

Some pages of this thesis may have been removed for copyright restrictions.

If you have discovered material in Aston Research Explorer which is unlawful e.g. breaches copyright, (either yours or that of a third party) or any other law, including but not limited to those relating to patent, trademark, confidentiality, data protection, obscenity, defamation, libel, then please read our [Takedown policy](#) and contact the service immediately (openaccess@aston.ac.uk)

The Integration of ProxiMAX Randomisation with CIS Display for the Production of Novel Peptides.

Andrew James Poole
Doctor of Philosophy

ASTON UNIVERSITY

September 2015

©Andrew James Poole

Andrew James Poole asserts his moral right to be identified as the author of this thesis.

This copy of the thesis has been supplied on condition that anyone who consults it is understood to recognise that its copyright rests with its author and that no quotation from this thesis and no information derived from it may be published without proper acknowledgement.

Aston University

The Integration of ProxiMAX Randomisation with CIS Display for the Production of Novel Peptides.

**Andrew James Poole
Doctor of Philosophy
September 2015**

Thesis Summary

Saturation mutagenesis is a powerful tool in modern protein engineering, which permits key residues within a protein to be targeted in order to potentially enhance specific functionalities. However, the creation of large libraries using conventional saturation mutagenesis with degenerate codons (NNN or NNK/S) has inherent redundancy and consequent disparities in codon representation. Therefore, both chemical (trinucleotide phosphoramidites) and biological methods (sequential, enzymatic single codon additions) of non-degenerate saturation mutagenesis have been developed in order to combat these issues and so improve library quality.

Large libraries with multiple saturated positions can be limited by the method used to screen them. Although the traditional screening method of choice, cell-dependent methods, such as phage display, are limited by the need for transformation. A number of cell-free screening methods, such as CIS display, which link the screened phenotype with the encoded genotype, have the capability of screening libraries with up to 10^{14} members.

This thesis describes the further development of ProxiMAX technology to reduce library codon bias and its integration with CIS display to screen the resulting library. Synthetic MAX oligonucleotides are ligated to an acceptor base sequence, amplified, and digested, subsequently adding a randomised codon to the acceptor, which forms an iterative cycle using the digested product of the previous cycle as the base sequence for the next. Initial use of ProxiMAX highlighted areas of the process where changes could be implemented in order to improve the codon representation in the final library. The refined process was used to construct a monomeric anti-NGF peptide library, based on two proprietary dimeric peptides (Isogenica) that bind NGF. The resulting library showed greatly improved codon representation that equated to a theoretical diversity of ~69%. The library was subsequently screened using CIS display and the discovered peptides assessed for NGF-TrkA inhibition by ELISA. Despite binding to TrkA, these peptides showed lower levels of inhibition of the NGF-TrkA interaction than the parental dimeric peptides, highlighting the importance of dimerization for inhibition of NGF-TrkA binding.

Keywords: non-degenerate, saturation mutagenesis, anti-NGF, codon randomisation,

Acknowledgements

I would like to thank my supervisor Dr Anna Hine for giving me the opportunity of this Ph.D. as well as her guidance and encouragement throughout the entirety of the process. My thanks are also extended to Dr Andy Sutherland, and his group, for offering help and feedback during our group meetings.

My thanks are also extended to my industrial sponsors, Isogenica, specifically Dr Chris Ullman, Dr Laura Frigotto, Dr Matt Smith, for his help with the library and MiSeq analysis, and Dr Gabriela Ivanova-Berndt for the mass spectrometry analysis. I would also like to thank everybody else at Isogenica for making me feel welcome during my time at the company.

I would also like to thank both past and present members of the research group. Dr Sam Hebaishi and Jenn Lines for offering continued help and insight throughout, along with Dr Mo Ashraf, Mike Tredgett, Marta Fraszczak and Jacob Kerin, as well as Dr Dave Nagel for his consultation and help regarding the protein expression and refolding.

My thanks are also extended to the members of my office and lab including Dr Heather Currinn, Dr James Barwell, Dr Marvin Dilworth, as well as many others, without whom this Ph.D. would have been far less enjoyable.

Finally I thank my family who have supported me throughout my entire life, I am truly grateful for everything you have done for me, and Jade for her love, understanding and support with all matters scientific or not throughout this time.

Contents

1. Chapter 1: Introduction.....	16
1.1. Site-Directed and Saturation Mutagenesis	16
1.2. Degenerate Saturation Mutagenesis	18
1.3. Saturation Mutagenesis with Limited Degeneracy	20
1.3.1. NNK/S Saturation.....	20
1.3.2. 22-c Trick	21
1.4. Non-degenerate Saturation Mutagenesis	21
1.4.1. Chemical Approaches to Non-degeneracy	21
1.4.2. PCR-Based Methodologies	25
1.4.3. Sequential, Enzymatic Single Codon Additions	28
1.5. Comparison of Saturation Mutagenesis Methods	30
1.5.1. Library Size/Diversity	30
1.5.2. Codon Bias	32
1.5.3. Encoded Truncation	32
1.5.4. Practicality of Application	33
1.6. Screening Technologies.....	34
1.6.1. <i>In vivo</i> Cell-Dependent Display Systems.....	34
1.6.2. <i>In vitro</i> Cell-Free Display Systems	37
1.7. Peptides as Therapeutic Agents.....	42
1.8. Nerve Growth Factor (NGF)	43
1.8.1. NGF Structure.....	43
1.8.2. NGF Receptors	45
1.8.3. NGF-Receptor Interaction	46
1.8.4. Clinical Use of Anti-NGF Therapy	48

1.9.	Project Outline	49
2.	Chapter 2: Materials and Methods.....	51
2.1.	Materials	51
2.1.1.	Media Recipes	51
2.1.2.	Broth Recipes	51
2.1.3.	Buffer Recipes	52
2.1.4.	Other Solutions	59
2.1.5.	Cell Lines	61
2.1.6.	Vectors.....	61
2.2.	Methods	62
2.2.1.	Enzyme Dependent Reactions	62
2.2.2.	ProxiMAX Procedure.....	64
2.2.3.	Refined ProxiMAX Procedure.....	69
2.2.4.	Electrophoresis	71
2.2.5.	Transformation of <i>Escherichia Coli</i>	74
2.2.6.	Plasmid Purification (Small scale)	75
2.2.7.	Ethanol Precipitation	75
2.2.8.	Phenol/Chloroform Extraction	76
2.2.9.	Protein Expression and Purification.....	76
2.2.10.	CIS Display.....	83
2.2.11.	NGF Inhibition Assay.....	85
3.	Chapter 3: ProxiMAX Randomisation: Single Reaction Equimolar Ligation Library	88
3.1	Introduction	88
3.2	MAX Oligonucleotide and Library Framework Preparation	90

3.3	ProxiMAX Saturation Cycling	92
3.4	ProxiMAX Saturation Cycling with Re-designed MAX Oligonucleotides	94
3.5	Completed Library Analysis.....	99
3.6	Discussion.....	104
4.	Chapter 4: Anti-NGF Peptide Library-ProxiMAX Process Refinement.	109
4.1.	Introduction	109
4.2.	Framework and MAX Oligonucleotide Preparation	111
4.3.	ProxiMAX Saturation Cycling of Anti-NGF Peptide Library	115
4.4.	Completed Anti-NGF Peptide Library Analysis	121
4.5.	ProxiMAX Saturation Cycling of Resynthesized LH Anti-NGF Peptide Library	127
4.6.	Resynthesized LH Anti-NGF Peptide Library Analysis.....	130
4.7.	Discussion.....	133
5.	Chapter 5: Recombinant Human Nerve Growth Factor Expression, Purification and Activity Testing in an Escherichia Coli Expression System	137
5.1.	Introduction	137
5.2.	Expression and purification of β -NGF using pJ434.....	138
5.3.	β -NGF Sub-Cloning into pETSUMO	141
5.4.	pETSUMO- β NGF Expression Optimisation in <i>E.coli</i> BI21.....	145
5.5.	pETSUMO- β NGF Expression and Purification in <i>E.coli</i> SHuffle.	149
5.6.	Preparation, Purification and Refolding of Insoluble SUMO- β NGF	152
5.7.	SUNO- β NGF Activity Testing	158
5.8.	Discussion.....	161
6.	Chapter 6: Anti-NGF Peptide Selection, Screening and Testing.....	165
6.1.	Introduction	165
6.2.	Biotinylation of rh- β NGF	166

6.3.	Library Selections Using CIS Display	169
6.4.	Cloning of Selection Output.....	171
6.5.	Screening of Selection Output.....	173
6.6.	Sequencing of Screening Output.....	179
6.7.	Anti-NGF Peptide Testing	182
6.8.	Discussion.....	195
6.8.1.	Biotinylation.....	195
6.8.2.	Library Screening	195
6.8.3.	Peptide Testing - ELISA Results	198
7.	Chapter 7: Discussion and Conclusions	204
7.1.	Summary of Results	204
7.2.	Discussion and Conclusions	209
7.2.1.	ProxiMAX Randomisation	209
7.2.2.	CIS Display	211
7.2.3.	Peptides: Therapeutics, Interactions and Optimisation	212
8.	References.....	216
9.	Appendices	232
9.1.	Appendix 1. Single Reaction Ligation Library Codon Representation Table	232
9.2.	Appendix 2. Anti-NGF PeptideLibrary Framework Sequences	233
9.3.	Appendix 3. 72-mer Anti-NGF Peptide Library Codon Representation Tables.....	234
9.4.	Appendix 4. 63-mer Anti-NGF Peptide Library Codon Representation Tables.....	236
9.5.	Appendix 5. Re-Synthesised Final Anti-NGF Peptide Library Codon Representation Tables.....	238
9.6.	Appendix 6. pET SUMO/CAT Positive Expression Control Plasmid Map (taken from Champion™ pET SUMO Protein Expression System manual, Invitrogen).....	240

9.7. Appendix 7. pET SUMO Sequencing Primers241

Table of Figures

Figure 1.1. The Genetic Code	19
Figure 1.2. NNK Limited Genetic Code.....	20
Figure 1.3. MAX Randomisation Schematic (taken from (Hughes et al., 2003))	27
Figure 1.4. Theoretical Library Diversity using Different Saturation Mutagenesis Methods (Ashraf et al., 2013).....	31
Figure 1.5. Library display methods illustration (taken from (Baxter et al., 2014)).....	41
Figure 1.6. NGF Structure (taken from (Wiesmann and De Vos, 2001)).....	44
Figure 1.7. NGF Dimerization (taken from (Wiesmann and De Vos, 2001)).....	44
Figure 1.8. NGF-TrkA-d5 Structure (taken from (Wiesmann et al., 1999)).....	47
Figure 3.1. ProxiMAX Randomisation Process Schematic.....	89
Figure 3.2. Picogreen Standard Curve	90
Figure 3.3. ProxiMAX Saturation Cycling.....	92
Figure 3.4 Oligonucleotide Contamination and Concatemers	94
Figure 3.5. Picogreen Standard Curve	95
Figure 3.6. Saturation Cycling with Re-designed MAX Oligonucleotides	97
Figure 3.7. Six Cycle Comparison of Saturation Cycling PCR Products	98
Figure 3.8. Sequencing Results Randomised Array	101
Figure 3.9. Codon Representation of Single Reaction Equimolar Library	102
Figure 4.1. ProxiMAX Randomisation Process Illustration.....	110
Figure 4.2 Original Anti-NGF Peptide Sequence Homology	111
Figure 4.3. Library Construction Overview.....	111
Figure 4.4. LH Framework Construction Overview	113
Figure 4.5. Refined Saturation Cycling and Quantification of LH Anti-NGF Library	117
Figure 4.6. Refined Saturation Cycling and Quantification of RH Anti-NGF Library	120
Figure 4.7. RH 6 cycle comparison and LH+RH ligation	121
Figure 4.8. Codon Representation of Full length (72-mer) Anti-NGF Peptide Library.....	123
Figure 4.9. Codon Representation of Truncated (63-mer) Anti-NGF Peptide Library	124

Figure 4.10. LH Internal Amplification Cycle Comparison	126
Figure 4.11. Saturation Cycling and Quantification of Re-synthesised LH Anti-NGF Library	129
Figure 4.12. Resynthesized LH Cycle Comparison.....	129
Figure 4.13. Codon Representation of Re-synthesised LH Anti-NGF Peptide Library.....	131
Figure 5.1 pJ434-NGF_optEc Plasmid Map	139
Figure 5.2. pJ434- β -NGF Expression and Purification.....	140
Figure 5.3. pETSUMO Plasmid Map (taken from Champion™ pET SUMO Protein Expression System manual, Invitrogen).....	141
Figure 5.4. β -NGF TA Cloning.....	142
Figure 5.5. pETSUMO- β NGF Colony Screening	143
Figure 5.6. pETSUMO- β NGF Sequencing.....	144
Figure 5.7 Initial pETSUMO- β -NGF Expression in <i>E.coli</i> BI21	146
Figure 5.8. pETSUMO- β -NGF Expression Optimisation in <i>E.coli</i> BI21.....	148
Figure 5.9. pETSUMO- β NGF Expression Optimisation in <i>E.coli</i> SHuffle	150
Figure 5.10. pETSUMO- β NGF Soluble Fraction Purification	152
Figure 5.11. pETSUMO- β NGF Soluble Fraction Purification	154
Figure 5.12. SUMO- β NGF Refolding.....	156
Figure 5.13. BCA Assay BSA Standard Curve	157
Figure 5.14. SUMO- β NGF Digestion and Purification.....	159
Figure 5.15. β -NGF Activity Assay.....	160
Figure 6.1. CIS Display Overview.....	166
Figure 6.2. rh- β NGF Biotinylation	168
Figure 6.3. CIS Display Recovery PCR	170
Figure 6.4. Selection Output Amplification and Re-introduction of Restriction Site	171
Figure 6.5. NcoI/NotI Cloning Digestion.....	172
Figure 6.6. Selection Output Screening.....	179
Figure 6.7. Colony Screening	180
Figure 6.8. Screening Output Sequencing.....	181

Figure 6.9. Simplified TrkA Inhibition ELISA Illustration	184
Figure 6.10. Example TrkA Inhibition ELISA Results	185
Figure 6.11. Initial Peptide Testing	188
Figure 6.12. Broad Concentration Range Peptide Testing.....	191
Figure 6.13. Library Peptide Dose Curves	192
Figure 6.14. Unnatural Amino Acid Peptide Dose Curves.....	193
Figure 6.15. Changes in Amino Acid Representation Before and After Selection for NGF Binding.....	196
Figure 6.16. NGF-TrkA-d5 binding pocket (original image taken from Wiesmann <i>et al.</i> (Wiesmann et al., 1999))	198

Table of Tables

Table 1.1. Library Size	31
Table 1.2. Encoded Bias (Ashraf et al., 2013)	32
Table 1.3. Encoded Truncation (Ashraf et al., 2013).....	33
Table 1.4. Min/max no. of Primers to Saturate Contiguous Codons.....	34
Table 2.1. Single Reaction Ligation MAX Oligonucleotide Sequences.....	64
Table 2.2 Re-designed Single Reaction Ligation MAX Oligonucleotide Sequences	65
Table 2.3 Single Reaction Ligation Library MAX Codon Identity	65
Table 2.4. Single Reaction Ligation Library MiSeq Primers	68
Table 2.5. Anti-NGF Peptide Library MiSeq Primers.....	68
Table 2.6. Refined MAX Oligonucleotide Sequences	69
Table 2.7. Anti-NGF Peptide Library MAX Codon Identity	70
Table 3.1. MAX Oligonucleotide Picogreen Measurements	91
Table 3.2. Library Build Overview.....	91
Table 3.3. Re-designed MAX Oligonucleotide Picogreen Measurements. Picogreen measurements	96
Table 3.4. MiSeq Library Length Distribution.....	101
Table 3.5. Library Sequence Diversity	103
Table 3.6. Mathematical Analysis of Library Diversity	103
Table 4.1. LH Anti-NGF Peptide Library Build Overview.....	112
Table 4.2. RH Anti-NGF Peptide Library Build Overview	112
Table 4.3. LH Hairpin Quantification.....	114
Table 4.4. RH Hairpin Quantification	115
Table 4.5. Anti-NGF Peptide Library MiSeq Length Distribution	122
Table 4.6. Mathematical Analysis of Anti-NGF Peptide Library Diversity	125
Table 4.7. Anti-NGF Peptide Library Sequence Diversity for 72-mer and 63-mer	125
Table 4.8. Re-synthesised LH Anti-NGF Peptide Library MiSeq Length Distribution.....	130

Table 4.9. Mathematical Analysis of Re-synthesized LH Anti-NGF Peptide Library Diversity.	132
Table 4.10. Re-synthesized LH Anti-NGF Peptide Library Sequence Diversity.....	132
Table 5.1. pETSUMO- β NGF Cloning	143
Table 5.2. SUMO- β NGF BCA Assay Quantification	157
Table 6.1. CIS Display Selections Plan	169
Table 6.2. Selection Output pHEN Cloning.....	173
Table 6.3. Library Peptide Identity and Sequences.....	182
Table 6.4. Unnatural Amino Acid Peptide Identity and Sequences.	183
Table 6.5 Consensus of Amino Acid Preferences in Anti-NGF Peptide Monomers After Taking Library Composition into Account.	197
Table 6.6. Comparison of Consensus and Actual Peptide Sequences	202

Abbreviations

Amp	Ampicillin
ATP	Adenosine triphosphate
bp	Base pair(s)
BSA	Bovine serum albumin
dNTPs	Deoxynucleotide
DMF	Dimethylformamide
DMT	<i>N,N</i> -Dimethyltryptamine
DNA	Deoxyribose nucleic acid
EDTA	Ethylenediaminetetraacetic acid
Fmoc	9-fluorenylmethyl carbamate
IPTG	Isopropyl β -D-1-thiogalactopyranoside
Kan	Kanamycin
LB	Luria broth
Mins	Minute(s)
NEB	New England Biolabs
NGF	Nerve Growth Factor
OD	Optical density
PAGE	Polyacrylamide gel electrophoresis
PBS	Phosphate buffered saline
PBST	Phosphate buffered saline/0.1% Tween
PCR	Polymerase chain reaction
PNK	Polynucleotide kinase
rh- β NGF	Recombinant human β nerve growth factor
RNA	Ribonucleic acid
Rpm	Revolutions per minute
w/v	Weight to volume
v/v	Volume to volume
X-gal	5-Bromo-4-Chloro-3 indolyl- β -D-galactopyranoside

Chapter 1

Introduction

1. Chapter 1: Introduction

Directed mutagenesis techniques are becoming ever-more important tools in the field of protein engineering. Rather than randomly making changes within a protein these techniques rely on more detailed targeting of key residues allowing rational structural changes to be implemented. These directed mutagenesis techniques have evolved from the substitution of a single critical residue with another, to the ability to fully randomise/saturate multiple residues either contiguously or at disparate locations in a protein. Whilst single substitutions may highlight the importance of a residue in a set tertiary structure without drastic alterations, the ability to target multiple positions can provide a more holistic overview of the roles that different residues play within a proteins tertiary structure. High-throughput protein engineering generates highly diverse libraries maximising the chance for novel improvements to be discovered, whether in the fields of stability, binding affinity etc. However, the high-throughput production of diverse protein libraries is only as powerful as the ability with which to screen them. Modern advances in high-throughput screening techniques allow libraries with an even greater number of members to be efficiently screened in less time than ever before.

Therefore the general aim of this project is to integrate and demonstrate new high-throughput methods of library generation and screening for a peptide that inhibits the binding of nerve growth factor (NGF) to its receptor.

1.1. Site-Directed and Saturation Mutagenesis

Site-directed mutagenesis in its simplest form involves the substitution of one codon with another one at specific single location. This usually involves the use of mutagenic primers containing the three altered nucleotides that are then annealed to the wild type ssDNA and subsequently incorporated. However, replacing a single codon with another one is a very low-throughput and laborious process as only a single mutant is generated at a time.

Saturation mutagenesis on the other hand is a method in which a single codon is replaced to encode all twenty amino acids, so creating a randomised library. This is hugely beneficial in terms of protein engineering as many variants of single gene can be generated quickly becoming a process that is truly high-throughput. Saturation mutagenesis has been used to improve the activity and stability of enzymes (Siloto and Weselake, 2012, Valetti and Gilardi, 2013, Reetz, 2013), engineering the binding of antibodies (Sidhu and Kossiakoff, 2007) and transcription factors (Pattanaik et al., 2010, Smith et al., 2013) as well as engineering regulatory elements (Patwardhan et al., 2009) and ribosome binding sites (Wang et al., 2009).

A number of techniques have been developed that allow further knowledge of the structure-function relationship of proteins to be gained, which particularly target regions critical to functionality. CASTing (combinatorial active site saturation test) is one such method that can be used to identify important catalytic residues within the active site of an enzyme. This is achieved by designing and generating small randomised libraries of enzyme mutants. Two spatially close residues around the enzyme's active site are randomised, which allows for any conformational effects that may not result from a single mutation (Reetz et al., 2005). The choice of positions to randomise is decided from analysis of the wild-type enzyme bound to a substrate. Due to the fact that multiple positions are randomised at the same time, high diversity is created and can be seen as a good alternative to error-prone PCR (Reetz et al., 2006b). To highlight the effectiveness of this process, CASTing was used on a lipase from *Pseudomonas aeruginosa*. Five pairs of interacting amino acids, critical to activity, were identified. This data was used to generate five mutagenized libraries ultimately resulting eight important hits that showed increased hydrolysis rates compared to the wild type enzyme (Reetz et al., 2005).

A second such method is BFIT (B factor iterative test), which is designed to identify residues involved in the stability of a protein (Reetz et al., 2006a). It was identified that the thermostability of mesophilic enzymes was proportional to their rigidity. B factors (values) were obtained in order to identify which positions at which to increase the enzymes' rigidity.

Those residues with the highest B factors, reflecting the most flexible bonds, were then chosen for saturation mutagenesis to form focussed libraries. The best gene was then used for a second round of saturation mutagenesis at another site and subsequently focussed through the remaining sites. This was applied lipase Lip A from *Bacillus subtilis* eventually resulting in the screening of 8000 clones with significant increases in thermostability observed (Reetz et al., 2006a, Reetz and Carballeira, 2007).

1.2. Degenerate Saturation Mutagenesis

Phosphoramidite chemistry is the industry standard for the synthesis of oligonucleotides. This process involves adding nucleoside phosphates, one base at a time (in the 3'→5' direction) to a solid support and then exposing it to an acid/base to remove its protecting groups which then allows the formation of a bond with a new nucleoside, added in solution. This process is repeated to form an oligonucleotide. This chemistry can be used either to make oligonucleotides with a single, specific sequence or to introduce randomised bases, which can be introduced during oligonucleotide synthesis by using mixed pools of nucleotides, rather than single nucleotides, at specific cycles during the synthesis process (Derbyshire et al., 1986).

Traditionally, to generate such randomised libraries, a synthetic cassette containing codons specified as NNN (where any combination of the four nucleotides is possible) is created using chemical synthesis. That cassette is then inserted into the original gene. This is relatively simple and creates large diversity that is only limited by the amount of positions that can be randomised due the ability to screen the resulting libraries.

The genetic code has inherent redundancy as there are 64 (4^3) possible combinations of nucleotides to encode only 20 amino acids. This degeneracy is not evenly represented across the amino acids with six codons encoding the most common amino acids whilst only a single codon encodes the least common (Figure 1.1). As multiple codons can encode the same amino acid there can be large disparities between codon representations within

conventional methods of saturation mutagenesis as the number of codons targeted is increased (Table 1.2). This in turn can lead to vast libraries, for example the full saturation of 10 amino acids would result in library with 1.024×10^{13} combinations (Kille et al., 2013), which can increase pressure on later screening efforts. The presence of termination codons within the genetic code also limits the quality of libraries generate using NNN as the percentage of truncated sequences will increase as the number of saturated positions is increased (Table 1.3). The degeneracy of the genetic code also limits the number of positions that can be randomised because of the ability to screen the resulting libraries.

		Second Position				
		T	C	A	G	
T	First Position	Phe	Ser	Tyr	Cys	T
		Phe	Ser	Tyr	Cys	C
		Leu	Ser	STOP	STOP	A
		Leu	Ser	STOP	Trp	G
C	First Position	Leu	Pro	His	Arg	T
		Leu	Pro	His	Arg	C
		Leu	Pro	Gln	Arg	A
		Leu	Pro	Gln	Arg	G
A	First Position	Ile	Thr	Asn	Ser	T
		Ile	Thr	Asn	Ser	C
		Ile	Thr	Lys	Arg	A
		Met	Thr	Lys	Arg	G
G	First Position	Val	Ala	Asp	Gly	T
		Val	Ala	Asp	Gly	C
		Val	Ala	Glu	Gly	A
		Val	Ala	Glu	Gly	G

Figure 1.1. The Genetic Code. All 64 possible combinations of nucleotides with their corresponding amino acids. Serine is used as an example of the most commonly occurring amino acids whilst tryptophan is used as an example of the least common amino acids.

1.3. Saturation Mutagenesis with Limited Degeneracy

1.3.1. NNK/S Saturation

In attempting to combat the issues observed with NNN saturation, it is possible to limit the degeneracy using methods such as NNK/S. The NNK/S method relies on using oligonucleotides that have limited degeneracy within the randomised codons. NNK/S, where N=A, C, T or G, K=G or T and S=G or C, reduces the degeneracy by half (down to 32 possible codons rather than a 64 possible codons) whilst still encoding all 20 amino acids (Reetz et al., 2008, Kille et al., 2013). Within this mix the ratio of the most common: least common is reduced (Figure 1.2) although a bias is still present, which becomes more significant the more positions that are randomised (section 1.5). Again, by limiting the codons used, encoded truncation is reduced compared with NNN although it is still present (section 1.5) (Tang et al., 2012).

		Second Position					
		T	C	A	G		
First Position	T	Phe	Ser	Tyr	Cys	T	
		Phe	Ser	Tyr	Cys	C	
		Leu	Ser	STOP	STOP	A	
		Leu	Ser	STOP	Trp	G	
	C	Leu	Pro	His	Arg	T	
		Leu	Pro	His	Arg	C	
		Leu	Pro	Gln	Arg	A	
		Leu	Pro	Gln	Arg	G	
	A	Ile	Thr	Asn	Ser	T	
		Ile	Thr	Asn	Ser	C	
		Ile	Thr	Lys	Arg	A	
		Met	Thr	Lys	Arg	G	
G	Val	Ala	Asp	Gly	T		
	Val	Ala	Asp	Gly	C		
	Val	Ala	Glu	Gly	A		
	Val	Ala	Glu	Gly	G		

Figure 1.2. NNK Limited Genetic Code. The 32 combinations of nucleotides using NNK **Serine** is used as an example of the most commonly occurring amino acids whilst **tryptophan** is used as an example of the least common amino acids.

1.3.2.22-c Trick

The 22c-trick reduces the codon : amino acid ratio to 22:20 (Kille et al., 2013). This PCR-based method is achieved for a single targeted residue by using a mix of 3 oligonucleotide primers with one of each carrying an NDT (where N=A, T, C or G; D= A, G or T (12 codons)), VHG (V= A, G or C; H= A, C or T (9 codons)) and a TGG codon. These in combination do reduce the codon to amino acid ratio and also eliminate the presence of termination codons but do still contain a redundant codon for both valine and leucine.

To analyse the effectiveness of the mutagenesis techniques, Leu426 of cyclohexanone monooxygenase (CHMO) was targeted with both the 22c-trick and NNK. Although the initial comparison of the 22c-trick to NNK was generally favourable, further mutagenesis studies of genes encoding CHMO and phenylacetone monooxygenase (PAMO) showed poor saturation with a high frequency of wild type bases in particular at the second and third positions (Kille et al., 2013).

1.4. Non-degenerate Saturation Mutagenesis

Due to the inherent redundancy within the genetic code, various methods of non-degenerate saturation have been devised, which aim to remove redundant codons altogether. These tend to be either chemical or oligonucleotide-based approaches but all share the same objectives of creating smaller, focused randomised libraries without redundancy. These key methods are summarised in the following sections.

1.4.1. Chemical Approaches to Non-degeneracy

The core methodology of all chemical approaches to non-degenerate saturation involves the use of either di- or tri-nucleotide phosphoramidite building blocks during oligonucleotide synthesis. As the construction of trinucleotide phosphoramidites is stepwise process from the original starting material via intermediate products to the final trinucleotide, it is of particular

importance to use suitable protecting groups. This allows selective deblocking functionality required for the next reaction step whilst also conferring stability stable during the final introduction of the phosphoramidite and throughout the following oligonucleotide synthesis.

1.4.1.1. Trinucleotide Phosphoramidites/Phosphotriesters

The use of trinucleotide phosphoramidites as a mutagenesis technique was first reported by Sondek and Shortle (1992), who tested the coupling efficiency of two blocked and protected trinucleotide phosphoramidites (dGCT and dGGT). Whilst increasing phosphoramidite concentration gave increasing coupling efficiency, it was notable that even the highest trinucleotide phosphoramidite concentration resulted in a coupling efficiency of only 4% compared with 99% for the same concentration of monomer phosphoramidite (Sondek and Shortle, 1992).

This principle was taken on further by Virnekas and co-workers, who employed a full set of 20 trinucleotide phosphoramidites, using two 3'-O-phenoxyacetyl (Pac) protected mononucleotides and seven dinucleotides (Virnekas et al., 1994). The approach enabled the synthesis of all 20 trinucleotides in the fewest possible coupling reactions, with a yield of 25-40% of trinucleotide phosphoramidites achieved. In order to test the trinucleotide synthesis, two sets of tetranucleotides were produced. The first used normal phosphoramidites whilst the other used trinucleotide phosphoramidites to bind to a support thymine. No significant difference was observed. The trinucleotides were subsequently used to make two primers for the light chain of an antibody. Although sequencing showed that all trinucleotide phosphoramidites had been incorporated correctly, uneven representation was observed. It was concluded that there were varying coupling rates during synthesis, as the original mixture of trinucleotide phosphoramidites were equally proportioned (Virnekas et al., 1994).

Two approaches attempted tried to overcome the issues associated with the 3'-OH-protecting group. Replacement of Pac by tert-butyldimethylsilyl (TBDMS; Lytle et al., 1995) yielded by-products such as isometric trimers, at an average coupling efficiency of 71%, although the final yield of oligonucleotide was low. Meanwhile Gaytan et al. (1998)

addressed the protecting group issue by using 9-fluorenylmethyl carbamate (Fmoc) for protection of the 5' and DMT (dimethoxytrityl) at the 3'-OH group of deoxyribose. Twenty Fmoc protected trinucleotide phosphoramidites were produced by combining five Fmoc-protected dinucleotide phosphoramidites and four DMT-protected monomers (Gaytan et al., 1998). These were incorporated into oligonucleotides and used to generate libraries of TEM-1- β -lactamase variants, although subsequent sequence analysis of clones showed uneven codon representation. As previously found by Virnekas et al (1994), this uneven codon representation correlated with differing trinucleotide reactivity.

As an alternative to improve codon representation, Ono *et al.* (1995) developed a method utilising phosphotriester chemistry where seven unprotected 3'-OH dimer precursors were extended in the 3' direction by coupling an *N*-acylated nucleoside to the 3'-OH. A coupling efficiency of 90% was achieved for the final oligonucleotide synthesis using these trinucleotides. This method also aimed to minimise the number of dimers needed for the synthesis of trinucleotides for all 20 amino acids. Resulting anti-sense sequences were then transformed into codons using template-mediated replication (Ono et al., 1995).

Clearly, different trimers exhibit different reaction rates. Therefore reaction factors (RFs) were determined. By assigning each trinucleotide an RF value, where an RF of 1.0 relates to the most reactive, and poorer reactivity is reflected in a higher RF value, it can be attempted to compensate for different reaction rates (Kayushin et al., 1996). Thus, a trimer with an RF value of 2.0 would be mixed at twice the concentration of one with an RF value of 1.0, in order to obtain equal incorporation into an oligonucleotide. This method was subsequently used to create two 12-codon libraries (Kayushin et al., 1999) though significant variations between codon representation were still observed. The methodology was further developed to allow the use of partially protected trimers with solid phase synthesis (Kayushin et al., 2000). Here they were able to increase the yield of the phosphotriesters whilst allowing the regeneration of the starting materials. However, further work from this group resulted in the commercialisation of a set of twenty 5' DMT-protected trinucleotide phosphoramidites (rather

than phosphotriesters) supplied by Glen Research Corporation (Gaytan et al., 2009, Yagodkin et al., 2007).

1.4.1.2. Microarray-Based Methods

As technology has advanced, phosphoramidite chemistry has been fused with micro-array methods to allow the parallel synthesis of short oligonucleotides. Many different methods have been developed such as photolabile 5' protecting groups (Nimblegen/Affymetrix), ink-jet printing with standard reagents (Agilent), photo-generated acid deprotection (Atactic/Xeotron) and electrolytic acid/base arrays (Oxamer/Combimatrix). Non-degenerate phosphoramidites have also been combined with microarrays (Gen9) allowing the construction large non-degenerate libraries, although these still suffer from the same problems as standard phosphoramidite chemistry using a solid support. Microarrays are used to produce many small oligonucleotides that are then joined to form larger oligonucleotides. If one oligonucleotide contains a deletion (n-1) this problem can be potentially exacerbated elongated with another n-1 oligonucleotide producing a longer n-2 oligonucleotide containing two deletions.

1.4.1.3. Chemical Approaches - Summary

Regardless of specific methodology, a major issue associated with phosphoramidite chemistry is the error rate during the chemical synthesis of oligonucleotides. This error rate can be as high as 10^{-3} to 10^{-2} (Tian et al., 2004) compared with an error rates observed in nature that can range for 10^{-8} to 10^{-7} (Schofield and Hsieh, 2003). Errors commonly occur when new phosphoramidite monomers fail to couple. These are usually terminated from growth by acetylation thus producing truncated oligonucleotides, however failure rates in termination can be up to 0.5% per position, which will in turn lead to deletion errors. Finally insertion rates can be up to 0.4% per base as a result of DMT cleavage by excess activator (Ma et al., 2012).

Another downfall of using chemical, trinucleotide-based approaches is the high cost associated with this type of production which is therefore not practical for the majority of laboratories. A number of other methods that do not involve such chemical synthesis have been developed to address the issue of redundancy involved in saturation mutagenesis.

1.4.2. PCR-Based Methodologies

1.4.2.1. Small Intelligent Libraries

Similar to the 22c-trick, this method relies on using four primers, two containing NDT (where N=A, T, C or G; D= A, G or T (12 codons)) and VMA degeneracies respectively (V= A, G or C; M= A or C (6 codons)) and two containing single ATG and TGG codons (Tang et al., 2012). This approach has the initial advantage over the 22c-trick in that it has a 1:1 codon to amino acid ratio and removes all termination codons and was combined with primer design software, DC-Analyzer, to assist with the design of small intelligent primers. The DC-Analyzer software was further adapted to create MDC-Analyzer to aid the design of degenerate primer sets in multiple contiguous sites (Tang et al., 2014).

However, like the problems faced with 22c-trick, the number of primers required to saturate multiple residues in close proximity increase substantially for every targeted position (64-128 primers for 3 saturated positions) (section 1.5). Therefore again this method becomes physically and financially impractical as more residues are targeted.

1.4.2.2. MAX Randomisation

MAX randomisation is another oligonucleotide based method of mutagenesis aimed at removing the redundancy and bias found in randomised gene libraries. Instead of using all possible combinations created from NNN, the target was to choose the twenty favoured codons for expression of each amino acid in *Escherichia Coli* (*E.Coli*) (Nakamura et al., 2000) without the use of complex chemistry techniques. This ensures that the ratio of codons

to amino acids is 1:1 no matter how many positions are randomised. It also in turn removes redundant and termination codons from the process (Hughes et al., 2003). Codon bias should also be addressed as there is only one codon for every amino acid so each should be represented equally.

In this process twenty individually-synthesised “selection” oligonucleotides were hybridised to a “template” oligonucleotide that has been conventionally randomised in certain areas. The selection oligonucleotides have a conserved region that pairs with their complementary base pair in the template sequence, which can also aid orientation to the correct alignment. Mis-annealing between the sets of oligonucleotides is dealt with using a PCR step as only the ligated selection strand is amplified (Figure 1.3). This method was illustrated by randomising three contacting positions within a synthetic zinc finger (Hughes et al., 2003). This process was also used to create sixty overlapping randomised gene libraries for zinc finger proteins (Hughes et al., 2005).

Compared with other methods, MAX randomisation is relatively easy to implement, though the process is limited by the fact that no more than two contiguous positions can be randomised at a single attempt, owing to the requirement of conserved regions to align the selection oligonucleotides with the template.



Figure 1.3. MAX Randomisation Schematic (taken from (Hughes et al., 2003)). A synthetic template oligonucleotide is made with appropriate codons randomised as NNN and invariant bases (represented as continuous lines) corresponding to the parental gene. For each randomised codon, 20 synthetic selection oligonucleotides, each comprising the appropriate complementary invariant region and a codon (the MAX codon) for optimal expression of a single amino acid, are hybridised with the template oligonucleotide. Base-pairing dictates that any single selection oligonucleotide will hybridise with its complement in the template. Selectional hybridisation generates a synthetic cassette for gene randomisation. Here, the template oligonucleotide contains three conventionally randomised codons. The invariant regions of the template are colour-coded to correspond with the complementary invariant regions of the appropriate selection oligonucleotides. Two additional, unique constant oligonucleotides are required in the hybridisation mixture to provide primer-binding and restriction sites at the ends of the cassette. Primer-binding sites are indicated by broken lines. Their location ensures that only the selection strand is amplified by PCR. The resulting DNA cassette is then digested with restriction enzymes, dephosphorylated (to prevent concatemerisation) and cloned.

1.4.2.3. Computational and Bioinformatics Library Design

Apart from these methods described previously, there are computational methods designed to identify key functional residues in proteins. To generalise these can be broadly split into methods such as 1. Sequence based statistical analysis; 2. Analysis based off topological properties of native protein structure; 3. Molecular dynamics simulation. Sequence based

statistical methods, such as ConSurf 2005 (Landau et al., 2005), have proved highly successful in identifying critical sites for protein function, where co-conservation of evolutionarily conserved residues reflect functional coupling between them. In the case of structure and topology analysis methods parameters of topological property networks, derived from residue interaction networks formed by protein tertiary structures, are used to highlight functionally important residues (del Sol et al., 2006). While these methods can highlight important residues they give little information of the larger conformational changes, unlike molecular dynamics simulations that are also designed to take this into account (Su et al., 2011). Potential library size can be reduced and focussed using data-driven protein engineering strategies. This can be achieved in multiple ways such as; 1. by *in silico* analysis of the potential fitness of recombinant proteins produced (SCHEMA), 2. Using protein family sequence alignment to analyse changes amino acid pairs to predict incompatibilities (FamClash), 3. Prediction of functional variants of a native protein by analysing key amino acids in critical region (HotSpot wizard and ConSurf-HSSP). This type of analysis aids the rational design of libraries that can greatly reduce the size of the desired library whilst keeping the quality of the sequences within it (Tang et al., 2014).

1.4.3. Sequential, Enzymatic Single Codon Additions

1.4.3.1. Slonomics™

Sloning Biotechnology describes a randomisation method based upon the addition of random trinucleotides through a more molecular biology based method (Van den Brulle et al., 2008). This method uses synthetic oligonucleotides that contain a self-complementary region, causing them to form hairpins, and a three nucleotide overhang. The two types of oligonucleotide used in this process are termed “splinkers” and “anchors”; where every splinkers structure is the same apart from its overhang, and the anchors have the same structure apart from the overhang and the three adjacent bases. The anchor oligonucleotide also has a biotin modification within the hairpin thus allowing it to bind to a streptavidin-

coated surface. A combination of 4096 anchors and 64 splinkers can be used to create a randomised library that covers all possible eventualities.

Initially a single anchor and splinker are ligated together using the complementary overhangs, then using the biotin modification immobilised onto a streptavidin-coated plate. Un-ligated material is washed away whilst ligated product remains bound, which is later digested using the restriction endonuclease *Eam1104I*. This releases a product elongated by three nucleotides that is then used as an acceptor for a new anchor oligonucleotide. This process is repeated five more times to make an 18bp fragment (Van den Brulle et al., 2008). This phase is termed the elongation phase. Many of these elongation reactions can be done parallel creating many independent elongation products.

A second phase termed “transposition” involves releasing the elongation block with *Eam1104I* and removing the splinker end of the product with *Esp31*. These can be assembled in a pair wise method, which is highly specific due to the specific overhangs, to form a longer fragment. This process can be repeated five times to create a fragment 462bp in length (T1 produces a fragment of 32bp; T2 produces a fragment of 61bp; T3 produces a fragment of 118bp; T4 produces a fragment of 233bp; T5 produces a fragment of 462bp).

SlonoMax® libraries also used the same methodology to allow non-degenerate codon mutagenesis in the form of arrays and at separate locations. This allows control over codon representation but is only made within the company and is not available for in-house use within standard laboratories. Since the acquisition of Sloning Biotechnology by Morphosys in 2010 this service is only available under license.

1.4.3.2. ProxiMAX Randomisation

This process utilises synthetic oligonucleotides to donate specific codons at their termini, at a non-degenerate ratio, to a conserved acceptor sequence via a blunt-ended ligation. This ligation is amplified to provide enough working material to maintain diversity, purified and then digested with type IIs restriction endonucleases. The use of type IIs restriction

endonucleases to cut down stream of their recognition site facilitates the removal of the donator sequence whilst leaving randomised codon in place (Ashraf et al., 2013) (Figure 3.1). This process can be repeated to form an iterative cycle thus enabling the ability to create a sequential array of randomised positions whilst keeping the inherent advantages of a codon to amino acid ratio of 1:1. Different sets of donor oligonucleotides can be used per cycle allow restriction of specific codons for each cycle. An advantage of this method is that it not only allows the use of all 20 amino acids at a single position but also allows fine control of the use of specific subsets of amino acids at controllable ratios for each. ProxiMAX randomisation has been used for the saturation of 11 consecutive codons with the loop of CDR3 loop of the variable heavy chain of an antibody (Ashraf et al., 2013) with good codon representation observed for the most part. Further detail and indeed development of ProxiMAX methodology is provided in Chapters 3 & 4.

1.5. Comparison of Saturation Mutagenesis Methods

Which approach to saturation mutagenesis is best? Key approaches must take into account library size/diversity; codon bias; truncation caused by termination codons (all are directly relevant to subsequent screening) and ease of application. The following paragraphs compare key available approaches to saturation mutagenesis in these contexts.

1.5.1. Library Size/Diversity

Currently, the highest-capacity screening methodologies can handle libraries with a maximum of 10^{14} components, whilst cloning limits (relating to phage display etc.) are around 10^{10} library components. Therefore saturation of multiple residues using degenerate mutagenesis can quickly result in large libraries that exceed screening and/or cloning capacity and as such, library size is a significant consideration when designing a saturated library (Table 1.1).

No. of Saturated Codons	NNN	NNK/S	22c-trick	Non-degenerate
2	4.10×10^3	1.02×10^3	4.84×10^2	4.00×10^2
4	1.68×10^7	1.05×10^6	2.34×10^5	1.60×10^5
6	6.87×10^{10}	1.07×10^9	1.13×10^8	6.40×10^7
8	2.81×10^{14}	1.10×10^{12}	5.49×10^{10}	2.56×10^{10}
10	1.15×10^{18}	1.13×10^{15}	2.66×10^{13}	1.02×10^{13}

Table 1.1. Library Size. Theoretical size of libraries generated using different saturation mutagenesis techniques. NNN=64, NNK/S= 32, 22c-trick=22 and non-degenerate=20 possible nucleotide combinations per saturated position.

Moreover, degeneracy of the genetic code has a great impact on diversity (a measure of the percentage of unique sequences within a library). Randomisation using NNN at single position starts with a potential library diversity of ~65% and rapidly falls as the number of saturated positions increase despite reducing the degeneracy a similar trend is also observed using NNK/S and even the 22c trick, which has just two degenerate codons. In contrast, all non-degenerate methods maintain a theoretical 100% diversity, no matter how many codons are saturated, such that library size then becomes the sole limiting factor when designing the library (Figure 1.4).



Figure 1.4. Theoretical Library Diversity using Different Saturation Mutagenesis Methods (Ashraf et al., 2013). Diversity was calculated using the formula $d = 1/(N \sum_k p_k^2)$ (Makowski and Soares, 2003) and is in agreement for a 12-mer peptide saturated with codon NNN (Krumpe et al., 2007).

1.5.2. Codon Bias

Whilst increased screening capacity may help to nullify the effect of diversity for libraries with more than three randomised codons, the screening process is again a limiting factor, since all display screens assume an equal concentration of library components. However, the interaction between proteins and ligands is not a linear relationship, as proteins in high concentrations with relatively low affinity can saturate the ligands whilst those in low concentrations, albeit with higher affinity, may not reach saturation binding levels (Hughes et al., 2003). Thus, since both affinity and concentration affect the magnitude of detected protein–ligand interactions (Ashraf et al., 2013), screening of biased protein libraries may deliver misleading results in terms of optimal “hits”. Again, only non-degenerate saturation has the potential to deliver unbiased libraries (Table 1.2).



Table 1.2. Encoded Bias (Ashraf et al., 2013). Ratios represent the theoretical relative concentrations of each individual gene combining any of the most common codons (leucine/arginine/serine, NNN/NNK; or leucine/valine, 22c trick) compared with each individual gene containing any combination of the rarest codons [methionine/tryptophan, NNN;cysteine/aspartate/glutamate/phenylalanine/histidine/isoleucine/lysine/methionine/asparagine/glutamine/tryptophan/ tyrosine, NNK; or 18 codons (omitting leucine/valine), 22c trick].

1.5.3. Encoded Truncation

Degenerate and limited degeneracy saturation methods both encode termination codons, which lead to truncated proteins that are liable to be non-functional, but more seriously, can cause aggregation (Ashraf et al., 2013) that will likely disrupt subsequent screening assays. Again, with degenerate mutagenesis, the effect is magnified as the number of saturated

positions increase. Both the 22c trick and all non-degenerate methodologies avoid this problem (Table 1.3).



Table 1.3. Encoded Truncation (Ashraf et al., 2013). Truncation is calculated as the percentage of sequences that contain one or more termination codons within the saturated region.

1.5.4. Practicality of Application

Whilst NNN and NNK degenerate / limited degeneracy approaches are experimentally facile, as detailed in the preceding paragraphs, the libraries encoded by these methodologies have numerous problems. The 22c trick and small intelligent libraries would appear to improve many of those problems, but practicality becomes an issue when saturating multiple codons, particularly where such codons are contiguous. For example, the number of primers required rapidly increases if two or more residues in close vicinity are targeted using the 22c-trick (27-54 primers are required to saturate 3 positions depending on whether or not both sense and anti-sense primers are needed). Both the numbers and associated synthesis costs soon become unmanageable practically if more residues need to be saturated. Slonomics™ also has a high number of primers involved, though these are handled robotically and can be re-used, as opposed to being specific to each library. In contrast, ProxiMAX would appear to be a favourable compromise in terms of library quality versus complexity of use and again, these primers can be re-used (Table 1.4).

No. of saturated codons	NNN/NNK/Trinucleotide phosphormaidites	22c-trick	Small intelligent libraries	Slonomics	ProxiMAX
3	2-3	27-54	64-128	4160	64
6		729-1458	4096-8192		
9		19683-39366	2.6-5.2x10 ⁶		
12		5.3x10 ⁵ -1.1x10 ⁶	1.7-3.4x10 ⁶		

Table 1.4. Min/max no. of Primers to Saturate Contiguous Codons. NN/NNK/trinucleotide oligonucleotides may be used as a DNA cassette, or as primers in PCR-based mutagenesis; SlonomicsTM and ProxiMAX require a fixed number of oligonucleotides and the numbers of primers for the 22c trick and small-intelligent libraries were calculated using the formulae in the respective publications for saturating consecutive codons.

1.6. Screening Technologies

Whilst the ability to create high quality highly diverse libraries is critical, the ability to screen the libraries shares equal importance as the choice of an inappropriate method can result in a natural bottle-neck in the overall process. As the title of this project suggests, the focus is not solely on creating a randomised library, but to combine both library generation and screening to maximise the efficiency of this process thus increasing the likelihood of developing novel peptides/proteins. In this case the ultimate goal of the thesis is to analyse binding events, hence the approaches described in the following section will relate to this.

1.6.1. *In vivo* Cell-Dependent Display Systems

1.6.1.1. Phage Display

Phage display is the most commonly used method of screening and involves the use of filamentous phage (Smith, 1985). Phage can be split into filamentous, such as M13 phage, or lytic bacteriophage, such as lambda (Beghetto and Gargano, 2011). DNA libraries are engineered into specialist phage vectors (phagemids) where mutant DNA is fused to the coat protein genes, normally PVIII or PIII in the case of filamentous phage or gpV/gpD for lambda phage, allowing the display of foreign peptide after transcription/translation using the host

cellular machinery. Filamentous phage are assembled in the periplasmic space and subsequently secreted making them ideal for the display of small peptides. On the other hand, lambda phage, which are assembled in the cytoplasm prior to cell lysis, are used for the display of larger proteins due to the sensitivity of their tertiary structure to the periplasmic space. The peptide-phage coat protein fusion is subsequently screened using affinity based selection, termed biopanning (Hoess, 2001). An immobilised target is incubated with the phage library allowing binding of suitable targets. This is washed to remove non-specifically bound phage and then enriched, usually by infection of the phage into bacteria and ensuing re-growth. During the biopanning process selective pressures can be introduced to increase the stringency in order to select subpopulations of peptides that best bind the target. However, these conditions are important in order to select the best population as the stringency needs to be high enough to isolate high affinity peptides without diminishing yield (Smith, 1985).

Although phage display has been proven to be the most successful form of display due to its robustness and stability, it does have some limitations as is the case with all cell-dependent display methods. The foremost of these is that phage display can be a laborious and time consuming procedure mainly due to the requirement of transformation in *E.coli*. As a result, due to the inefficiencies of the transformation process the maximum size of a phage library is approximately 10^{10} members although libraries of 10^{12} have been reported (Sidhu et al., 2000). Some foreign proteins have been difficult to display, whilst larger proteins have also had problems with display due to folding and secretion problems (Fernandez-Gacio et al., 2003, Levin and Weiss, 2006).

1.6.1.2. Yeast and Bacterial Cell Surface Display

Both yeast and bacterial display use a similar system to that of phage display where the required library DNA is fused to the coding sequence of a cell wall protein, leading to the expression of the library on the cell surface (Samuelson et al., 2002, Ullman et al., 2011). In the case of yeast surface display, the library can be fused to either α -agglutinin or flocculin

membrane proteins. Yeast display has the advantage of eukaryotic machinery allowing display of mammalian proteins in a native-like state (Gai and Wittrup, 2007). With bacterial cell surface display the peptide can be expressed in both gram-positive and gram-negative bacteria in a fusion with membrane proteins or bacterial flagella (Bessette et al., 2004, Daugherty, 2007). Once display on the surface the peptides can undergo biopanning against a specific immobilised target or in conjunction with cell sorting methods (Rockberg et al., 2008). However the disadvantages of these systems, like that of phage display, are that they rely on transformation so can be laborious and time consuming, whilst affinity maturation can be complicated by the number of other proteins expressed on the cell surface.

1.6.1.3. Baculovirus Display

Baculovirus display can be used to display peptide libraries either on the host cell surface or on budding virions by utilizing the baculovirus to infect eukaryotic cells. The library is fused to the major baculovirus envelope protein gp67 under the transcriptional control of the polyhedron gene promoter (Makela and Oker-Blom, 2008). Cell surface expression can be particularly beneficial for peptides that require post-translational modifications.

1.6.1.4. Lambda Repressor Display

In lambda repressor display both library peptides and target are fused to separate lambda transcription repression monomers within a host cell. Interaction of the library and target promotes dimerization of the monomers which represses transcription of the *toF* immediate-early gene. As a result lysis of the host by the lambda phage is inhibited allowing identification of target binding peptides (Hu et al., 1990).

1.6.2. *In vitro* Cell-Free Display Systems

All cell-free display mechanisms require some method to link the screened phenotype with the encoded genotype. This link can be either covalent or non-covalent as discussed in the following paragraphs.

1.6.2.1. Cell-Free Non-covalent Linkages

1.6.2.1.1. Ribosome Display

Ribosome display was originally developed using an *E.coli* cell lysate for the display of peptides (Mattheakis et al., 1994). In this process a DNA library undergoes *in vitro* transcription/translation where it is transcribed into RNA and subsequently translated using the S30 ribosomal extract from *E.coli*. The ribosome stalls on the mRNA, due to the absence of a termination codon normally required for ribosomal release, resulting in a complex between the ribosome, with the nascent peptide bound, and the encoding mRNA (Mossner and Pluckthun, 2001). This creates a physical linkage between the phenotype (protein) and the genotype (genetic material coding the protein). A C-terminal spacer also prevents steric hindrance from the ribosomal tunnel thus allowing the displayed peptide to fold correctly. The complex is disrupted using EDTA and the released RNA is amplified using reverse-transcription PCR. Ribosome display in both prokaryotic and eukaryotic systems have successfully displayed antibody fragments (Mattheakis et al., 1994, Hanes and Pluckthun, 1997, He et al., 2007, He and Taussig, 1997, Hanes et al., 1999, He and Taussig, 2002) as well as the selection of high affinity peptides (Zahnd et al., 2004) .

However, this system has a couple of major flaws such as its sensitivity to RNase activity and the stability of the mRNA-ribosome-peptide complex. The stability can be improved using lowered temperatures, increased magnesium concentration and chloramphenicol to halt the ribosome (Mattheakis et al., 1994) although these combined changes limit the selective pressures that can be applied. The use of purified transcription and translation

components (PUREsystem (Shimizu et al., 2001, Shimizu et al., 2005)) was shown to improve the recovery of mRNA 395-fold from the selection of an anti-IL-13 scFv.

1.6.2.1.2. CIS Display

CIS display utilises the ability of the bacterial replication initiator protein RepA to bind to DNA. By fusing the peptide library to the RepA gene after *in vitro* transcription/translation, a genotype-phenotype link is created with RepA-peptide fusion and its encoding DNA. Non-binding peptides are washed away and the remaining DNA is eluted and amplified by PCR to form a DNA library ready for the next round of selection. After several rounds of selection recovered DNA is cloned for the identification of individual target binding peptide sequences (Odegrip et al., 2004, Eldridge et al., 2009). The mechanisms of CIS display will be further discussed in chapter 6 (Figure 6.1).

CIS display has successfully been used for the affinity selection of peptide ligands to DO1 and M2 antibodies as well as a non-antibody target lysozyme (Odegrip et al., 2004), with comparable results to those using ribosome and mRNA display. DNA-based systems have the advantage that they are considerably more resilient, than other selection systems, to nucleases and can be generated quickly using normal PCR procedures. Unlike the tight control of parameters that is normally required when using RNA-based display technologies, simplified selection conditions such as no control of divalent cation concentration and the complexes do not require incubation under sterile or ribonuclease-free conditions make DNA-based systems straighter forward to carry out.

The stability of RepA–DNA complexes was demonstrated by incubating *in vitro* expressed C-RepA with an anti-C antibody for 48 h before elution and recovery of associated DNA. No reduction in DNA yield was observed compared with that obtained using standard selection conditions (Odegrip et al., 2004). However it was stated the quality of the library DNA itself is the most variable factor in the technology with the level of deletions and insertions varying from 0-75% depending on the batch used.

1.6.2.1.3. STABLE Display

Streptavidin-biotin linkage in emulsion (STABLE) display requires each molecule of the DNA library to be biotinylated whilst peptides are expressed as streptavidin fusions (Doi et al., 2007). Due to the high affinity between streptavidin and biotin a genotype-phenotype link is created although a capture of efficiency ~1% was reported. Photocleavage of a 2-nitro benzyl linker between the DNA and biotin can aid elution of selected peptide-DNA complexes.

1.6.2.2. Cell-Free Covalent Linkages

1.6.2.2.1. mRNA Display

mRNA display is related to ribosome display, although it differs by to the formation of a covalent link, via puromycin, between the template and protein.

Puromycin mimics amino-acyl tRNA thus covalently binding the nascent peptide as a result of the peptidyl transferase activity of the ribosome (Nemoto et al., 1997, Roberts and Szostak, 1997). Puromycin enters the A site of the ribosome allowing the ribosome, via its peptidyl transferase activity, to move the nascent peptide onto the *O*-methyl tyrosine of puromycin thus covalently linking the library mRNA to its peptide. The RNA is stabilised by forming an RNA/DNA hybrid by using the DNA primer that delivered the puromycin in a reverse transcription step. An efficiency of 10-40% of protein/mRNA coupling has been reported (Wilson et al., 2001, Takahashi et al., 2003, Millward et al., 2007). This has been used in the incorporation of unnatural amino acids (Li et al., 2002) and probing tissue specific mRNA libraries (Hammond et al., 2001). Once again the susceptibility to RNase degradation can be a limiting factor of mRNA display, although the screening ability of much larger libraries is greater when compared with *in vivo* techniques requiring host cell transformation.

1.6.2.2.2. P2A System

The P2A system utilises the expression of the P2A bacteriophage replication initiation protein. A covalent bond formed with the 5' phosphate of its encoding strand is caused by a catalytic tyrosine creating a single stranded nick at the viral origin of replication. A scFv can be fused to the P2A protein thus creating a covalent genotype-phenotype link (Reiersen et al., 2005). Enrichment rates of 14-300-fold have been reported when this system was used to select for tetanus toxin binders, although mis-linking to different genotypes have caused issues with panning results.

1.6.2.2.3. M.HaeIII System

A similar concept to that of the P2A system is the M.HaeIII system, which utilizes the capacity of HaeIII methyltransferase to covalently link DNA. M.HaeIII forms a covalent bond with a fluorinated GGFC recognition sequence fused to the library molecule, thus creating a genotype-phenotype link (Bertschinger and Neri, 2004). However, the production of free M.HaeIII can cause non-specific binding to non-fluorinated recognition sequences in other DNA molecules, thus reducing the efficiency of the process.

1.6.2.3. *In vitro* Compartmentalisation

In vitro compartmentalisation utilises water-in-oil emulsions to simulate the natural compartments of an organism in order to trap DNA and *in vitro* transcription/translation components (Tawfik and Griffiths, 1998). By precisely mixing mineral containing surfactants in water femtolitre droplets with a 1µm diameter can be created, which contain single DNA molecules from a library. By localising the DNA library molecule and expressed peptide the fidelity of the genotype-phenotype link can be improved, although it important to minimise compartment fusion during peptide expression as this can be limitation (Bertschinger and Neri, 2004).



Figure 1.5. Library Display Methods Illustration (taken from (Baxter et al., 2014)). Library display for selection against a target in commonly used library display systems which make use of cellular expression of libraries (top panel) or in vitro cell-free expression (bottom panel). Target of interest, against which libraries are screened, is shown in pink. For the majority of display systems shown, the target is immobilized on a solid support (black dashed lines) via linker (green) and libraries are panned against it in vitro. Library-encoding DNA is shown as a yellow ribbon, or mRNA as a red ribbon, displayed peptide is shown as a light blue oval, with its target-binding site shown as a dark blue triangle. Linker molecules between displayed peptide and the molecule on which it is displayed are shown in grey. Cell walls are shown as yellow rectangles.

1.7. Peptides as Therapeutic Agents

Traditional therapeutic agents fall in to two distinct categories; small molecular weight molecules <500 Da and larger biologics >5000 Da (Craik et al., 2013). Traditionally the use of small molecules was limited to <500 Da in order to favour the bioavailability from oral dosages. With the development of recombinant protein expression and improved protein purification, proteins (>5000 Da), such as insulin and engineered antibodies, became increasingly popular due to their potency and selectivity. The major advantage of highly selective therapeutics is that they tend to greatly reduce non-specific side effects in comparison with small molecules drugs. However due to their increased size and solubility they are not suitable for oral delivery and are rather delivered by either injection or intranasal routes.

With the development of genome screening/proteomics the number of protein-protein interactions (PPIs) is becoming an increasingly important area with more than 320,000 hypothesised and ~39,000 experimentally confirmed (Baxter et al., 2014).

Peptides can potentially fill this 500-5000 Da gap in therapeutics. Peptides are common within the natural world with the identification more than 7000 naturally occurring, ranging in physiological roles from hormones, neurotransmitters, growth factors ion channels or antimicrobial agents (Padhi et al., 2014, Buchwald et al., 2014, Giordano et al., 2014, Robinson et al., 2014). Their larger sizes and secondary structures allow more interaction with the target thus conferring increased specificity with fewer potential side effects when compared to the small molecule drugs. There are more than one hundred peptide based drugs currently on the market with the majority of them consisting of 8-10 amino acids although they also go up to 45 amino acids long (Craik et al., 2013). Currently the majority of peptides-based therapeutics are administered via injection although developments in peptide modification, such as cyclization, *N*-Methylation and intramolecular hydrogen bonds, allows the peptide to retain bioactivity while improve bioavailability to the extent where they are becoming favourable as therapeutics for oral delivery (Diao and Meibohm, 2013).

Conventionally peptides have been unsuitable for oral delivery due acidic and enzymatic degradation in the gastrointestinal tract.

1.8. Nerve Growth Factor (NGF)

Nerve growth factor (NGF), the target protein of the current study, was first described over 60 years ago by Levi-Montalcini & Hamburger (Levi-Montalcini and Hamburger, 1951) and is the founding member of the neurotrophin family. The neurotrophin family plays a critical role in controlling the development and survival of neuronal populations in the central and peripheral nervous system (Snider, 1994, Aloe et al., 1997). Neurotrophins act upon two classes of receptors; the high affinity Trk receptors, and the low affinity p75 neurotrophic receptor (p75^{NTR}) (Yano and Chao, 2000).

1.8.1. NGF Structure

The neurotrophin family, which includes brain-derived neurotrophic factors (BDNF), neurotrophin-3 (NT-3), neurotrophin-4/5 (NT-4/5) and neurotrophin-6 (Nt-6), all share sequence homology with approximately 50% conservation (Wiesmann and De Vos, 2001). The NGF gene is located on human chromosome 1 (Edwards et al., 1988), and like most other members of neurotrophin family, biologically active NGF consists of a homo-dimer of two NGF monomers. The structure of NGF was shown to consist of a novel protein fold (McDonald et al., 1991) where the monomeric form of NGF contains 2 pairs of anti-parallel β -pleated strands with three loop structures at one end (Bradshaw et al., 1994) and a cysteine knot at the other (Figure 1.6 ref (Wiesmann and De Vos, 2001)). The cysteine knot consists of three disulfide bonds, two of which form a closed ring with the third disulfide bond penetrating the ring. This confers stability to the molecule and has been found in other dimeric growth factors, such as platelet-derived growth factor and transforming growth factor- β , which do not share any other significant sequence homology with the neurotrophin family.

NGF, and the wider neurotrophin family, forms a parallel homo-dimer with an elongated core formed by the central β sheets Figure 1.7 (Wiesmann and De Vos, 2001).



Figure 1.6. NGF Structure (taken from (Wiesmann and De Vos, 2001)). Ribbon diagram depicting the structure of the NGF monomer (PDB code 1BFT). The secondary structure elements are labelled and depicted according to McDonald *et al.* The termini as well as the loop regions, L1-L4, are labelled in red, and the cysteine residues forming the cysteine-knot motif near the top of the molecule are shown in grey and yellow in ball-and-stick rendering.



Figure 1.7. NGF Dimerization (taken from (Wiesmann and De Vos, 2001)). Ribbon diagrams of experimentally determined neurotrophin dimers. The secondary structure elements are depicted as determined with option 'molauto' in program Molscript 2 (Kraulis, 1991). All N and C termini are labelled; unlabelled ends are due to disordered segments in the crystal structures. In all cases, the monomers dimerize in parallel fashion, positioning the N and C termini at the same end of the molecule (top in this figure). Loops important for p75^{NTR} binding (L1, L3, L4) or Trk specificity (L2, L4) are labelled. NGF dimers (left: unbound NGF, PDB access code 1BET; right: NGF from the complex with the second Ig-like domain of its TrkA receptor, PDB access code 1WWW).

1.8.2. NGF Receptors

NGF acts upon two receptors; TrkA (part of the Trk family of receptor tyrosine kinases) and p75^{NTR}. The Trk family share sequence homology and generally consist of an cysteine rich extracellular domain (domain 1), three leucine rich repeats (domain 2), another cysteine rich cluster (domain 3) and two immunoglobulin (Ig)-like domains (domains 4 and 5) (Schneider and Schweiger, 1991). The extracellular domain and intracellular kinase domain are linked by a single transmembrane helix. A sequence homology of >75% is observed for the intracellular kinase domain (Chao, 1992) whilst the extracellular domain show sequence conservation of 50-55% (Lamballe et al., 1991). Domain 5 of the Trk family, which includes the EF loop, shows the most highly conserved regions with 9, of 11, identical residues (Ultsch et al., 1999). Whilst NGF is specific to TrkA, TrkB is the receptor for BDNF and NT-4 whereas TrkC is the receptor for NT-3 (Kaplan and Miller, 1997), although NT-3 does also activate TrkA albeit at significantly higher concentrations than NGF.

There are two isoforms of TrkA that differ from one another by an additional 6 amino acids near the transmembrane domain in their extracellular domain, with the additional insert appearing to relax TrkA specificity resulting in enhanced NT-3 mediated signaling (Clary and Reichardt, 1994). NGF-TrkA binding results in autophosphorylation that can lead to phosphorylation-dependent recruitment sites for adaptor molecules and enzymes that mediate cytosolic/endosomal pathways such as the Ras-mitogen activated protein kinase (MAPK), extracellular signal-regulated kinase (ETK), phosphatidylinositol 3-kinase (PI3K)-Akt and Phospholipase C (PLC)- γ (Aloe et al., 2012).

The second receptor for NGF is p75^{NTR}, which is as transmembrane glycoprotein that shows equivalent binding to all members of the neurotrophin family at approximately nanomolar levels (Hallböök et al., 1991). The cytoplasmic domain of p75^{NTR} contains a death domain, consisting of six α helices, that shares sequence homology to those found in other apoptosis inducing factors. The extracellular domain of p75^{NTR} contains four cysteine rich domains that is consistent to the tumor necrosis factor receptor family (Iacarusio et al., 2011). These receptors tend to have a variable number of cysteine rich repeats containing three disulfide

bonds, which when in complex with their ligand they bind along a groove formed by two of their subunits (Naismith and Sprang, 1998). The cell mediated effect of NGF-p75^{NTR} binding is dependent on the presence or absence of TrkA. If TrkA is not present, NGF-p75^{NTR} binding will lead to apoptosis (Frade et al., 1996) whereas NGF- p75^{NTR} binding in the presence of TrkA will increase the binding affinity of NGF to TrkA which in turn promotes survival (Meldolesi et al., 2000).

1.8.3. NGF-Receptor Interaction

NGF engages the second Ig-like domain (domain 5) of TrkA through two distinct patches. The crystal structure of NGF-TrkA-d5 was described by Wiesmann *et al.* (Wiesmann et al., 1999) and showed that the NGF dimer bound to two copies of TrkA domain 5 through its central β sheet region (Figure 1.8). TrkA-d5 contacts NGF through its C-terminal pole with the cysteine knot, N and C termini at the top of the molecule, leaving the residues important in the binding of p75^{NTR} exposed. This backs up the hypothesis that NGF can bind TrkA and p75^{NTR} simultaneously. As mentioned above, two distinct patches termed the 'specificity patch' and the 'conserved patch' are required for NGF-TrkA binding, and consist of the N-terminus of NGF in contact with the ABED sheet of TrkA-d5 and residues from the central β sheet of NGF and loops AB, C'D and EF of TrkA-d5 respectively (Wiesmann et al., 1999). The 'specificity patch' shows low sequence homology with other neurotrophins and is thought to be specific for NGF-TrkA, whereas the 'conserved patch' features conserved residues in comparison with other neurotrophin and Trk receptors.

In its unbound state the residues involved in the 'specificity patch' are disordered, however when bound to TrkA these residues at the N-terminal of each NGF monomer form a short segment of helix that packs against the receptor. The sidechain of Ile6, the central hydrophobic residue in the patch, penetrates into a hydrophobic pocket of the ABED sheet and at the bottom of the pocket is a solvent exposed free domain of a disulfide bridge. This disulfide is conserved across all Trk receptors, however in TrkB this pocket is more hydrophilic whilst in TrkC the pocket is absent completely (Ultsch et al., 1999). The

importance of this patch for the activity of NGF is demonstrated by the removal of 10 residues from NGF causing a 300-fold drop in TrkA affinity (Kahle et al., 1992), whilst a 9-fold decrease in TrkA affinity is caused the truncation of the first five N-terminal residues (Shih et al., 1994).

Unlike the 'specificity patch', the 'conserved patch' involves residues from both NGF subunits, which are in contact with the AB, C'D, and EF loops at the C-terminal pole of TrkA-d5 (Wiesmann et al., 1999). The patch is formed by the NGF surface residues Trp21, Ile32, Phe54 and Phe86, whose sidechains pack against residues in the EF loop of TrkA.



Figure 1.8. NGF-TrkA-d5 Structure (taken from (Wiesmann et al., 1999)). Overall structure of the complex. **a, b**, Two orientations related by a rotation of 90° about the horizontal axis. The NGF monomers are red and blue; TrkA-d5 is green. The termini, some relevant loops and the secondary structure elements are labelled. In **a**, loops L2 and L4 of NGF and the C-terminus of TrkA-d5 (residue 382) point towards the membrane.

The binding site of NGF to p75^{NTR} has been interpreted from binding studies using neurotrophin mutants. As a result of these studies, two spatially distinct regions have been identified on the surface of NGF. The first of these regions involves residues from the L3 loop and C-terminal tail of NGF and is mainly composed of residues with a positive charge. The

identification of this patch was the result of alanine scanning experiments on NT-3 resulted in a 100-fold decrease in p75^{NTR} affinity (Urfer et al., 1994, Rydén and Ibáñez, 1997).

The second patch involved in NGF binding of p75^{NTR} is formed from positively charged residues from L1 and L4 loops. Alanine substitution of Lys32 Lys34 or Lys95 in NGF resulted in a significant decrease p75^{NTR} affinity (Ibáñez et al., 1992) whilst triple alanine substitutions of Lys32 Lys34 or Glu35 showed no reduction in TrkA binding (Rydén et al., 1997).

1.8.4. Clinical Use of Anti-NGF Therapy

NGF-TrkA binding on nociceptive neurons activates phospholipase C which results in sensitisation of TRPV1, a non-selective ligand-gated channel that generates the action potential resulting in pain signal transmission (Winston et al., 2001, Ji et al., 2002). NGF also increases TRPV1 expression and its trafficking to the plasma membrane (Ji et al., 2002, Stein et al., 2006).

Increased levels of NGF have been implicated in a number of pain states, including inflammatory and neuropathic pain states (Sevcik et al., 2005), neurogenic overactive bladder and interstitial cystitis (Lowe et al., 1997, Oddiah et al., 1998), prostatitis (Miller et al., 2002), asthma (Watson et al., 2006) and cancer-induced bone pain (Jimenez-Andrade et al., 2011). The most common intervention strategies to date in this area involve blocking the NGF molecule, so preventing its association with TrkA. To this end, an anti-TrkA monoclonal antibody was shown to inhibit the perception of pain in both inflammatory and neuropathic pain models (Ugolini et al., 2007).

The administration anti-NGF antibodies has also shown good analgesic effect in a number of animal models for human disease, such as fracture pain (Koewler et al., 2007), cancer pain (Mantyh et al., 2010), pancreatic pain (Zhu et al., 2011) and arthritic joint pain (Ghilardi et al., 2012). Of these anti-NGF antibodies, Tanzeumab has probably been the most successful. It is a humanized IgG₂ monoclonal antibody that binds with high affinity and specificity to NGF (Abdiche et al., 2008), and is now used as a treatment for osteoarthritis.

The development of novel anti-NGF peptides, as an alternative to antibody therapy, to inhibit the the NGF/TrkA interaction would be an extremely useful addition to the existing arsenal of pain-modulating therapies and is thus the ultimate target of this study.

1.9. Project Outline

Therefore, this project aims to combine optimised peptide library generation (using ProxiMAX randomisation) with CIS display to produce and screen a randomised library based on two anti-NGF peptides, which bind NGF, previously-developed by Isogenica Ltd. Isogenica's original anti-NGF peptides were hypothesised to have a helical structure and to dimerize through cysteine residues present at their C-termini. To further develop these peptides, this project aimed to develop high affinity monomeric (rather than dimeric) peptide(s) based around the same binding motif. The binding affinity of the selected peptides would then be screened (CIS display) using NGF-binding as the selection criterion with the hypothesis that NGF-binding might inhibit the NGF-TrkA interaction in a manner analogous to that of the antibody Tanzeumab. This hypothesis was tested by assessing the peptide'(s) ability to disrupt the NGF-TrkA interaction using an NGF-TrkA inhibition ELISA.

Chapter 2

Materials and Methods

2. Chapter 2: Materials and Methods

2.1. Materials

2.1.1. Media Recipes

2.1.1.1. Antibiotic selective LB agar

LB Broth Powder (Sigma-Aldrich)	2% w/v
Bacto Agar (DIFCO)	2% w/v

Dry ingredients were dissolved in ddH₂O and sterilised by autoclaving at 121°C for 20 minutes. Solutions were left to cool to approximately 50°C and 50-100 µg/ml sterile antibiotic solution was added as required.

2.1.2. Broth Recipes

2.1.2.1. LB

LB Broth Powder (Sigma-Aldrich)	2% w/v
---------------------------------	--------

Powder was dissolved in ddH₂O and sterilised by autoclaving at 121°C for 20 minutes. It was left to cool to approximately 50°C and 50-100 µg/ml sterile antibiotic solution was added as required.

2.1.2.2. 2TY

2TY Powder (Invitrogen)	3.1% w/v
Glucose	2% w/v

Powder was dissolved in ddH₂O and sterilised by autoclaving at 121°C for 20 minutes. It was left to cool to approximately 50°C and 50-100 µg/ml sterile antibiotic solution was added as required.

2.1.2.3. S.O.C Medium (Invitrogen)

Tryptone	2% w/v
Yeast Extract	0.5% w/v
NaCl	0.01 M
KCl	0.0025 M
MgCl ₂	0.01 M
MgSO ₄	0.01 M
Glucose	0.02 M

2.1.3. Buffer Recipes

2.1.3.1. TBE (1x)

Tris(hydroxymethyl)aminomethane	0.089 M
Boric Acid	0.089 M
EDTA solution (pH 8.0)	0.002 M

2.1.3.2. TAE (1x)

Tris(hydroxymethyl)aminomethane	0.04 M
Glacial acetic acid	0.04 M
EDTA solution (pH 8.0)	0.001 M

2.1.3.3. SDS Tris-Glycine Running Buffer (1x)

Tris base	0.025 M
Glycine	0.192 M

Sodium dodecyl sulfate	0.1% w/v
------------------------	----------

2.1.3.4. NuPAGE® MES SDS Running Buffer (1x) pH 7.3

2-(<i>N</i> -morpholino)ethanesulfonic acid	0.05 M
Tris base	0.05 M
Sodium dodecyl sulfate	0.1% w/v
EDTA	0.01 M

2.1.3.5. Blue/orange Loading Buffer

Orange g	0.4%
Bromophenol blue	0.03%
Xylene cyanol FF	0.03%
Ficoll® 400	15%
Tris-HCl (pH 7.5)	0.01 M
EDTA (pH 8.0)	0.05 M

2.1.3.6. Bromophenol Blue Loading Dye

Tris-HCl (pH 7.6)	0.01 M
Bromophenol Blue	0.03%
Xylene cyanol FF	0.03%
Glycerol	60%
EDTA	0.06 M

2.1.3.7. NEB 6x Gel Loading Dye, Blue

Ficoll® 400	15%
EDTA	0.066 M
Tris-HCl (pH 8.0)	0.0198 M
SDS	0.102%
Bromophenol Blue	0.09%

2.1.3.8. SDS-PAGE Sample Buffer (1x)

Tris-HCl (pH 6.8)	0.0625 M
Glycerol (100%)	10% v/v
B-mercaptoethanol	2% v/v
Bromophenol Blue	0.1% w/v
Sodium dodecyl sulfate	2% w/v

2.1.3.9. TE Buffer

Tris-HCl (pH 7.5)	0.01 M
EDTA (pH 8.0)	0.001 M

2.1.3.10. NEB T4 DNA Ligase Buffer (1x)

Tris-HCl (pH 7.5)	0.05 M
MgCl ₂	0.01 M
Dithiothreitol	0.01 M
ATP	0.001M

2.1.3.11. Thermo Scientific Ligase Buffer (1x)

Tris-HCl	0.04 M
MgCl ₂	0.01 M
Dithiothreitol	0.01 M
ATP	0.0005 M

2.1.3.12. NEB Taq DNA Polymerase Buffer (1x)

Tris-HCL	0.01 M
KCl	0.05 M

MgCl ₂	0.0015 M
-------------------	----------

2.1.3.13. NEB ThermoPol Buffer (1x)

Tris-HCl	0.02 M
(NH ₄) ₂ SO ₄	0.01 M
KCl	0.01 M
MgSO ₄	0.002 M
Triton®X-100	0.1% v/v
pH 8.8 at 25°C	

2.1.3.14. Promega Pfu Polymerase Buffer (1x)

Tris-HCl (pH 8.8)	0.02 M
KCl	0.01 M
(NH ₄) ₂ SO ₄	0.01 M
MgSO ₄	0.002 M
Triton®X-100	0.1%
BSA	0.1 mg/ml

2.1.3.15. Thermo Scientific Pfu Buffer

Tris-HCl (pH 8.8)	0.2 M
(NH ₄) ₂ SO ₄	0.1 M
KCl	0.1 M
BSA	1 mg/ml
Triton X-100	1% (v/v)

2.1.3.16. NEB Buffer 2 (1x)

Tris-HCl (pH 7.5)	0.01 M
NaCl	0.05 M

MgCl ₂	0.01 M
Dithiothreitol	0.001 M

2.1.3.17. NEB Buffer 4 (1x)

Potassium acetate	0.005 M
Tris-acetate	0.002 M
Magnesium acetate	0.001 M
Dithiothreitol	0.0001 M

2.1.3.18. NEB T4 PNK Buffer (1x)

Tris-HCl (pH 7.6)	0.07 M
MgCl ₂	0.01 M
Dithiothreitol	0.0005 M

2.1.3.19. Antarctic Phosphatase Buffer (1x)

Bis-Tris-Propane-HCl	0.05 M
MgCl ₂	0.0010 M
ZnCl ₂	0.0001 M

2.1.3.20. Protein Expression and Purification Buffers

2.1.3.20.1. Lysis Buffer (pH 8.0)

NaH ₂ PO ₄	0.05 M
NaCl	0.3 M
Imidazole	0.01 M

2.1.3.20.2. Denaturing Lysis Buffer (pH 8.0)

Urea	8 M
NaH ₂ PO ₄	0.1 M
Tris-HCl	0.01 M
β-Mercaptoethanol	0.005 M

2.1.3.20.3. Native Column Wash Buffer (pH 8.0)

NaH ₂ PO ₄	0.05 M
NaCl	0.3 M
Imidazole	0.02 M

2.1.3.20.4. Native Column Elution Buffer (pH 8.0)

NaH ₂ PO ₄	0.05 M
NaCl	0.3 M
Imidazole	0.25 M

2.1.3.20.5. Denaturing Column Wash Buffer (pH 6.3)

Urea	8 M
NaH ₂ PO ₄	0.1 M
Tris-HCl	0.01 M
β-Mercaptoethanol	0.005 M

2.1.3.20.6. Denaturing Column Elution Buffer 1 (pH 5.9)

Urea	8 M
NaH ₂ PO ₄	0.1 M
Tris-HCl	0.01 M
β-Mercaptoethanol	0.005 M

2.1.3.20.7. Denaturing Column Elution Buffer 2 (pH 4.5)

Urea	8 M
NaH ₂ PO ₄	0.1 M
Tris-HCl	0.01 M
β-Mercaptoethanol	0.005 M

2.1.3.20.8. Solubilisation Buffer (pH8.0)

Urea	8 M
NaH ₂ PO ₄	0.1 M
Tris-HCl	0.01 M
β-Mercaptoethanol	0.005 M

2.1.3.20.9. Refolding buffer

NaH ₂ PO ₄	0.1 M
L-Arginine	0.1 M
Glutathione (reduced)	0.005 M
Glutathione (oxidised)	0.0005 M

2.1.3.20.10. Native Dilution Elution Buffer (pH 8.0)

NaH ₂ PO ₄	0.05 M
NaCl	0.3 M

2.1.3.20.11. SUMO Protease –Salt (1x)

Tris-HCl (pH8.0)	0.05 M
Igepal (NP-40)	0.2% v/v
Dithiothreitol	0.001 M

2.1.4. Other Solutions

2.1.4.1. Thermo Scientific PEG 4000 Solution

Polyethylene glycol 50% w/v

2.1.4.2. ATP

ATP solutions were prepared using 100 mM stock solution (Bioline) and sterile double distilled H₂O.

2.1.4.3. dNTPs

dNTP solutions were prepared using 100 mM stock solution (Bioline) and sterile double distilled H₂O and then mixed at an equimolar concentration.

2.1.4.4. X-Gal (5-Bromo-4-Chloro-3 indolyl-β-D-galactopyranoside)

X-Gal (5-Bromo-4-Chloro-3 indolyl-β-D-galactopyranoside) was as purchased a 50 mg/ml solution in DMF from Promega (UK). This was diluted down with DMF to a concentration of 20 mg/ml and subsequently stored at -20°C.

2.1.4.5. Ampicillin Solution

Stock solutions with a final concentration 50 mg/ml were prepared using ampicillin sodium salt (Sigma-Aldrich-Aldrich) and double distilled water. It was filter sterilised and stored at -20°C.

2.1.4.6. Kanamycin Solution

Stock solutions with a final concentration 50 mg/ml were prepared using ampicillin sodium salt (Sigma-Aldrich) and double distilled water. It was filter sterilised and stored at -20°C.

2.1.4.7. IPTG (Isopropyl β -D-1-thiogalactopyranoside)

IPTG was dissolved in ddH₂O to make a final concentration of 1 M. It was filter sterilised and stored at -20°C.

2.1.4.8. Lysozyme (Thermo Scientific)

Lysozyme 0.2 mg/ml

Lysozyme (Thermo Scientific) was reconstituted in double distilled water to a concentration of 0.2 mg/ml

2.1.4.9. 10% Ammonium Persulfate

Ammonium Persulfate (Sigma-Aldrich) 10% w/v

2.1.4.10. 20% Sodium Dodecyl Sulfate

Sodium Dodecyl Sulfate (Sigma-Aldrich) 20% w/v

2.1.4.11. CaCl₂ Solution

CaCl₂ stock solution was dissolved ddH₂O to make a final concentration of 1 M and sterilised by autoclaving.

2.1.5. Cell Lines

2.1.5.1. *E.coli* DH5 α Genotype

(F- Φ 80lacZ Δ M15 Δ (lacZYA-argF) U169 recA1 endA1 hsdR17 (rk-, mk+) phoA supE44 λ - thi-1 gyrA96 relA1).

2.1.5.2. One Shot $^{\circledR}$ Mach1 $^{\text{TM}}$ -T1R Genotype

F- Φ 80lacZ Δ M15 Δ lacX74 hsdR(rK- mK +) Δ recA1398 endA1 tonA

2.1.5.3. *E.coli* SHuffle $^{\circledR}$ Genotype

F' lac, pro, lacI^q / Δ (ara-leu)7697 araD139 fhuA2 lacZ::T7 gene1 Δ (phoA)PvuII phoR ahpC* galE (or U) galK latt::pNEB3-r1-cDsbC (SpecR, lacI^q) Δ trxB rpsL150(StrR) Δ gor Δ (malF)3

2.1.5.4. *E.coli* BL21 (DE3) Genotype

F- *ompT* hsdSB (rB-mB-) gal dcm (DE3)

2.1.5.5. *E.coli* TG1

F'[traD36 lacI^q Δ (lacZ) M15 proA⁺B⁺] glnV (supE) thi-1 Δ (mcrB-hsdSM)5 (r_k⁻ m_k⁻ McrB⁻) thi Δ (lac-proAB)

2.1.6. Vectors

2.1.6.1. *Sma*I-phosphatased pUC19

*Sma*I-phosphatased pUC19 was purchased from Thermo Scientific (formerly Fermentas).

2.1.6.2. pJ434-NGF_optEc

The plasmid pJ434 containing the synthetic gene for NGF expression, optimised for expression in *E.coli*, was purchased from DNA 2.0.

2.1.6.3. pET SUMO

The plasmid pET SUMO was purchased from Invitrogen as part of the Champion™ pET SUMO Expression System.

2.2. Methods

2.2.1. Enzyme Dependent Reactions

2.2.1.1. Phosphorylation Reactions

Unless otherwise stated, phosphorylation reactions were carried out in 1x PNK buffer (2.1.3.18), 1 mM ATP (2.1.4.2), with 5 units *T4 PNK* (NEB) and up to 300 pmol of DNA. The reaction was incubated at 37°C for 30 minutes and the enzyme was then heat inactivated at 65°C for 20 minutes.

2.2.1.2. Filling-in Reactions

Unless otherwise stated ligation reactions were carried out in 1x NEB buffer 2 (2.1.3.16) with 5 units *DNA Polymerase I, Large (Klenow) Fragment* (NEB), 1 mM dNTPs. This reaction was incubated at 37°C for 30 min followed by 65°C for 20 min.

2.2.1.3. Ligations

Unless otherwise stated ligation reactions were carried out in 1x ligase buffer (2.1.3.10 or 2.1.3.11) with 1 unit of *T4 DNA ligase* (NEB or Thermo Scientific) in 20 µl volumes. These contained 50-100 ng of the appropriate vector and 3-fold molar excess of insert DNA. Cohesive end ligations were incubated at 22°C for 15-120 minutes, whilst 16°C for 12-16 hours was used for blunt ended ligations. The enzyme was then heat inactivated at 65°C for 10 minutes.

2.2.1.4. Polymerase Chain Reaction (PCR) Reactions

Unless otherwise stated, PCR reactions were carried out in 1x appropriate buffer (2.1.3.122.1.3.13), 100 µM dNTPs (2.1.4.3), 1.5 mM MgCl₂ (if not in the PCR buffer), the appropriate forward and reverse primers (Eurofins Genomics) and 1 pg - 1 ng of DNA. Enzyme concentrations varied depending on the manufacturers recommendations. PCR reactions were carried out under a standard PCR cycle 30 cycles of (95°C, 30s; 55°C, 30s; 72°C, 1 min).

2.2.1.5. Restriction Digest Reactions

Unless otherwise stated restriction digests were performed in 1x appropriated buffer (2.1.3.16 or 2.1.3.17) and, if required, supplemented with BSA to a final concentration of 0.1 µg/ µl to prevent enzyme star activity. DNA and enzyme concentrations varied depending on the manufacturers recommendations.

2.2.1.6. Dephosphorylation Reactions

Dephosphorylation reactions were performed using 1x antarctic phosphatase buffer (2.1.3.19) with 1-5 µg of DNA and 5 units of Antarctic Phosphatase. This was incubated at 37°C for 15 minutes and heat inactivated at 70°C for 5 minutes.

2.2.2. ProxiMAX Procedure

2.2.2.1. Original Oligonucleotide Hybridisation

Complementary pairs of 'MAX' oligonucleotides (Table 2.1 and Table 2.2; MAX_{R1} – MAX_{R6} and MAX_{RC}) and base sequences (synthesised by Eurofins Genomics) were mixed together, at 10 µM final individual concentrations in H₂O. These were then hybridised by incubating at 94°C for 5 minutes followed by cooling at 1°C per min to 4°C. The concentration of the hybridised oligonucleotides was then measured using the PicoGreen® assay (Life technologies) and the concentration adjusted to 1 µM.

Oligo Name	Sequence
Base	5' - PHO - ATCCGATCCTAGTGTATTCTTCGCTGTTCTCTGACTGAT - 3'
Base _{RC}	5' - ATCAGTCAGAGAACAGCGAAGAATACTAGGATCGGAT - 3'
MAX _{Fwd R1}	5' - GTGCTACGATGTCATTGCGAGTCACGT MAX - 3'
MAX _{Fwd R2}	5' - AGGTAGATCAGTGACACGGAGTCACGT MAX - 3'
MAX _{Fwd R3}	5' - ACAGAACAGGCACTTAGGGAGTCACGT MAX - 3'
MAX _{Fwd R4}	5' - GATCTCACAGTCAGATGGGAGTCACGT MAX - 3'
MAX _{Fwd R5}	5' - TTCGACAGTAGCATCTCGGAGTCACGT MAX - 3'
MAX _{Fwd R6}	5' - ATCGACCGTAACTTGAGCGAGTCACGT MAX - 3'
MAX _{RC}	5' - (MAX) _{RC} TACGTGACTC - 3'
Base (rev) primer	5' - ATCAGTCAGAGAACAGCG - 3'
Primer 1	5' - GTGCTACGATGTCATTGC - 3'
Primer 2	5' - AGGTAGATCAGTGACACG - 3'
Primer 3	5' - ACAGAACAGGCACTTAGG - 3'
Primer 4	5' - GATCTCACAGTCAGATGG - 3'
Primer 5	5' - TTCGACAGTAGCATCTCG - 3'
Primer 6	5' - ATCGACCGTAACTTGAGC - 3'

Table 2.1. Single Reaction Ligation MAX Oligonucleotide Sequences. Sequences for the forward and reverse MAX oligonucleotides, base oligonucleotides and the appropriate cycle primers. The annotation 'MAX' refers to the randomised MAX codons whose sequences are highlighted in Table 2.3.

Oligo Name	Sequence
Base	5' PHO- CATAGATCCAGCCATCGCACAGTCTAGTACGCCTCAAACCTCTCATCCCCGACCATCGCACAGTCTACATT-3'
Base _{RC}	5' -AATGTAGACTGTGCGATGGTTCGGGATGAGAGTTTGAGGCGTACTAGACTGTGCGATGGCTGGATCTATG-3'
MAX _{Fwd R1}	5' -GGTCGCAATACAGTAACGGAGTCGTCAT MAX -3'
MAX _{Fwd R2}	5' -AGGTCAGACATCGGTGCGGAGTCGTCAT MAX -3'
MAX _{Fwd R3}	5' -GCCACTTCCGATTACGCCGAGTCGTCAT MAX -3'
MAX _{Fwd R4}	5' -TCACCAATGAGTTGCCTGGAGTCGTCAT MAX -3'
MAX _{Fwd R5}	5' -TACACCTGAGCGATAAAGCGAGTCGTCAT MAX -3'
MAX _{Fwd R6}	5' -CATTCTGTGATCTCTGCCGAGTCGTCAT MAX -3'
MAX _{RC}	5' - (MAX) _{RC} ATGACGACTC-3'
Base (rev) primer	5' -AATGTAGACTGTGCGATG-3'
Fwd Primer1	5' -GGTCGCAATACAGTAACG-3'
Fwd Primer2	5' -AGGTCAGACATCGGTGCG-3'
Fwd Primer3	5' -GCCACTTCCGATTACGCC-3'
Fwd Primer4	5' -TCACCAATGAGTTGCCTG-3'
Fwd Primer5	5' -TACACCTGAGCGATAAAGC-3'
Fwd Primer6	5' -CATTCTGTGATCTCTGCC-3'

Table 2.2 Re-designed Single Reaction Ligation MAX Oligonucleotide Sequences. Re-designed sequences for the forward and reverse MAX oligonucleotides, base oligonucleotides and the appropriate cycle primers. The annotation 'MAX' refers to the randomised MAX codons whose sequences are highlighted in Table 2.3.

Codon	Sequence
A	GCG
C	TGC
D	GAC
E	GAA
F	TTT
G	GGC
H	CAT
I	ATT
K	AAA
L	TTA
M	ATG
N	AAC
P	CCG
Q	CAG
R	CGT
S	TCT
T	ACC
V	GTG
W	TGG
Y	TAT

Table 2.3 Single Reaction Ligation Library MAX Codon Identity. Identity of the MAX codons located at the 3' end of the MAX oligonucleotide used for the single reaction ligation library.

2.2.2.2. PicoGreen® Assay

Where dsDNA concentration was assessed, the concentration of each oligonucleotide pair was measured in triplicate, against λ DNA standards, using PicoGreen® reagent (Life technologies). Lambda DNA was diluted 300x in TE buffer (2.1.3.9) to a concentration of 1ng/ μ l, and subsequently serially diluted down to 0.2 ng/ μ l. A sample of each oligonucleotide was diluted 50x, and Picogreen reagent 200x with TE buffer (2.1.3.9). Diluted oligonucleotide (45 μ l) was mixed with 45 μ l of diluted picogreen reagent and applied to a 96 well plate in triplicate. Fluorescence was measured on a SpectraMAX Gemini EM microplate fluorimeter (Molecular Devices), with excitation and emission wavelengths of 480 nm and 520 nm respectively. Concentrations of dsDNA were calculated using the linear regression formula generated from the standard curve.

2.2.2.3. Oligonucleotide Sequencing

To ensure that the sequences were correct and that the MAX codons were intact, a sample of oligonucleotides were sequenced. Samples of the oligonucleotides were phosphorylated and blunt-ended in a 50 μ l reaction containing; 25 μ l hybridised oligonucleotide, 1 mM dNTPs, 10 mM ATP, 10 x PNK buffer, 5 units *Klenow* fragment (NEB), and 5 units *T4 Polynucleotide Kinase* (NEB) incubated at 37°C for 30 min and then 65°C for 20 min. After this, 4 ng of the phosphorylated/blunt-ended oligonucleotides were ligated into pUC19 in a 20 μ l reaction containing; 1x ligase buffer, 20 ng pUC19 DNA/*Sma*I (Thermo Scientific) and 1 unit T4 DNA ligase (NEB; 400 cohesive end units), and incubated at 16°C for 18 hours and 65°C for 20 min. Twenty μ l of the ligation were transformed into competent *E.coli* DH5 α and screened using ampicillin resistance and blue/white screening. Samples of positive colonies were taken and amplified using colony PCR in a 20 μ l reaction containing; 1x Taq polymerase buffer, 100 μ M dNTPs, 50 pmol pUC19 forward and reverse primers and 1 unit Taq polymerase. These underwent PCR with cycle conditions: 2 min at 95°C, followed by 30 cycles of (95°C, 30s; 55°C, 30s; 72°C, 1 min). These were electrophoresed on a 2% agarose/TAE gel to check for successful amplification. One μ l of colony PCR product was

added to a 10 µl reaction containing 3.2 pmol of a pUC19 forward primer, and sent for sequencing at the Functional Genomics and Proteomics Unit (University of Birmingham).

2.2.2.4. Original ProxiMAX Oligonucleotide Ligation

Appropriate 1 µM hybridised oligonucleotide stocks (i.e Round 1 oligonucleotide pairs for cycle 1) were combined together to form an equimolar mixture. Ten pmol of this mixture of oligonucleotide pairs was ligated to 3.3 pmol of base sequence, in a 20 µl reaction containing 1x NEB buffer 2, 1mM ATP, 5 units *Nt.Afl* (NEB) and 1 µl *T4 DNA ligase* (NEB; 400 cohesive end units). The reaction was incubated at room temperature for 2 hours followed by 37°C for 30 minutes.

2.2.2.5. Original ProxiMAX Oligonucleotide PCR

The template was serially diluted to 1/10, 1/100 and 1/1000 and duplicate 100 µl amplifications were set up. These contained 50 pmol primers (the appropriate cycle primer and a universal primer for the base sequence), 100 µM dNTPs, 1 unit *Pfu* DNA polymerase (Promega), 1x *Pfu* buffer and 1 µl of the diluted template. These underwent PCR with cycle conditions: 2 min at 95°C, followed by 30 cycles of (95°C, 30s; 54°C, 30s; 72°C, 1 min). The two PCR reactions were then combined and processed using a MinElute PCR Purification Kit (Qiagen) according to manufacturer's instructions.

2.2.2.6. Original ProxiMAX Oligonucleotide Digestion

MinElute-purified DNA was re-suspended in 30 µl H₂O, with 25 µl digested in a 50 µl reaction containing 1x fast digest buffer and 10 units *MlyI* (Thermo Scientific). The reaction was incubated at 37°C for 1 hr and then 65°C for 20 min, and the resulting product was electrophoresed on a 3% agarose/TAE gel to check the digestion was successful. Undigested material was retained for later examination. The concentration of the digested product was

then measured using a Nanodrop 2000c (Thermo Scientific), and the volume required for ~3.3 pmol was calculated. The process was then repeated using the next set of oligonucleotide pairs and primer (R2 and primer 2 for cycle 2, etc.), but using the digested cycle 1 product rather than the original base sequence. Reiteration employed the next set of oligonucleotides as indicated in Table 2.1, Table 2.2 and Table 2.6 for each cycle.

2.2.2.7. MiSEQ Tagging Reaction

Finished library products were amplified by PCR with the reaction containing 10 pmol MiSEQ primers (Table 2.4 and Table 2.5), 100 μ M dNTPs, 1 unit *Pfu* DNA polymerase (Promega) or 1 unit *Phusion HSII* (Thermo Scientific) and 1 x *Pfu* buffer or 1x HF buffer. These underwent PCR with cycle conditions: 2 min at 95°C, followed by 15 cycles of (95°C, 30s; 55°C, 30s; 72°C, 1 min). The PCR reactions were cleaned using a QiaQuick PCR Purification Kit (Qiagen) according to manufacturer's instructions and sent to Isogenica for MiSEQ sequencing.

MiSEQ Fwd	5' -AATGATACGGCGACCACCGAGATCTACACTCTTTCCCTACACGACGCTCTTCCGATCTNNNNNCATTCTGTGATCTCTGCC-3'
MiSEQ Rev	5' -CAAGCAGAAGACGGCATAACGAGATTACAAGGTGACTGGAGTTCAGACGTGTGCTCTTCCGATCTACTAGACTGTGCGATGGC-3'

Table 2.4. Single Reaction Ligation Library MiSeq Primers. The sequences of the forward and reverse primers used for MiSeq analysis of the "one-pot" ligation library. Primers were purchased from Eurofins Genomics at 0.05 μ mol synthesis scale and PAGE-purified.

MiSeqFor	5' -AATGATACGGCGACCACCGAGATCTACACTCTTTCCCTACACGACGCTCTTCCGATCTNNNNNCACAGGAAACAGGATCTACCATG-3'
MiSeqRev03	5' -CAAGCAGAAGACGGCATAACGAGATGCCTAAGTGACTGGAGTTCAGACGTGTGCTCTTCCGATCTTGGTGAAGATCAGTTGGGGC-3'
MiSeqRev04	5' -CAAGCAGAAGACGGCATAACGAGATTGGTCAGTGACTGGAGTTCAGACGTGTGCTCTTCCGATCTTGGTGAAGATCAGTTGGGGC-3'

Table 2.5. Anti-NGF Peptide Library MiSeq Primers. The sequences of the forward and reverse primers used for MiSeq analysis of the anti-NGF peptide library. Primers were purchased from Eurofins Genomics at 0.05 μ mol synthesis scale and PAGE-purified.

2.2.3. Refined ProxiMAX Procedure

2.2.3.1. Refined Oligonucleotide Hybridisation

Single stranded MAX hairpins were diluted from stock to ~40 μM in 0.5x ThermoPol buffer (2.1.3.13) and self-hybridised by heating to 95°C for 2 minutes followed by ramp cooling down to 25°C over 45 minutes. These were quantified by UV spectrometry and diluted down to a working concentration of 2.4 μM with 0.5x ThermoPol buffer (2.1.3.13).

Oligo Name	Sequence
RH MAX _{R1}	5' - (MAX) _{RC} TACGTGACTCGCAATGACATCGTAGCACttttGTGCTACGATGTCATTGCGAGTCACGT MAX -3'
RH MAX _{R2}	5' - (MAX) _{RC} AGGTAGATCAGTGACACGGAGTCACGTAttttAGGTAGATCAGTGACACGGAGTCACGT MAX -3'
RH MAX _{R3}	5' - (MAX) _{RC} ACAGAACAGGCACTTAGGGAGTCACGTAttttACAGAACA GGCACCTAGGGAGTCACGT MAX -3'
LH MAX _{R1}	5' - MAX TACGTGACTCCCATCTGACTGTGAGATCttttGATCTCACAGT CAGATGGGAGTCACGTA (MAX) _{RC} -3'
LH MAX _{R2}	5' - MAX TACGTGACTCCGAGATGCTACTGTGCGAAttttTTCGACAGTAG CATCTCGGAGTCACGTA (MAX) _{RC} -3'
LH MAX _{R3}	5' - MAX TACGTGACTCGCTCAAGTTACGGTTCGATttttATCGACCGTAA CTTGAGCGAGTCACGTA (MAX) _{RC} -3'
RH Fwd Primer 1	5' -GTGCTACGATGTCATTGC-3'
RH Fwd Primer 2	5' -AGGTAGATCAGTGACACG-3'
RH Fwd Primer 3	5' -ACAGAACAGGCACTTAGG-3'
LH Fwd Primer 1	5' -GATCTCACAGTCAGATGG-3'
LH Fwd Primer 2	5' -TTCGACAGTAGCATCTCG-3'
LH Fwd Primer 3	5' -ATCGACCGTAACTTGAGC-3'
RH Universal Rev Primer	5' -GCCGGTACAGGTCTCCGT-3'
LH Universal Rev Primer	5' -CGGCGGTTAGAACGCGGC-3'

Table 2.6. Refined MAX Oligonucleotide Sequences. Sequences for the left (LH) and right (RH) MAX oligonucleotide hairpin and the appropriate cycle primers. The annotation 'MAX' refers to the randomised MAX codons whose sequences are highlighted in Table 2.7.

Codon	Sequence
A	GCT
D	GAT
E	GAA
F	TTC
G	GGC
H	CAT
I	ATC
K	AAG
L	CTG
N	AAC
P	CCG
Q	CAG
R	CGT
S	TCT
T	ACC
V	GTG
W	TGG
Y	TAC

Table 2.7. Anti-NGF Peptide Library MAX Codon Identity. Identity of the MAX codons located at the donor end of the top strand of the MAX oligonucleotide hairpins used for the anti-NGF peptide library.

2.2.3.2. Refined ProxiMAX Oligonucleotide Ligation

Appropriate 2.4 μ M MAX hairpin stocks (i.e. Round 1 oligonucleotide pairs for cycle 1) were ligated individually to 0.4 μ M base sequence, in a 20 μ l reaction containing 1 Thermo Scientific ligase buffer, 5% w/v PEG (Thermo Scientific) and 5 μ l *T4 DNA ligase* (Thermo Scientific). The reaction was incubated at 22°C for 15 min followed by 65°C for 10 minutes.

2.2.3.3. Refined ProxiMAX Oligonucleotide PCR

Quadruple 100 μ l amplifications were set up containing 50 pmol primers (the appropriate cycle primer and a universal primer for the base sequence), 20 μ M dNTPs, 2 units *Phusion Hot Start II* high-fidelity DNA polymerase (Thermo Scientific), 1 x Phusion HF buffer and 8 μ l of the single hairpin ligation. These underwent initial denaturation at 98°C for 45 secs followed by 3 cycles of (98°C, 10s; 52°C, 30s; 72°C, 20s), 13 cycles of (98°C, 10s; 55°C,

30s; 72°C, 20s) and a final extension of 72°C for 8 min. The four PCR reactions were then combined and cleaned using a QIAquick PCR Purification Kit (Qiagen) according to manufacturer's instructions. DNA concentration was assessed by either UV using a nanodrop 2000c (Thermo Scientific), or PCR products were electrophoresed, imaged and pixel density of the respective bands measured using imageJ. PCR products were then mixed to give an equimolar mix of MAX hairpins, digested as described in 2.2.2.6 and purified by agarose gel extraction (2.2.4.2.1 and 2.2.4.2.2).

2.2.4. Electrophoresis

2.2.4.1. Agarose gel electrophoresis

Agarose gels were made by dissolving 2% or 3% molecular grade agarose (Invitrogen) in 100 ml 1x TAE buffer, and ethidium bromide was added at a final concentration of 0.5 µg/ml. The gel was poured into an electrophoresis tank casting tray, set up according to manufacturer's instructions and allowed to set. Once set the comb was removed and the tank was filled up with 1x TAE buffer. DNA was mixed with loading buffer (2.1.3.5, 2.1.3.6 or 2.1.3.7), loaded into the wells and a constant voltage of 10 V/cm was applied to gel until the dye front had migrated a sufficient distance. The gel was then viewed using a UV transilluminator (UVP), or using GeneSnap photographic software (GeneSnap).

2.2.4.2. Agarose gel purification of DNA (Low Melting Point Agarose Gel)

2.2.4.2.1. Spin Column Purification

Agarose gels were prepared using low melting point agarose (Invitrogen) in 1x TAE buffer with a final concentration of 0.5 µg/ml ethidium bromide. The gel was poured into an electrophoresis tank, set up according to manufacturer's instructions and allowed to set. Once set the comb was removed and the tank was filled up with 1x TAE buffer (2.1.3.2). DNA was mixed with loading buffer (2.1.3.5, 2.1.3.6 or 2.1.3.7), loaded into the wells and a

constant voltage of 10 V/cm was applied to gel until the dye front had migrated a sufficient distance. The required DNA band was excised and purified using a GENE CLEAN turbo kit (MP Bio), QIAquick or MinElute Gel extraction kit (Qiagen) according to the manufacturer's instructions.

2.2.4.2.2. D-tube Dialyzer (Merck Millipore)

Agarose gels were prepared using low melting point agarose (Invitrogen) in 1x TAE buffer (2.1.3.2) with a final concentration of 0.5 µg/ml ethidium bromide. The gel was poured into an electrophoresis tank, set up according to manufacturer's instructions and allowed to set. Once set the comb was removed and the tank was filled up with 1x TAE buffer (2.1.3.2). DNA was mixed with loading buffer (2.1.3.5, 2.1.3.6 or 2.1.3.7), loaded into the wells and a constant voltage of 10 V/cm was applied to gel until the dye front had migrated a sufficient distance. The DNA fragment was excised from the agarose gel with a clean, sharp scalpel and purified using D-tube Dialyzers (Merck Millipore) according to the manufacturer's instructions

2.2.4.3. TBE-Polyacrylamide gel electrophoresis

Polyacrylamide gels were made using 10x TBE buffer (2.1.3.1), 40% 37:5:1 acrylamide:bisacrylamide (National diagnostics), 10% APS (2.1.4.9) and TEMED (N',N',N',N'-Tetraethylmethylethylene diamine) (National diagnostics). The electrophoresis tank was set up according to manufacturer's instructions and the gels poured and set. DNA samples were mixed with loading buffer, loaded onto the gel and constant voltage of 100V was applied for 1 hour, or until the dye front had travelled an appropriate distance. The gel was then removed, stained with a 1x TBE/ethidium bromide buffer (final concentration of 0.5 µg/ml) for 10 minutes and imaged on a UV transilluminator (UVP) or using GeneSnap photographic software (GeneSnap).

2.2.4.4. Tris-Glycine Polyacrylamide Gel Electrophoresis

Polyacrylamide resolving gels made were using 1.5 M Tris-HCl (pH 8.8.), 30% acrylamide/bisacrylamide (37:5:1) (National diagnostics), 20% SDS (2.1.4.10), 10% APS (2.1.4.9) and TEMED (National diagnostics). Polyacrylamide stacking gels were made using 0.5 M Tris-HCl (pH6.8.), 30% acrylamide/bisacrylamide (37:5:1) (National diagnostics), 20% SDS (2.1.4.10), 10% APS (2.1.4.9) and TEMED (National diagnostics). The electrophoresis tank was set up according to manufacturer's instructions and the gels placed within with 1x SDS Tris-Glycine running buffer (2.1.3.3). Protein samples were mixed with 2x SDS sample loading buffer (2.1.3.8), loaded onto the gel and constant voltage of 150V was applied for 1 hour and 10 minutes, or until the dye front had travelled an appropriate distance. The gel was then removed, stained with Instant blue protein stain (Expedeon) for 30 minutes and imaged using GeneSnap photographic software (GeneSnap) under white light.

2.2.4.5. Bis-Tris Polyacrylamide Gel Electrophoresis

Precast bis-tris protein gels were purchased from Invitrogen. The electrophoresis tank was set up according to manufacturer's instructions and the gels placed within with 1x NuPAGE® MES-SDS running buffer (2.1.3.4). Protein samples were mixed with 2x SDS sample loading buffer (2.1.3.8), loaded onto the gel and constant voltage of 180V was applied for 45 minutes, or until the dye front had travelled an appropriate distance. The gel was then removed, stained with Instant blue protein stain (Expedeon) for 30 minutes and imaged using GeneSnap photographic software (GeneSnap) under white light.

2.2.4.6. Western Blotting

2.2.4.6.1. Semi-Dry Method

PVDF membrane was pre-wetted in 100% methanol and then equilibrated for 10-15 minutes in 1x transfer buffer (Thermo Scientific) along with filter paper. After equilibration this was then assembled on a semi-dry blotter (Thermo Scientific) according to the manufacturer's protocol and transferred at 25V for 20-45 minutes. After transfer the membrane was then washed with ultrapure water.

2.2.4.6.2. Protein Detection

The membrane was blocked with 5% w/v milk in PBS with the primary HRP-conjugated antibody diluted to the appropriate working concentration and was then washed three times for 10 minutes with PBS + 0.2% Tween. The membrane was then equilibrated with EZ-ECL buffer for 3 minutes and then dried in the dark. The membrane was then imaged using UViChem imaging equipment and captured for 20 minutes.

2.2.5. Transformation of *Escherichia Coli*

2.2.5.1. CaCl₂ Method

Thirty ml LB broth (2.1.2.1) was inoculated with a single *E.coli* DH5a and incubated overnight at 37°C. The next day, 30 ml of fresh LB broth was inoculated with 0.3 ml of the overnight culture and placed in an incubator for 2 hours. The cells were then harvested by centrifugation at 4000 rpm for 5 min, the supernatant removed, the cells re-suspended with 6 ml ice cold 50 mM CaCl₂ (2.1.4.11) and placed on ice for 10 min. This procedure of harvest, supernatant removal, re-suspension and incubation on ice was repeated two more times with the final re-suspension in 1.2 ml (rather than 6.0 ml) ice cold CaCl₂. The cells were then placed on ice for 20 min. One hundred µl of competent cells were added to 5 ng transformed DNA in pre chilled 1.5 ml microcentrifuge tubes and left on ice for 30 min. After 30 min the

cells were heat shocked in a 37°C water bath for 30 sec and then transferred back to ice for 2 min. Sterile LB broth (500 µl) was added to each microcentrifuge tube and then incubated in a 37°C water bath for 40 min. For the use of blue/white screening, after the 40 min incubation 200 µl of transformations were added to 50 µl 2 % X-GAL (2.1.4.4) and 10 µl 1 M IPTG (2.1.4.7). These were then plated out on LB agar + AMP plates (2.1.1.1) and incubated overnight at 37°C.

2.2.5.2. Chemically Competent *E.coli*

One vial per transformation of the particular strain was thawed on ice for 10 minutes and transformed according to the manufacturer's protocol.

2.2.6. Plasmid Purification (Small scale)

Plasmid DNA was purified from cells grown in LB broth (2.1.2.1) using a Wizard™ miniprep kit (Promega) according to the manufacturer's protocol.

2.2.7. Ethanol Precipitation

DNA was precipitated by adding 1/10th the volume of 3 M sodium acetate (pH5.5) and 2x volume of ice-cold 100% ethanol. This mixture was then incubated at either -20°C overnight or -80°C for 1 hour, and the DNA subsequently pelleted by centrifugation (14,000 rpm) at 4°C for 20 minutes. The supernatant was aspirated and the pellet was washed with 70% ethanol. The pellet was then dried via aspiration/evaporation and resuspended in an appropriate buffer.

2.2.8. Phenol/Chloroform Extraction

DNA was extracted by the addition of an equal volume phenol: chloroform: isoamyl alcohol (25:24:1), mixed and centrifuged at 14000 rpm for 30 seconds. The upper aqueous phase was removed and the process repeated two more times. To remove any residual phenol the recovered aqueous phase was mixed with an equal volume of chloroform: isoamyl alcohol (24:1) and subsequently vortexed and centrifuged at 14000 rpm for 30 minutes. The upper aqueous phase was removed and the DNA recovered by ethanol precipitation (2.2.7) before resuspension in the appropriate buffer.

2.2.9. Protein Expression and Purification

2.2.9.1. pJ434-NGF_optEc

2.2.9.1.1. Expression

pJ434-NGF_optEc was transformed into *E.coli* SHuffle® T7 Competent (2.2.5.2) and grown overnight on LB agar+50 µg/ml kanamycin (2.1.1.1) at 30°C. Two hundred ml LB broth +50 µg/ml kanamycin (2.1.4.6) was inoculated with a single colony and incubated overnight at 30° whilst shaking at approximately 200 rpm. Fresh LB broth +50 µg/ml kanamycin was inoculated 10:1 with overnight culture was and incubated 30°C whilst shaking at approximately 200 rpm until an OD_{600nm} 0.4-0.6. The cultures were induced with 0.4-1.0 mM IPTG (2.1.4.7) and incubated at 30°C for 4hours or 16°C overnight. Cultures were pelleted by centrifugation at 10,000 xg and the resulting pellets stored at -20°C.

Prior to induction a 10 ml sample of culture was taken and split into two 5 ml samples to allow comparison of induced vs. un-induced protein expression. Time-point samples (500 µl) were taken at 0, 2 and 4 hours and pellet by centrifugation at 10,000 xg for 1 min. The supernatant was discarded and the cell pellet resuspended in 80 µl 1x SDS sample buffer (2.1.3.8), boiled at 95°C for 10 minutes and analysed by SDS-PAGE.

2.2.9.1.2. Cell Lysate Production (Sonication)

E.coli pellets were resuspended in 0.1x original culture volume of native cell lysis buffer (2.1.3.20.1) with lysozyme (2.1.4.8) at a final concentration of 0.2 mg/ml and incubated on ice for 10 minutes. The resuspended cells were then sonicated 10x at 90% power for 20 secs with 2 minutes on ice between each sonication event. Cell debris and insoluble material were pelleted by centrifugation at 16,000 xg for 20 minutes at 4°C and the soluble fraction transferred to a fresh tube.

2.2.9.1.3. Cell Lysate Production (Bugbuster™)

E.coli cell pellets were resuspended in Bugbuster™ master mix (Merck Millipore) at 5 ml per 1g wet cell paste. These were incubated at room temperature for 20-30 minutes and the insoluble debris pelleted by centrifugation at 16,000 xg for 20 minutes at 4°C. Supernatant containing the soluble fraction was transferred to a fresh tube.

2.2.9.1.4. Purification

Cell lysate as produced in 2.2.9.1.2 or 2.2.9.1.3 was mixed with 1 ml (0.5 ml bed volume) Ni-NTA (Qiagen) and incubated at room temperature whilst mixing end-over-end for 1 hour. The mixture was loaded onto a poly-prep® chromatography column (BioRad), allowed to flow through and that fraction collected. The column was washed 2x with native column wash buffer (2.1.3.20.3), followed by 4x with native column elution buffer (2.1.3.20.4). Twenty µl of each fraction was taken for analysis whilst the remaining fractions were stored at -80°C in 25% glycerol. Sample fractions were mixed with 20 µl 2x SDS sample buffer (2.1.3.8) and analysed by SDS-PAGE (2.2.4.4, 2.2.4.5).

2.2.9.2. pET SUMO-βNGF

2.2.9.2.1. TA Cloning

β-NGF gene was amplified out of pJ434-NGF_optEc and inserted into pETSUMO plasmid using TA cloning with specific primers to amplify the β-NGF gene. Amplification was undertaken using the general PCR procedure as described in 2.2.1.4 with a primer annealing temperature of 51°C. A 3:1 insert: vector molar ratio was used for the ligation, which was performed according to the general ligation procedure described 2.2.1.3. The pET SUMO-βNGF was transformed into One Shot® Mach1™-T1R Competent Cells (2.1.5.2) as described in 2.2.5.2 and resulting clones screened by colony PCR (2.2.2.3). Plasmid DNA was extracted and purified by miniprep (2.2.6) and sent for sequencing at Eurofins Genomics.

2.2.9.2.2. Expression

pET SUMO β-NGF was transformed into both SHuffle® T7 Competent *E.coli* and (NEB) *E.coli* BL21 (DE3) One Shot® (2.1.5.3 & 2.1.5.4) and grown overnight on LB agar+50 µg/ml kanamycin (2.1.1.1) at 30°C and 37°C respectively. LB broth +50 µg/ml kanamycin (200 ml) (2.1.4.6) was inoculated with a single colony of either cell line and incubated overnight at 30/37°C whilst shaking at approximately 200 rpm. Fresh LB broth +50 µg/ml kanamycin was inoculated 10:1 of overnight culture was and incubated 30/37°C whilst shaking at approximately 200 rpm until an OD_{600nm} 0.4-0.6. The cultures were induced with 1.0 mM IPTG (2.1.4.7) and incubated at 30/37°C for 4hours or 16°C overnight. Cultures were pelleted by centrifugation at 10,000 xg and stored at -20°C.

Prior to induction, a 10 ml sample of culture was taken and split into two 5 ml samples to allow comparison of induced vs. un-induced protein expression. Time-point samples (500 µl) were taken at 0, 2 and 4 hours and pelleted by centrifugation at 10,000 xg for 1 min. The supernatant was discarded and the cell pellet resuspended in 80 µl 1x SDS sample buffer (2.1.3.8), boiled at 95°C for 10 minutes and analysed by SDS-PAGE (2.2.4.4, 2.2.4.5).

2.2.9.2.3. Soluble Fraction Purification

E.coli cell pellets were resuspended in Bugbuster™ master mix (Merck Millipore) at 5ml per 1g wet cell paste. These were incubated at room temperature for 20-30 minutes and the insoluble debris pelleted by centrifugation at 16,000 x g for 20 minutes at 4°C. Supernatant containing the soluble fraction was transferred to a fresh tube.

Cell lysate as was mixed with 1 ml (0.5 ml bed volume) Ni-NTA (Qiagen) and incubated at room temperature whilst mixing end-over-end for 1 hour. The mixture was loaded onto a poly-prep® chromatography column (BioRad), allowed to flow through and that fraction collected. The column was the washed 2x with native column wash buffer (2.1.3.20.3), followed by 4x with native column elution buffer (2.1.3.20.4). Twenty µl of each fraction was taken for analysis whilst the remaining fractions were stored at -80°C in 25% glycerol. Sample fractions were mixed with 20 µl 2x SDS sample buffer (2.1.3.8) and analysed by SDS-PAGE (2.2.4.4, 2.2.4.5).

2.2.9.2.4. Purification under Denaturing Conditions

The cell pellet generated from 2.2.9.2.2 was resuspended in 0.1 original culture volume of denaturing lysis buffer (2.1.3.20.2) and mixed with 1 ml (0.5 ml bed volume) Ni-NTA (Qiagen) and incubated at room temperature whilst mixing end-over-end for 1 hour. The mixture was loaded onto a poly-prep® chromatography column (BioRad), allowed to flow through and that fraction collected. The column was the washed 2x denaturing column wash buffer (2.1.3.20.5), followed by 4x with denaturing column elution buffer 1 (2.1.3.20.6) and 4x with denaturing column elution buffer 2 (2.1.3.20.7). Samples (20 µl) of each fraction were taken for analysis whilst the remaining fractions were stored at -80°C in 25% glycerol. Sample fractions were mixed with 20 µl 2x SDS sample buffer (2.1.3.8) and analysed by SDS-PAGE (2.2.4.4, 2.2.4.5).

2.2.9.2.5. Inclusion Body Preparation (Bugbuster™)

The insoluble pellet generated from 2.2.9.2.3 was resuspended the same volume of Bugbuster™ master mix as previously used, to lyse the cell pellet, and incubated at room temperature for 5 minutes. Six volumes of 1:10 diluted Bugbuster™ master mix in deionised water was added, vortexed for 1 min and the inclusion bodies collected by centrifugation at 5,000 xg for 15 minutes at 4°C. The supernatant was removed and the inclusion bodies resuspended in 0.5 volume (of the original volume) 1:10 diluted Bugbuster™ master mix. This was repeated three more times but final resuspension was centrifuged at 16,000 xg for 15 minutes at 4°C and the supernatant removed. Inclusion body pellets were then stored at -80°C.

2.2.9.2.6. Inclusion Body Solubilisation

Inclusion body pellets as prepared in 2.2.9.2.5 were resuspended in solubilisation buffer (2.1.3.20.8) and mixed end-over-end at room temperature for 2 hours. Insoluble debris was pelleted by centrifugation at 16,000 xg for 20 minutes, following which the supernatant was transferred to a clean tube. Pelleted insoluble debris was again resuspended in solubilisation buffer and mixed end-over-end at room temperature for 2 hours to allow analysis of solubilisation efficiency.

2.2.9.2.7. Inclusion Body Purification

Solubilised inclusion bodies as prepared in 2.2.9.2.6 were mixed with 1 ml (0.5 ml bed volume) Ni-NTA (Qiagen) and incubated at room temperature whilst mixing end-over-end for 1 hour. The mixture was loaded onto a poly-prep® chromatography column (BioRad), allowed to flow through and the fraction collected. The column was washed 2x denaturing column wash buffer (2.1.3.20.5), followed by 4x with denaturing column elution buffer 1 (2.1.3.20.6) and 4x with denaturing column elution buffer 2 (2.1.3.20.7). 20 µl of each fraction

was taken for analysis whilst the remaining fractions were stored at -80°C with 25% glycerol. Sample fractions were mixed with 20 µl 2x SDS sample buffer (2.1.3.8) and analysed by SDS-PAGE (2.2.4.4, 2.2.4.5).

2.2.9.2.8. Refolding

Purified solubilised inclusion bodies prepared as described in 2.2.9.2.7 were incubated with 1ml (0.5ml bed volume) Ni-NTA resin (Qiagen) per 4 ml solubilised inclusion bodies and mixed by inversion at room temperature for 45-60minutes. This was then passed through a poly-prep chromatography column (BioRad) and the flow through saved for later analysis. The resin was washed with 4 bed volumes of denaturing wash buffer (2.1.3.20.5) and the fractions saved for later analysis. The resin was then resuspended 1:1 v/v in refolding buffer (2.1.3.20.9) transferred out of the column, diluted 50-fold in refolding buffer and rolled for 5 minutes. The resin was then pelleted, the supernatant removed, resuspended in fresh refolding buffer (1:50 dilution) and rolled for 5 minutes. This was repeated again but after re-suspension it was mixed end-over-end at 4°C overnight. The next day this was passed through a new poly-prep chromatography column (BioRad) and washed with 4 bed volumes of native wash buffer (2.1.3.20.3). Soluble refolded protein was then eluted with 4x 1 bed volume native elution buffer (2.1.3.20.4) and fractions saved. Elution fractions were diluted 5-fold in dilution buffer (2.1.3.20.10) to reduce the imidazole concentration, glycerol was added to a 25% final concentration and the resulting fractions were stored at -80°C.

2.2.9.3. BCA Protein Quantification Assay

Protein concentration was determined using the BCA assay in the manner described in the manufacturer's protocol.

2.2.9.4. SUMO-NGF Cleavage

One unit of SUMO protease was added per 5 µg SUMO-NGF fusion with 1x SUMO protease buffer (2.1.3.20.11). NaCl concentration was kept between 100 mM and 300 mM for optimal reaction conditions. The reaction was incubated at 30°C for 6 hours and then stored at -20°C. Twenty µl was removed and prepared for analysis by adding 20 µl 2x SDS sample buffer (2.1.3.8) and analysed by SDS-PAGE.

2.2.9.5. NGF Activity Assay

TrkA-Fc chimera (125 ng/50 µl; R&D Systems) was incubated on a NUNC F96 Maxisorp plate (Sigma-Aldrich) at 4°C overnight. The plate was washed 3x in PBS/0.1% Tween and 2x PBS. This was then blocked for 1hr at room temperature with Blocker™ 1% casein (Thermo Scientific) followed by 4x washes with PBS/0.1% Tween and 2x PBS. Recombinant human β-NGF (30 ng; R&D Systems) was mixed with 50µl 0.1% casein (1:10 diluted Blocker™ 1% casein in PBS/0.1% Tween). NGF solution (55 µl/well) was transferred into the NUNC Maxisorp plate and incubated for 40 minutes at room temperature with 50 µl/well 1:200 biotinylated anti-human β-NGF antibody (R&D Systems) in 0.1% casein in PBS/0.1% Tween. The plate was washed 4x in PBS/0.1% Tween and 2x PBS. Streptavidin-HRP (Sigma-Aldrich, 1:1000 dilution) in 0.1% casein/PBS/0.1% Tween, 50 µl/well was added to the plate, which was then incubated for 30 minutes at room temperature followed by 4x washes with PBS/0.1 Tween and 2x PBS. Finally, TMB reagent (50 µl/well; eBiosciences) was incubated on the plate for 5-20 minutes, quenched with 50 µl/well 0.5M H₂SO₄ and the absorbance read at 450nm.

2.2.10. CIS Display

2.2.10.1. Rh β -NGF Biotinylation

EZ-Link™ Sulfo-NHS-Biotin (Thermo Scientific) was reconstituted with ultrapure water to 10mM concentration and was added to rh β -NGF (R&D systems) at a 20-fold molar excess. This was incubated on ice for 2 hours and the reaction was stopped with the addition of 250 μ l 1M Tris-HCl (pH 7.4). Free biotin was removed by dialysis using a Slide-A-Lyzer dialysis cassette (MWCO 3KDa) with PBS as an exchange buffer. Exchange buffer was replaced after 2 hours (twice) followed by overnight at 4°C.

2.2.10.2. Library Selections

An *in vitro* transcription/translation reaction was set up containing 2 μ g library template DNA along with in Isogenica proprietary buffer, amino acid mix and cell lysate to a total volume of 50 μ l. This was incubated for 1 hour at 37°C and subsequently put on ice for 5 minutes. Dynabeads® M-280 Streptavidin (Life technologies) were prewashed 3x with PBS and resuspended in the original volume of 2% BSA/PBS/0.1% Tween. Unspecific binders from the *in vitro* transcription/translation were discarded using unblocked uncoated beads by mixing for 30 minutes with 2% BSA/PBS (+/- 1mg/ml heparin depending on stringency). Ten μ g of biotinylated rh β -NGF (2.2.10.1) was bound to 50 μ l prewashed beads for 1 hour in PBS followed by 2x PBS washes and blocked with 2% BSA/PBS. Deselection supernatant was transferred to coated beads and washed on a KingFisher™ Flex Magnetic Particle Processor (Thermo Scientific) according to the designed selection plan. Bound DNA was then heat eluted at 75°C in 1x ThermoPol buffer (2.1.3.13) for 10 minutes, the beads were captured and the supernatant transferred to a fresh Eppendorf tube. Selected DNA was then amplified using reactions containing 10 μ M recovery primer, 2 μ M dNTPs, 1 x KOD buffer, 25 mM MgSO₄ 0.5 units KOD Hot Start DNA polymerase (Merck Millipore Millipore) and 10 μ l of the eluted DNA. These underwent initial denaturation at 95°C for 2 min followed by 35 cycles of (95°C, 30s; 52°C, 20s; 72°C, 1 min), and a final extension of 72°C for 7 min. The resulting

product was purified using Promega Wizard™ columns according to the manufacturer's protocol and the resulting DNA was used for another round of selections.

2.2.10.3. Library Screening

2.2.10.3.1. Selection Output Cloning

The output from the final round of selections was digested with *NcoI* (NEB) and *NotI* (NEB) (2.2.1.5) and ligated (2.2.1.3) into an Isogenica proprietary phagemid vector. The ligations were purified using phenol/chloroform extraction (2.2.8), ethanol precipitation (2.2.7) and the phagemid was transformed into *E.coli* TG1 (2.1.5.5) as described in 2.2.5.2

2.2.10.3.2. Peptide Phage Expression

Individual colonies from selection output cloning (2.2.10.3.1) were picked into 120 µl 2TY (2.1.2.2) with 100 µg/ml ampicillin (2.1.4.5) and 2% glucose. This was incubated at 37°C, 225 rpm until cloudy. Glycerol was then added to 25% (v/v) and these precultures were stored at -80°C.

Thirty µl of preculture was transferred to 300 µl 2TY-Amp-Glu (2.1.2.2, 2.1.4.6) and incubated at 37°C until the OD_{600nm} was 0.3. Approximately 10⁸ pfu (plaque forming units) of M13K07 helper phage (NEB) was added and incubated at 37°C with shaking @225 rpm. The cultures were then pelleted by centrifugation at 3000 xg for 10 mins, the supernatant discarded and pellets resuspended in 600 µl 2TY-Amp (2.1.2.2,2.1.4.6) +50 µg/ml (2.1.4.6). This was subsequently incubated at 37°C, with shaking @ 225 rpm overnight and the following day the cultures were pelleted by centrifugation at 3000 xg for 10 mins. The supernatant was kept and stored at 4°C ready for analysis by ELISA.

2.2.10.3.3. Phage expression ELISA screening

A NUNC F96 Maxisorp plate (Sigma-Aldrich) was coated with 50 ng/well recombinant human β -NGF (R&D Systems) and incubated overnight at 4°C. The plate was washed 4x PBS/0.1% Tween and 2x PBS. This was then blocked for 1hr at room temperature with Blocker™ 1% casein (Thermo Scientific) followed by 4x washes with PBS/0.1% Tween and 2x PBS. Supernatant produced from (2.2.10.3.2) was diluted 2x in 0.1% casein in PBS/0.1% Tween and 100 μ l/well was added to the Maxisorp plate and incubated at room temperature for 1 hour. The plate was washed again with 4x PBS/0.1% Tween and 2x PBS. Mouse anti-M13 HRP conjugated antibody (Sigma-Aldrich; 1:5000 dilution, 50 μ l/well) in 0.1% casein/PBS/0.1% Tween was incubated on the plate for 30 minutes at room temperature followed by 4x washes with PBS/0.1 Tween and 2x PBS. TMB reagent (eBiosciences; 50 μ l/well) was incubated on the plate for 5-20 minutes, the reaction was quenched with 50 μ l/well 0.5M H₂SO₄ and the absorbance read at 450nm.

2.2.11. NGF Inhibition Assay

TrkA-Fc chimera (125 ng/50 μ l; R&D Systems) was incubated on a NUNC F96 Maxisorp plate (Sigma-Aldrich) at 4°C overnight. The plate was the washed 3x in PBS/0.1% Tween and 2x PBS. This was then blocked for 1hr at room temperature with Blocker™ 1% casein (Thermo Scientific) followed by 4x washes with PBS/0.1% Tween and 2x PBS. Thirty ng recombinant human β -NGF (R&D Systems) was mixed with 50 μ l of appropriate peptide concentrations in 0.1% casein in PBS/0.1% Tween. NGF/peptide solutions (55 μ l/well) were transferred into the NUNC Maxisorp plate and incubated for 40 minutes at room temperature with 50 μ l/well 1:200 biotinylated anti-human β -NGF antibody (R&D Systems) in 0.1% casein in PBS/0.1% Tween. The plate was washed 4x in PBS/0.1% Tween and 2x PBS. Streptavidin-HRP (Sigma-Aldrich; 1:1000 dilution, 50 μ l/well) in 0.1% casein/PBS/0.1% Tween was incubated on the plate for 30 minutes at room temperature followed by 4x washes with PBS/0.1 Tween and 2x PBS. TMB reagent (eBiosciences; 50 μ l/well) was

incubated on the plate for 5-20 minutes, quenched with 50 μ l/well 0.5M H₂SO₄ and the absorbance read at 450nm.

Chapter 3

ProxiMAX Randomisation: Single Reaction Equimolar Ligation Library

3. Chapter 3: ProxiMAX Randomisation: Single Reaction Equimolar Ligation Library

3.1 Introduction

The original ProxiMAX method (2.2.2) relied on the use of single stranded oligonucleotides that were subsequently hybridised together (2.2.2.1) and quantified (2.2.2.2) to donate an equimolar mix of MAX codons to an acceptor piece of DNA in a single reaction (Figure 3.1). MAX codons were chosen based on preferred usage in *E.coli* as described in (Nakamura et al., 2000). MAX oligonucleotides contained a single stranded 5' region to reduce the formation of concatamers. Blunt ended ligation was used to ligate the donor MAX oligonucleotide to acceptor sequence (2.2.2.4). In order to keep point mutations to a minimum high fidelity *Pfu* DNA polymerase was used to amplify the acceptor:donor complex. As this is an iterative process, the amount of template employed could influence the maximum number of randomised codons that can be added is the ability to functionally screen the final library.

To assess the ProxiMAX method, in its original format, it would be used to add a randomised array of codons, over six cycles, on to a non-specific piece of acceptor DNA. Specific subsets of codons based on their structural qualities were used in each cycle (Table 3.2). From this data the process could be analysed and any flaws could be adjusted in order to further refine the method.

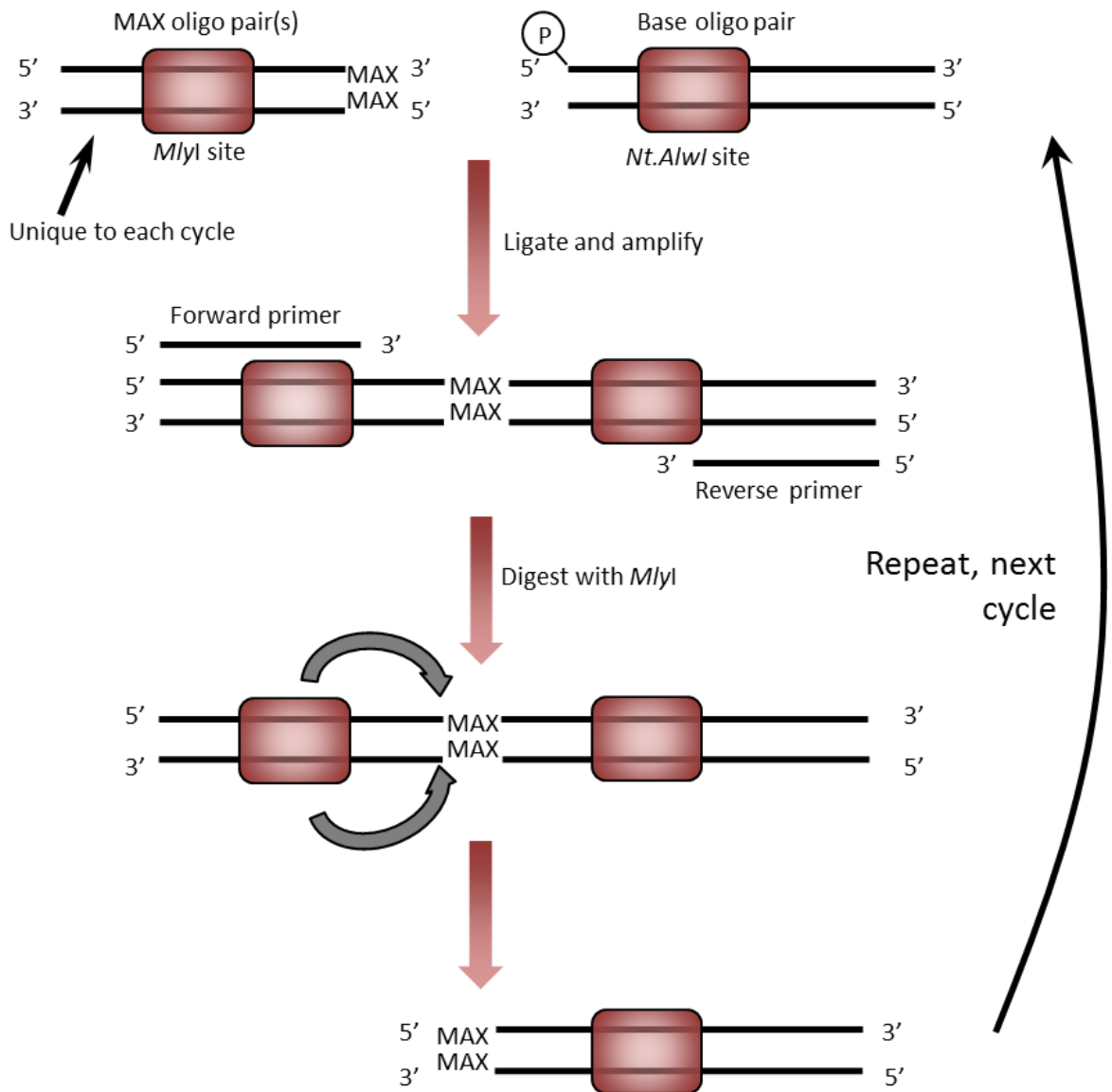


Figure 3.1. ProxiMAX Randomisation Process Schematic. Specially designed 'MAX' oligonucleotides (Table 2.1 and Table 2.2) are hybridised together. They are then ligated to a conserved base sequence, whilst concurrently undergoing a single strand digestion with *Nt.AflwI* to cleave base/base ligation. The ligation is amplified using *Pfu* DNA polymerase and the resulting product cleaned using QIAGEN Minelute kit. The cleaned product is digested with *MlyI*, and the ligation/amplification/digestion process is repeated using the digested product of the previous cycle as the base sequence.

3.2 MAX Oligonucleotide and Library Framework Preparation

Before saturation cycling could proceed, the single stranded forward and reverse MAX oligonucleotides, as well as the library framework sequence (termed base sequence), were hybridised by heating to 94°C for 5 minutes followed by cooling at 1°C per min to 4°C (2.2.2.1).

To ensure the MAX oligonucleotides were successfully hybridised and could be used at an equimolar concentration when combined, the concentration of the individual hybridised oligonucleotide pairs was calculated using a Quant-iT™ PicoGreen® dsDNA assay (2.2.2.2) as shown in Figure 3.2 and Table 3.1. PicoGreen binds exclusively to double-stranded DNA and therefore allows the quantification of successfully hybridised double stranded oligonucleotides whilst single stranded oligonucleotides should not affect quantification.

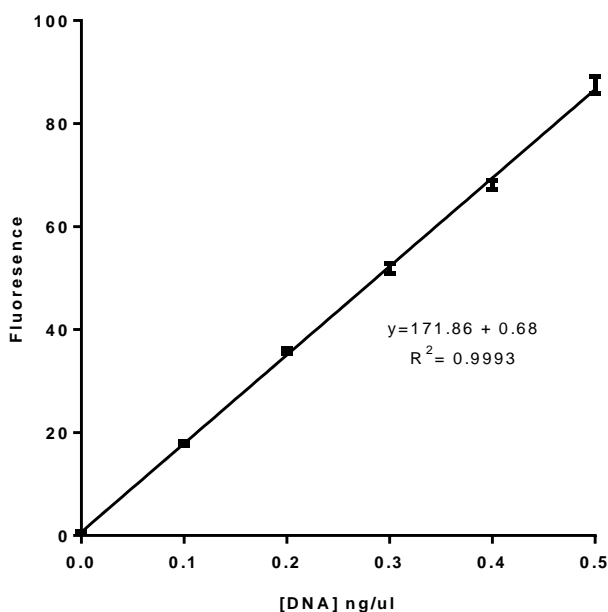


Figure 3.2. Picogreen Standard Curve. Lambda DNA was diluted to a range of 0-1.0 ng/μl in TE buffer. This was further diluted 1:1 with 200x diluted picogreen reagent and fluorescence measured at 480nm excitation and 520nm emission. A standard curve was plotted with DNA concentration on the x axis and fluorescence on the y axis.

Oligo	Fluorescence				[DNA] ng/ μ l	Mol	Concentration / μ M
	1	2	3	Mean			
1A	119.54	130.65	120.02	123.40	71.05	8.28E-06	8.28
1G	146.20	148.09	152.92	149.07	85.98	1.00E-05	10.02
1I	104.42	104.76	116.99	108.72	62.51	7.29E-06	7.29
1L	115.93	120.33	122.44	119.57	68.82	8.02E-06	8.02
1V	118.42	117.00	115.75	117.06	67.35	7.85E-06	7.85
2F	134.36	132.76	125.24	130.79	75.34	8.78E-06	8.78
2W	136.01	133.91	133.25	134.39	77.44	9.03E-06	9.03
2Y	76.34	78.52	75.06	76.64	43.84	5.11E-06	5.11
3D	103.03	99.67	105.89	102.86	59.10	6.89E-06	6.89
3E	102.35	101.28	106.09	103.24	59.32	6.91E-06	6.91
4N	121.34	117.91	115.76	118.34	68.10	7.94E-06	7.94
4Q	114.09	111.51	112.71	112.77	64.86	7.56E-06	7.56
4S	133.98	138.60	126.79	133.12	76.70	8.94E-06	8.94
4T	171.92	169.00	167.26	169.39	97.81	1.14E-05	11.4
5H	123.54	128.37	116.38	122.76	70.68	8.24E-06	8.24
5K	128.15	130.42	130.70	129.76	74.74	8.71E-06	8.71
5R	134.95	127.06	126.90	129.64	74.67	8.70E-06	8.7
6C	60.84	190.00	113.44	121.43	69.90	8.15E-06	8.15
6M	147.31	143.72	142.96	144.66	83.42	9.72E-06	9.72
6P	118.61	119.68	124.66	120.98	69.64	8.12E-06	8.12
BASE	160.00	163.64	161.42	161.69	93.32	3.63E-06	3.63

Table 3.1. MAX Oligonucleotide Picogreen Measurements. 50x diluted hybridised MAX oligonucleotides were mixed with 200x diluted picogreen reagent and the fluorescence measured at 480nm excitation and 520nm emission. Concentration was then calculated using the standard curve from Figure 3.2.

After quantification, the concentration of the appropriate oligonucleotide for each cycle of the library build (Table 3.2) was adjusted to make 1 μ M stocks to be used in the ProxiMAX saturation cycling procedure.

Pos.	R1	R2	R3	R4	R5	R6
Codons	AGILV	FWY	DE	NQST	HKR	CMP
No.	5	3	2	4	3	3

Table 3.2. Library Build Overview. The identity of the corresponding groups of MAX codons in each cycle. To demonstrate the ProxiMAX technique specific sub-groups with related structural properties were grouped together.

3.3 ProxiMAX Saturation Cycling

Initially a 39 bp base sequence (Table 2.1) was used as a framework on to which an equimolar group of 31 bp cycle 1 MAX oligonucleotides (Table 2.1) were ligated (2.2.2.4) to form a fragment with a sequence length of 70 bp. This provided an acceptor: donor complex large enough to purify using standard spin columns whilst small enough to eventually resolve the difference in size between cycles via electrophoresis. The first cycle contained an equimolar mix of MAX oligonucleotides, as described in 2.2.2.4, which were ligated to the base template sequence in a single 20 µl reaction. This ligation was subsequently amplified (2.2.2.5) using the appropriate base and cycle primers (Table 2.1) and examined by 3% agarose gel electrophoresis (2.2.4.1), as shown in Figure 3.3.

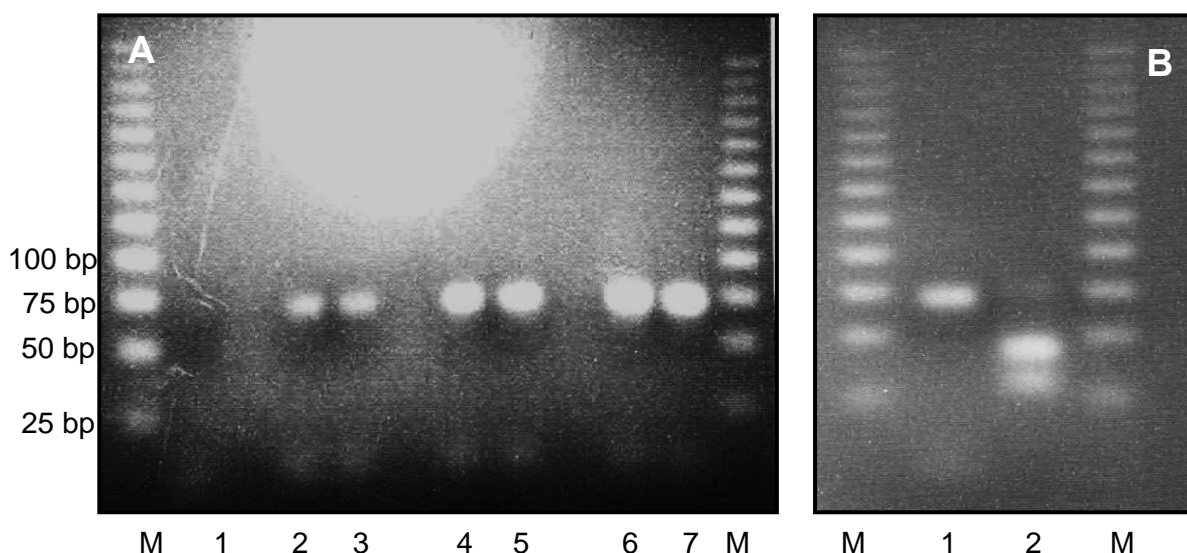


Figure 3.3. ProxiMAX Saturation Cycling. A: Round 1 PCR. Agarose gel image of PCR products generated from diluted round 1 ligation (A, G, I, L, V). Lanes: 1: Negative control (no template DNA); 2-3: 1/1000 ligation dilution; 4-5: 1/100 ligation dilution; 6-7: 1/10 ligation dilution. Each dilution appeared to be the correct length of 70 bp. Samples were electrophoresed on 3% agarose/TAE gel against 0.36 µg of Promega 25 bp step ladder. **B: Round 1 Digestion.** PCR products underwent clean-up and subsequently digested with *Mly*I forming two fragments of 42 bp and 28 bp respectively. Lanes: 1: Undigested PCR product; 2: Digested PCR product. Samples were electrophoresed on 3% agarose/TAE gel against 0.36 µg of Promega 25 bp step ladder.

Figure 3.3 A clearly shows a band in lanes 2-7 that is slightly smaller than the 75 bp marker, with some slight primer dimerization occurring below the 25 bp marker. This corresponds to the expected 70 bp size of the PCR product, with no contamination observed in the negative

control of lane 1, so was therefore purified and digested (2.2.2.6) according to the ProxiMAX procedure.

Analysis of the digestion on an agarose gel (Figure 3.3 B) showed that the digestion was successful in forming two smaller bands (lane 2) at the expected sizes of 42 bp and 28 bp, with some undigested material still present at 70 bp. Lane 1 contained a control of undigested PCR product as control to measure the success of the digestion. The first round of saturation cycling appeared to be successful so the product was subsequently used in the next cycle of ProxiMAX randomisation.

However after progressing onto the second cycle some fundamental problems manifested themselves. An equimolar mix of cycle 2 MAX oligonucleotides were ligated to the digested product carried through from cycle 2 and amplified in the same manner as previously described. Cycle 2 PCR products visualised on a 3% agarose/TAE gel (2.2.4.1) showed a product of corresponding to approximately the right size, of 73bp (lanes 2-7), however a product of a similar size (circled) is visible in the negative control (lane 1) (Figure 3.4). The negative control contained the same reaction components except without the template DNA to amplify, which obviously cast doubt over the validity of the results. As well as contamination despite the use of *Nt.A/wI* as nicking enzyme to prevent concatamer formation some higher molecular weight laddering also occurred (arrowed). Even after repeated attempts at this second cycle and the previous cycle (using different reagents) the issue of contamination was still persistent in the same manner as previously observed. The source of the contamination was investigated (results not shown) and it was eventually discovered that the MAX oligonucleotide primer stocks had been unintentionally contaminated by other workers. As new oligonucleotide stocks had to be ordered it was decided to re-design the oligonucleotide sequences (Table 2.6) to avoid these issues in case any other reagents were contaminated. Therefore if there was any contamination present it should no longer be amplified up as contrastingly different primer sequences were now used.

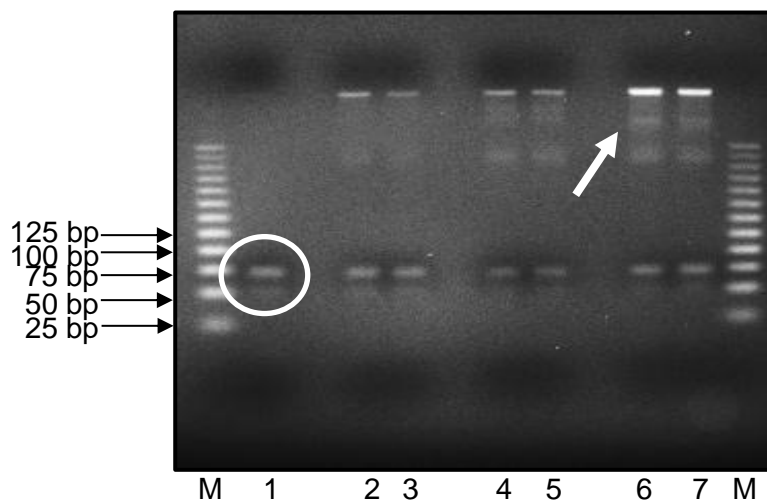


Figure 3.4 Oligonucleotide Contamination and Concatemers. Agarose gel image of PCR products generated from diluted round 2 ligation (F, W, and Y). Lanes: 1: Negative control (no template DNA); 2-3: 1/1000 ligation dilution; 4-5: 1/100 ligation dilution; 6-7: 1/10 ligation dilution. Each dilution appeared to be the correct length of 73 bp with smaller molecular weight products (~50 bp) visible. Higher molecular weight concatamers (arrowed) were also visible in lanes 2-7 whilst there was contamination (circled) visible in lane 1. Samples were electrophoresed on 3% agarose/TAE gel against 0.36 μ g of Promega 25 bp step ladder.

3.4 ProxiMAX Saturation Cycling with Re-designed MAX Oligonucleotides

MAX oligonucleotide sequences were re-designed to be different from that of the originals (Table 2.2). The length of the MAX sequence was kept at 31 bp but the sequence was altered to avoid the amplification of any previous contamination. To aid in the handling of the DNA the conserved base sequence was extended from 39 bp to 69 bp thus meaning that a successful ligation of a MAX sequence to it would create a product of 100 bp.

Again the new oligonucleotides were purchased as ssDNA so had to undergo hybridisation, as described in 2.2.2.1, and quantification using a Quant-iT™ PicoGreen® dsDNA assay (2.2.2.2) as shown in Figure 3.5 and Table 3.3. The new oligonucleotides were then ready for saturation cycling using the same library build as described in Table 3.2.

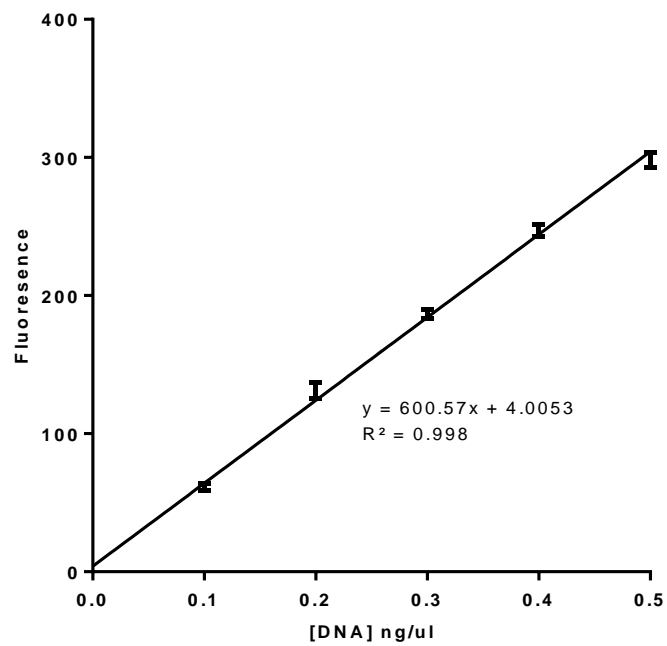


Figure 3.5. Picogreen Standard Curve. Lambda DNA was diluted to a range of 0-1.0 ng/ μ l in TE buffer. This was further diluted 1:1 with 200x diluted picogreen reagent and fluorescence measured at 480 nm excitation and 520nm emission. A standard curve was plotted with DNA concentration on the x axis and fluorescence on the y axis.

Oligo	Fluorescence				[DNA] ng/ μ l	Mol	Concentration/ μ M
	1	2	3	Mean			
A	225.69	221.95	231.48	226.37	36.97	4.31E-06	4.31
C	288.70	306.27	233.23	276.07	45.25	5.27E-06	5.27
D	186.87	195.45	188.30	190.21	30.95	3.61E-06	3.61
E	160.78	167.83	164.48	164.36	26.65	3.11E-06	3.11
F	290.57	302.80	298.81	297.39	48.80	5.69E-06	5.69
G	185.39	225.02	225.34	211.92	34.57	4.03E-06	4.03
H	249.44	295.33	277.43	274.07	44.91	5.23E-06	5.23
I	139.37	142.93	213.14	165.15	26.78	3.12E-06	3.12
K	152.94	164.71	167.01	161.55	26.18	3.05E-06	3.05
L	284.79	265.74	331.34	293.96	48.23	5.62E-06	5.62
M	225.47	223.16	220.73	223.12	36.43	4.25E-06	4.25
N	310.86	291.46	290.87	297.73	48.85	5.69E-06	5.69
P	98.78	230.79	297.98	209.18	34.11	3.98E-06	3.98
Q	224.64	256.63	224.32	235.20	38.44	4.48E-06	4.48
R	267.17	285.13	284.47	278.92	45.72	5.33E-06	5.33
S	146.75	141.38	144.01	144.05	23.27	2.71E-06	2.71
T	260.81	260.88	297.64	273.11	44.76	5.22E-06	5.22
V	301.17	318.45	315.17	311.60	51.16	5.96E-06	5.96
W	206.44	218.05	212.27	212.25	34.62	4.04E-06	4.04
Y	296.41	296.28	304.57	299.09	49.08	5.72E-06	5.72
BASE	236.08	268.37	251.1	251.85	41.22	9.05E-07	0.91

Table 3.3. Re-designed MAX Oligonucleotide Picogreen Measurements. Picogreen measurements. 50x diluted hybridised MAX oligonucleotides were mixed with 200x diluted picogreen reagent and the fluorescence measured at 480 nm excitation and 520 nm emission. Concentration was then calculated using the standard curve from Figure 3.5.

The ligation and PCR of first cycle of the library build using redesigned MAX oligonucleotide was performed successfully (Figure 3.6 A). Importantly the negative control in lane 1 was clear and showed no sign of the previous contamination. Lanes 2-7 showed a product approximately 100 bp in size, albeit extremely faint in lane 2, as expected. A smaller band of approximately 65-70 bp was also observed in lanes 2-7. Although the presence of the secondary product could reduce the efficiency of the MAX oligonucleotides, ligation to the base sequence in this case it was deemed suitable to continue as the concentration of MAX oligonucleotides used was sufficiently high to cover the relatively small theoretical library diversity of 1.08×10^3 , so reduced ligation efficiency should only have a minimal effect. The

saturation cycling was continued successfully for a further 5 cycles according to the plan described in Table 3.2 and the resulting PCR's visualised on 3% agarose gels (Figure 3.6 B-F). The lower molecular weight band was present throughout the entire process.

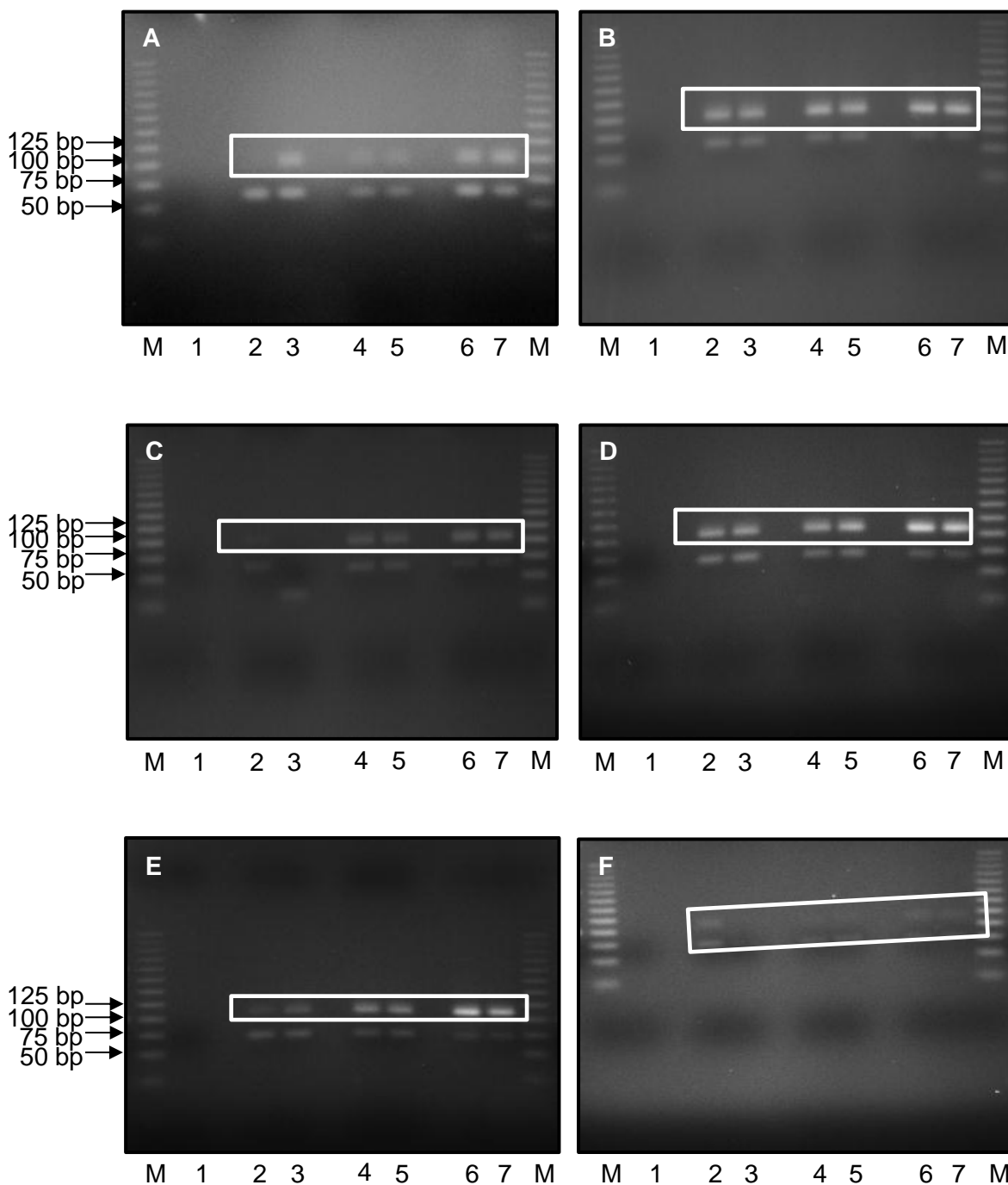


Figure 3.6. Saturation Cycling with Re-designed MAX Oligonucleotides. Agarose gel image of PCR products generated from each cycle ligation using redesigned MAX oligonucleotides (A: Round 1: A, G, I, L, V; B: Round 2: F, W, Y; C: Round 3: D, E; D: Round 4: N, Q, S, T; E: Round 5: H, K, R; F: Round 6: C, M, P). Lanes: 1: Negative control (no template DNA); 2-3: 1/1000 ligation dilution; 4-5: 1/100 ligation dilution; 6-7: 1/10 ligation dilution. Anticipated MW of rounds 1-6 PCR products: R1: 100 bp; R2: 103 bp; R3: 106 bp; R4: 109 bp; R5: 112 bp; R6: 115 bp. Lower molecular weight products were also observed

during some of the rounds. Samples were electrophoresed on 3% agarose/TAE gel against 0.36 µg of Promega 25 bp step ladder.

To determine whether the saturation cycling had successfully added a codon per cycle the PCR product of every cycle was electrophoresed on a 10% polyacrylamide gel (2.2.4.3) with the round 1 PCR product in lane 1 through to the round 6 PCR product in lane 6 (Figure 3.7). The increase in size of the PCR product was evident from 100 bp in round 1 to 115 bp in round 6 showing that each cycle had added a single codon. The lower molecular weight band that was observed throughout the process was also visible and it too showed an increase in size throughout the saturation cycling procedure.

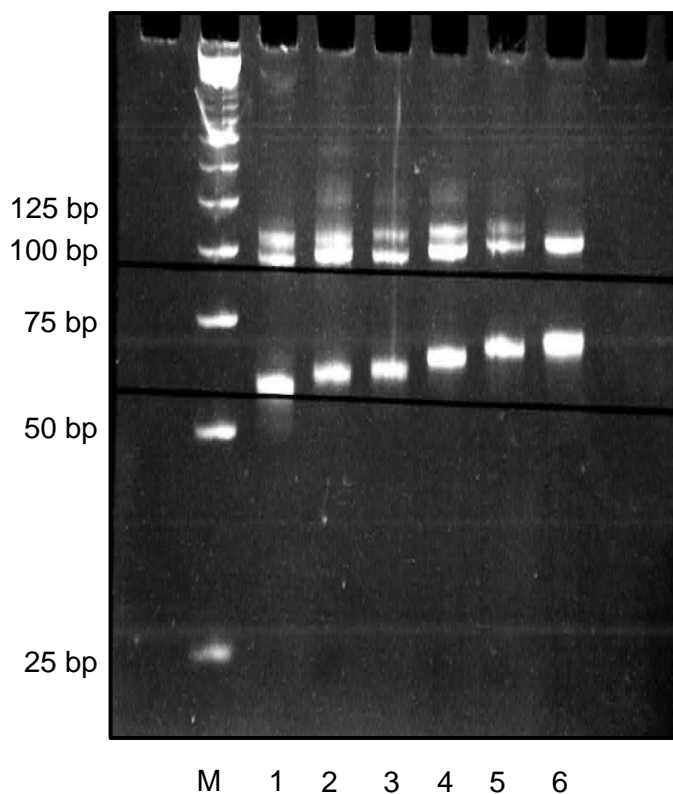


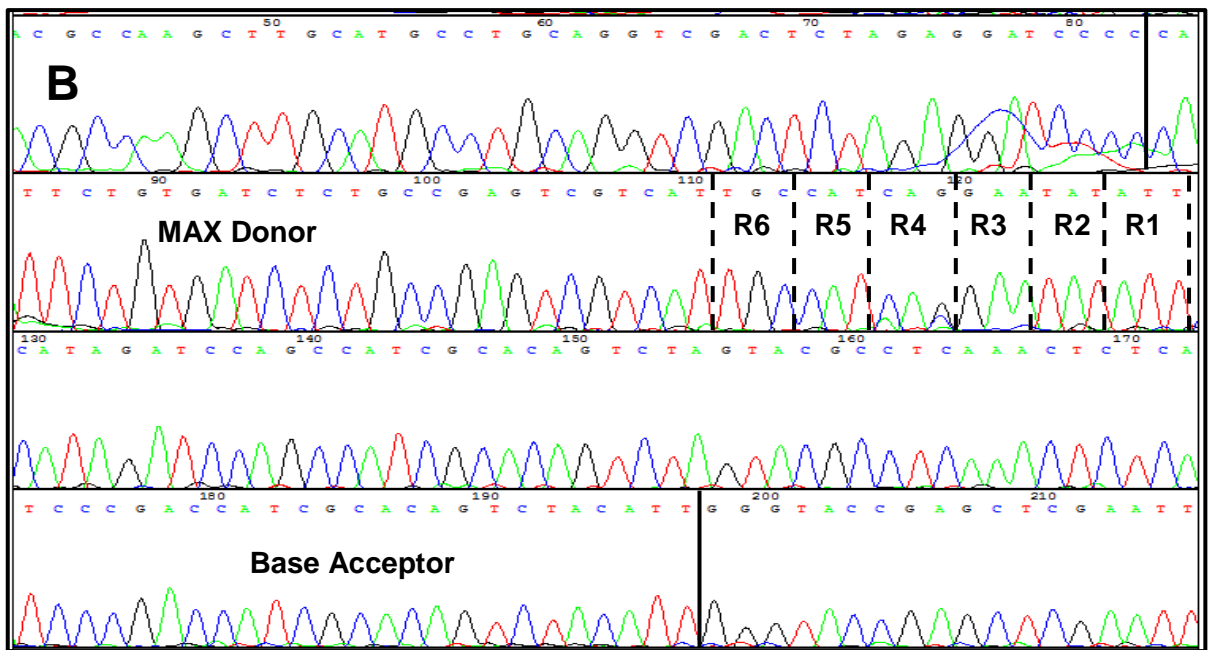
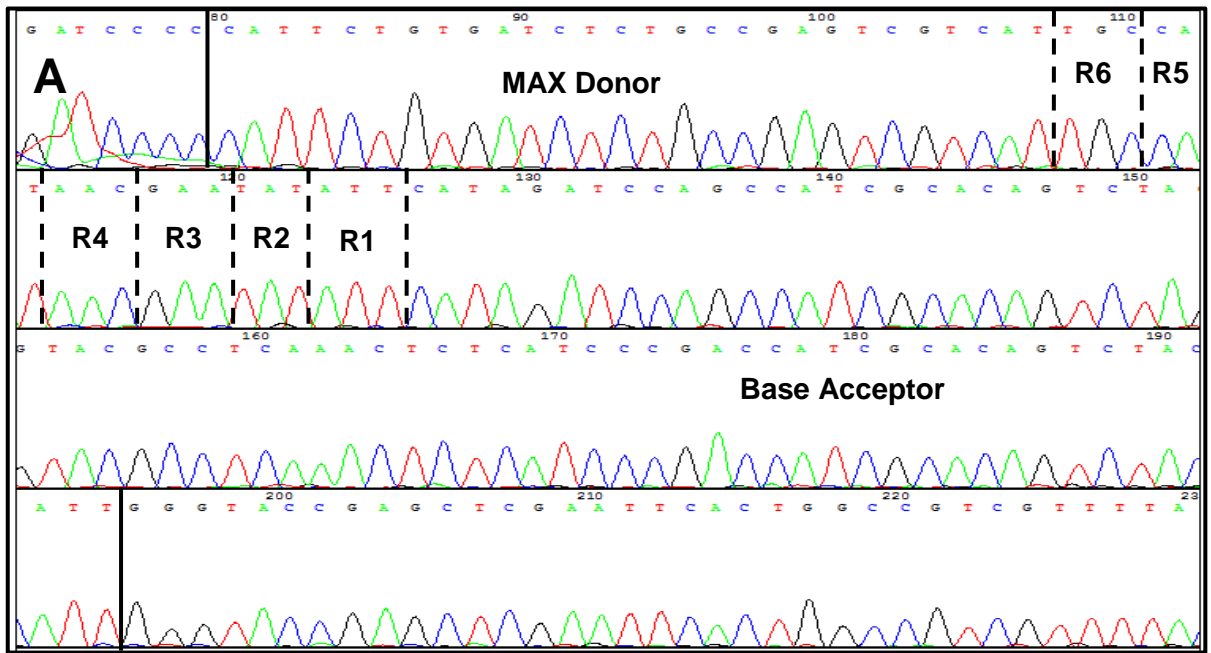
Figure 3.7. Six Cycle Comparison of Saturation Cycling PCR Products. Agarose gel image of the PCR products generated from each round of saturation cycling. Lanes: 1: Round 1 PCR product (100 bp); 2: Round 2 PCR product (103 bp); 3: Round 3 PCR product (106 bp); 4: Round 4 PCR product (109 bp); 5: Round 5 PCR product (112 bp); 6: Round 6 PCR product (115 bp). Correct size PCR products were seen to be increasing throughout the saturation cycling process, as well as the lower molecular weight product (~55 bp-70 bp). Samples were electrophoresed on 10% polyacrylamide/TBE gel against a Promega 25 bp step ladder.

3.5 Completed Library Analysis

In order to assess whether the ProxiMAX process had worked successfully, the cycle 6 PCR product, that should contain the full length 6 randomised positions, was purified (2.2.4.2), phosphorylated (2.2.1.1), blunted-end ligated into the multiple cloning site of *Sma*I phosphatased pUC19 (2.1.6.1) and sent to undergo sequencing using standard M13 primers at the University of Birmingham's Functional Genomics, Proteomics and Metabolomics Facility. As it was seen to be increasing in size through the process it was deemed prudent that the lower molecular weight product, observed in Figure 3.7, was also sent for sequencing.

The sequencing results (Figure 3.8 A & B) showed the correct sequence for the cycle 6 MAX donator and the base acceptor within the pUC19 multiple cloning site. These regions were flanking a series of six codons corresponding to an appropriate MAX codon per cycle. The "wobble" in the sequence read immediately upstream of the MAX donator sequence present in all the sequencing results was determined to be an artefact from the sequencing reaction. The sequencing results of the smaller molecular weight product (Figure 3.8 C) again showed the full sequence of the cycle 6 MAX donator oligonucleotide followed by the expected codons based on the mixes that were added at each cycle. However it only showed a partial sequence for the base acceptor suggesting that there was a secondary primer annealing site allowing creating of the smaller product in the first cycle of PCR. Although reduced in size this was still able to undergo the same processes as the full size product thus creating an array of 6 randomised codons albeit on shorter DNA framework.

This showed that the process of adding a single correct codon cycle by cycle was functioning correctly although it was noted that in this small sample there was virtually no diversity. In fact all showed the same codons added at each cycle apart from a glutamine (CAG) present in round 4 of Figure 3.8 B as opposed to asparagine (AAC) seen in the others. In order to better understand diversity of the library the undigested cycle 6 PCR product was tagged with MiSeq primers (Table 2.4) and analysed using Illumina MiSeq next-generation sequencing.



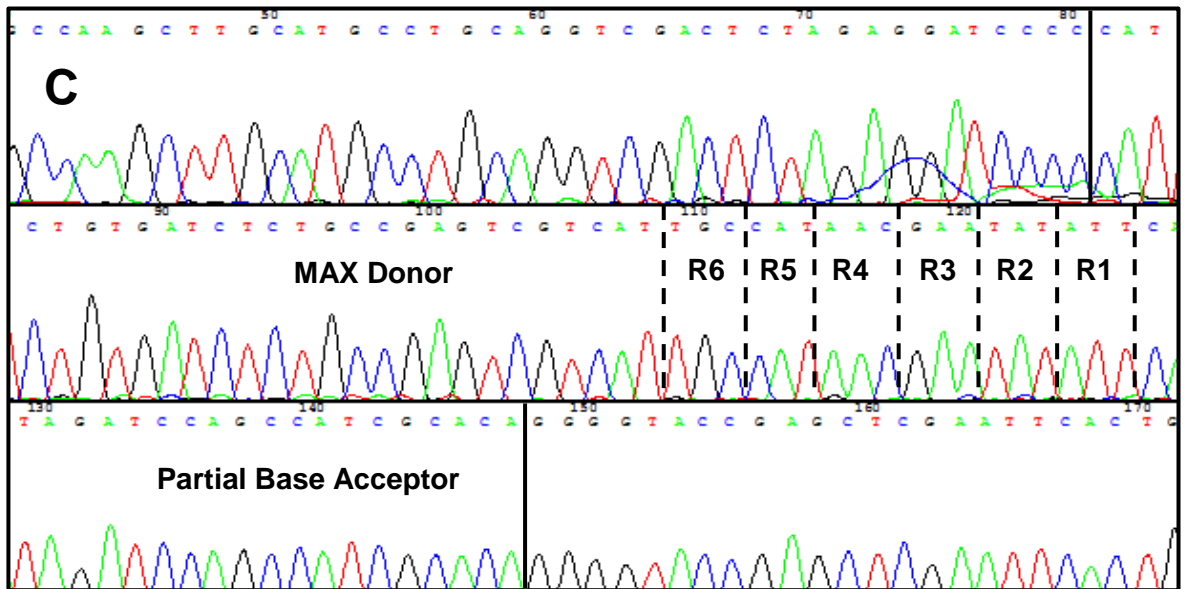


Figure 3.8. Sequencing Results Randomised Array. Round 6 PCR products were inserted into the pUC19 plasmid, transformed into *Escherichia Coli* DH5α and subsequently cloned. The resulting colonies were screened using colony PCR and positives were sequenced using an ABI 3730 capillary sequencer (University of Birmingham). At the 5' end is the round 6 MAX donator region, followed by each MAX codon added by a round of saturation cycling, and the base acceptor at the 3' end (A & B), and a partial 3' base acceptor (C).

The MiSeq next-generation sequencing read a total of 31611 sequences with 26467 having the correct 10 bp flanking regions. Just over 95% of those sequences were the correct length and contained the full length library. The majority of the remaining 4.93% consisted of sequences containing either a 1 bp deletion (4.39%) or 1 codon deletion (0.45%) (Table 3.4). Due to the use of small subsets of codons at each cycle the theoretical expected library size of 1.08×10^3 was relatively small and the sequencing results easily covered 100% of the library (Table 3.6).

Length	Count	%
18	25163	95.07%
17	1161	4.39%
15	120	0.45%
16	10	0.04%
12	6	0.02%

Table 3.4. MiSeq Library Length Distribution. The cycle 6 PCR product was tagged with MiSeq primer (Table 2.4) as described in 2.2.2.7. A total of 31611 sequences were analysed with 26467 having the correct 10 bp flanking regions. 95.07% of these sequences were the correct length with sequences containing a 1bp deletion or 1 nucleotide deletion the next highest frequency (4.39% and 0.45% respectively).

Analysis of the codon representation of each cycle however showed there was significant bias to single codons at each position (Figure 3.9). When comparing the expected codon representation to the observed positions 1, 2, 3 and 5 showed virtually 100% representation of a single codon (R1: I, R2: W, R3: E, R5: H), although whilst position 4 and 6 showed slightly more varied representation they were still significantly biased (R4: N, R6: C). Further analysis did highlight a mistake in the R3 aspartic acid oligonucleotide explaining its absence although all other biases appeared to be as a result of the procedure.

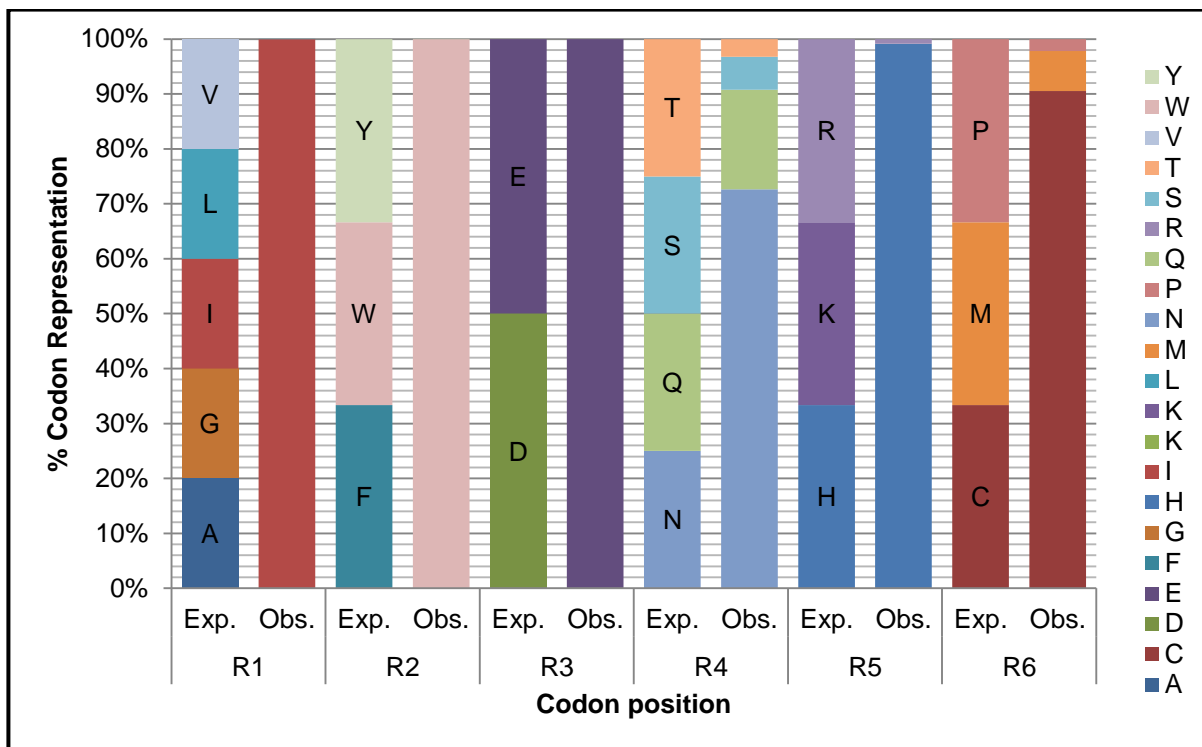


Figure 3.9. Codon Representation of Single Reaction Equimolar Library. Next-generation sequencing results using MiSeq tagged cycle 6 PCR products. Library was assembled as described 2.2.3 and sequenced using a MiSeq sequencer according to the manufacturer's instructions. Data represent the analysis of 26467 sequences with the flanking region, which comprised 95.07% of correct length sequences.

Table 3.5 backed up the severe bias observed in the codon representation. A single sequence of the library was present 16222 times (out of 25163) whereas there were only 53 unique sequences present. In total this library only represented 9.7% of its potential diversity (Table 3.6). From this library data it was clear that although the process of codon-by-codon additions was working correctly the library diversity and codon representation was far from acceptable.

Occurrences	Count
1	53
2	18
3	5
4	4
5	6
6	4
9	1
12	1
26	1
43	1
75	1
171	1
318	1
431	1
745	1
1315	1
4136	1
16222	1

Table 3.5. Library Sequence Diversity. The number of sequences observed and the frequency they occurred within the library. Based on a theoretical maximum diversity of 1.08×10^3 and a total of 25163 read, if the library was evenly represented the most common occurrence should be ~23 copies.

Theoretical expected Library Diversity (Dmax)	1.08×10^3
No. of MiSeq sequences with correct flanks & 18 nt long	25163
Expected number of variants in Sequenced library ($V = D_{\max}(1 - e^{-T/D_{\max}})$)	1.08×10^3
No. of different peptide sequences	105
Expected Completeness of library (V/D_{\max})	100.0%
Diversity represented (No. of different sequences in library / V)	9.7%

Table 3.6. Mathematical Analysis of Library Diversity. Mathematical analysis of potential library diversity as described in (Bosley and Ostermeier, 2005). Dmax: Theoretical expected Library Diversity; V: Expected number of variants in Sequenced library.

3.6 Discussion

Despite the cycle-by-cycle additions working correctly the codon representation was greatly biased. Given the theoretical library size of 1080 compared to the number of correct length sequences read (25163), if the library was evenly represented there should be approximately 23 copies of each sequence (Table 3.5), although due to the biased codon representation this was not the case. Due to the fact that 100% of the potential library diversity is covered by the next generation sequencing there is no doubt that these results are correct.

Having identified the areas where codon bias, as well other issues, can be introduced it is necessary to implement changes to the ProxiMAX process in order to minimise these. Whilst this may initially complicate the process it is necessary in order to achieve a core goal of the process- to produce high quality libraries with good control over codon representation. Improvements could include, but are not limited to: 1. The use of hairpin MAX oligonucleotides to increase stability; 2. Alternative methods of oligonucleotide quantification to improve the accuracy of MAX oligonucleotide stock quantification; 3. Individual ligations, rather than a single pool, of MAX oligonucleotides that are subsequently pooled after a quantification step; 4. Optimised PCR cycle conditions to reduce the amplified bias in earlier cycles; 5. Optimal digestion conditions to minimise any *MlyI* star activity; 6. A gel purification steps after the digestion to minimise the carry-over of any unwanted products to the following cycle. Some of these approaches will be further discussed in Chapter 4.

As this process consists of a series of sequential steps to construct the randomised regions there are a number of specific areas the codon bias may be introduced, namely; differing oligonucleotide quality, error in oligonucleotide concentration, T4 ligase sequence preference during blunt end ligation, amplification bias during PCR or *MlyI* star activity and sequence preference. Whilst the stock MAX oligonucleotides are supplied at a specified concentration in truth there may be variation in the net concentration across the all the different sets. This in combination with the likelihood that the hybridisation is not 100% efficient across the board made it necessary to quantify the stock MAX oligonucleotides prior to use. However, error during the quantification process can have great ramifications later and throughout the

ProxiMAX process potentially leading, or at least contributing, to the codon bias that was observed.

Further analysis of the whole library shows that 95.5 % of the single nucleotide deletions (n-1), which equated to 4.4% of the total library, contain a deletion in the 3rd nucleotide of the R6 addition. This primarily consisted of a 3' guanine deletion (98.6%) in the codons for methionine and proline (ATG and CCG) with the methionine codon making up the majority of deletions at 89.1%. The most likely explanation for this deletion is error during oligonucleotide synthesis as the nucleotide at the 3' position of each MAX codon is the terminal nucleotide added during synthesis of the MAX oligonucleotide. As the majority of these deletions were observed in the R6 methionine codon the error may be localised to a single defective oligonucleotide, although the number of 3' guanine deletions observed in the proline codon as may suggest a larger issue with the guanine addition at the terminal position for all MAX oligonucleotides. Guanine is also present at the terminal position at R1 alanine (GCG) and valine (GTG), R2 tryptophan (TGG) and R4 glutamine (CAG). Position 1 was almost completely biased to isoleucine with neither alanine nor valine present in the either the full library or the n-1 deletions. Therefore it is not possible to tell whether these were incomplete or not. On the other hand R2 tryptophan and R4 glutamine were present in comparable percentages in the complete library and the n-1 sequences with no 3' guanine deletions at these positions were observed. Based on this it is unlikely that this larger problem with oligonucleotide synthesis, although it cannot be completely ruled out, and is more likely to be localised to the R6 methionine, and possibly the R6 proline, oligonucleotide.

The codon representation observed in these n-1 sequences is largely the same as observed in the full length library, with the exception of R6 where the majority of sequences contain the methionine as previously discussed. If the methionine deletions are corrected and incorporated into the complete library the representation for the methionine codon increases from 6.9% to 10.7%. The remaining n-1 deletions (0.2% of the overall population) occur at such low numbers and in spurious positions throughout the library sequence that they are

most likely due to general error rates associated with polymerases used in PCR and sequencing.

Error in oligonucleotide quantification may have been introduced by using the Picogreen[®] assay to quantify the oligonucleotides after hybridisation. A downside to using this assay is that the Picogreen[®] reagent is light sensitive and can quickly degrade, therefore quantification measurements can be variable and may not give a true representation of the oligonucleotide concentration. Secondly, once quantified and stored, the hybridised double-stranded oligonucleotides may dissociate, over time, from one another causing variations in the true concentrations of the double-stranded oligonucleotide stocks. As result of these potential variations in oligonucleotide stock concentrations, oligonucleotides may be comparatively over- or under-represented.

The use of T4 DNA ligase for blunt ended ligation in a single reaction of mixed oligonucleotides was also considered as a source from which codon bias could be introduced. As there are no apparent specificity factors involved in blunt-ended ligation one would assume that ligase would exert itself equally on all constituent members in single reaction of mixed oligonucleotides. However, if T4 DNA ligase demonstrates sequence specificity and favours certain sequences/terminal codons over others this variation would be carried through the individual cycle, and the ProxiMAX process as a whole, leading to wide ranging codon representations and biases.

Due to the cyclical nature of PCR any bias introduced in the earlier cycles would also be amplified exponentially during the later cycles and effectively diluting out those under represented sequences. This may be a contributing factor to the extreme codon bias observed in early cycles (bias in R3 due to erroneous oligonucleotide) with this reducing slightly in the later cycles. Optimising PCR conditions and reducing the number of cycles may help to reduce this.

Another factor that may have an effect on the procedure is the restriction digest. As is the case with many other restriction endonucleases *MlyI* is susceptible to star activity/relaxed specificity if the digestion is not carried out under optimal conditions. Factors such as high

enzyme concentration, ionic strength, high pH and glycerol concentration (>5%) can contribute to star activity. In the case of *MlyI* it is advised by the manufacturers not to exceed 15 units/ μg of DNA. Typically 10 units of *MlyI* were used to digest the PCR, which in turn would typically contain $\sim 1\text{-}5$ μg of DNA, therefore as this was well within the working guidelines star activity as a result of high enzyme concentration should be minimised. The ionic conditions and pH should also be optimal for the digest as the PCR underwent spin column purification prior to the digest. Finally, glycerol concentration should have minimal effect as the final concentration in the digestion was 1% (1 μl of the enzyme, containing 50% glycerol, in a 50 μl reaction). Taking this into account, analysis of the MiSeq data showed that incorrect products represented <0.8% of the total library (taking in to account for the 4.2% n-1 deletions from the faulty R6 methionine oligonucleotide as previously discussed), which is in line with general experimental error. Visual inspection of the digestions on agarose gels showed clean digestions with no unwanted by products, although when dealing with such short oligonucleotides an agarose gel may not be able to resolve the difference. Therefore, based on this evidence it is unlikely that any potential star activity would have had a significant effect on the observed codon representation, although as with any enzymatic reaction it cannot be completely ruled out as to having a potential small contributory effect. A more poignant question would be whether *MlyI* exhibits any major sequence preference outside of its recognition sequence? Whilst due to the use of a precise recognition site, unlike the blunt-ended ligation, it is a specific enzymatic reaction this may also be a factor that introduces codon bias when using *MlyI* to digest multiple different sequences in a single reaction.

Therefore in brief conclusion, although the process of cycle-by-cycle additions appeared to be working correctly it was obviously necessary to further refine the process in order to improve the codon representation at each position.

Chapter 4

Anti-NGF Peptide Library-ProxiMAX Process Refinement

4. Chapter 4: Anti-NGF Peptide Library-ProxiMAX Process Refinement.

4.1. Introduction

An issue with the single reaction ProxiMAX method is that T4 DNA ligase appears to have sequence preference when undertaking blunt ended ligations (Ashraf et al., 2013). Although all enzymatic reactions may be less than 100% efficient, it was concluded that blunt ended ligation using T4 DNA ligase was the primary enzymatic candidate for introducing codon bias into a library as both PCR and digestion rely on specific targets (primers sequence for PCR and recognition site for restriction digests).

Therefore, changes to the ProxiMAX methodology needed to be introduced to circumvent the issue of ligase sequence specificity. A simple way of doing this, rather than using a single reaction containing a mix of MAX of oligonucleotide ligating to an acceptor sequence, was to set up multiple, single ligation reactions containing a single MAX donor that would ligate to the acceptor. These single reactions would then be amplified separately, quantified and mixed together at an equimolar concentration. Although this procedure may consume slightly more time and material it was deemed beneficial.

The use of single stranded oligonucleotides was also considered to be an area where changes could be made. Previously, after hybridisation double stranded oligonucleotides were quantified using Quant-iT™ PicoGreen® dsDNA assay, although its sensitivity to light may cause erroneous results. To overcome this issue, it was decided to use single stranded oligonucleotides that would self-hybridise to form hairpins, which are subsequently quantified by UV spectrometry. These hairpins should be more stable whilst they should also help to reduce concatamer formation by reducing the availability of ligation positions i.e. they are only able to ligate at one end. No nicking enzymes, to prevent concatamer formation would be required, thus providing process simplification. The separate reaction, amplification and quantification method should help resolve this issue too as the PCR products would be quantified before mixing.

To reduce the carryover of unwanted 5'-phosphorylated products that would be suitable for subsequent ligation, an agarose gel purification step was introduced after the *MlyI* digestion, between cycles.

The refined ProxiMAX protocol is illustrated in Figure 4.1. This refined ProxiMAX protocol was used to build a library for a monomeric anti-NGF peptide where an 11 amino acid motif within the peptide would be targeted with different subsets of MAX codons, as described in the following sections.

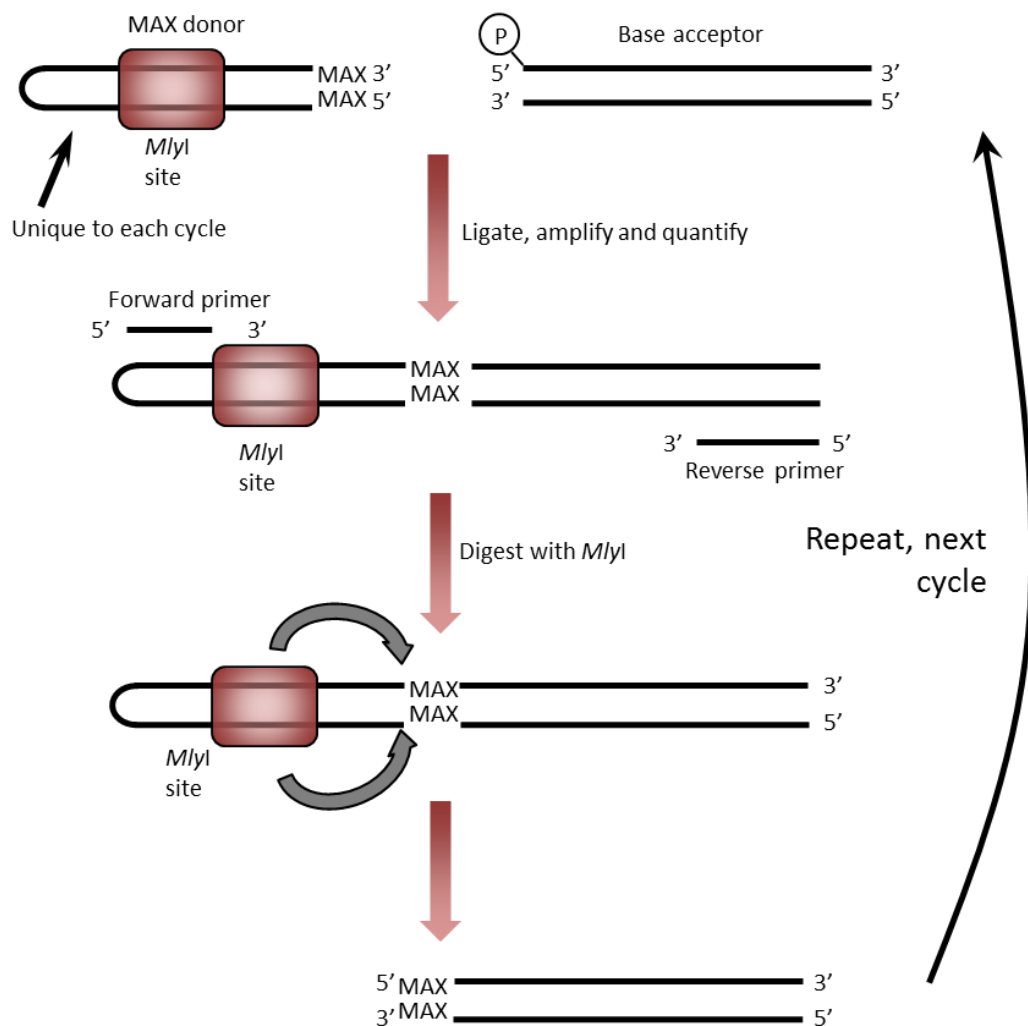


Figure 4.1. ProxiMAX Randomisation Process Illustration. Specially designed 'MAX' hairpins (Table 2.6) are self-hybridised. They are then individually ligated to a conserved base sequence and amplified using *Phusion Hotstart II* polymerase, the resulting product cleaned using QIAGEN QiaQuick kit and subsequently quantified. The cleaned products are mixed to an equimolar concentration, digested with *MlyI* and gel purified to remove unwanted digested material. The ligation/amplification/digestion process is repeated using the digested product of the previous cycle as the base sequence.

	LH Framework							LH ProxiMAX Library				
	LH-6	LH-5	LH-4	LH-3	LH-2	LH-1	LH0	LH1	LH2	LH3	LH4	LH5
Codons	M	A	A	F	K	Q/P	E	GAVS	WFYIVH	P	All (exc. C&M)	NEQDKRH
No.	1	1	1	1	1	2	1	4	6	1	18	7

Table 4.1. LH Anti-NGF Peptide Library Build Overview. The identity of the corresponding groups of MAX codons using LH MAX hairpins in each cycle. The Q/P mutation added at position LH-1 was introduced by a mutagenic primer rather than ProxiMAX randomisation.

	RH ProxiMAX Library						RH Framework			
	RH6	RH5	RH4	RH3	RH2	RH1	RH0	RH-1	RH-2	RH-3
Codons	VILA	YWFL	NEQDKRH	DE	WIRFY	PIVL	S	A	A	A
No.	4	4	7	2	5	4	1	1	1	1

Table 4.2. RH Anti-NGF Peptide Library Build Overview. The identity of the corresponding groups of MAX codons using RH MAX hairpins in each cycle, where DNA encoding the framework sections serves as the acceptor sequence in the revised ProxiMAX process.

As with previous libraries, before the saturation cycling could begin, the frameworks (9.2) needed to be prepared. The RH framework, which consisted of two full complementary single stranded oligonucleotides of 72 bp in length, were obtained from Eurofins Genomics and hybridised by heating to 94°C for 5 minutes followed by cooling at 1°C per min to 4°C (2.2.2.1). The resulting product was amplified using specific primers, in a similar manner as described in 2.2.1.4, and the amplicon subsequently gel purified (2.2.4.2.2).

However, the LH framework was required to be longer in length (152 bp), which was not possible to create from two fully complementary single stranded oligonucleotides due to manufacturer production limitations. In order to overcome this issue, two single stranded oligonucleotides (90 bp and 80 bp respectively) were designed with a complementary 18 bp at the 3' end. These were hybridised by heating to 94°C for 5 minutes followed by cooling at 1°C per min to 4°C (2.2.2.1) and the remaining single stranded sequence filled in using *DNA Polymerase I, Large (Klenow) Fragment* (2.2.1.2) (Figure 4.4). The product was amplified using specific primers, in a similar manner as described in 2.2.1.4. In order to introduce a point mutation at position LH-1 (Table 4.1) a second PCR reaction that was identical to the first apart from a mutagenic primer designed to introduce the point mutation. This was amplified alongside the first reaction under the same conditions. Both LH frameworks were gel purified (2.2.4.2.2), quantified using a nanodrop 2000c (Thermo Scientific) and mixed to equimolar concentrations.

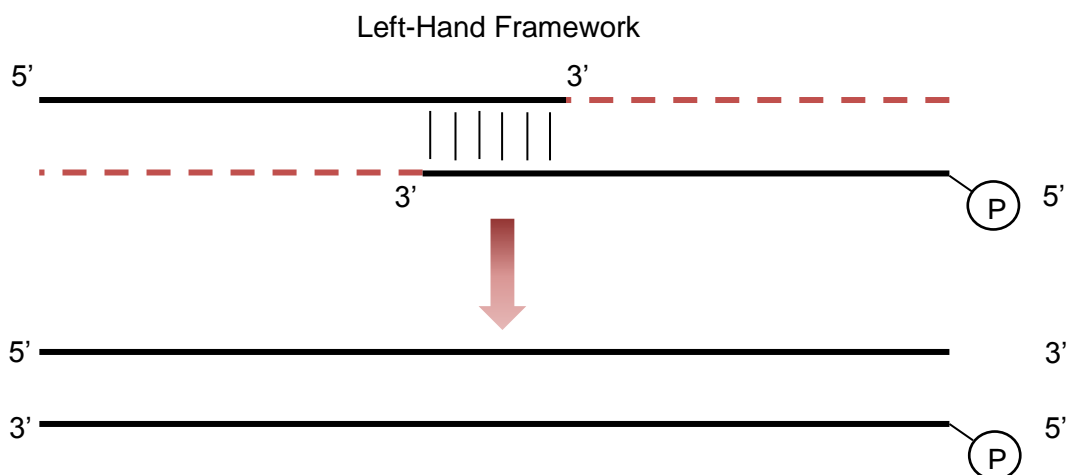


Figure 4.4. LH Framework Construction Overview. RH framework was constructed by standard hybridisation of two complementary single stranded oligonucleotides (2.2.2.1) by

incubating at 94°C for 5 minutes followed by cooling at 1°C per min to 4°C. LH framework was constructed using two single stranded oligonucleotides with a 20 bp complementary region at the 3' end, which was then filled in as described in 2.2.1.2. Frameworks were amplified by PCR (2.2.1.4) using a mutagenic primer to add the mutated position at LH-1.

To allow additions to LH and RH frameworks two different sets of MAX codon donor oligonucleotides were required (9.2). Single stranded MAX hairpins were self-hybridised by heating to 95°C for 2 minutes followed by ramp cooling down to 25°C over 45 minutes. These were quantified in triplicate by UV spectrometry and diluted down to a working concentration of 2.4 μ M (Table 4.3 and Table 4.4).

Amino Acid	Codon	MW	Cycle 1		Cycle 2		Cycle 3	
			Mean ng/ μ l	μ M	Mean ng/ μ l	μ M	Mean ng/ μ l	μ M
A	GCT	26887.6	1222	45.4	1053	39.2	1057	39.3
D	GAT	26886.6	1337	49.7	941	35.0	1070	39.8
E	GAA	26886.6	1235	45.9	996	37.1	1010	37.6
F	TTC	26886.6	1123	41.8	1001	37.2	1029	38.3
G	GGC	26888.6	1098	40.8	961	35.7	1069	39.8
H	CAT	26886.6	1103	41.0	987	36.7	981	36.5
I	ATC	26886.6	1151	42.8	1021	38.0	1285	47.8
K	AAG	26886.6	1302	48.4	1124	41.8	1279	47.6
L	CTG	26887.6	1157	43.0	1010	37.6	1179	43.8
N	AAC	26886.6	1143	42.5	980	36.4	1101	40.9
P	CCG	26888.6	1148	42.7	939	34.9	1080	40.2
Q	CAG	26887.6	1160	43.1	1000	37.2	1213	45.1
R	CGT	26887.6	1132	42.1	1024	38.1	1135	42.2
S	TCT	26886.6	1165	43.3	1035	38.5	1429	53.1
T	ACC	26887.6	2318	86.2	1413	52.6	1284	47.8
V	GTG	26887.6	2048	76.2	1061	39.5	1197	44.5
W	TGG	26887.6	1830	68.1	1025	38.1	1045	38.9
Y	TAC	26886.6	2074	77.1	972	36.1	1061	39.5

Table 4.3. LH Hairpin Quantification. MAX hairpins were diluted from stock to ~40 μ M in 0.5x ThermoPol buffer (2.1.3.13) and self-hybridised by heating to 95°C for 2 minutes followed by ramp cooling down to 25°C over 45 minutes. Hairpins were quantified by UV spectrophotometer in triplicate and diluted down to a working concentration of 2.4 μ M in 0.5x ThermoPol buffer (2.1.3.13).

Amino Acid	Codon	MW	Cycle 1		Cycle 2		Cycle 3	
			Mean ng/ μ l	μ M	Mean ng/ μ l	μ M	Mean ng/ μ l	μ M
A	GCT	26887.6	981	36.5	1050	39.1	1010	37.5
D	GAT	26887.6	1089	40.5	1213	45.1	1281	47.6
E	GAA	26886.6	925	34.4	931	34.6	1063	39.5
F	TTC	26886.6	992	36.9	984	36.6	1003	37.3
G	GGC	26888.6	973	36.2	969	36.0	1024	38.1
H	CAT	26886.6	974	36.2	1098	40.8	1058	39.3
I	ATC	26886.6	933	34.7	1038	38.6	995	37.0
K	AAG	26886.6	984	36.6	1024	38.1	1001	37.2
L	CTG	26887.6	868	32.3	989	36.8	989	36.8
N	AAC	26886.6	946	35.2	1033	38.4	1033	38.4
P	CCG	26888.6	954	35.5	966	35.9	966	35.9
Q	CAG	26887.6	940	35.0	1021	38.0	1021	38.0
R	CGT	26887.6	908	33.8	974	36.2	974	36.2
S	TCT	26886.6	987	36.7	989	36.8	989	36.8
T	ACC	26887.6	934	34.7	944	35.1	944	35.1
V	GTG	26887.6	858	31.9	977	36.3	977	36.3
W	TGG	26887.6	948	35.3	1034	38.5	1038	38.6
Y	TAC	26886.6	879	32.7	962	35.8	1079	40.1

Table 4.4. RH Hairpin Quantification. MAX hairpins were diluted from stock to $\sim 40 \mu\text{M}$ in 0.5x ThermoPol buffer (2.1.3.13) and self-hybridised by heating to 95°C for 2 minutes followed by ramp cooling down to 25°C over 45 minutes. Hairpins were quantified by UV spectrophotometer in triplicate and diluted down to a working concentration of $2.4 \mu\text{M}$ with 0.5x ThermoPol buffer (2.1.3.13).

4.3. ProxiMAX Saturation Cycling of Anti-NGF Peptide Library

Once the MAX hairpins and library frameworks were prepared, the saturation cycling process could begin on both library fragments. To start the LH library, the 152 bp LH framework was ligated separately to the appropriate 36 bp MAX hairpins, according the LH library design in Table 4.1 (2.2.3.2), to form a fragment with a sequence length of 188 bp. The individual ligations were subsequently amplified separately (2.2.3.3) using the appropriate LH universal and cycle primers (Table 2.6) and examined by 3% agarose gel electrophoresis (2.2.4.1), as shown in Figure 4.5 A. Lanes 2-5 show the various MAX hairpin::LH framework PCR products. The pixel density of the individual PCR products was analysed using ImageJ software to give a relative concentration of each product. Based on these relative

concentrations, the PCR reactions were mixed at varying proportions in order to form an equimolar mix of MAX hairpin: LH framework complexes. The equimolar mix of PCR products was then digested with *MlyI* (2.2.2.6) forming two fragments with lengths 155 bp and 33 bp respectively and the larger sized fragment was gel purified (2.2.4.2). This gel-purified DNA fragment was used as the acceptor for the second cycle and the whole process was continued iteratively for a total of five cycles (Figure 4.5 B-D). As illustrated in Table 4.1 the LH3 position was only a single addition (due to critical importance in the peptides' activity) and unlike with the other cycles not quantified and hence is not shown.

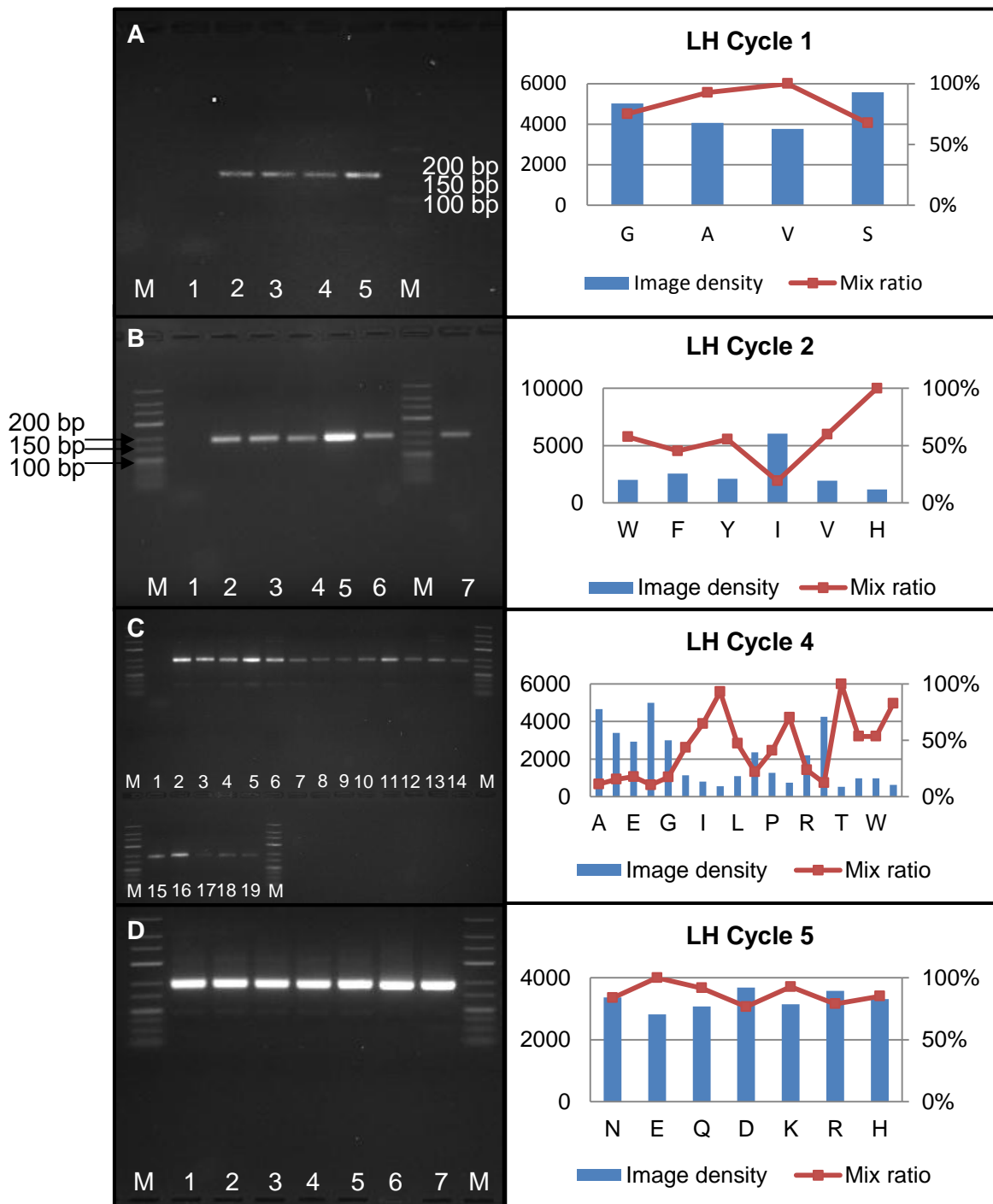


Figure 4.5. Refined Saturation Cycling and Quantification of LH Anti-NGF Library. Agarose gel image of PCR products generated from each cycle of LH additions. **A: Cycle 1:** Lane 1: Negative control; 2: G; 3: A; 4: V; 5: S. **B: Cycle 2:** Lane 1: Negative control; 2: W; 3: F; 4: Y; 5: I; 6: V; 7: H. **C: Cycle 4:** Lane 1: Negative control; 2: A; 3: D; 4: E; 5: F; 6: G; 7: H; 8: I; 9: K; 10: L; 11: N; 12: P; 13: Q; 14: R; 15: S; 16: T; 17: V; 18: W; 19: Y. **D: Cycle 5:** Lane 1: N; 2: E; 3: Q; 4: D; 5: K; 6: R; 7: H. Expected molecular weights; R1: 188 bp; R2: 191 bp; R3: 194 bp; R4: 197 bp; R5: 200 bp. Correct size products are highlighted whilst there are other molecular weight products also visible. Samples were electrophoresed on 3% agarose/TAE gel against 0.1 μ g of Thermo Scientific low range generuler. PCR products were quantified by pixel density after gel electrophoresis and appropriately adjusted to equimolar concentrations.

Both the LH and RH libraries were constructed concurrently. The RH library framework of 72 bp was ligated separately to the appropriate 36 bp MAX hairpins, according to the RH library design in Table 4.2 (2.2.3.2), to form a fragment with a sequence length of 108 bp. The individual ligations were subsequently amplified separately (2.2.3.3) using the appropriate RH universal and cycle primers (Table 2.6) and examined by 3% agarose gel electrophoresis (2.2.4.1), as shown in Figure 4.6 A. Lanes 2-5 show the various MAX hairpin: RH framework PCR products. Some minor products with higher and lower molecular weight products are also visible. The pixel density of the individual PCR products was analysed using ImageJ software to give a relative concentration of each product from which the PCR reactions were mixed at varying proportions in order to form an equimolar mix. This was then digested with *MlyI* (2.2.2.6) forming two fragments with lengths 75 bp and 33 bp respectively and the larger sized fragment was gel purified (2.2.4.2).

This gel purified DNA fragment was used as the acceptor for the second cycle and the whole process was continued iteratively for a total of six cycles (Figure 4.6 B-F). Secondary products of both higher and lower molecular weights were observed throughout the process suggesting possible secondary primer annealing sites or concatamer formation although the quantification and purification steps should negate their overall impact.

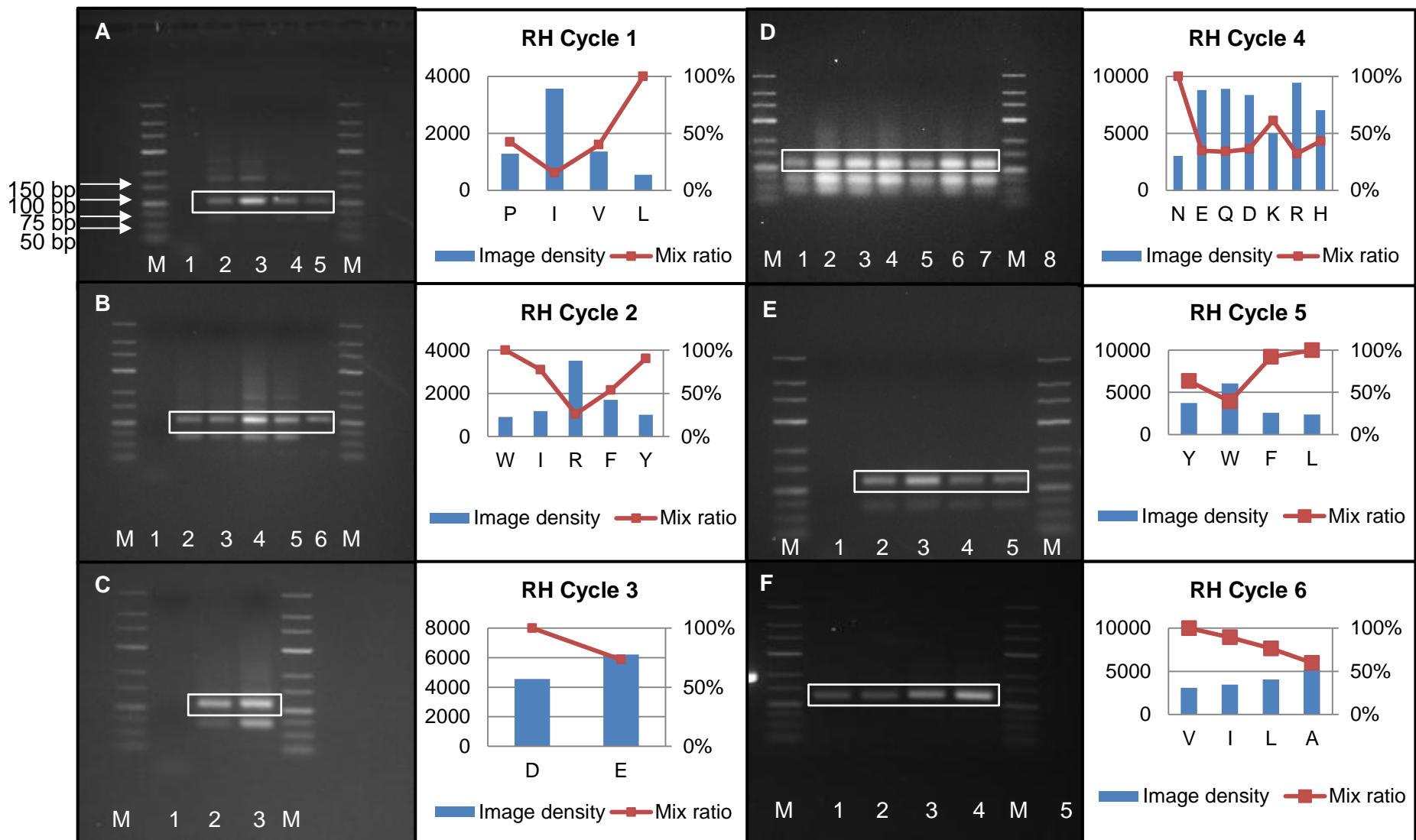


Figure 4.6. Refined Saturation Cycling and Quantification of RH Anti-NGF Library. Agarose gel image of PCR products generated from each cycle of RH additions. **A: Cycle 1:** Lane 1: Negative control; 2: P; 3: I; 4: V; 5: L. **B: Cycle 2:** Lane 1: Negative control; 2: W; 3: I; 4: R; 5: F; 6: Y. **C: Cycle 3:** Lane 1: Negative control; 2: D; 3: E. **D: Cycle 4:** Lane: 1: N; 2: E; 3: Q; 4: D; 5: K; 6: R; 7: H; 8: Negative control. **E: Cycle 5:** Lane 1: Negative control; 2: Y; 3: W; 4: F; 5: L. **B: Cycle 6:** Lane 1: V; 2: I; 3: L; 4: A; 5: Negative control. Expected molecular weights; R1: 108 bp; R2: 111 bp; R3: 114 bp; R4: 117 bp; R5: 120 bp; R6: 123 bp. Correct size products are highlighted whilst there are other molecular weight products also visible. Samples were electrophoresed on 3% agarose/TAE gel against 0.1 µg of Thermo Scientific low range generuler. PCR products were quantified by pixel density after gel electrophoresis and appropriately adjusted to equimolar concentrations.

To determine whether the saturation cycling had successfully added a codon per cycle the PCR product of every cycle was electrophoresed on a 10% polyacrylamide gel (2.2.4.3), with the round 1 PCR product in lane 1 through to the round 6 PCR product in lane 6 (Figure 4.7 A). The increase in size of the PCR product was evident from 108 bp in cycle 1 to 120 bp in cycle 5 showing that each cycle had added a single codon. Unfortunately the cycle 6 product was mis-loaded and was not visible on the gel, although its size had been confirmed previously from the agarose gel electrophoresis to be approximately correct. As these were un-purified mixes of the PCR products some different molecular weight products are also visible across the lanes. Unfortunately due to its larger size it was not possible to resolve a 3bp difference between LH library PCR products.

Once both LH and RH library fragments were complete they were blunt end ligated to each other (2.2.1.3) to form a full length library sequence of 257 bp, which was amplified by PCR (2.2.1.4) and electrophoresed (2.2.4.1) (Figure 4.7 B). This was subsequently tagged with MiSeq primers (2.2.2.7, Table 2.5) and sent for next-generation sequencing.

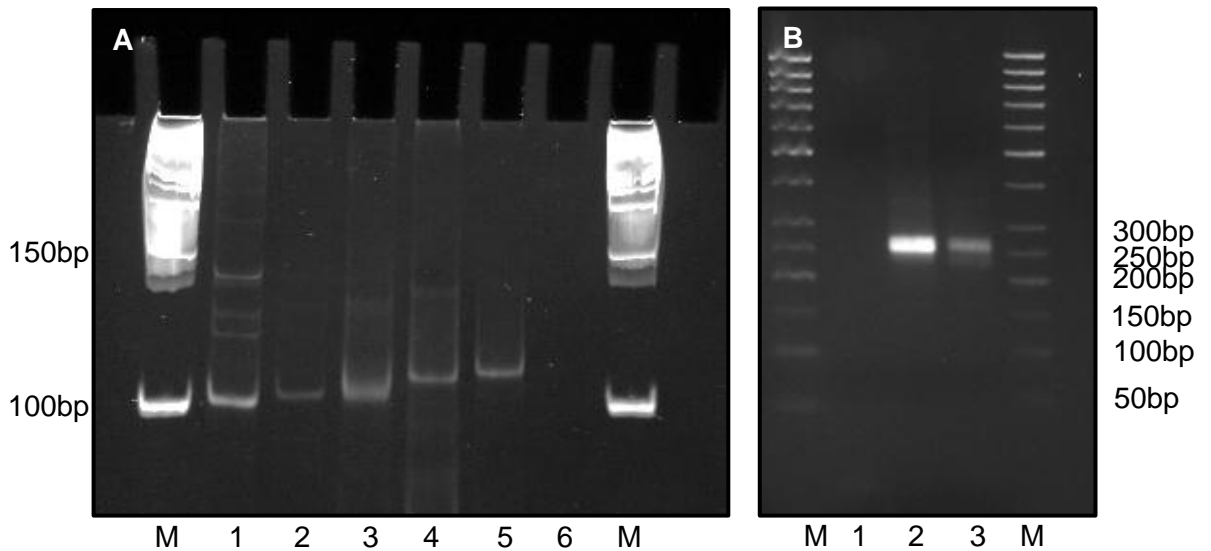


Figure 4.7. RH 6 cycle comparison and LH+RH ligation. **A:** Polyacrylamide gel image of the RH PCR products from every saturation cycling round. Lanes: 1: Round 1 PCR product; 2: Round 2 PCR product; 3: Round 3 PCR product; 4: Round 4 PCR product; 5: Round 5 PCR product; 6: Round 6 PCR product. Expected molecular weights; R1: 108 bp; R2: 111 bp; R3: 114 bp; R4: 117 bp; R5: 120 bp; R6: 123 bp. The molecular weight of the PCR products is seen to be increasing the saturation cycling progresses (R6 PCR product in lane 6 was misloaded so is not visible). Samples were electrophoresed on 10% polyacrylamide/TBE gel against a Thermo Scientific low range generuler. **B:** Agarose gel image of ligated LH and RH library fragments. Lanes: 1: Negative control (no template DNA); 2-3: PCR products of LH + RH ligation. Samples were electrophoresed on 2% agarose/TAE gel against 0.5 μ g of Thermo scientific 50 bp ladder.

4.4. Completed Anti-NGF Peptide Library Analysis

The MiSeq next-generation sequencing read a total of 321340 sequences with 281289 having the correct 10 bp flanking regions. Based on the way NGS data was analysed the length of read corresponding to the full length library should be 72 bp. As demonstrated in Table 4.5, only 5.0% of the correctly-flanked sequences contained the full length library (72 bp) with its corresponding 1bp deletion and 1 codon deletion equating to 0.9% and 1.7% respectively (Table 4.5). The majority of the library consisted of truncated sequences making up 61.4% of the sequences read with its corresponding 1 bp deletion (9.0%) or 1 codon deletion (8.7%) the next two most frequent.

Length (bp)	Count	%
63	172676	61.4%
62	25325	9.0%
60	24540	8.7%
72	14073	5.0%
61	6615	2.4%
59	5628	2.0%
69	4861	1.7%
57	4503	1.6%
71	2426	0.9%

Table 4.5. Anti-NGF Peptide Library MiSeq Length Distribution. The cycle 6 PCR product was tagged with MiSeq primer (Table 2.5) as described in 2.2.2.7. A total of 321340 sequences were analysed with 281289 having the correct 10bp flanking regions. 5.0% of these sequences were the correct length (72) with the respective 1 bp deletion (71) or 1 nucleotide deletion (69) making up 0.9% and 1.7%. The majority of the library (61.4%) consisted of a truncated sequence (63) with the respective 1 bp deletion (62) or 1 nucleotide deletion (60) the next highest frequencies (9.0% and 8.7% respectively).

Obviously there had been a serious issue in the process resulting in the truncation of the library but to examine the encoded amino acid distribution and to discover the location of the truncation, the data were nevertheless analysed.

The codon representation of the 72-mer full length library (that made up 5% of the sequence read) was vastly improved (Figure 4.8) compared to the previous single reaction library (Chapter 4). Whilst not perfect, the observed codon representation was getting much closer to the expected levels with positions LH1 and LH5 showing particularly good correlation between the design and the obtained product. Other positions also showed reasonable correlation, although some codons were still over represented compared with others that were under represented. However position LH 4 showed tyrosine codon was significantly over represented, which was compounded by the fact that this position had the most codons added (18), which should have resulted in an expected codon representation 5.6% each.

Analysis of the truncated library (63-mer) showed that positions LH2-LH4 were missing resulting in the 3 codon truncation, (Figure 4.9) although the source of this truncation was unclear. The observed codon representation for those positions it contained were broadly similar to those observed in Figure 4.8 and much improved on those observed in Figure 3.9.

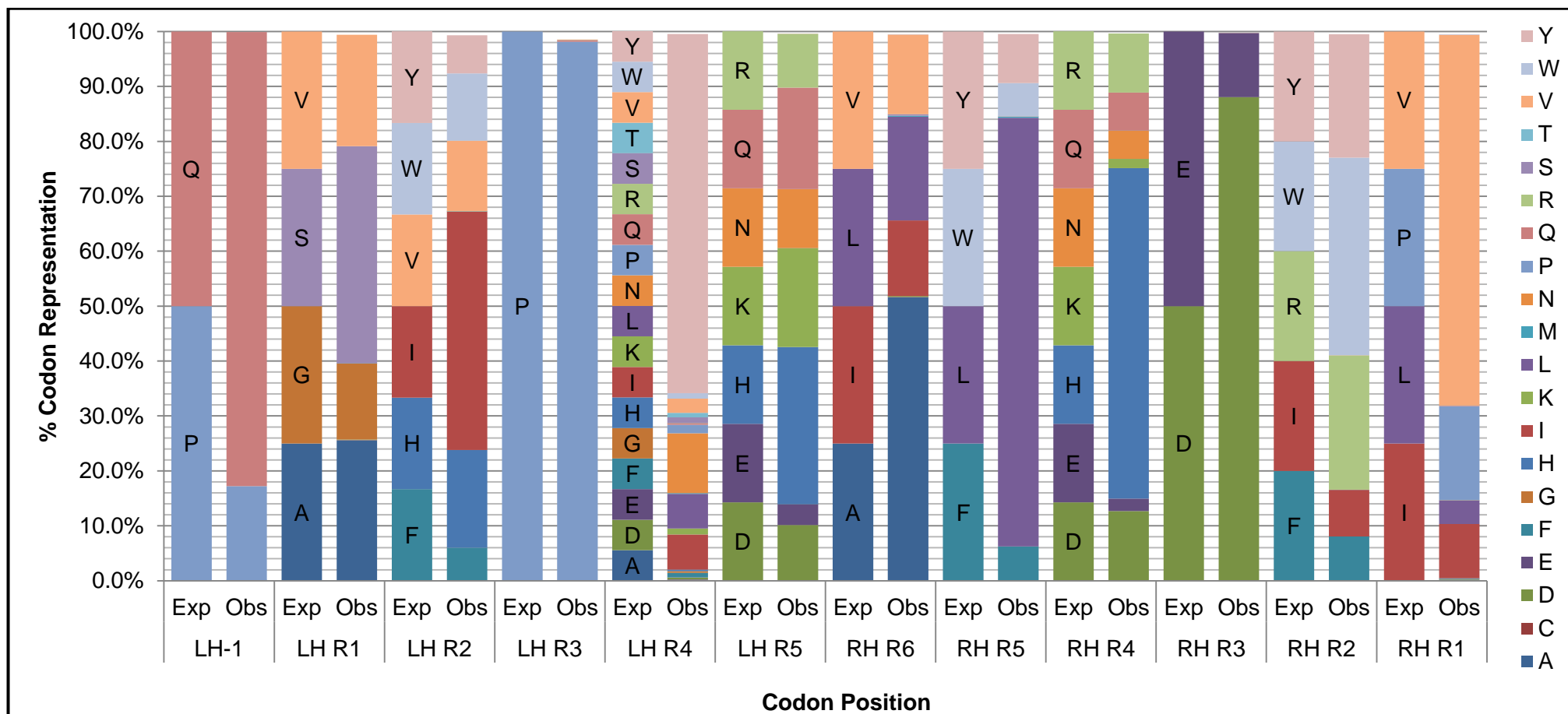


Figure 4.8. Codon Representation of Full length (72-mer) Anti-NGF Peptide Library. Next-generation sequencing results using MiSeq tagged cycle 6 PCR products. Library was assembled as described in 2.2.3 and sequenced using a MiSeq sequencer according to the manufacturer's instructions. Expected codon representation is compared to observed codon representation and data represents the analysis of 281289 sequences with the flanking region, which comprised 5.0% of correct length sequences.

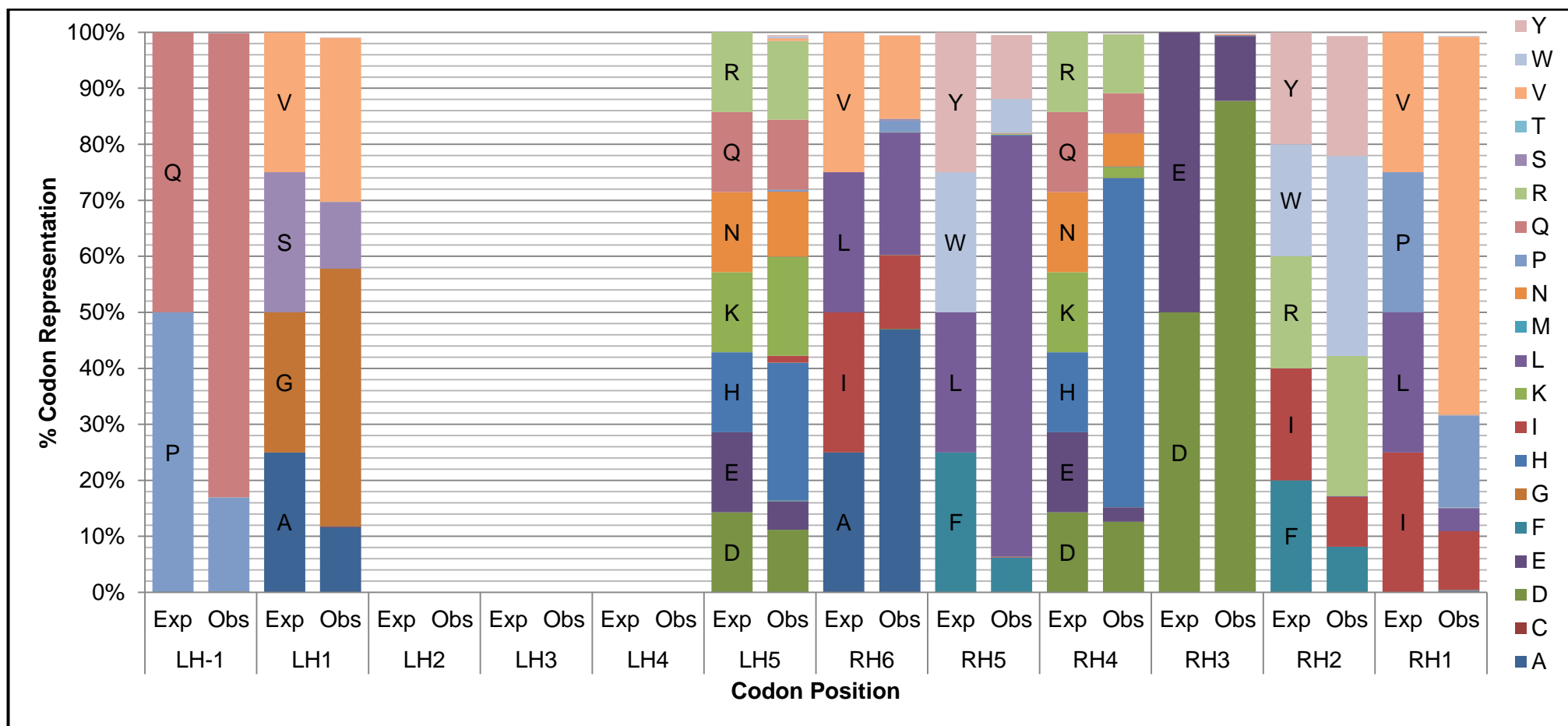


Figure 4.9. Codon Representation of Truncated (63-mer) Anti-NGF Peptide Library. Next-generation sequencing results using MiSeq tagged cycle 6 PCR products. Library was assembled as described in 2.2.3 and sequenced using a MiSeq sequencer according to the manufacturer's instructions. Expected codon representation is compared to observed codon representation and data represents the analysis of 281289 sequences with the flanking region, which comprised 61.4% of correct length sequences.

Mathematical analysis of the sequencing data suggested that the full length (72-mer) library represented close to 87% diversity in those sequences read (Table 4.6), although the 14073 sequences that corresponded to this only covered 0.1% of the theoretical diversity of the library. In contrast, even by adjusting the theoretical diversity of the truncated library to take into account for those missing positions the diversity represented was only 42.7% (Table 4.6). Finally, just fewer than 92% of the sequences that corresponded to the full length occurred only once compared to 70% for the truncated library (Table 4.7).

	72-mer	63-mer
Theoretical expected Library Diversity (Dmax)	2.70x10 ⁷	2.51x10 ⁵
No. of MiSeq sequences with correct flanks & 72/63 nt long	14073	172676
Expected number of variants in Sequenced library (V=Dmax(1-e ^{-T/Dmax}))	1.41x10 ⁴	1.25x10 ⁵
No. of different peptide sequences	12228	53341
Expected Completeness of library (V/Dmax)	0.1%	49.8%
Diversity represented (No. of different sequences in library / V)	86.9%	42.7%

Table 4.6. Mathematical Analysis of Anti-NGF Peptide Library Diversity. Mathematical analysis of potential library diversity as described in (Bosley and Ostermeier, 2005). Dmax: Theoretical expected Library Diversity; V: Expected number of variants in Sequenced library.

Occurrences	72-mer		63-mer	
	Count	Percentage	Count	Percentage
1	11238	91.9%	37641	70.6%
2	663	5.4%	6101	11.4%
3	164	1.3%	2665	5.0%
4	60	0.5%	1511	2.8%
5	35	0.3%	1017	1.9%
6	21	0.2%	729	1.4%
7	15	0.1%	515	1.0%

Table 4.7. Anti-NGF Peptide Library Sequence Diversity for 72-mer and 63-mer. The number of times the same sequence was observed and the frequency they occurred within the library.

The truncation was not observed during the library build because the difference in size was too large to resolve on either agarose or polyacrylamide gel electrophoresis. To overcome the issue of resolving power and to investigate where/when the truncation had occurred, an LH internal primer was designed for use in analytical gels. When used in conjunction with the appropriate MAX primers this would shorten the LH framework whilst keeping the saturated portion intact thus creating a PCR product small enough to give resolution between the difference between cycles.

PCR product from every LH cycle were amplified (2.2.1.4) with the LH internal primer an appropriate cycle primer and was electrophoresed on a 10% polyacrylamide gel (2.2.4.3) (Figure 4.10). Lanes: 1-2: Cycle 1 PCR product; 3-4: Cycle 2 PCR product; 5: Cycle 3 PCR product; 6-7: Cycle 4 PCR product; 8-9: Cycle 5 PCR product. Cycles 1, 2 and 3 looked normal (70bp, 73bp and 76bp respectively), however in cycle 4 a smaller molecular weight product (the truncated library) appeared below the expected band and this was then preferentially amplified in the final cycle.

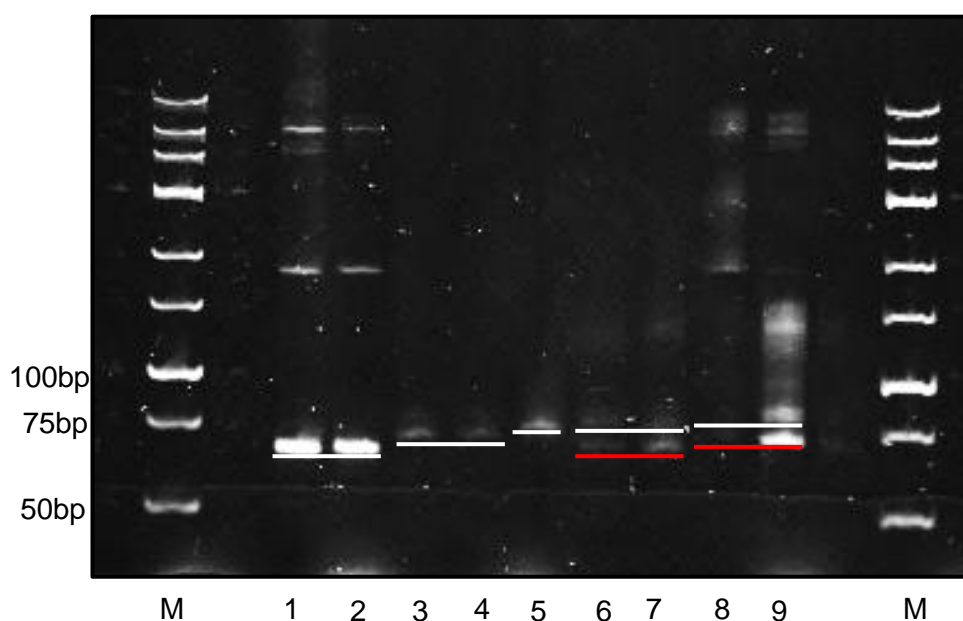


Figure 4.10. LH Internal Amplification Cycle Comparison. Polyacrylamide gel image of LH PCR products from each round of the saturation cycling process. To enable resolution on a polyacrylamide gel the LH framework was shortened using an internal primer whilst leaving the randomised portion unaltered. Lanes: 1-2: Round 1 PCR product; 3-4: Round 2 PCR product; 5: Round 3 PCR product; 6-7: Round 4 PCR product; 8-9: Round 5 PCR product. Expected molecular weights; R1: 65 bp; R2: 68 bp; R3: 71 bp; R4: 74 bp; R5: 77 bp. Expected PCR products, underlined white are seen to be increasing in size throughout the process. Lower molecular weight products, underlined red, are generated in round 4 (lanes

6-7) and begin to increase in size. The products were electrophoresed on 10% polyacrylamide/TBE gel against a Thermo Scientific low range generuler. The gel was stained with a 1x TBE/ethidium bromide buffer (final concentration of 0.5 µg/ml) for 10 minutes and imaged.

4.5. ProxiMAX Saturation Cycling of Resynthesized LH Anti-NGF Peptide Library

Due to the truncation in the LH library and significant bias observed in the LH4 position of the full length library it was decided that the LH library should be re-synthesised to overcome these issues. Although not perfect it was decided that the RH library was at an acceptable level of representation, so that no further action was required. Once the new LH library had been generated, it would be ligated to the original RH library to form the complete, full-length anti-NGF library.

Analysing the codon representation from the previous library (Figure 4.8 and Figure 4.9) it was thought that some of the bias may be as a result of the method of quantification. Although quantification by pixel density allows a relative comparison between bands on a gel, error can still be introduced. This may either be from error in initial sample pipetting or from gel loading, thus creating bias in the final library. Therefore it was decided to change the quantification method to measuring the DNA concentration using a nanodrop 2000c.

Once again, the 152 bp LH framework was ligated separately to the appropriate 36 bp MAX hairpins, according the LH library design in Table 4.1 (2.2.3.2), to form a fragment with a sequence length of 188 bp. The individual ligations were subsequently amplified separately (2.2.3.3) using the appropriate LH universal and cycle primers (Table 2.6) and examined by 3% agarose gel electrophoresis (2.2.4.1) (Figure 4.5). Based on the concentrations determined by nanodrop analysis, the PCR reactions were mixed at varying proportions in order to form an equimolar mix of MAX hairpin: LH framework complexes (Figure 4.11). The equimolar mix of PCR products was then digested with *MlyI* (2.2.2.6) forming two fragments with lengths 155 bp and 33 bp respectively and the larger sized fragment was gel purified (2.2.4.2). This gel purified DNA fragment was used as the acceptor for the second cycle and the whole process was continued iteratively for a total of five cycles (Figure 4.5 B-D).

MAX Codons		[DNA] ng/ul				
		LH1	LH2	LH3	LH4	LH5
A	GCT	15.5			40.5	
C	TGC					
D	GAT				14.2	56.7
E	GAA				24.8	38.6
F	TTC		16.0		34.4	
G	GGC	14.7			38.4	
H	CAT		21.9		37.3	55.2
I	ATC		15.3		27.6	
K	AAG				66.0	42.9
L	CTG				52.9	
M	ATG					
N	AAC				41.2	33.1
P	CCG			22.1	43.0	
Q	CAG				52.9	42.8
R	CGT				55.2	57.8
S	TCT	21.3			47.0	
T	ACC				55.0	
V	GTG	17.8	28.1		49.2	
W	TGG		19.0		36.1	
Y	TAC		19.7		40.2	

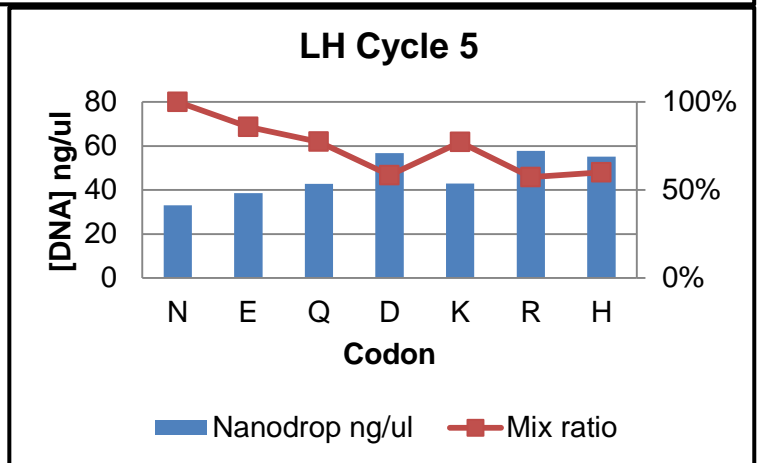
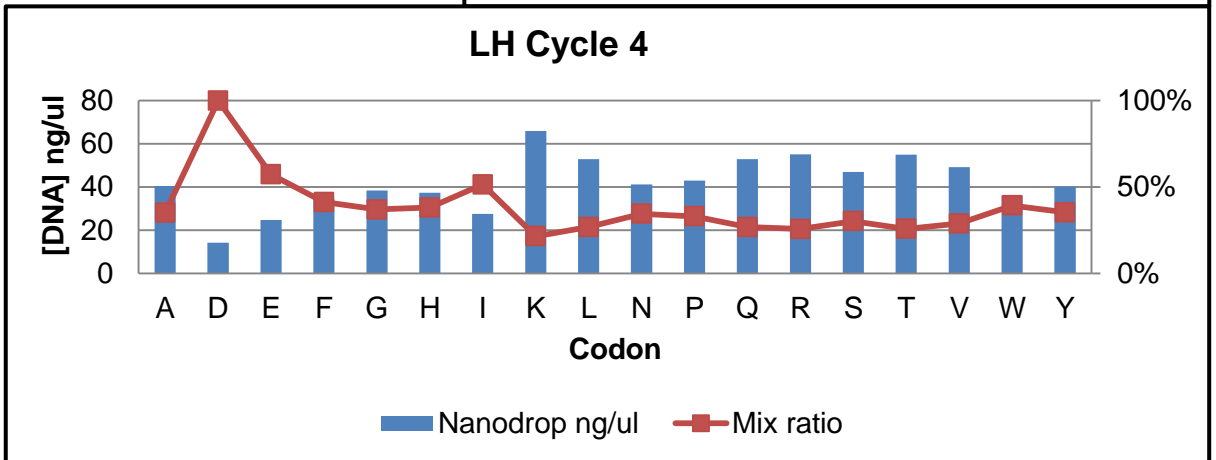
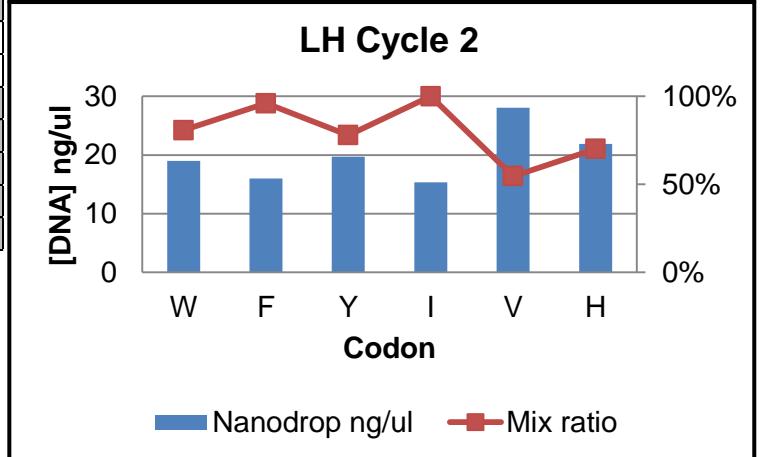
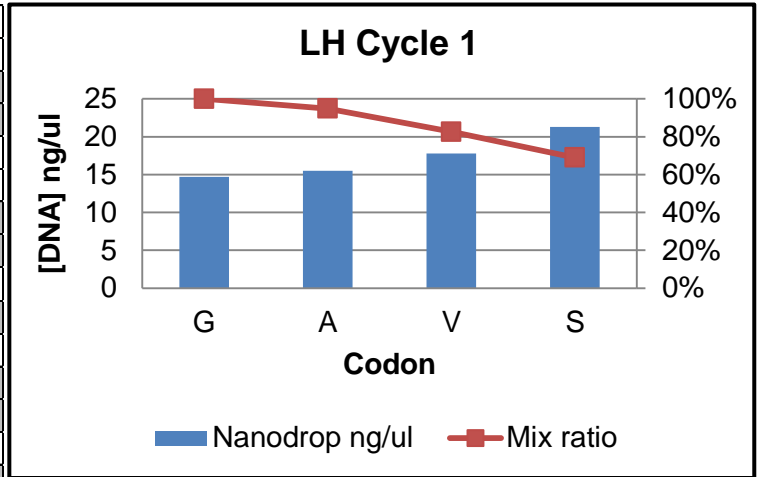


Figure 4.11. Saturation Cycling and Quantification of Re-synthesised LH Anti-NGF Library. Products generated from each cycle of LH additions were quantified by UV spectrophotometry using a nanodrop 200c (Thermo Scientific) and mixed at an equimolar concentration. Cycle 1: G, A, V, S. Cycle 2: W, F, Y, I, V, H. Cycle 4: A, D, E, F, G, H, K, L, N, P, Q, R, S, T, V, W, Y. Cycle 5: N, E, Q, D, K, R, H.

To analyse whether re-synthesised LH saturation cycling had successfully added a codon per cycle, the PCR product of every cycle were amplified with the LH internal primer and an appropriate cycle primer (Table 2.6) and was electrophoresed on a 10% polyacrylamide gel (2.2.4.3) with the round 1 PCR product in lane 1 through to the round 5 PCR product in lane 5 (Figure 4.12). The increase in size of the PCR product was evident from 70 bp in cycle 1 to 82 bp in cycle 5 showing that each cycle had added a single codon. Again as these were unpurified mixes of the PCR products some different molecular weight products are also visible across the lanes. Both library fragments were ligated together in the manner previously described (2.2.1.3), tagged with MiSeq primers (2.2.2.7) and sent for next-generation sequencing.

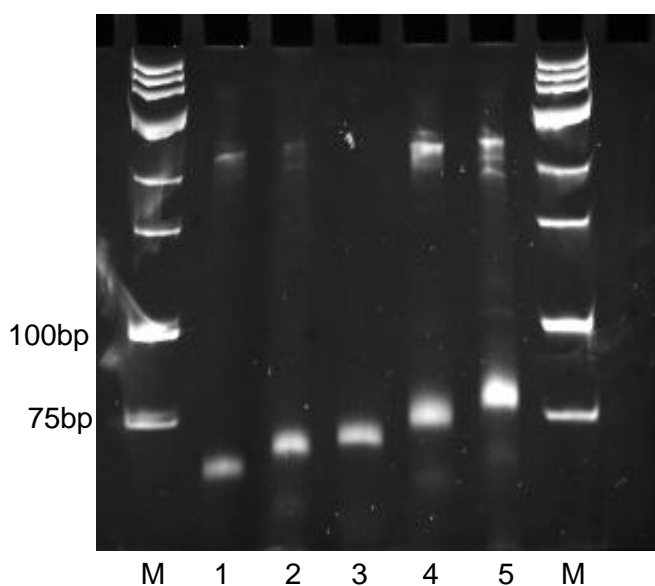


Figure 4.12. Resynthesized LH Cycle Comparison. Polyacrylamide gel image of PCR products generated from the amplification LH cycle ligations using an LH internal primer to allow resolution. Lanes: 1: Round 1 PCR product; 2: Round 2 PCR product; 3: Round 3 PCR product; 4: Round 4 PCR product; 5: Round 5 PCR product. Expected molecular weights: R1: 65 bp; R2: 68 bp; R3: 71 bp; R4: 74 bp; R5: 77 bp. Samples were electrophoresed on 10% polyacrylamide/TBE gel against a Thermo Scientific low range generuler.

4.6. Resynthesized LH Anti-NGF Peptide Library Analysis

The MiSeq next-generation sequencing read a total of 589734 sequences with 458911 having the correct 10 bp flanking regions. Based on the way NGS data was analysed the length of read corresponding to the full length library should be 72 bp. This showed that 71.0% of those sequences were the correct length and contained the full length library (72 bp) with its corresponding 1 bp deletion (71 bp) and 1 codon deletion (69 bp) equating to 13.2% and 5.2% of total flanked sequences respectively (Table 4.8).

Length (bp)	Frequency	%
72	326047	71.0%
71	60684	13.2%
69	23743	5.2%
70	14080	3.1%
68	6666	1.5%
63	6628	1.4%

Table 4.8. Re-synthesised LH Anti-NGF Peptide Library MiSeq Length Distribution. The cycle 6 PCR product was tagged with MiSeq primer (Table 2.5) as described in 2.2.2.7. A total of 589734 sequences were analysed with 458911 having the correct 10bp flanking regions. 71.0% of these sequences were the correct length with sequences containing a 1bp deletion or 1 nucleotide deletion the next highest frequency (13.2% and 5.2% respectively).

As the same RH library was used as in the previous full-length library construction (4.4) the codon representation for the RH section remained the same. Codon representation in the LH library was improved (Figure 4.13) when compared to previous libraries, with the exception of LH-1 position. Position LH4 showed much a better balance in observed codon representation between the 18 used and was in general closer to the expected values. Positions LH1, 2, and 5 were also showed improvement although they showed a remarkable similarity in the codon bias to those seen in Figure 4.8, albeit in reduced levels.

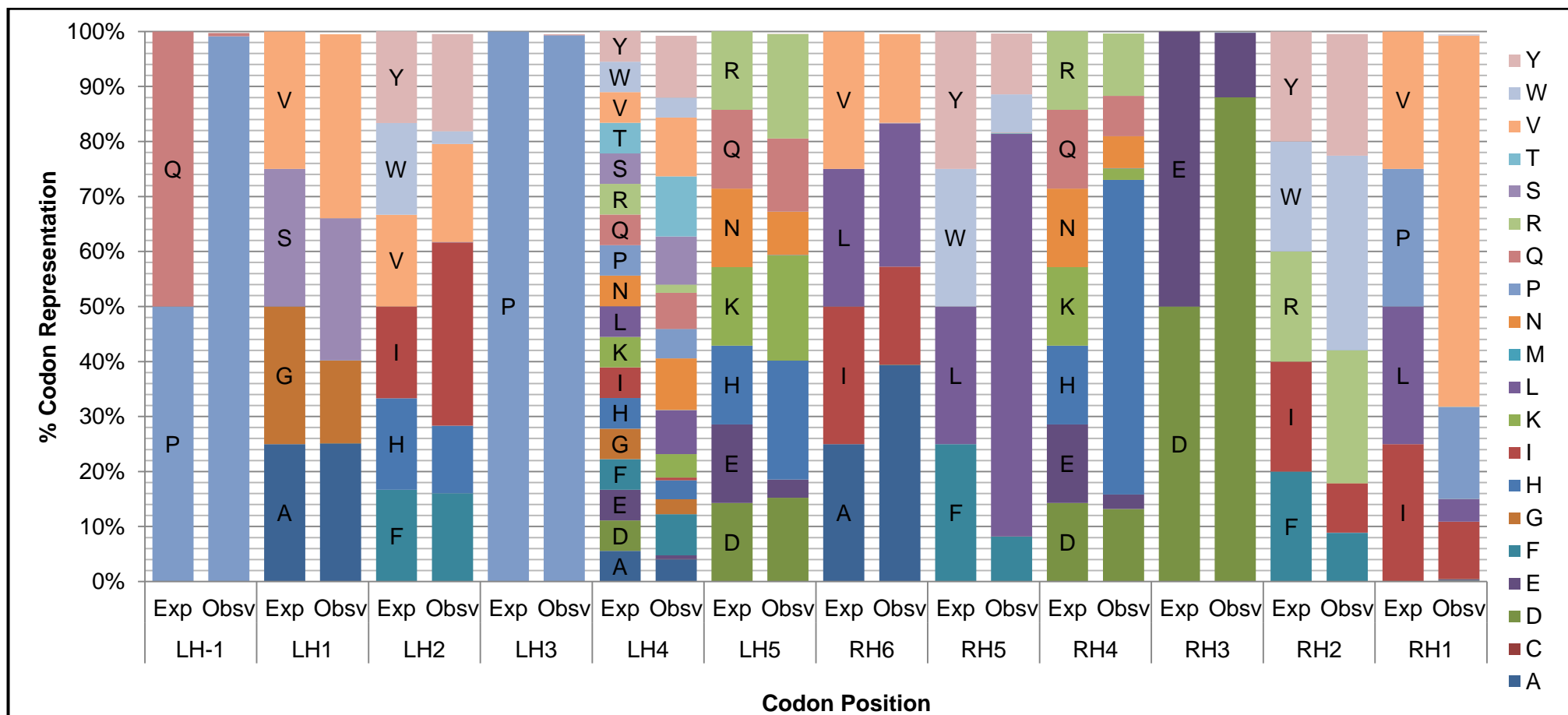


Figure 4.13. Codon Representation of Re-synthesised LH Anti-NGF Peptide Library. Next-generation sequencing results using MiSeq tagged cycle 6 PCR products. Library was assembled as described 2.2.3 and sequenced using a MiSeq sequencer according to the manufacturer's instructions. Expected codon representation is compared to observed codon representation and data represents the analysis of 589734 sequences with the flanking region, which comprised 71.0% of correct length sequences.

Mathematical analysis of the sequencing data suggested that the full length (72-mer) library represented 69.1% diversity (Table 4.9), with the 326047 sequences that corresponding to 1.2% coverage of the theoretical diversity of the library. Within the library 81.3% of the sequences that corresponded to the full length occurred only once (Table 4.10) with duplicate (10.5%) and triplicate (3.5%) sequence occurrences the next frequent.

Theoretical expected Library Diversity (Dmax)	2.70x10 ⁷
No. of MiSeq sequences with flanks & 72 nt long	326047
Expected number of variants in Sequenced library (V=Dmax(1-e ^{-T/Dmax}))	3.24x10 ⁵
No. of different peptide sequences	222683
Expected Completeness of library (V/Dmax)	1.2%
Diversity represented (No. of different sequences in library / V)	68.7%

Table 4.9. Mathematical Analysis of Re-synthesized LH Anti-NGF Peptide Library Diversity. Mathematical analysis of potential library diversity as described in (Bosley and Ostermeier, 2005). Dmax: Theoretical expected Library Diversity; V: Expected number of variants in Sequenced library.

Occurrences	Count	Percentage
1	181014	81.3%
2	23278	10.5%
3	7832	3.5%
4	3542	1.6%
5	2078	0.9%

Table 4.10. Re-synthesized LH Anti-NGF Peptide Library Sequence Diversity. The number of times the same sequence was observed and the frequency they occurred within the LH library.

4.7. Discussion

Despite the truncation in the first attempt of building the anti-NGF peptide library the observed codon representation was greatly improved compared to the previous library (chapter 3), which showed that refinement of the ProxiMAX process had been largely successful.

The truncation observed in Figure 4.9 appeared to be caused by the carry-over of undigested material from the first cycle product through cycles 2 and 3. The sequential use of 3 sets of MAX oligonucleotides (Cycle 1: set 1; Cycle 2: set 2; Cycle 3: set 3; Cycle 4: set 1; Cycle 5: set 2) meant that in cycle 4 this (cycle 1) sequence was amplified (Figure 4.10) when its complementary primers were introduced. This was still only present in low concentrations after PCR in cycle 4 due to dilution through the cycles 2 and 3. This truncated product would then have been digested in cycle 4 and the process resumed for the position 5 codon to be added. Despite the gel purification of the *MlyI* digestion, due to a lack of resolving power from agarose gels there was obviously some carryover. PAGE purification may be a more appropriate purification method when dealing with such small size differences.

Despite an extremely biased LH4 position, with a represented library diversity of 86.9% (Table 4.6) the full length 72-mer library results from the initial synthesis (4.4) looked extremely encouraging. However as these sequences only made up 5% of all the sequences read (Table 4.5) it only equated to 0.1% coverage of the library, so should be considered with caution. In contrast, the truncated library was poor, showing a represented diversity of 49.8% with 42.7% coverage (Table 4.7), when taking into account for a reduced library size of 2.51×10^5 . With a higher percentage of library coverage these results can be taken as more accurate representation, although the codon representation for those positions present in both the 72-mer and 63-mer showed reasonable similarity.

In contrast, the represented diversity of the final anti-NGF peptide library (Table 4.9) was good (68.7%) with 1.2% of the potential library covered. In this case the bias observed in the LH-1 position is due to an error introducing a primer-directed randomised codon rather than using ProxiMAX randomisation. However, the RH portion of this library was the same as that

in the truncated 63-mer and both show remarkable similarity adding validity to the consistency of sequencing data.

In both libraries the percentage of n-1 deletions are the high end of what is expected/accepted with a combined 9.9% for the 63/72mer library and 13.2% for the final library. Whilst broadly similar, the increased n-1 percentage in the final library may be in part due to use of first RH library portion that had been in storage whilst the new LH portion was synthesised. This increased time in storage may have facilitated the deterioration of some the sequences leading to increase n-1 sequences when the two library portions were ligated. Having said that, the high percentages in both libraries could also indicate the stock oligonucleotides, whether them being framework oligonucleotides or MAX oligonucleotides, may contain truncated. The most likely source is the LH library framework due to the filling-out reactions used to generate it (Figure 4.4), although it may be the case that other oligonucleotides contained errors introduced during their synthesis.

Interestingly, while the use of separate ligation reactions did help negate the influence of T4 DNA ligase sequence preference allowing the observed and expected codon representations to align more closely there was still variations observed throughout the library (in particular the LH portion of Figure 4.13). Therefore the poignant question is whether these differences are down to general experimental error or are they indicative larger problems associated with other areas of the process where this bias may be introduced? Obviously once the individual PCR products are quantified and pooled there is the chance for the *MlyI* digestion to potentially introduce codon bias, either through <100% reaction efficiency or possible sequence preference, that is then carried through to the following cycle. However, the sporadic nature of these variations in codon representations from cycle to cycle do not seem to follow an obvious pattern (unlike the sequence preference observed for T4 DNA ligase (Ashraf et al., 2013)). For example, in Figure 4.13 valine at position LH1 shows +8.4% over representations compared to only +1.1% at position LH2. Whilst these differences are not vast, unlike those observed in Figure 3.9, this seems to be typical range of variation once ligase preference accounted for. Visual analysis of the codon representation presented in

Ashraf *et al.* shows a similar situation to that of the codon representation in Figure 4.13, in that whilst there is some variation in the percentage codon representation there is no obvious pattern with some codons showing some over representation at one position and not at others. Furthermore, these types of variations are also observed in Frigotto *et al.* using a version of ProxiMAX that has undergone further optimisation. Therefore I am inclined to surmise that these variations are due to minor experimental error associated with factors such liquid handling, oligonucleotide quantification, <100% reaction efficiencies rather than larger issues such as *MlyI* sequence preference.

In conclusion, although not perfect, the final anti-NGF peptide library showed that ProxiMAX could be undertaken in a normal laboratory using standard molecular biology techniques without the need for specialist equipment. As the library was to an acceptable standard it was now taken forward to undergo CIS display in order to screen for novel mutants.

Chapter 5

Recombinant Human Nerve Growth Factor Expression, Purification and Activity Testing in an *Escherichia Coli* Expression System

5. Chapter 5: Recombinant Human Nerve Growth Factor Expression, Purification and Activity Testing in an Escherichia Coli Expression System

5.1. Introduction

An immobilised target for the anti-NGF peptide library was required for the selection and screening process of CIS display. Therefore it was necessary to express biologically active NGF in sufficient yield for use in CIS display.

As NGF contains three disulfide bonds with non-consecutive cysteine pairs, expression of recombinant human NGF (rhNGF) is usually performed eukaryote cell lines such as murine myeloma derived NSO. However mammalian cell culture can be costly and produces relatively low yields. Expression of rhNGF has previously been attempted in the periplasm of *E.coli*. (Fujimori et al., 1992, Negro et al., 1992), although these formed aggregates and after subsequent solubilisation and refolding the yield of biologically active rhNGF was low. NGF has been expressed in the periplasm of *E.coli* using co-expression of disulfide bond formation proteins (Dsb's) (Kurokawa et al., 2001).

With the advances in cell line engineering it is possible to attempt bacterial cytoplasmic expression using the NEB *E.coli* SHuffle cell line. *E.coli* SHuffle are an engineered *E.coli* K12 cell line that constitutively expresses a chromosomal copy of the disulfide bond isomerase DsbC (which lacks its signal sequence, retaining it in the cytoplasm) designed to promote disulfide bond formation in the cytoplasm. DsbC promotes the correction of mis-oxidized proteins into their correct form (Besette et al., 1999, Levy et al., 2001) and is also a chaperone that can assist in the folding of proteins that do not require disulfide bonds (Chen et al., 1999).

As well as expressing DsbC the *E.coli* SHuffle cell line has deletions in the genes for glutaredoxin reductase and thioredoxin reductase that allows disulfide bonds to form in the cytoplasm. The lethality of this combination of mutations is suppressed by a mutation in the peroxiredoxin enzyme (*ahpC**).

NGF is physiologically processed from a pre-pro peptide to give a 13.5 kDa protein with no other posttranslational processing. It contains an 18 amino acid signal peptide (1-18) followed by a 103 amino acid pro-sequence (19-121), which contains two glycosylation points (positions 69 and 114). The active subunit (β NGF) is 120 amino acids (122-241) and forms an active homodimer (Rattenholl et al., 2001b). Therefore, as expression would be attempted in a prokaryote system it was decided to express the β subunit.

5.2. Expression and purification of β -NGF using pJ434

The β -NGF gene was synthesised and inserted into the bacterial expression vector by DNA 2.0. The plasmid map of this vector is illustrated in Figure 5.1. This is a low copy number vector that is IPTG inducible, contains an ampicillin resistance gene for selectivity and the β -NGF was cloned downstream of a T7 promoter.

Initially pJ434-NGF_optEc (2.1.6.2) was transformed into SHuffle® T7 Competent *E.coli* (2.1.5.3). To start with expression conditions such as temperature, incubation time and IPTG concentration were varied to determine the optimal conditions for expression. Final expression conditions were established as IPTG induction concentration of 0.6 mM and incubation of 16°C overnight (2.2.9.1.1) (data not shown). To lyse the cell pellet both chemical lysis, using Bugbuster™ (2.2.9.1.3), and sonication (2.2.9.1.2) were used to analyse which was the most efficient lysis method. It was decided that sonication was more efficient at lysing large cell pellets although chemical lysis provided a better quality lysate with less degradation. Cleared cell lysate was then purified using Ni-NTA his tag affinity purification (Figure 5.2 A).

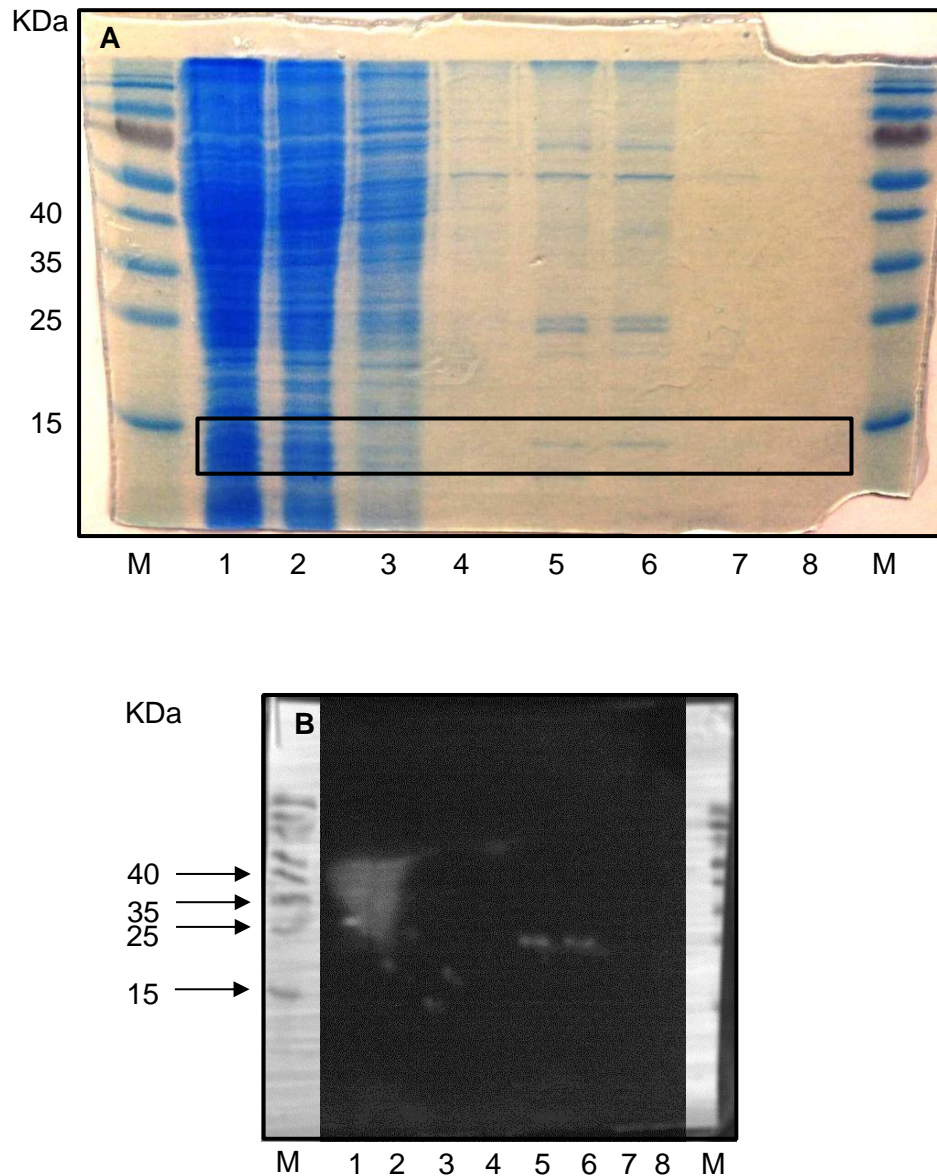


Figure 5.2. pJ434- β -NGF Expression and Purification. **A:** SDS-PAGE gel image of protein generated in 2.2.9.1.1 and subsequently purified in 2.2.9.1.2 and 2.2.9.1.4. Lanes 1: Raw cleared lysate; 2: Column flow through; 3-4: Column washes; 5-8: Column eluent. Expected molecular weight of β -NGF is \sim 13.5 KDa (appropriate size area is boxed). Samples were electrophoresed on 15% polyacrylamide gel. **B:** Western blot of the SDS-PAGE gel (A) using an anti-His antibody. Lanes 1: Raw cleared lysate; 2: Column flow through; 3-4: Column washes; 5-8: Column eluent. Smudging in lanes 1 and 2 resulted from blotting procedure.

Whilst some extremely faint bands that were approximately the correct size (\sim 13.5 KDa) were visible in the eluted fractions (lanes 5-8) analysis by western blot, as described in 2.2.4.6 using HisG mouse monoclonal antibody-HRP conjugate (Figure 5.2 B) showed that these were not the correct protein, although lanes 5-6 did show bands at higher molecular weight. As there appeared that there was no significant yield of the correct protein present in

the soluble fraction it was decided to modify the expression system in order to improve solubility.

5.3. β -NGF Sub-Cloning into pETSUMO

In order to try and improve the solubility it was decided to express β -NGF as a C-terminal fusion with a small ubiquitin-related modifier (SUMO) purchased from Life Technologies, which is claimed to increase expression and solubility of recombinant SUMO fusion proteins. The SUMO protein is cleaved by SUMO protease, a cysteine protease that specifically recognises its tertiary structure (Li and Hochstrasser, 1999, Mossessoiva and Lima, 2000). This results in the production of native protein with no extra amino acids between the protein and the cleavage site (Figure 5.3).



Figure 5.3. pETSUMO Plasmid Map (taken from Champion™ pET SUMO Protein Expression System manual, Invitrogen). Champion™ pET SUMO Expression System was purchased from Life Technologies. It contains: the T7 lac promoter for high-level, IPTG-inducible expression of the gene of interest in *E.coli*; Kanamycin resistance gene for selection in *E.coli*; N-terminal polyhistidine (6xHis) tag for detection and purification of recombinant fusion proteins; N-terminal SUMO fusion protein for increased expression and solubility of recombinant fusion proteins and generation of native protein following cleavage by SUMO Protease; lacI gene encoding the lac repressor to reduce basal transcription from the T7lac promoter in the pET SUMO vector and from the lacUV5 promoter in the *E.coli* host chromosome; pBR322 origin for low-copy replication and maintenance in *E.coli*.

The β NGF gene was amplified out of pJ434-NGF_optEc using *Taq* polymerase, as described in 2.2.9.2.1, to add single 3' A overhangs (Figure 5.4). Lane 1 showed a clean negative control whilst lane 2 showed a band corresponding the β NGF gene with the correct size of 360 bp.

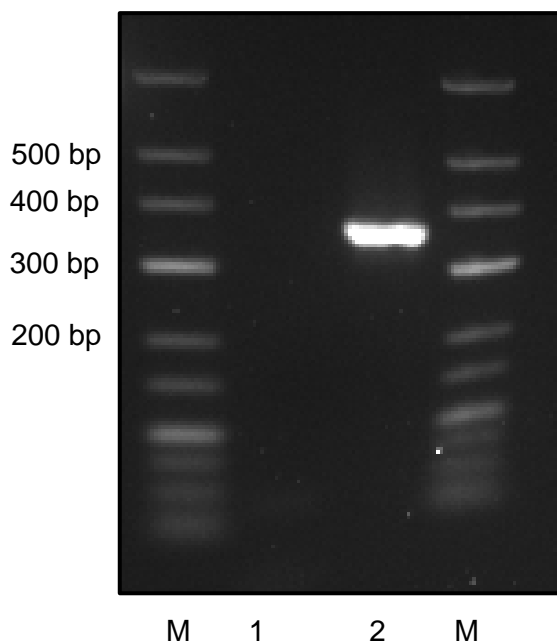


Figure 5.4. β -NGF TA Cloning. Agarose gel image of the amplified β NGF gene to be used in pET SUMO TA cloning. β NGF gene was amplified out of pJ434-NGF_optEc and inserted into pETSUMO plasmid using TA cloning with specific primers to amplify the β -NGF gene as described in 2.2.9.2.1. Expected molecular weight of the β NGF gene is 360 bp. Lanes: 1: Negative control; 2: β -NGF gene. The products were electrophoresed on 1.5% agarose/TAE gel.

The amplified β NGF gene was subsequently ligated into pETSUMO (2.1.6.3) and cloned into One Shot® Mach1™-T1R Competent Cells (2.1.5.2) as described in 2.2.5.2. Alongside this ligation various controls were also undertaken to analyse the effectiveness of the transformation (Table 5.1).

	Colonies
β NGF ligation	623
Self-ligation	~1000
Linear pETSUMO	8
Transformation Control (pUC19)	~1500
No vector (+ Kanamycin)	0
No vector (- Kanamycin)	Lawn

Table 5.1. pETSUMO- β NGF Cloning. Amplified β NGF gene was ligated into pETSUMO with a 3:1 insert: vector molar ratio at 16°C overnight. The pET SUMO- β NGF was transformed into One Shot® Mach1™-T1R Competent Cells (2.1.5.2) and plated onto LB agar+Kan along with relevant controls.

Colonies were picked and analysed by colony PCR (as described in 2.2.2.3) using a forward external primer (complementary to SUMO) and a reverse internal primer (complementary to β NGF) to ensure the gene was in the correct orientation (Figure 5.5). All lanes showed a product of the correct size although the quality was varied and the secondary products were also visible in (lanes 4, 6 and 7 especially). Several of the best looking clones were picked, purified by miniprep (2.2.6) and sequenced using forward and reverse sequencing primers by Eurofins Genomics (9.7, Figure 5.6). Clones showing the correct sequences in the correct reading frame could then be used for expression.

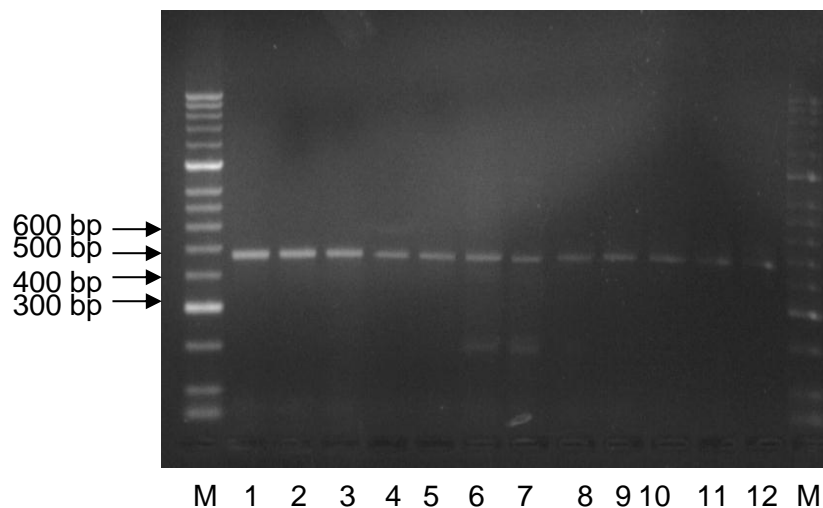


Figure 5.5. pETSUMO- β NGF Colony Screening. Agarose gel image of the PCR products generated from pETSUMO- β NGF colony screening. Products were generated using an external primer, complementary to pETSUMO, and an internal primer commentary to β NGF. Expected molecular weight of the PCR products from clone containing the correct vector and insert is ~490 bp. The products were electrophoresed on 1.5% agarose/TAE gel. Lanes: 1-12: Individual clones.

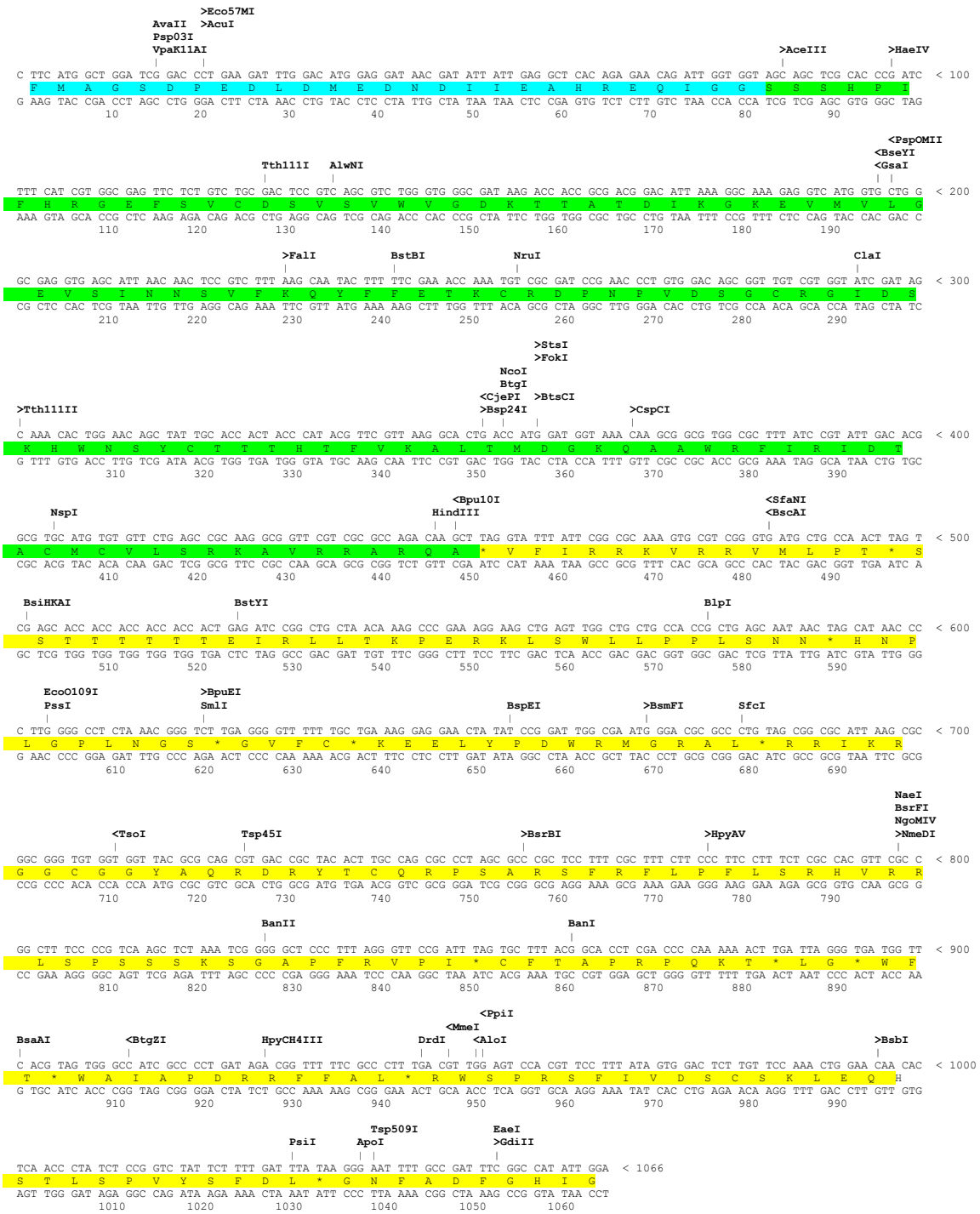


Figure 5.6. pETSUMO-βNGF Sequencing. Good quality clones that showed the insert in the correct orientation were used to inoculate fresh LB+Kan (2.1.2.1) and grown overnight at 37 °C. Plasmid DNA was extracted and purified by miniprep (2.2.6) and sent for sequencing at Eurofins Genomics. βNGF gene is highlighted in green, C-terminal of SUMO in blue and the plasmid backbone in yellow.

5.4. pETSUMO-βNGF Expression Optimisation in *E.coli* B121.

After sequence verification pETSUMO-βNGF was transformed into *E.coli* B121 cells (2.1.5.4) as described in 2.2.5.2. Initial optimisation was undertaken in this cell line as these were supplied with the Champion™ pET SUMO Expression System kit (Life Technologies). Once the initial expression parameters for the SUMO-βNGF fusion were deduced different cell lines could be used. The expression control vector pETSUMO/CAT (9.6) was also transformed and expressed in parallel to pETSUMO-βNGF.

Initially, overnight precultures of both pETSUMO/CAT and pETSUMO-βNGF were diluted 50-fold in fresh 10 ml LB+50 µg/ml Kanamycin (2.1.2.1), and when cultures had reached OD_{600nm} 0.4-0.8, induced with 0.4mM IPTG (2.1.4.7) and grown at 30°C (to potentially aid solubility) for 4 hours. Whole cell protein was analysed by boiling the pellets for each time point in 1x SDS sample buffer (2.1.3.3, 2.1.3.4) (Figure 5.7). Lanes 1-3 show un-induced expression samples at times 0, 2 and 4 hours while lanes 4-6 show induced expression samples at times 0, 2 and 4 hours. The expression levels of the control pETSUMO/CAT were at reasonable levels in the induced samples while there was little/or no expression observed in the un-induced samples across the time course (Figure 5.7 A). There was little non-specific expression of pETSUMO-βNGF in the un-induced samples, with a small amount visible across the time course in the induced samples (Figure 5.7 B). Therefore it was concluded that expression conditions would need to be further optimised in order to improve the yield of SUMO-βNGF fusion.

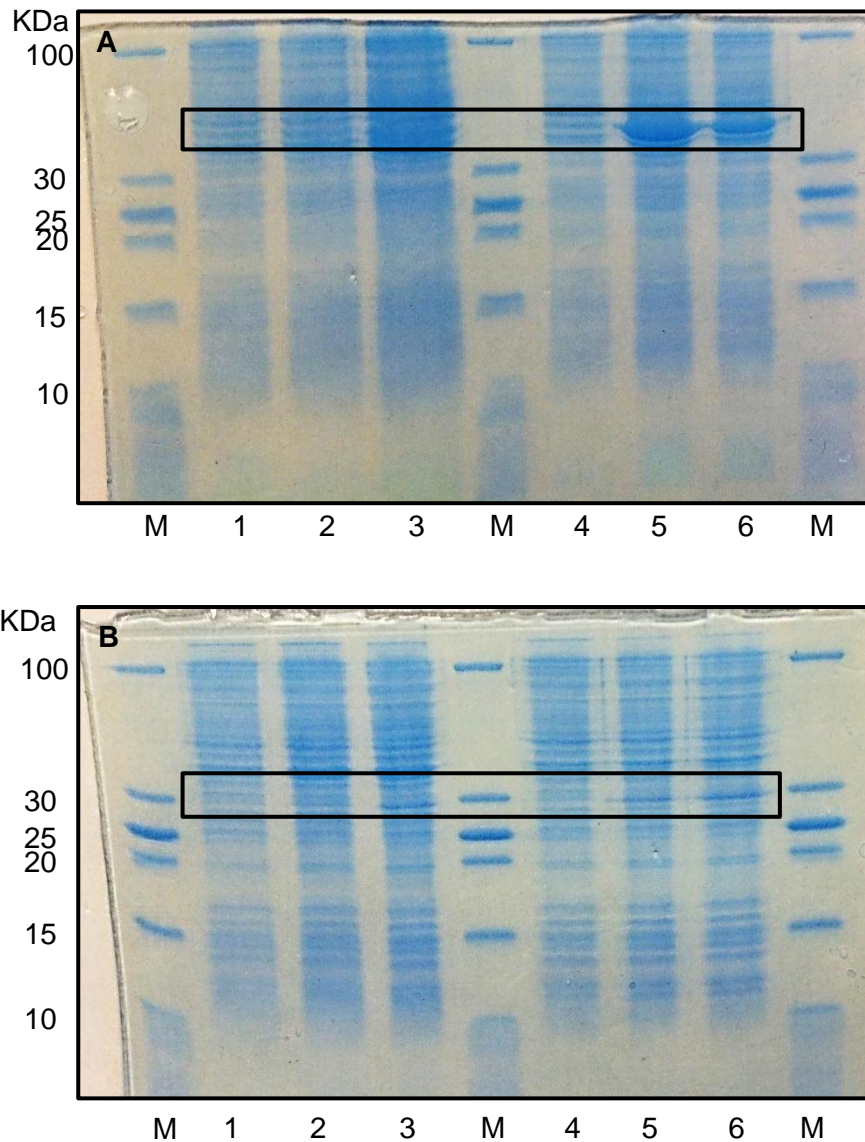


Figure 5.7 Initial pETSUMO-β-NGF Expression in *E.coli* BI21. SDS-PAGE gel image of whole cell protein generated in 2.2.9.2.2. **A: Positive expression control pETSUMO/CAT (9.6)** Lanes: 1: Un-induced, 0 hours; 2: Un-induced 2 hours; 3: Un-induced 4 hours; 4: Induced, 0 hours; 5: Induced 2 hours; 6: Induced 4 hours; **B: pETSUMO-βNGF:** Lanes: 1: Un-induced, 0 hours; 2: Un-induced 2 hours; 3: Un-induced 4 hours; 4: Induced, 0 hours; 5: Induced 2 hours; 6: Induced 4 hours. Expected molecular weight of SUMO-βNGF and pET SUMO/CAT is ~30 kDa and ~39 kDa respectively (appropriate size area is boxed). Samples were electrophoresed on 15% polyacrylamide gel alongside a Thermo Scientific 10-100 kDa pageruler and stained with instant blue stain (Expedeon).

A point noted from the first expression was that due to the 50-fold dilution of the precultures, prior to induction, was that it took a considerable time for them to reach the lower induction threshold of OD_{600nm} 0.4, meaning that the cells were induced at the low end of the range. Therefore for it was decided to only dilute the precultures 10-fold, thus reducing the time taken to reach an OD_{600nm} 0.4-0.8 and the likelihood the cells were in log phase. The concentration of IPTG (2.1.4.7) used for induction was increased from 0.4mM to 1.0mM. Lanes 1-3 show un-induced expression samples at times 0, 2 and 4 hours while lanes 4-6 show induced expression samples at times 0, 2 and 4 hours. Once again the expression levels of the control pETSUMO/CAT were at reasonable levels in the induced samples while there was little/or no expression observed in the un-induced samples across the time course (Figure 5.8 A), although overall protein levels increased as result of increased cell numbers. Similarly, there was little non-specific expression of pETSUMO- β NGF in the un-induced samples, but under this alternative protocol, there was much improved expression of the SUMO- β NGF fusion in the induced samples (Figure 5.8 B, lanes 5 & 6).

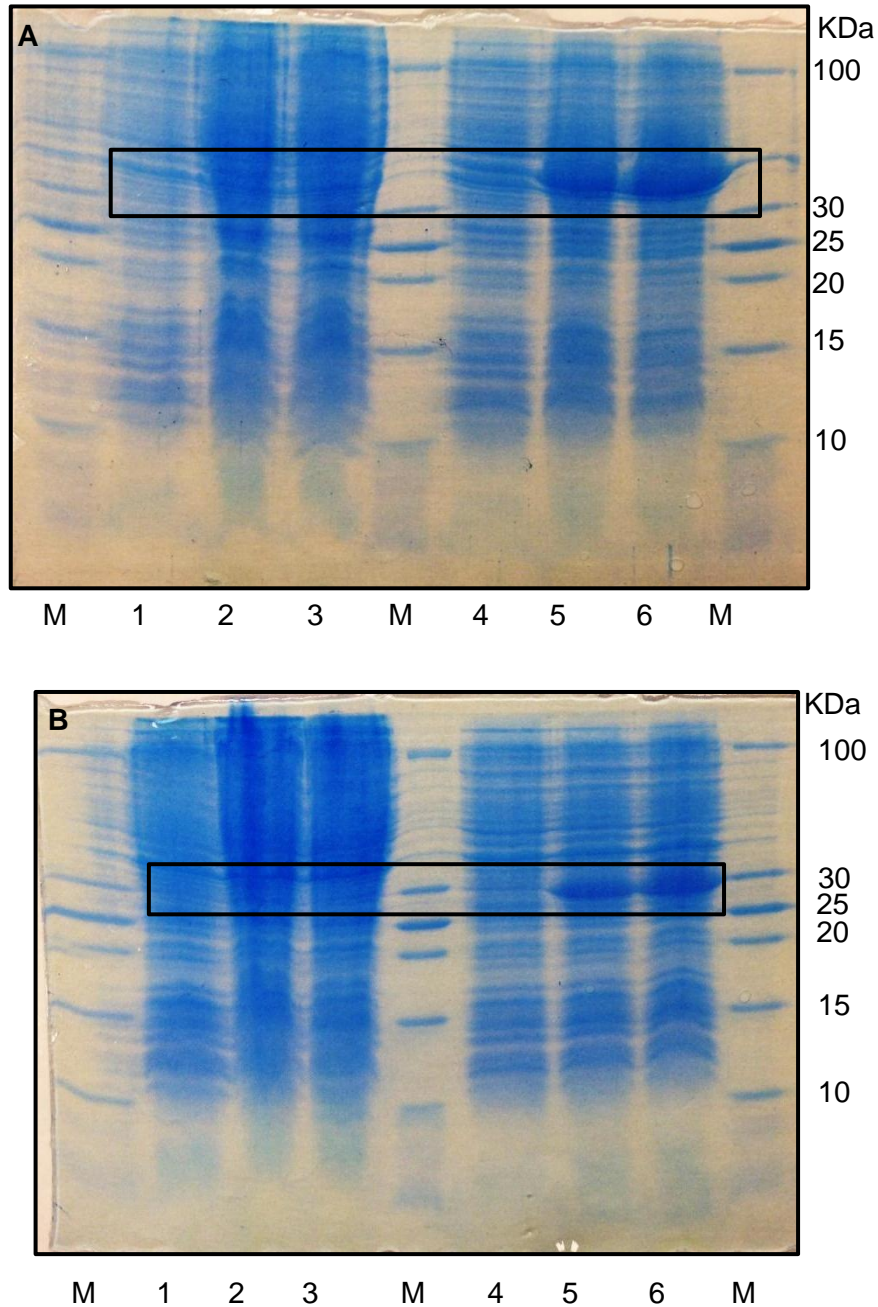


Figure 5.8. pETSUMO-β-NGF Expression Optimisation in *E.coli* BI21. SDS-PAGE gel image of whole cell protein generated in 2.2.9.2.2. **A: Positive expression control pETSUMO/CAT (9.6)** Lanes: 1: Un-induced, 0 hours; 2: Un-induced 2 hours; 3: Un-induced 4 hours; 4: Induced, 0 hours; 5: Induced 2 hours; 6: Induced 4 hours. **B: pETSUMO-βNGF:** Lanes: 1: Un-induced, 0 hours; 2: Un-induced 2 hours; 3: Un-induced 4 hours; 4: Induced, 0 hours; 5: Induced 2 hours; 6: Induced 4 hours. Expected molecular weight of SUMO-βNGF and pET SUMO/CAT is ~30 kDa and ~39 kDa respectively (appropriate size area is boxed). Samples were electrophoresed on 15% polyacrylamide gel alongside a Thermo Scientific 10-100 kDa pageruler and stained with instant blue stain (Expedeon).

5.5. pETSUMO-βNGF Expression and Purification in *E.coli* SHuffle.

As the expression levels of the fusion appeared reasonable in *E.coli* BL21 it was decided to move onto expression in the NEB *E.coli* SHuffle cell line (2.1.5.3). This time pETSUMO-βNGF was transformed into the *E.coli* SHuffle cell line as described in 2.2.5.2. Overnight precultures were diluted 10-fold into fresh LB+50 µg/ml Kanamycin (2.1.2.1), induced with 1.0mM IPTG (2.1.4.7) when cultures had reached OD_{600nm} 0.4-0.8 and grown at 30°C (Figure 5.9 A) for 4 hours. Lanes 1-3 show un-induced expression samples at times 0, 2 and 4 hours while lanes 4-6 show induced expression samples at times 0, 2 and 4 hours. The expression levels observed in the induced pETSUMO-βNGF were good while there was little/ expression observed in the un-induced samples across the time course, although once again overall protein levels increased as result of increased cell numbers. To ensure that the protein being expressed was the SUMO-βNGF fusion a western blot using HisG mouse monoclonal antibody-HRP conjugate was performed as described in 2.2.4.6 (Figure 5.9 B). Once again lanes 1-3 show un-induced expression samples at times 0, 2 and 4 hours while lanes 4-6 show induced expression samples at times 0, 2 and 4 hours. This showed bright band at the correct size corresponding to the SUMO-βNGF fusion. There was a constant background expression of the fusion visible in the un-induced samples but there was a distinct increase in the intensity of the bands in the induced samples across the time course.

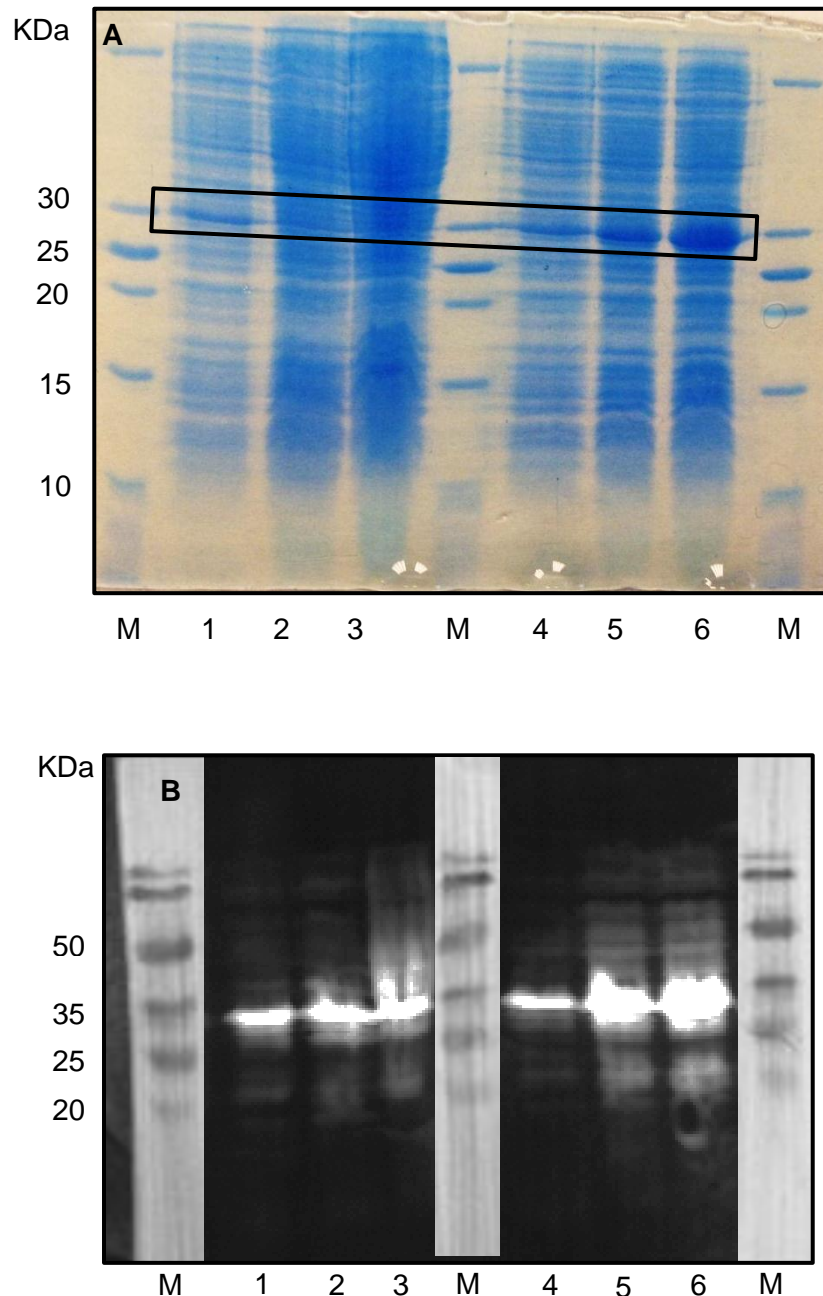


Figure 5.9. pETSUMO- β NGF Expression Optimisation in *E.coli* Shuffle. **A:** SDS-PAGE gel image of whole cell protein generated in 2.2.9.2.2. Lanes: 1: Un-induced, 0 hours; 2: Un-induced 2 hours; 3: Un-induced 4 hours; 4: Induced, 0 hours; 5: Induced 2 hours; 6: Induced 4 hours. Expected molecular weight of SUMO- β NGF is ~30 KDa (appropriate size area is boxed). Samples were electrophoresed on 15% polyacrylamide gel alongside a Thermo Scientific 10-100 kDa pageruler and stained with instant blue stain (Expedeon). **B:** Western blot of the SDS-PAGE gel (A) using an anti-His antibody. Lanes: 1: Un-induced, 0 hours; 2: Un-induced 2 hours; 3: Un-induced 4 hours; 4: Induced, 0 hours; 5: Induced 2 hours; 6: Induced 4 hours.

Once the expression of the SUMO- β NGF fusion had been optimised in the *E.coli* SHuffle cell line the process was up scaled for 500 ml expressions and the resulting cultures pelleted. In order to undergo purification the cell pellets were lysed using BugbusterTM (Merck Millipore) (2.2.9.1.3) and the soluble fraction was purified using Ni-NTA resin for His-tag affinity purification as described in 2.2.9.2.3 (Figure 5.10 A). Unfortunately little/or no protein corresponding to the correct size of the fusion (~30 KDa) was observed in the column eluent (lanes 5-8) along with little visible in the un-purified soluble fraction (lane 1), column flow through (lane 2) and column washes (lanes 3-4). This suggested that the expressed fusion was still not soluble but in order to confirm this hypothesis the insoluble and soluble fractions were analysed by SDS-PAGE (2.2.4.4) (Figure 5.10 B). A band of the correct size was visible (arrowed) in the insoluble fraction (lane 1) whilst very little was observed in the soluble fraction (lane 2). Despite the best attempts (i.e. expressing as fusion and using specialised cell lines) it seemed clear that it would be difficult to express soluble protein in the cytoplasm. Therefore it was decided to express the SUMO- β NGF fusion in the insoluble fraction and attempt to solubilise, purify and refold it

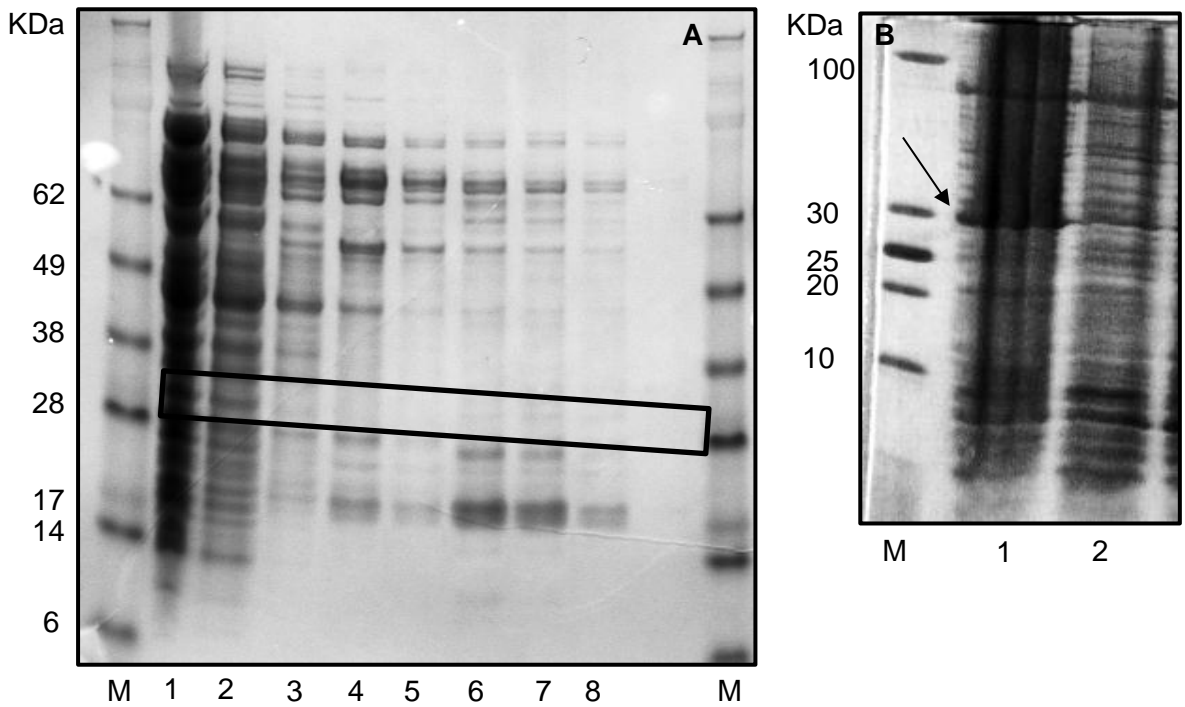


Figure 5.10. pETSUMO-βNGF Soluble Fraction Purification. A: SDS-PAGE gel image of whole cell protein generated in 2.2.9.2.2 that subsequently underwent purification as described in 2.2.9.2.3. Lanes: 1: Un-induced, 0 hours; 2: Un-induced 2 hours; 3: Un-induced 4 hours; 4: Induced, 0 hours; 5: Induced 2 hours; 6: Induced 4 hours. Expected molecular weight of SUMO-βNGF is ~30 KDa (appropriate size area is boxed). Lanes: 1: Un-purified soluble fraction; 2: Column flow through; 3-4: Wash 1-2; 5-8: Elution 1-4. **B:** SDS-PAGE gel image of soluble and insoluble protein generated in 2.2.9.2.2. Lanes: 1: Un-purified insoluble fraction; 2: Un-purified soluble fraction. SUMO-βNGF is indicated in the insoluble fraction (lane 1) by arrow. Samples were electrophoresed on 4-12% polyacrylamide gel.

5.6. Preparation, Purification and Refolding of Insoluble SUMO-βNGF

Two methods were initially examined for purifying the insoluble fraction; purification under denaturing conditions (2.2.9.2.4) and inclusion body purification using Bugbuster™ (2.2.9.2.5).

Purification under denaturing conditions meant that the whole cell protein (soluble and insoluble fractions) was denatured and then purified by Ni-NTA his tag affinity purification (Figure 5.11 A). Unbound and low affinity proteins were washed away and bound protein was eluted down a pH gradient. A large band corresponding to the correct size of the SUMO-βNGF fusion was visible in the un-purified denatured lysate (lane 2) with low levels present during the wash and first elution steps (lanes 5-6 and 7-10 respectively). The second elution

at pH 4.5 (lanes 11-14) showed a larger proportion of the fusion being eluted, especially in the first 2 fractions at this pH. Although the purification process had worked fairly well, non-specific binders were still present in the majority of the fractions.

Purification of inclusion bodies involved the same initial cell lysis procedure as used when purifying the soluble fraction (2.2.9.2.3), although the insoluble fraction was kept whilst the soluble fraction could be discarded. The inclusion bodies were then washed (2.2.9.2.5), solubilised (2.2.9.2.6) and purified (2.2.9.2.7) (Figure 5.11 B). Again a large band corresponding to the SUMO- β NGF fusion was observed in the solubilised inclusion body fraction (lane 1) with traces visible in the column flow through (lane 2) and column washes (lanes 3-4). SUMO- β NGF levels started to increase in the first elution fractions (lanes 5-7) whilst by the second elution significant levels were visible (lanes 8-10). Finally to note was that the fractions produced by inclusion body purification seemed to contain significantly fewer contaminating proteins and was cleaner in general. Therefore it was decided that this was the preferred method of purification.

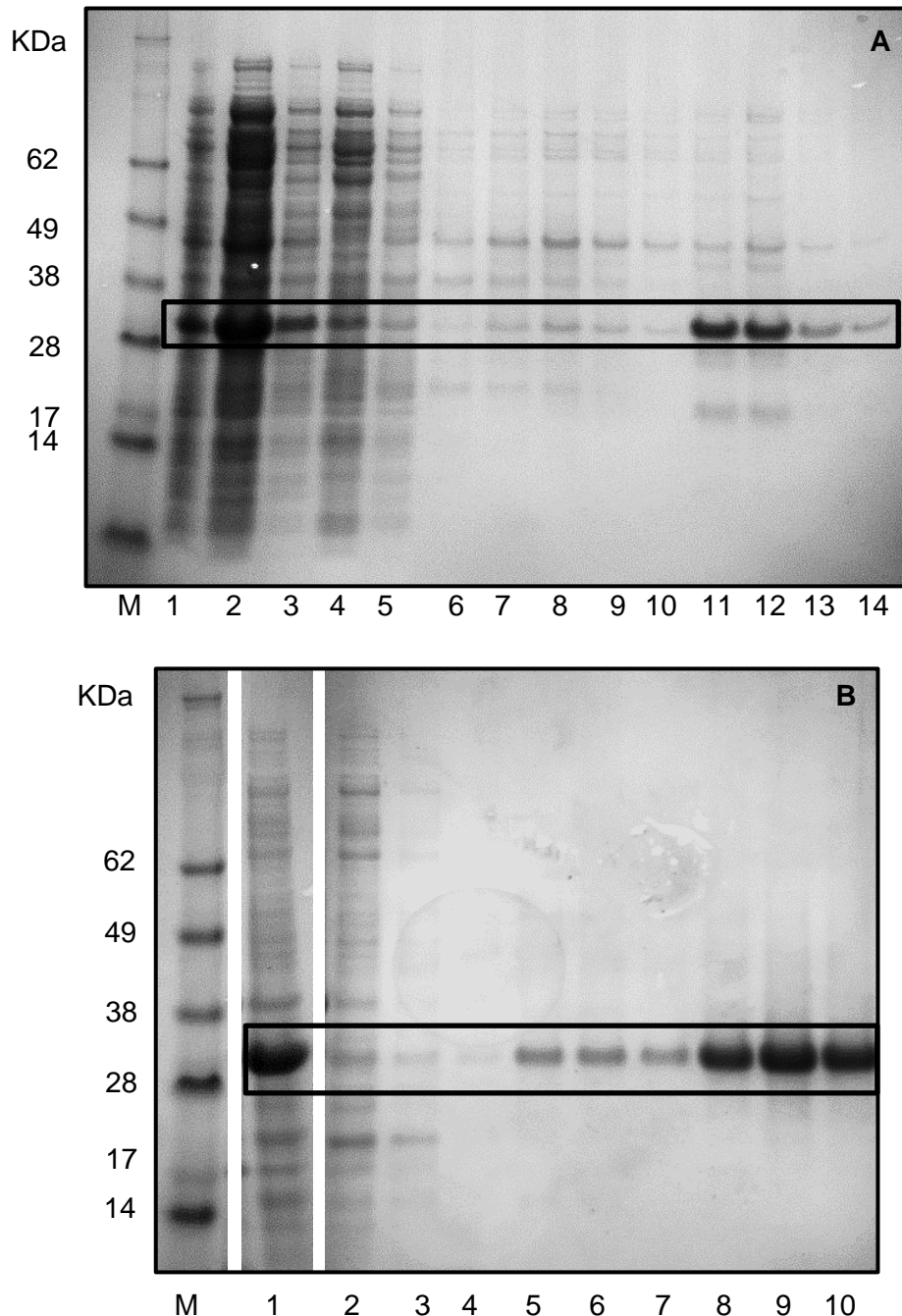


Figure 5.11. pETSUMO- β NGF Insoluble Fraction Purification. A: SDS-PAGE gel image of whole cell protein generated in 2.2.9.2.2 and purified under denaturing conditions as described in 2.2.9.2.4. Lanes: 1: Cell pellet prior to resuspension in denaturing buffer; 2: Denatured un-purified lysate; 3: Remaining pelleted material post resuspension in denaturing buffer; 4: Denatured column flow through; 5-6: Column washes (pH 6.3); 7-10: Column elution buffer 1 (pH 5.9); 11-14: Column elution buffer 2 (pH 4.5). **B:** SDS-PAGE gel image of inclusion bodies generated from soluble lysate production, (2.2.9.2.3), prepared (2.2.9.2.5) solubilised (2.2.9.2.6) and purified as described in 2.2.9.2.7. Lanes: 1: Solubilised inclusion bodies; 2: Column flow through; 3-4: Column wash (pH 6.3); 5-7: Column elution buffer 1 (pH 5.9); 8-10: Column elution buffer 2 (pH 4.5). Expected molecular weight of SUMO- β NGF is ~30 KDa (appropriate size area is boxed). In both A & B samples were electrophoresed on 4-12% polyacrylamide gel.

Once the solubilised fusion was purified it was necessary to refold it. After discussions with colleagues who had previous success with a similar method it was decided to attempt a hybrid refolding method of solid phase and dilution refolding. Solid phase refolding has the advantage of proteins being spatially separated from each other during refolding (thus reducing aggregation) whilst dilution refolding reduces the time for potential unwanted intermediate products to form (Arakawa and Ejima, 2014).

In this case proteins would be bound to a solid phase of Ni-NTA followed by dilution in a specific refolding buffer as described in 2.2.9.2.8 (Figure 5.12). L-Arg and a 10:1 ratio of GSH: GSSG was included in the refolding buffer to aid disulfide formation. A portion of denatured SUMO- β NGF fusion was still present in the column flow through prior to refolding (lane 1) meaning that the binding capacity of the resin had been exceeded. The post refolding showed no obvious protein present (lane 3). The elution fractions containing refolded soluble protein in native (non-denaturing) buffer (lanes 5-8) showed high levels of protein corresponding to the correct size if the SUMO- β NGF fusion, although there was significantly less visible in the first fraction (lane 5) possibly due to equilibration to the new buffer. There was still a significant amount of protein that remained bound the resin (lane 9). Finally, as a check to see whether the refolding process had been successful, the same elution fractions as observed in lanes 5-8 were electrophoresed in SDS sample buffer without the reducing agent (lanes 10-13). β NGF normally acts as a homodimer so should bind to itself, as observed in the higher molecular weight products observed in these fractions.

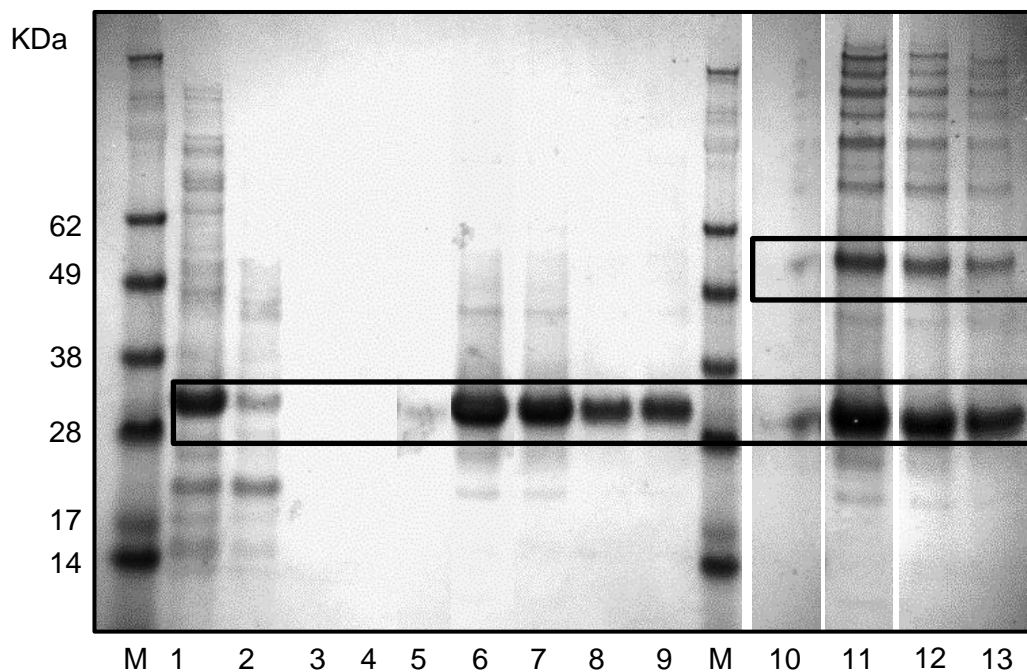


Figure 5.12. SUMO- β NGF Refolding. SDS-PAGE gel image of refolded SUMO- β NGF generated in 2.2.9.2.8 and purified under denaturing conditions as described in 2.2.9.2.4. Lanes: 1: Column flow through prior to refolding; 2: Denaturing wash; 3: Post-refolding flow through; 4: Native column wash; 5-8: Native elution's (reducing conditions); 9: Ni-NTA resin; 10-13: Native elution's (non-reducing conditions). Expected molecular weight of SUMO- β NGF is ~30 KDa (appropriate size area is boxed). Samples were electrophoresed on 4-12% polyacrylamide gel.

As there appeared to be soluble SUMO- β NGF it was necessary to quantify the concentration to allow the subsequent activity testing later in the process. The method of quantification chosen was the BCA assay (Thermo Scientific) (2.2.9.3) and the concentration of the refolded fraction were measured compared to BSA standard curve (Figure 5.13 and Table 5.2).

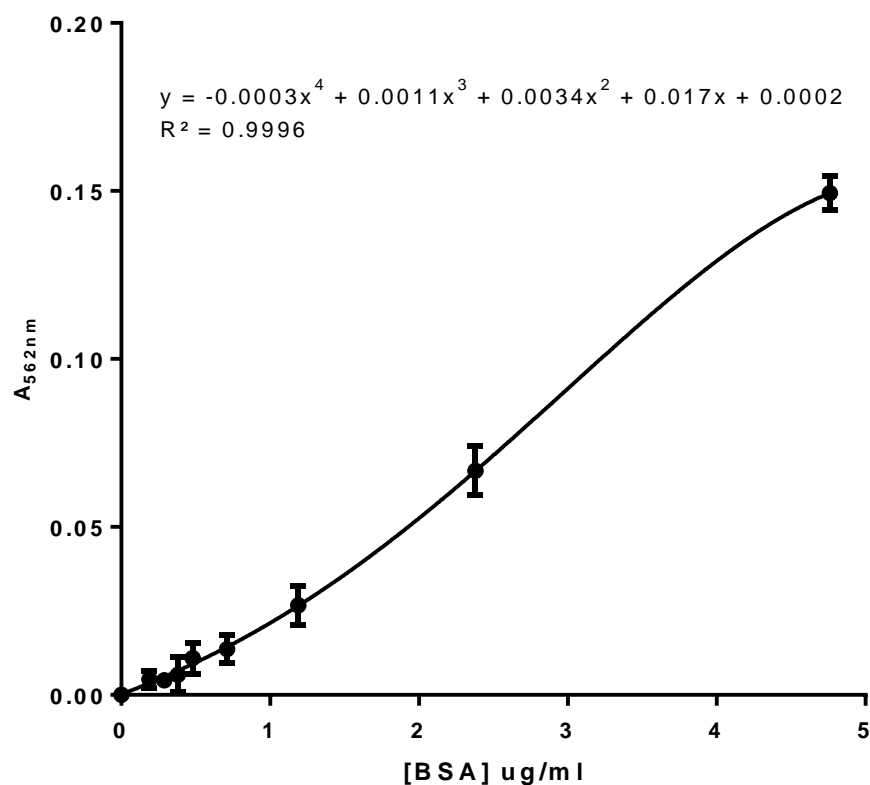


Figure 5.13. BCA Assay BSA Standard Curve. BSA was diluted to an initial range of 0-100 $\mu\text{g/ml}$. This was further diluted 21-fold with BCA working reagent and incubated at 37 °C for 30 min. The plate was then cooled to room temperature and the absorbance measured at 562nm.

	$A_{562\text{nm}}$					[Dilution] ug/ml	[Refolded] ug/ml
	1	2	3	Mean	Blank Corrected Mean		
RF1	0.147	0.150	0.153	0.150	0.084	2.8	59.2
RF2	0.168	0.166	0.171	0.168	0.102	3.3	69.3
RF3	0.137	0.140	0.139	0.139	0.072	2.5	53.1

Table 5.2. SUMO- β NGF BCA Assay Quantification. SUMO- β NGF samples were diluted 21-fold with BCA working reagent and incubated at 37 °C for 30 min. They were then cooled to room temperature and the absorbance measured at 562nm. Concentration of each sample was then calculated using BSA standard curve.

5.7. SUMO- β NGF Activity Testing

Once the SUMO- β NGF fusion had been refolded and quantified it was necessary to cleave the SUMO tag from β NGF. One unit of SUMO protease was added per 5 μ g SUMO- β NGF fusions with 1x SUMO protease buffer (2.1.3.20.11) whilst NaCl concentration was kept between 100 mM and 300 mM for optimal reaction conditions. The reaction was incubated at 30°C for 6 hours (Figure 5.14 A). Lane 1 shows undigested SUMO- β NGF fusion with a molecular weight of ~30 KDa whereas lane 2 shows digested fusion. A small amount of undigested material is visible at ~30 KDa with two small fragments appearing close to the 14 and 17 KDa markers (β NGF and SUMO respectively).

In order to purify the two proteins from one another it was necessary to undergo Ni-NTA his tag affinity purification again (2.2.9.1.4). The tag was present at the N-terminal of SUMO so this should bind to the resin while β NGF should be eluted in the column flow through (Figure 5.14 B). However no protein was present in the column flow through (lane 1) or column washes (lanes 2-3). SUMO was visible when protein bound to the column was eluted (lanes 4-7) although β NGF was not. By boiling a sample of the Ni-NTA with 1x SDS sample buffer (2.1.3.8) and it showed that the β NGF was bound to the resin (lane 8). This was repeatable and despite different elution conditions the β NGF would not elute from the column.

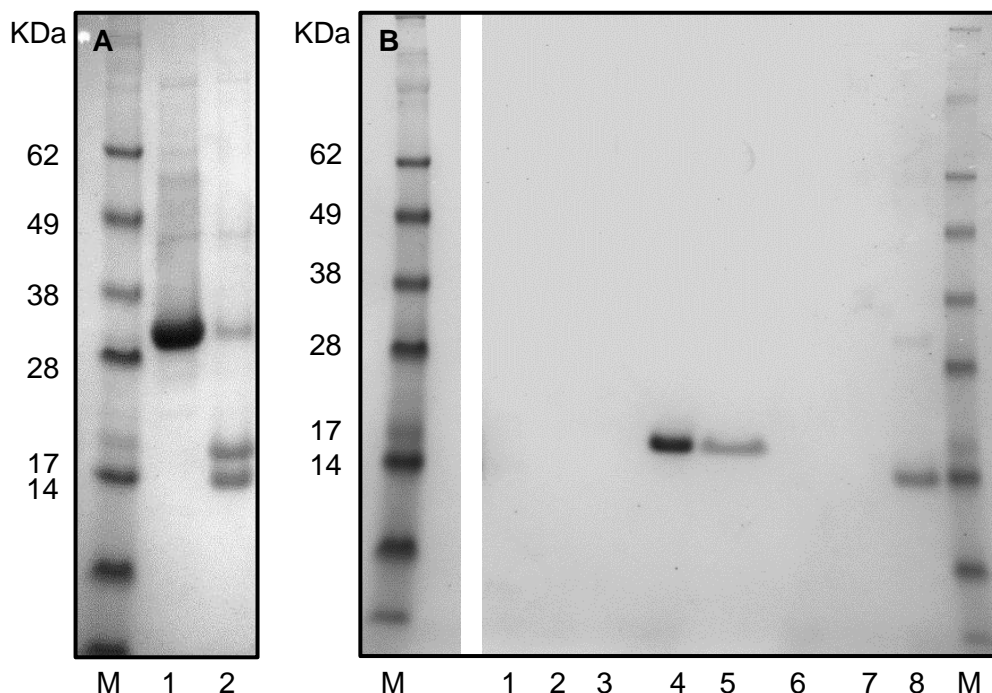


Figure 5.14. SUMO- β NGF Digestion and Purification. **A:** SDS-PAGE gel image of SUMO- β NGF cleavage after treatment with SUMO protease (2.2.9.4). Lanes: 1: Undigested SUMO- β NGF fusion; 2: Digested SUMO- β NGF fusion. Expected molecular weight of SUMO- β NGF is ~30 KDa whereas cleaved SUMO is ~16 KDa and β NGF is ~14 KDa. Some undigested SUMO- β NGF fusion is still present in the cleaved sample in lane 2. **B:** SDS-PAGE gel image of Ni-NTA purified cleaved SUMO- β NGF fusion (2.2.9.1.4). Lanes: 1: Column flow through; 2-3: Column washes; 4-7: Column elutions; 8: Ni-NTA resin. Expected molecular weight of SUMO- β NGF is ~30 KDa (appropriate size area is boxed). In both A & B samples were electrophoresed on 4-12% polyacrylamide.

As it was not possible to separate the cleaved SUMO- β NGF fusion as originally intended it was decided to test whether the cleaved un-purified β NGF was active before more purification attempts were made. This was undertaken using a TrkA binding assay (2.2.9.5) where TrkA, a receptor for NGF, was immobilised and the un-purified β NGF cleavage (as well as relevant controls) were washed over it and the binding was assessed using a monoclonal mouse human β NGF antibody (Figure 5.15).

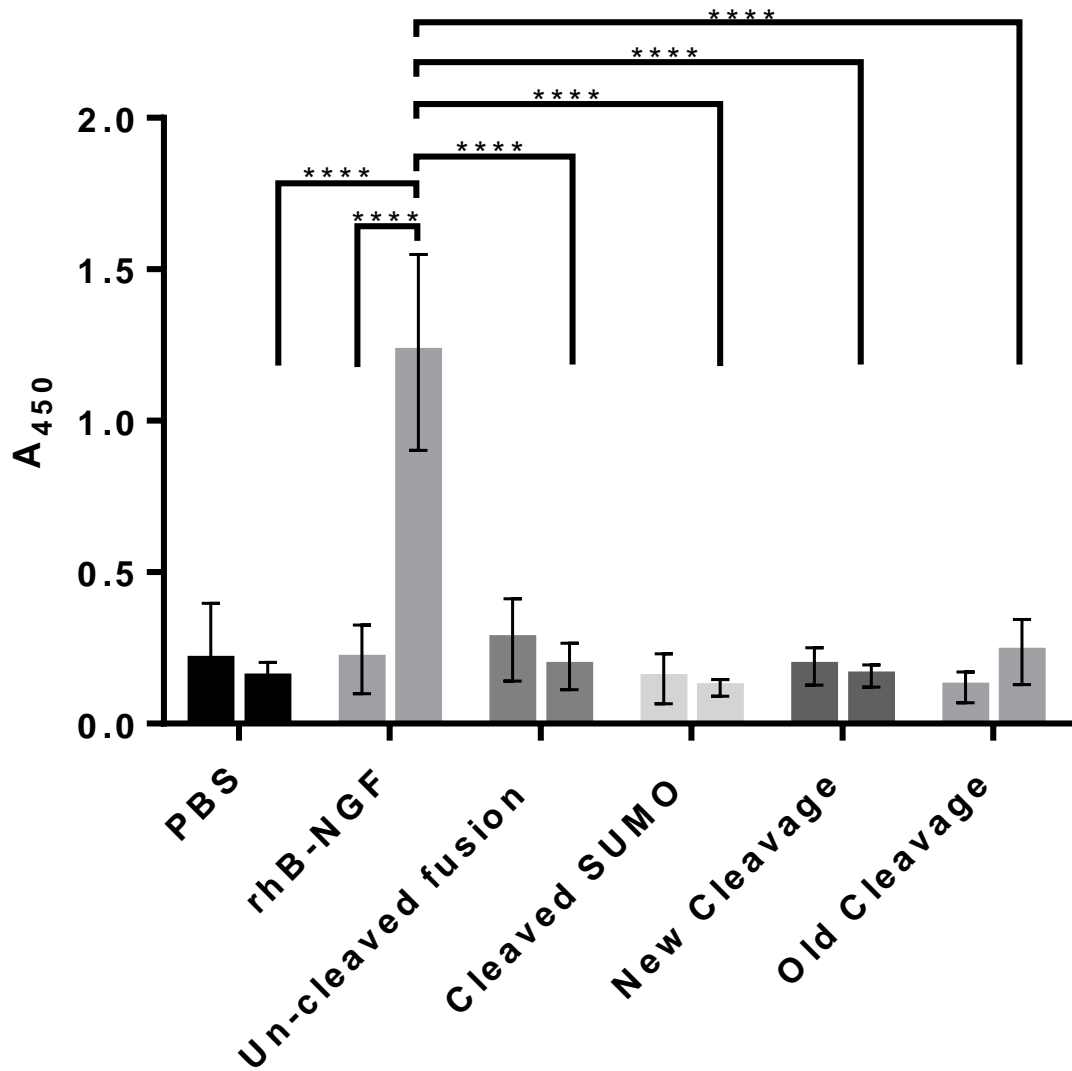


Figure 5.15. β -NGF Activity Assay. Expressed NGF activity was tested using a NGF-TrkA binding assay as described in 2.2.9.5. PBS was used as a negative control and rh- β NGF (purchased from R&D systems) as a positive control. The activity of un-cleaved and cleaved fusions were tested as well as purified SUMO ($-\beta$ NGF). Each compound tested (right column) was analysed alongside a background binding control where no TrkA was bound (left column). Statistical analysis was conducted in GraphPad Prism 6.0. A two-way ANOVA was used (* $p < 0.05$, ** $p < 0.01$, *** $p < 0.001$, **** $p < 0.0001$).

With each sample analysed (right column), a negative control using blocked plastic with no TrkA was used (left column) to measure non-specific binding to the well itself. A negative control of PBS (+/- TrkA) was used to analyse background absorbance from TrkA alone. A positive control of recombinant human β -NGF (rh β -NGF) purchased from R&D systems was used as a benchmark for TrkA binding. Un-cleaved fusion and purified SUMO were tested alongside two cleavage reactions (an old cleavage that had been stored at 4°C and new fresh cleavage) to test as many different variants as possible. Two way ANOVA statistical analyses were used to assess the significance of any differences between different groups. The negative controls PBS +/-TrkA showed low levels of absorption at 450nm with no significant difference observed between the two. rh β -NGF+TrkA showed a significant difference between both rh β -NGF-TrkA and PBS+TrkA thus giving a good positive control and so demonstrating that the assay was working correctly. There was a significant difference observed between rh β -NGF+/-TrkA bars for the un-cleaved fusion, cleaved fusion, new cleavage and old cleavage respectively. No significant difference between +TrkA and -TrkA for the un-cleaved fusion, cleaved fusion, new cleavage and old cleavage was observed. This data showed that the expressed β NGF appeared to have little or no activity in binding to its receptor TrkA.

5.8. Discussion

Although apparently showing optimal expression, albeit not producing soluble protein, based on the results of the TrkA binding assay it was obvious that the expressed β NGF was not active (Figure 5.15). Two way ANOVA statistical analysis showed that the rh β -NGF was bound to TrkA significantly compared to when there was no TrkA present ($p < 0.0001$). Likewise there was a significant difference observed between rh β -NGF+TrkA and the cleaved fusions +TrkA, whilst there was no significant difference observed between cleaved fusions +/-TrkA. There may be a few reasons why the expressed β NGF showed no biological activity.

To begin with, to attempt cytoplasmic expression may have been a factor in its lack of activity. Cytoplasmic expression was attempted because NGF was required for not only the selection process but also other crystallization studies and due to the amount required cytoplasmic expression, if successful, was deemed the most appropriate for scaling up due to the low and inactive yields generated from periplasmic expression previously. (Fujimori et al., 1992, Negro et al., 1992, Rattenholl et al., 2001a). Whilst expression in a prokaryotic system meant that there was no post-translational modification such as glycosylation possible, this should not have been a factor as there are no glycosylation sites of the β -NGF subunit. If the pro-form of NGF was being expressed the lack of post translational modification would have then been an issue as there are two glycosylation points (Asp69 and Asp114), although as previously stated these are outside the desired β -NGF subunit. Ultimately although the cell line co-expressed disulfide bond isomerase (DsbC), to aid disulfide bond formation, and mutations to allow disulfide formation in the cytoplasm they were not enough to allow the formation of soluble protein resulting in the formation of inclusion bodies. While cytoplasmic expression may have been a factor in protein solubility it was ultimately null and void due to this formation insoluble aggregate which subsequently had to undergo solubilisation, meaning that the disulfide bonds formed during expression had to be broken, and refolding. Therefore the more likely explanation for the expressed NGFs lack of biological activity is mis-folding during the refolding process.

The refolding procedure itself may have caused the protein to refold incorrectly. The dilution method of refolding was chosen over the dialysis method as this reduces the time for aggregates to form, and has been successfully used for other members of the neurotrophin family. Whilst L-Arg and GSSG/GSH was used to help the formation of disulfide bond refolding whilst immobilised on Ni-NTA may have interfered with correct refolding as the protein may bind the resin through multiple sites (Arakawa and Ejima, 2014), thus restricting refolding. In hindsight it may have proved more successful if refolding was undertaken whilst free in solution rather than while Immobilised. In the end refolding by dilution may have produced better results allowing longer timespan for disulfide bond formation, although ultimately all refolding methods will involve some form of compromise, be it the amount of

active protein generated or the time taken. Mis-folding of the SUMO-NGF fusion would explain the higher order aggregates in Figure 5.12. β -NGF contains three intra-monomer disulfide bonds (Cys136- Cys201, Cys179- Cys229, Cys189- Cys231) that form the cysteine knot. The presence of the higher order aggregates in Figure 5.12 could be as a result of inter-monomer disulfide bonds strongly suggesting that the NGF monomers are incorrectly folded. This inter-monomer folding may have been reduced by increasing the dilution/lowering the protein concentration to reduce the proximity of the molecules during refolding. Apart from possible mis-folding due to the methodology, there is also evidence to show that the pro sequence of NGF can aid the correct folding of mature β NGF (Rattenholl et al., 2001b). Pro-NGF acts as an intramolecular chaperone for β NGF, through hydrophobic interaction of tryptophan residues, by facilitating oxidative folding. Therefore, ultimately by attempting to express mature β NGF it may have reduced the likelihood of generating correctly folded β NGF. Finally it is worth noting that it is stated in the manual that SUMO protease recognises the tertiary structure of the SUMO protein and as this was digested successfully it would suggest that SUMO, at least, was folded correctly.

Despite not being able to express active β NGF it was necessary to carry on to the screening and selection process. In order undertake this it would be necessary to purchase rh- β NGF and use particularly tight conditions in order to maximise the efficiency of the selection process as large quantity of rh- β NGF would not be available.

Chapter 6

Anti-NGF Peptide Selection, Screening and Testing

6. Chapter 6: Anti-NGF Peptide Selection, Screening and Testing.

6.1. Introduction

Whilst it is important to produce the highest quality DNA library, a natural bottleneck in the mutagenesis process is the ability to efficiently screen the resulting libraries. There are a number of different methods that can be used as described in chapter 1. In this case CIS display (proprietary technology of Isogenica) was chosen for selections and screening of the anti-NGF peptide library created in chapter 4

CIS display utilises the ability of the bacterial replication initiator protein RepA to bind to DNA. Downstream of the RepA gene are two elements named *Cis* and *Ori*. Having transcribed *RepA*, RNA polymerase stalls on *Cis*, which is a non-coding region that contains a rho-dependent transcriptional terminator. This delay allows nascent RepA protein to be produced by the ribosome, whilst the mRNA is still bound, albeit transiently, to *Cis* via the stalled RNA polymerase (Praszkier and Pittard, 1999, Praszkier et al., 2000). The translated RepA protein is subsequently able to bind non-covalently to the downstream *ori* region (a plasmid origin of replication) (Odegrip and Haggard-Ljungquist, 2001), thus creating a phenotype to genotype relationship. Thus by fusing a library in frame, upstream of the *repA* sequence, the expressed protein, fused to RepA protein, which in turn is physically linked to the DNA that encoded it via the RepA/*Ori* interaction. The DNA library undergoes *in vitro* transcription/translation to form a pool of protein–DNA complexes and the library pool then is incubated with an immobilized target. Non-binding peptides are washed away and the remaining DNA is eluted and amplified by PCR to form a DNA library ready for the next round of selection. After several rounds of selection recovered DNA is cloned for the identification of individual target binding peptide sequences (Odegrip et al., 2004, Eldridge et al., 2009). DNA-based systems have the advantage that they are considerably more resilient, than other selection systems, to nucleases and can be generated quickly using normal PCR procedures. This process is illustrated in Figure 6.1.

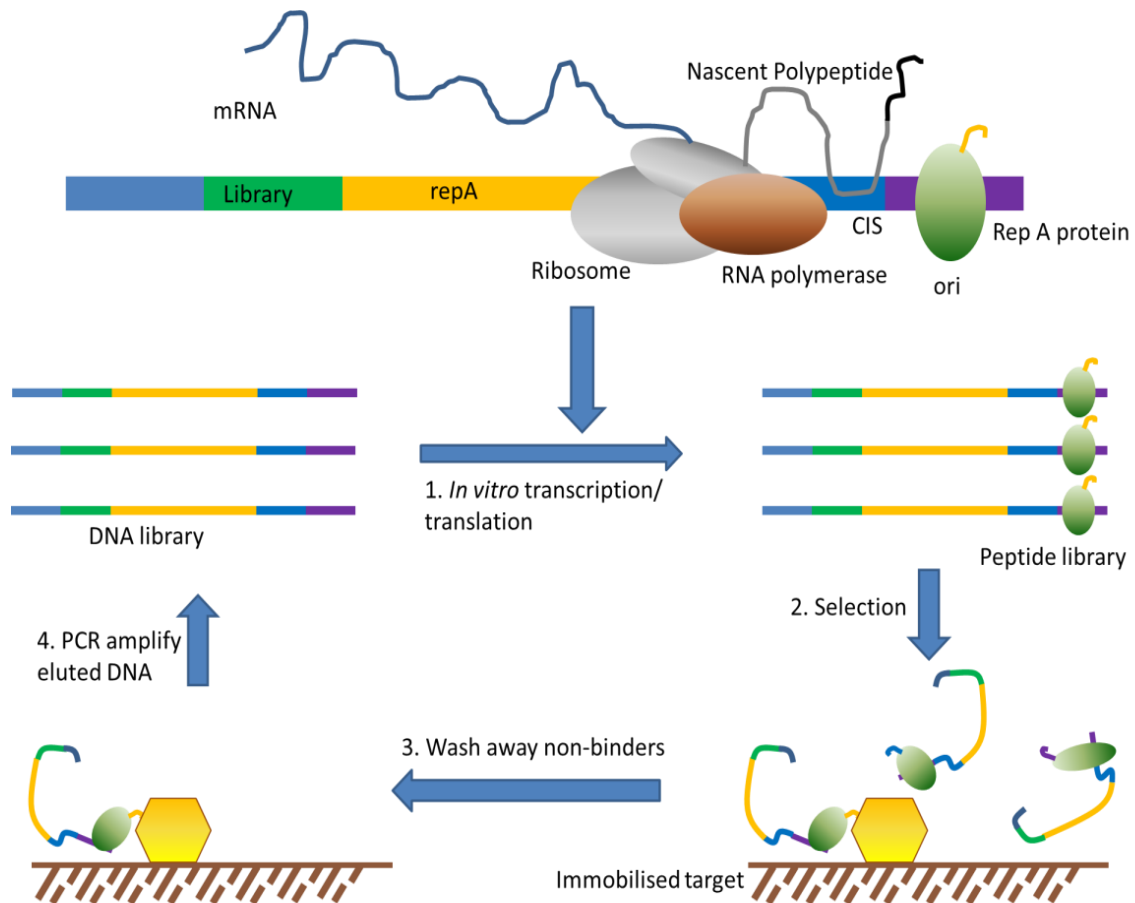


Figure 6.1. CIS Display Overview. CIS display (Isogenica, UK) is an *in vitro* DNA based screening method that creates a genotype to phenotype link between a peptide and the nucleic acid that encodes it (Odegrip et al., 2004). During transcription the RNA polymerase stalls on the non-coding *Cis* region, downstream of the *repA* sequence. Nascent RepA protein non-covalently binds to the downstream *ori* region creating a phenotype to genotype relationship. By placing a library upstream of the *repA* sequence the expressed protein will be attached to RepA protein, linking it to the DNA that encoded it. The library pool is incubated with an immobilized target, non-binding peptides are washed away and the remaining DNA is eluted and amplified by PCR to form a DNA library ready for the next round of selection. After several rounds of selection recovered DNA is cloned for the identification of individual target binding peptide sequences.

6.2. Biotinylation of rh-βNGF

As it was not possible at this time to successfully produce biologically active (chapter 5) rh-βNGF was purchased from R&D systems for use as an immobilised target.

In order to be used as a streptavidin-immobilised target for CIS display the rh-βNGF needed to be biotinylated. This was achieved using EZ-Link™ Sulfo-NHS-Biotin (Thermo Scientific) with free biotin subsequently removed by dialysis (2.2.10.1). Due to limited amount rh-βNGF it was decided to assess the efficiency of the biotinylation process using matrix assisted laser

desorption ionization (MALDI) coupled to time of flight (TOF) mass spectrometry (Figure 6.2), which only required a small volume of the biotinylated rh- β NGF compared to traditional biotinylation assays e.g. HABA assay.

As shown in Figure 6.2 A, native rh- β NGF was used as a control, which showed a high peak at 13580.46 Da. Peaks approximately half the size were also observed as a result of double charged molecules. An increase in the molecular weight of biotinylated rh- β NGF was observed (Figure 6.2B) with an obvious difference size difference between native rh- β NGF (red) and biotinylated rh- β NGF (blue) in Figure 6.2C. A single biotin (with linker) adds ~339.5 Da to the molecular weight of the protein. Further analysis of the observed peaks in the biotinylated sample showed that the most of the rh- β NGF had 4-5 biotins attached with an overall range of 2-6 biotins observed (Figure 6.2 D). Therefore it was deemed the rh- β NGF was sufficiently biotinylated and could be used for CIS display.

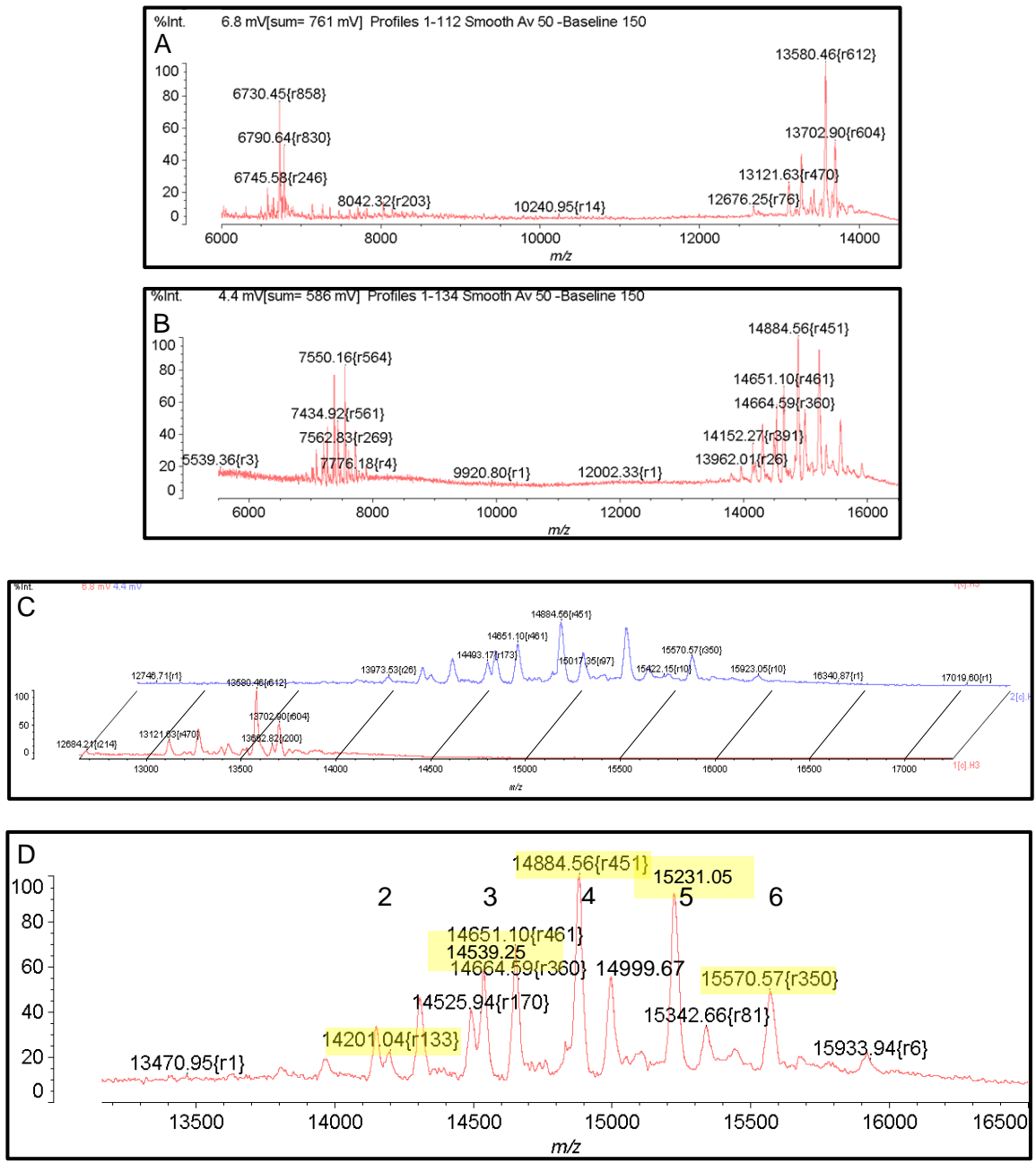


Figure 6.2. rh-βNGF Biotinylation. EZ-Link™ Sulfo-NHS-Biotin (Thermo Scientific) was added to rhβ-NGF (R&D systems) at a 20-fold molar excess. This was incubated on ice for 2 hours and the reaction was stopped with the addition of 250 μl 1M Tris-HCl (pH 7.4). Free biotin was removed by dialysis using a Slide-A-Lyzer dialysis cassette (MWCO 3KDa) with PBS as an exchange buffer. Exchange buffer was replaced after 2 hours (twice) followed by overnight at 4°C. Biotinylation of samples was then assessed using MALDI-TOF mass spectrometry.

6.3. Library Selections Using CIS Display

Once the rh- β NGF was biotinylated it could be used for selections using CIS display according to the selection plan as described in Table 6.1.

Round	ITT Vol/ μ l	Input DNA/ μ g	Biotinylated rh β -NGF/ μ g	Bead vol/ μ l	Wash type		
					0.1% Casein	PBST	PBS
1	250 (5x50)	10	10	50		5x	2x
2	100 (2x50)	4	3	20		5x	2x
3A	50	2	1	10		5x	2x
3B	50	2	1	10	5x	5x	2x
4A	50	2	0.5	10		5x	2x
4B	50	2	0.5	10	10x	5x	2x

Table 6.1. CIS Display Selections Plan. Overview of planned CIS display conditions for each round. To increase the stringency across the process the ratio of input DNA: Biotinylated NGF (immobilised target) was increased round by round as well as increasing the stringency of wash conditions. +/- heparin in the *in vitro* transcription/translation (ITT) was also used.

The plan (Table 6.1) allowed for four rounds of selections with stringency increasing throughout the process in order to select the best peptides. Initial increases in stringency were to be achieved by increasing the ratio of input DNA to biotinylated rh β -NGF. For example, the ratio was 1:1 in the first round compared 4:1 in the final round. Subsequently, more wash steps were included (in rounds 3 and 4) to remove low affinity binders. Finally, the selections would also include +/- heparin, used as intramolecular crowding agent, in the *in vitro* transcription/translation reaction (ITT) to vary the selection stringency.

The first round of sections (+/- heparin) commenced as described in 2.2.10.2 with the recovery PCR illustrated in Figure 6.3 A. This showed a product in lanes 2 (+heparin) and 4 (-heparin) of ~1300bp corresponding to the anticipated size of recovered DNA, with lanes 1 and 3 showing no visible contamination in the negative controls. The process was then continued as described in the selections plan (Table 6.1) with the relevant recovery PCR's shown in Figure 6.3 B-F.

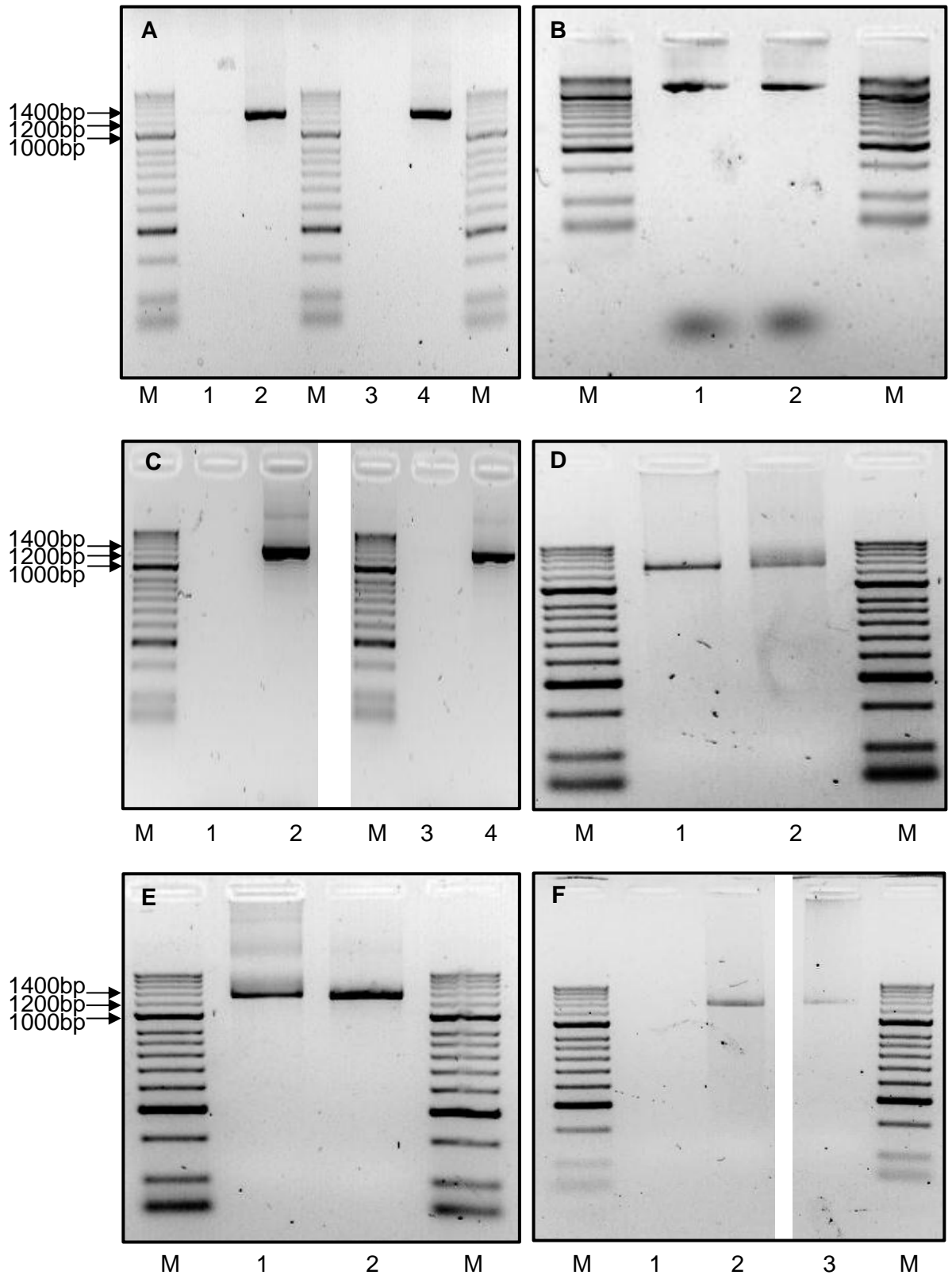


Figure 6.3. CIS Display Recovery PCR. Agarose gel image of the recovery PCR products generated from the eluted selection DNA. **A:** Round 1: Lane 1: Negative control; 2:+Heparin; 3: Negative control; 4:-Heparin. **B:** Round 2: Lane 1: +Heparin; 2:-Heparin. **C:** Round 3A: Lane 1: Negative control; 2:+Heparin; 3: Negative control; 4:-Heparin. **D:** Round 3B: Lane 1: +Heparin; 2:-Heparin. **E:** Round 4A: Lane 1: +Heparin; 2:-Heparin. **F:** Round 4B: Lane 1: Negative control; 2:+Heparin; 3: -Heparin. Expected molecular weight of the recovery PCR product is ~1400 bp. The products were electrophoresed on 3% agarose/TAE gel.

The PCR products in the recovery PCR of each round of selections were the correct size (~1400 bp) and there was no contamination observed in the negatives controls (where shown). PCR products in Figure 6.3 F appear faint due to residual ethanol from purification causing poor loading of the agarose gel. However, this product was subsequently deemed acceptable when determined by nanodrop quantification.

6.4. Cloning of Selection Output

To allow for subsequent screening the output from the selection process need to be cloned in to an appropriate expression vector. To allow this the restriction site for *NotI* was reintroduced using a mutagenic primer with a 1 nucleotide substitution, which also shortened the PCR product by removing the now redundant sequence that was needed for the selections (Figure 6.4). The appropriate negative controls in lanes 1, 3, 5, and 7 showed no sign of contamination whilst a PCR product (~225bp) for each stringency from the last round of selections was present in lanes 2, 4, 6, and 8.

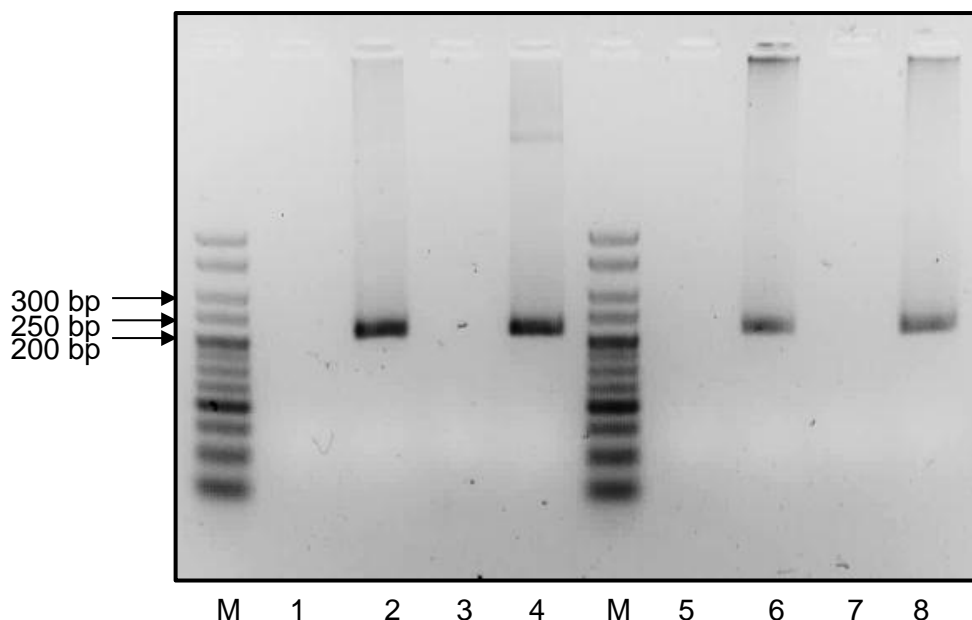


Figure 6.4. Selection Output Amplification and Re-introduction of Restriction Site. Agarose gel image of the PCR products generated as a result of reintroducing *NcoI/NotI* restriction sites necessary for subsequent cloning. Lanes: 1: Negative control; 2: Round 4A (+heparin) selection output; 3: Negative control; 4: Round 4A (-heparin) selection output; 5: Negative control; 6: Round 4B (+heparin) selection output; 7: Negative control; 8: Round 4B

(-heparin) selection output. Expected molecular weight of the recovery PCR product is ~225 bp. The products were electrophoresed on 1.5% agarose/TAE gel.

Both the shortened selection output and the phagemid into which it would be cloned were then digested with *NcoI* and *NotI* (2.2.1.5) to allow subsequent cloning. Figure 6.5 A shows the digested vector with uncut plasmid in lane 1, followed by *NcoI* and *NotI* linearised plasmid in lanes 2 and 3 respectively and finally *NcoI/NotI* double digested plasmid in lanes 4. The anticipated linearized phagemid size of ~5.7 Kbp corresponded to the bands observed in lanes 2 and 3, with a smaller band of ~5 Kbp present in the double digest in lane 4.

The digestions of selection output are shown in Figure 6.5 B with lanes 1, 3, 5 and 7 corresponding to undigested PCR product while lanes 2, 4, 6, and 8 correspond to *NcoI/NotI* digested PCR product. Residual ethanol from the purification buffer led to poor loading and hence faint bands for the digests.

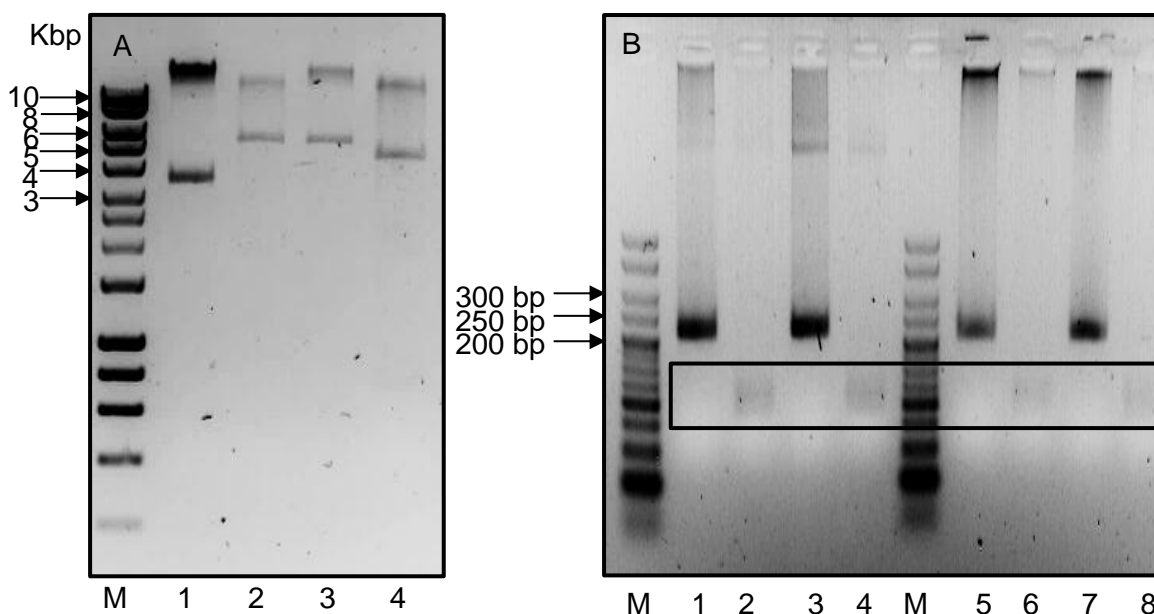


Figure 6.5. *NcoI/NotI* Cloning Digestion. An agarose gel image of *NcoI/NotI* digests for subsequent cloning; an Isogenica proprietary phagemid vector (pHEN) (A) and the output from the final round of selections (B). **A:** pHEN digestion. Lanes: 1: Uncut pHEN; 2: *NcoI* cut pHEN; 3: *NotI* cut pHEN; 4: *NcoI/NotI* cut pHEN. **B:** Selection output digestion. Lanes: 1: Uncut round 4A (+heparin); 2: *NcoI/NotI* cut round 4A (+heparin); 3: Uncut round 4A (-heparin); 4: *NcoI/NotI* cut round 4A (-heparin); 5: Uncut round 4B (+heparin); 6: *NcoI/NotI* cut round 4B (+heparin); 7: Uncut round 4B (-heparin); 8: *NcoI/NotI* cut round 4B (-heparin). Expected molecular weight of the recovery PCR product is ~125 bp. The products were electrophoresed on 1% (A) and 2% (B) agarose/TAE gels respectively.

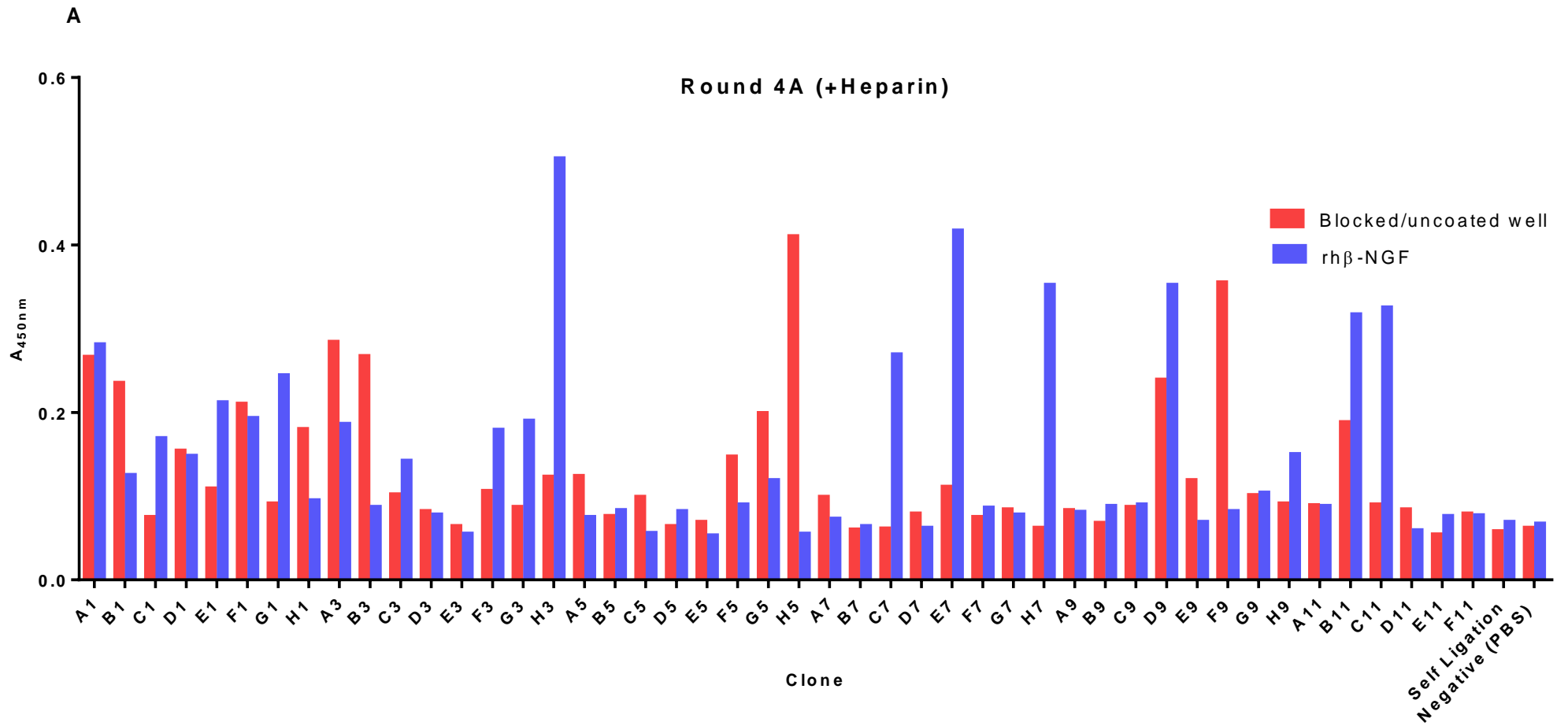
Digested phagemid and inserts were then ligated together with a 3:1 insert: vector molar ratio at 22°C for 30 mins followed by 70°C for 5 mins and transformed into *E.coli* TG1 cell line (Zymo Research) as described in 2.2.5.2 **Error! Reference source not found.** along with appropriate controls (Table 6.2). Each selection stringency showed a good number of clones whilst there were a low number of clones in the background self-ligation control. The transformation control vector pUC18 showed high numbers of clones showing that the transformation process was efficient and the antibiotic controls showed that there was no latent ampicillin resistance in the cells prior to transformation.

	Colonies
R4A+ ligation	572
R4A- ligation	836
R4B+ ligation	636
R4A- ligation	524
Self-ligation	92
Linear pHEN	0
Transformation Control (pUC18)	~3000
No vector (+ Ampicillin)	0
No vector (-Ampicillin)	Lawn

Table 6.2. Selection Output pHEN Cloning. NcoI/NotI digested product from the last round of selections was ligated into pHEN with a 3:1 insert: vector molar ratio at 22°C for 30 mins followed by 70°C for 5 mins. The pHEN ligation was transformed into ready competent *E.coli* TG1 (2.2.5.2) and plated onto LB agar 2% Glucose/Amp (2.1.1.1) along with relevant controls.

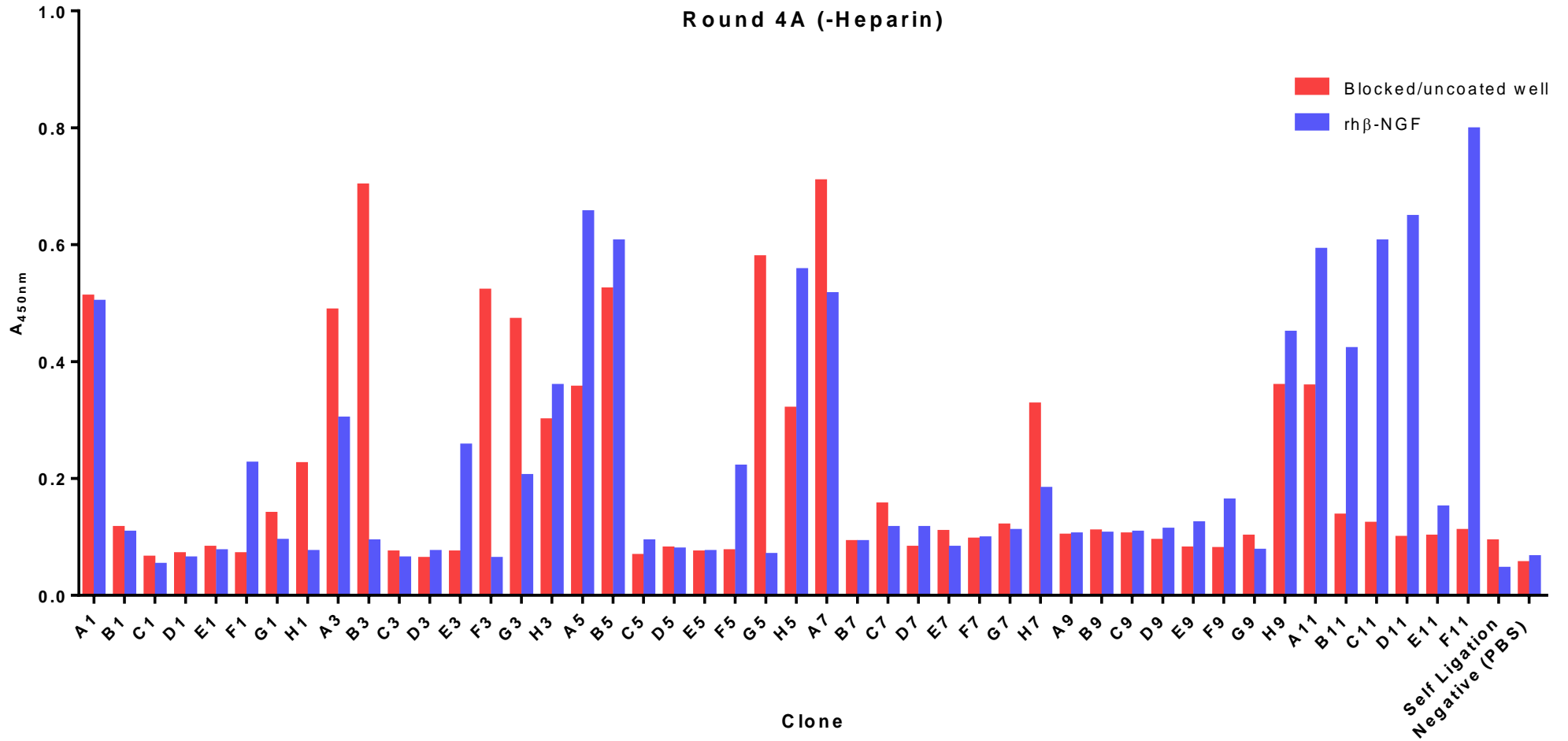
6.5. Screening of Selection Output

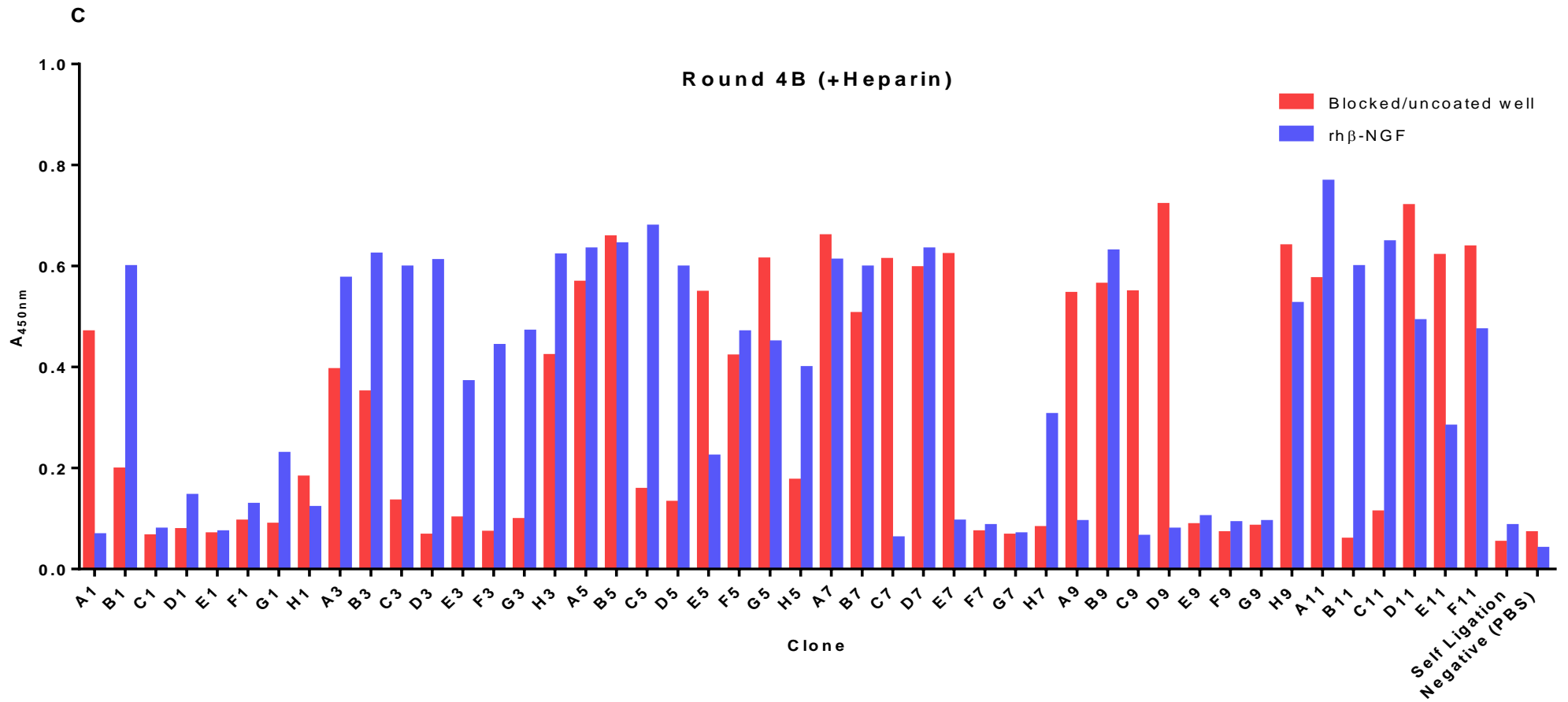
Individual clones were picked and expressed on phage as described in 2.2.10.3.2. Once expressed each phage, expressing a single selected peptide, was then screened for NGF binding by ELISA, using rh-βNGF as an immobilised target (2.2.10.3.3) (Figure 6.6). A negative control used to analyse non-specific background binding to the ELISA plate included by incubating PBS alone on uncoated wells. A separate control of self-ligated phagemid was also used to gauge background binding of phage (not expressing any peptide) to rh-βNGF. A single 96-well ELISA plate was used for each selection stringency with round 4A+heparin, 4A-heparin, 4B+heparin and 4B-heparin illustrated in Figure 6.6 A, B, C and D respectively.

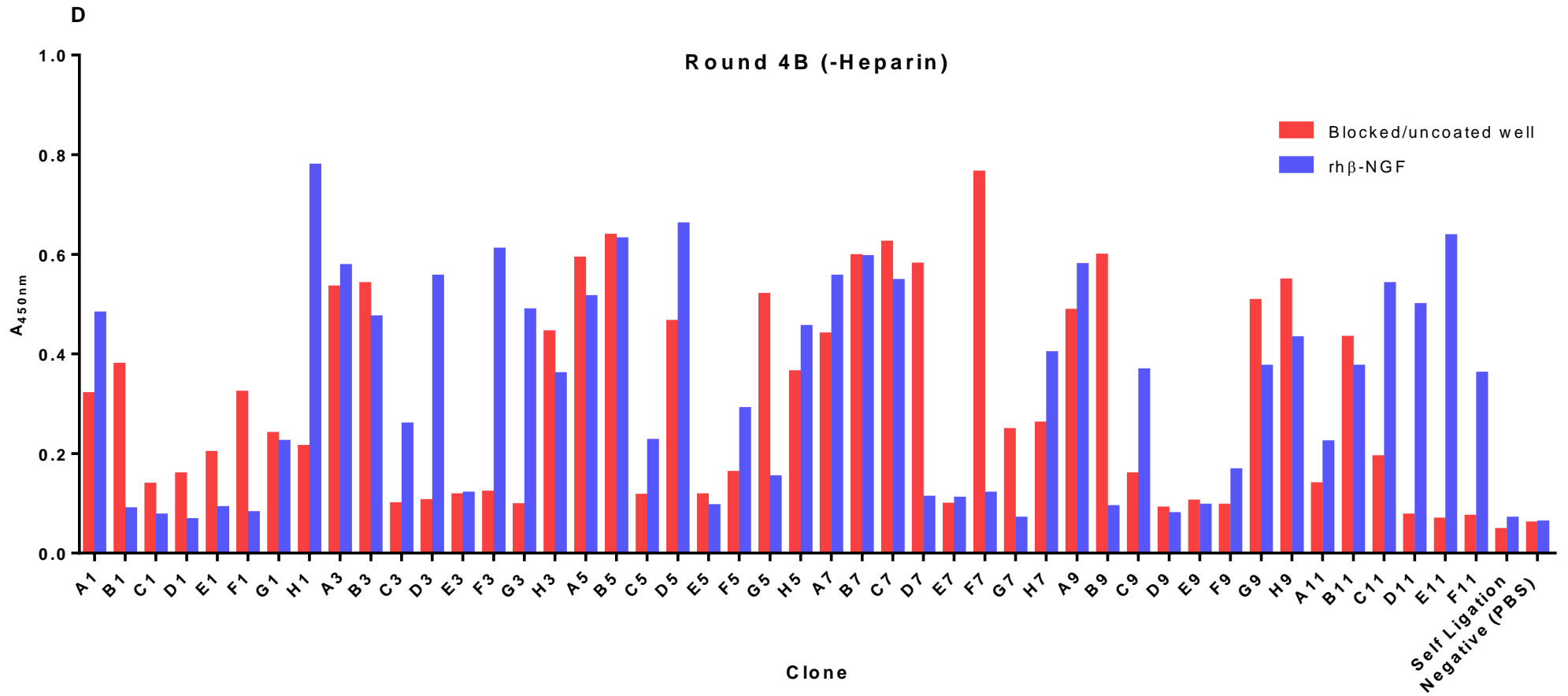


B

Round 4A (-Heparin)







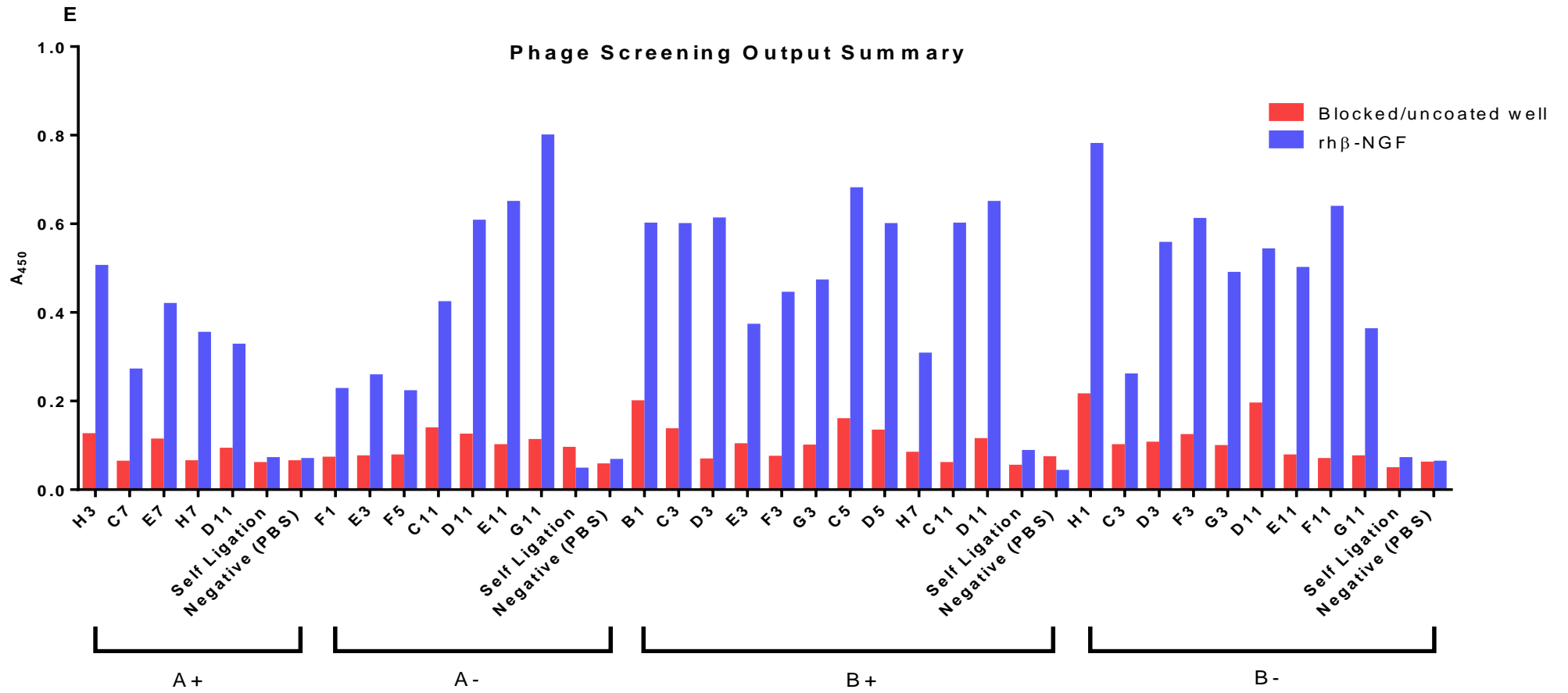


Figure 6.6. Selection Output Screening. The output from the selection process underwent ELISA screening, with an immobilised target of rh-BNGF, as described in 2.2.10.3. Negative phage expression controls of self-ligated vector (no insert) and PBS were used. Every expressed peptide was tested –NGF (red) and +NGF (blue). **A:** Round 4A (+heparin); **B:** Round 4A (-heparin); **C:** Round 4B (+heparin); **D:** Round 4B (-heparin). **E:** Phage screening summary.

In general the number of binders from the more stringent rounds of selection (4B+/-heparin) appeared to be higher than the numbers observed in the less stringent (4A+/-heparin). Additional specificity testing using BSA as a non-specific target (results not shown) narrowed down the number of potential NGF binding peptides to those that exhibited the best NGF binding affinity compared to non-specific binding, as illustrated in Figure 6.6 E.

6.6. Sequencing of Screening Output

After screening it was necessary to sequence the positive screening hits in order to verify constituent amino acid sequence to ensure they fell within the original library design. To do this the glycerol stocks of the positively screened clones were amplified using colony PCR (as undertaken in 2.2.2.3) as illustrated in Figure 6.7. The negative control in lane 1 showed no contamination while a sample of the PCR products from positively screened clones for each selection stringency showed clean single bands at the anticipated molecular weight (Lanes: 2-4: Round 4A (+heparin) colonies; 5-7: Round 4A (-heparin) colonies; 8-10: Round 4B (+heparin) colonies; 11-13: Round 4A (+heparin) colonies).

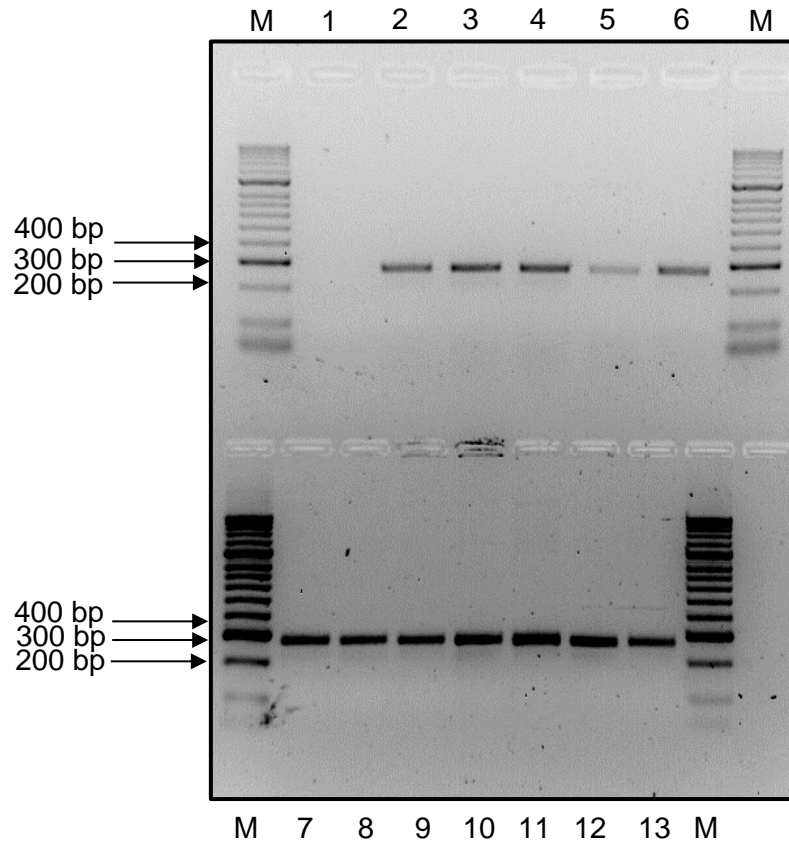


Figure 6.7. Colony Screening. Agarose gel image of the products generated from screening of positive identified from Figure 6.6. Lanes: 1: Negative control; 2-4: Round 4A (+heparin) colonies; 5-7: Round 4A (-heparin) colonies; 8-10: Round 4B (+heparin) colonies; 11-13: Round 4A (+heparin) colonies. Expected molecular weight of ~290 bp. The products were electrophoresed on 1.5% agarose/TAE gel.

The colony PCR products were sent for sequencing at Beckman-Coulter using standard M13 sequencing primers. In total 32 clones, spanning the 4 selection stringencies, were sequenced with 12 unique correct sequences returned (Figure 6.8 A). The 12 unique correct sequences activity could be tested using a TrkA inhibition ELISA. A number of the sequences returned that were not correct, according to the original library design, consisted of n-1 deletions (Figure 6.8 B) with some n-2, n-3, repeated sequences and nonsense sequences completing the set. Firstly, these peptides may have originally been correct NGF binders but deletions may have been introduced by either the glycerol stock colony PCR or the sequencing reaction. These n-1 sequences were re-sequenced with some returned as correct sequences whilst others still contained a deletion. A second hypothesis is that the n-1 deletions were introduced prior to the selections process and subsequently pulled through

the selections due to the presence of the cysteine potentially interacting with those present in rh-βNGF. Interestingly, as a result of the subsequent frameshift caused by the deletion a number of the n-1 sequences contained a poly-arginine tail. Those peptides with the poly-R tail all came from selections with heparin, so it may have been possible that there was some charge interaction that may have promoted binding. However, as these did not conform to the original library they were not taken on for further testing although could be an interesting lead for future work. To note, B+C3 contained a single nucleotide deletion in the 3' framework rather than the saturated library, meaning that the frameshift did not cause a cysteine to be translated.

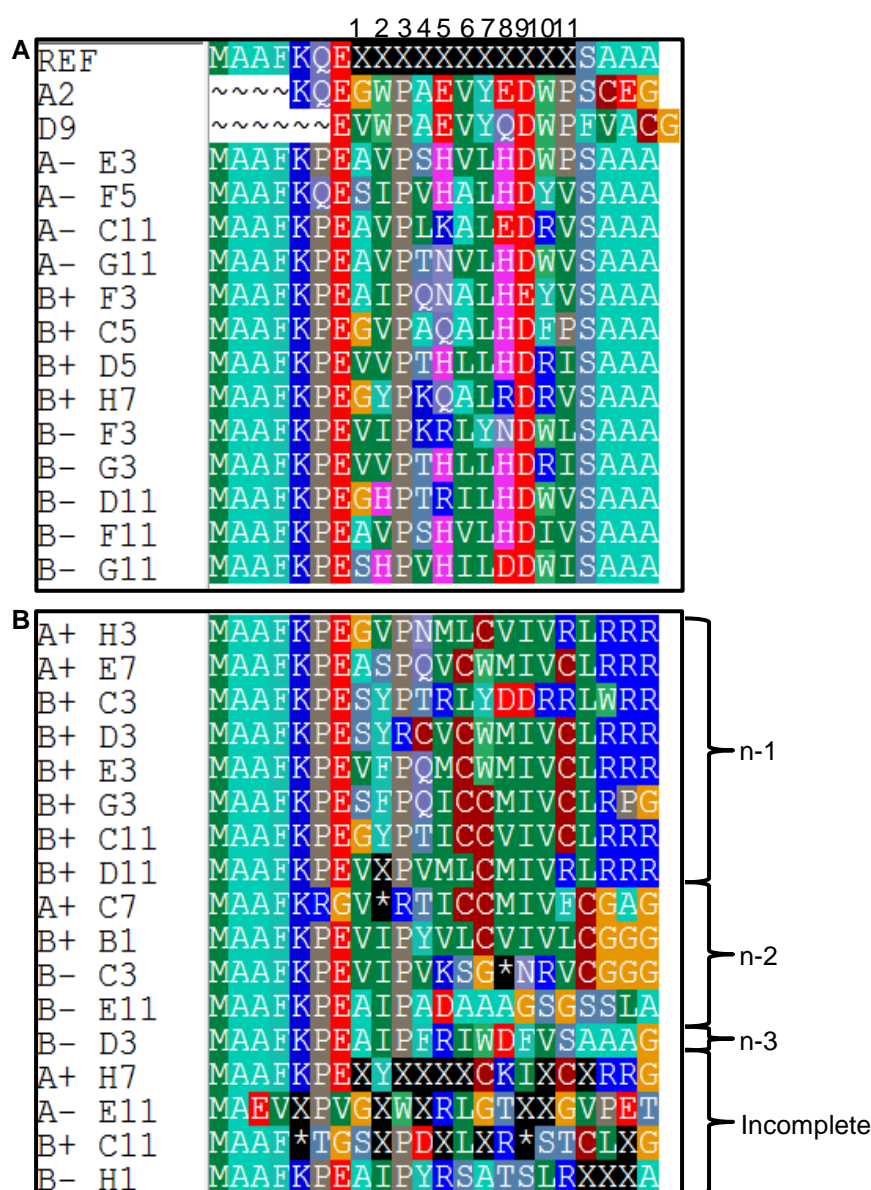


Figure 6.8. Screening Output Sequencing. PCR products amplified from colony glycerol stocks were sent for sequencing at Beckman-Coulter using M13 sequencing primers. Sequencing results returned full correct sequences (A) with the remaining, consisting of n-1,-

2, -3 and incomplete sequences (B). Correct sequences are compared to the original library build (Table 4.1 and Table 4.2) and the original anti-NGF peptides (A2 and D9).

6.7. Anti-NGF Peptide Testing

The 12 peptides (with the original A2 and D9 controls) pulled through the selection and screening process were synthesised by Alta Biosciences (Table 6.3) and quantified by UV spectrometry. These would be tested alongside a set of anti-NGF peptides containing unnatural amino acid substitutions obtained from Isogenica (Table 6.4). Based on original spot analysis the 11 amino acid motif was saturated. Although the termini showed no significant effect on activity they were optimised to the most preferred from the SPOT analysis. On request of Isogenica additional amino acids were added to flanking regions of the randomised section in an effort to encourage additional ionic interactions and hydrogen bonding. The cysteine present at the C-terminal was hypothesized to allow the peptides to work as dimers. As the purpose of this library was to find a high affinity monomer this was removed, hence some design differences from the original peptides.

Name	MW/ Da	Sequence
A2	2110.3	KQEGWPAEVYEDWPSCEG
D9	2053.3	EVWPAEVYQDWP FVGACG
A-E3	2332.7	MAAFKPEAVPSHVLHDWPSAAA
B-F11	2261.6	MAAFKPEAVPSHVLHDI VSAAA
A-G11	2325.7	MAAFKPEAVPTNVLHDWVSAAA
A-C11	2285.7	MAAFKPEAVPLKALEDRV SAAA
B+F3	2329.7	MAAFKPEAIPQNALHEYV SAAA
B+C5	2226.6	MAAFKPEGVPAQALHDFPSAAA
B+H7	2377.8	MAAFKPEGYPKQALRDRV SAAA
B-D11	2405.8	MAAFKPEGHPTRILHDWV SAAA
B-G11	2406.8	MAAFKPE SHPVHILDDWISAAA
A-F5	2356.7	MAAFKQESIPVHALHDYV SAAA
B-G3	2374.8	MAAFKPEVVP THLLHDRI SAAA
B-F3	2492.0	MAAFKPEVIPKRLYNDWLSAAA

Table 6.3. Library Peptide Identity and Sequences. Synthesised by Alta Biosciences and quantified by UV spectrometry.

Name	MW/ Da	Sequence	Unnatural Amino Acid Identity
D9	1929.5	KQEGWPAEV1EDWPSA	1=Tic
E4	1859.9	KQ5GWP2EVY2DWPSA	
E5	1888.0	KQE2WPA2VYE2WPSA	2=Aib
E7	1906.4	KQEG3PAEVYEDWPSA	
E9	1929.5	KQEGWPAEV3EDWPSA	
E10	1906.4	KQEGWPAEVYED1PSA	3=(D-Tic)
E11	1906.4	KQEGWPAEVYED3PSA	
F1	1944.5	KQEGWPAEVYED4PSA	4=(1-Nal)
F2	1944.5	KQEGWPAEVYED5PSA	
F3	1944.5	KQEG4PAEVYEDWPSA	
F4	1944.5	KQEG5PAEVYEDWPSA	5=(2-Nal)
F6	1906.4	KQEG1PAEVYEDWPSA	
G8	1932.0	KQE2WP2EVY2DWPSA	6=(L-Hyp)
H5	1949.4	KQEGW6AEVYEDWPSA	
H7	1908.5	KQEGWPAEVYED7PSA	
H8	1993.5	KQEGWPAEV8EDWPSA	7=alpha-methyl-L-PheOH
H9	1931.5	KQEGWPSEV7EDWPSA	
H10	1970.5	KQEG8PAEVYEDWPSA	8=(D-Dip)
H11	1908.5	KQEG7PAEVYEDWPSA	
H12	1970.5	KQEGWPAEVYED8PSA	

Table 6.4. Unnatural Amino Acid Peptide Identity and Sequences. Tic: L-1,2,3,4-Tetrahydroisoquinoline- 3-carboxylic acid; Aib: α -Aminoisobutyric acid; (L-Hyp): L-Hydroxyproline; (1-Nal): β -(1-Naphthyl)-L-alanyl; (2-Nal): β -(2-Naphthyl)-L-alanyl; (D-Tic) D-1,2,3,4-Tetrahydroisoquinoline- 3-carboxylic acid; (D-DIP): D-3,3-Diphenylalanine.

Both sets of peptide were tested using a TrkA inhibition ELISA (2.2.11) with the aim that active peptides should bind to rh- β NGF and in so doing prevent its binding to its immobilised receptor TrkA. TrkA was coated to a 96-well ELISA plate and then a mix of rh- β NGF and

peptides, at differing concentrations, were incubated on the plate. Non-binders were washed away and rh- β NGF was assessed using a monoclonal biotinylated anti-human β -NGF antibody and streptavidin-HRP. A simple schematic of this is illustrated in Figure 6.9.

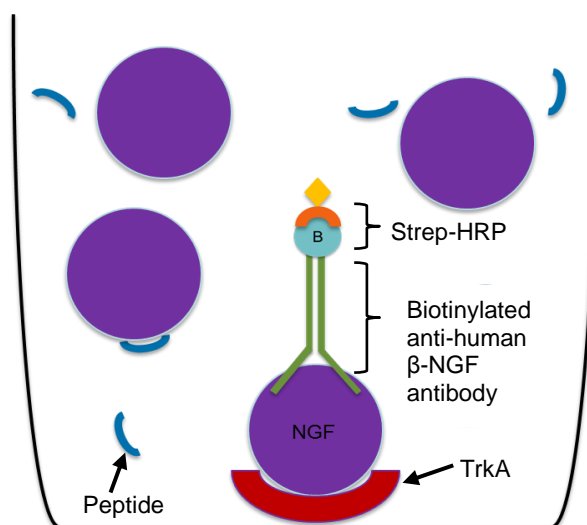


Figure 6.9. Simplified TrkA Inhibition ELISA Illustration. TrkA-Fc chimera was coated on a NUNC F96 Maxisorp plate. Recombinant human β -NGF was mixed with appropriate peptide concentrations separately and then transferred into the NUNC Maxisorp plate and non-binders subsequently washed away. Binders would then be detected using biotinylated anti-human β -NGF antibody and streptavidin-HRP followed by ELISA development using TMB reagent.

To aid interpretation an example of the anticipated results from a TrkA inhibition ELISA is illustrated in Figure 6.10. To ensure that results would be obtained a number of controls would also be run alongside the peptide testing. The first negative control would not contain any TrkA, NGF or peptide, and so effectively a measure of background absorbance from an empty well. A second negative control would measure any absorbance of TrkA alone without NGF or peptide. Finally, a third negative control would measure background binding of NGF to the plate without the TrkA or any peptide present. All of these should show low levels of absorbance at 450nm. A positive control using NGF and TrkA (with no peptide) would measure un-inhibited NGF binding and should result in a high absorbance. For every peptide used a control to measure binding for the NGF-peptide complex without TrkA present was conducted, which should give a low level of absorbance at 450nm. Finally when testing the activity of each peptide the absorbance, indicating the NGF-TrkA binding, should decrease as the peptide concentration increases.

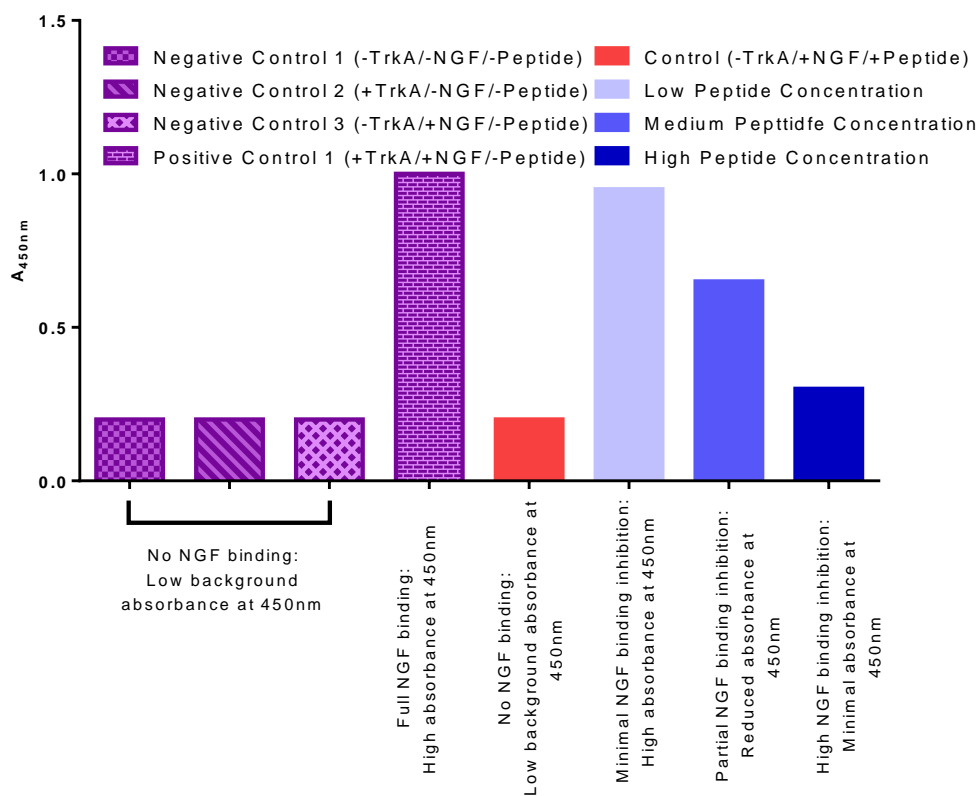
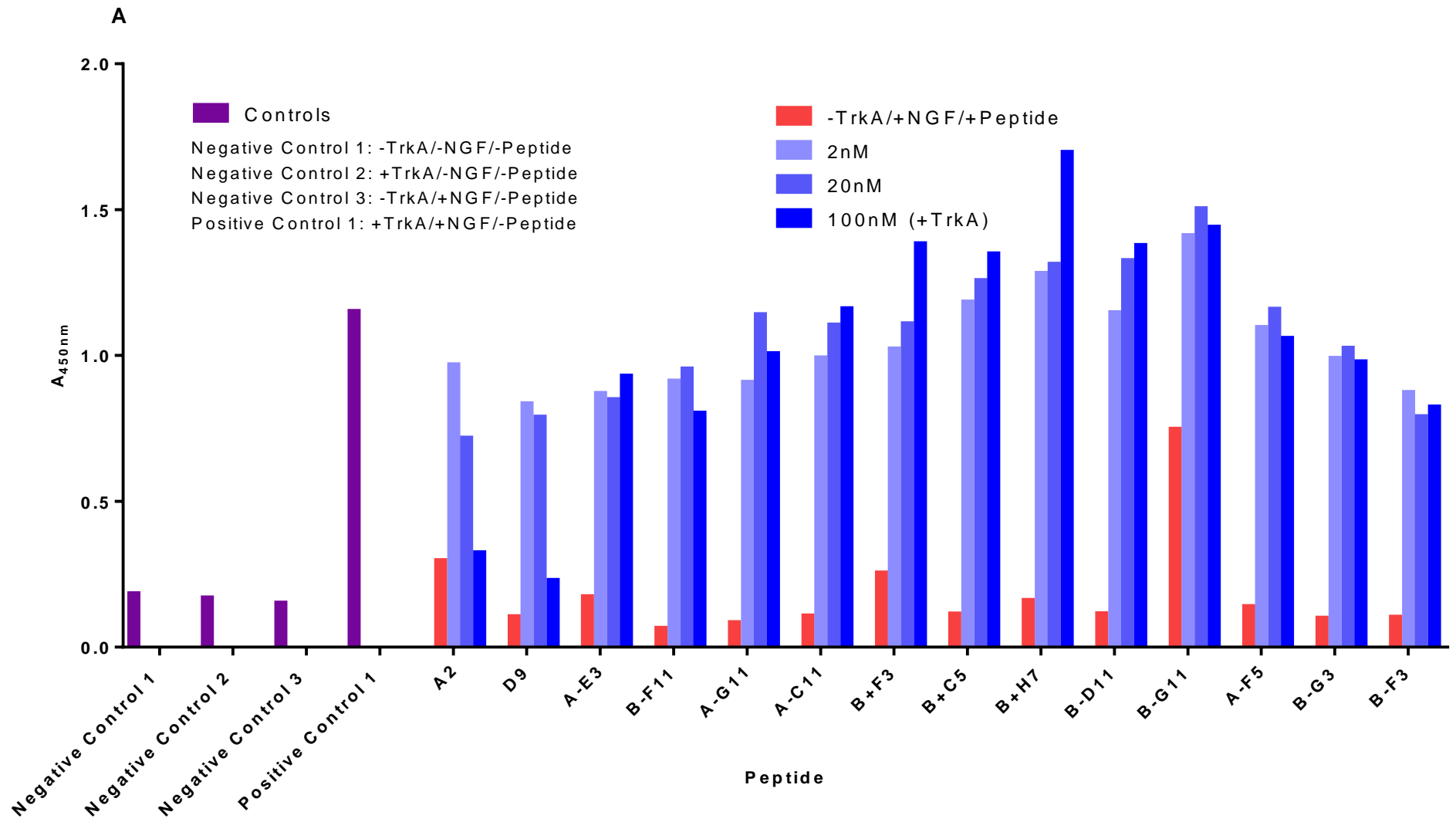


Figure 6.10. Example TrkA Inhibition ELISA Results. Expected results of the TrkA inhibition ELISA. Low background absorbance's would be expected from the negative controls whilst high absorbance from the positive control. Absorbance would decrease as peptide concentration was increased due to their inhibitory effect on NGF-TrkA binding.

The original A2 and D9 peptides showed a working concentration range of 2nM-100nM, so it was deemed prudent to use this as a starting reference point for the concentration at which the new peptides would be tested (Figure 6.11). Positive and negative controls of rh-βNGF +/-TrkA without any peptide were included. As expected, the A2 and D9 controls showed activity by inhibiting rh-βNGF binding over this concentration range whereas the library peptides showed little, if any, inhibition (Figure 6.11 A). The unnatural amino acid peptides performed marginally better with some show a low level of inhibition (e.g.F4 and G8) although inhibition levels were not nearly as strong as A2 and D9 controls (Figure 6.11B). Therefore it was decided to test a broader concentration range in order to determine the peptides working concentration range.



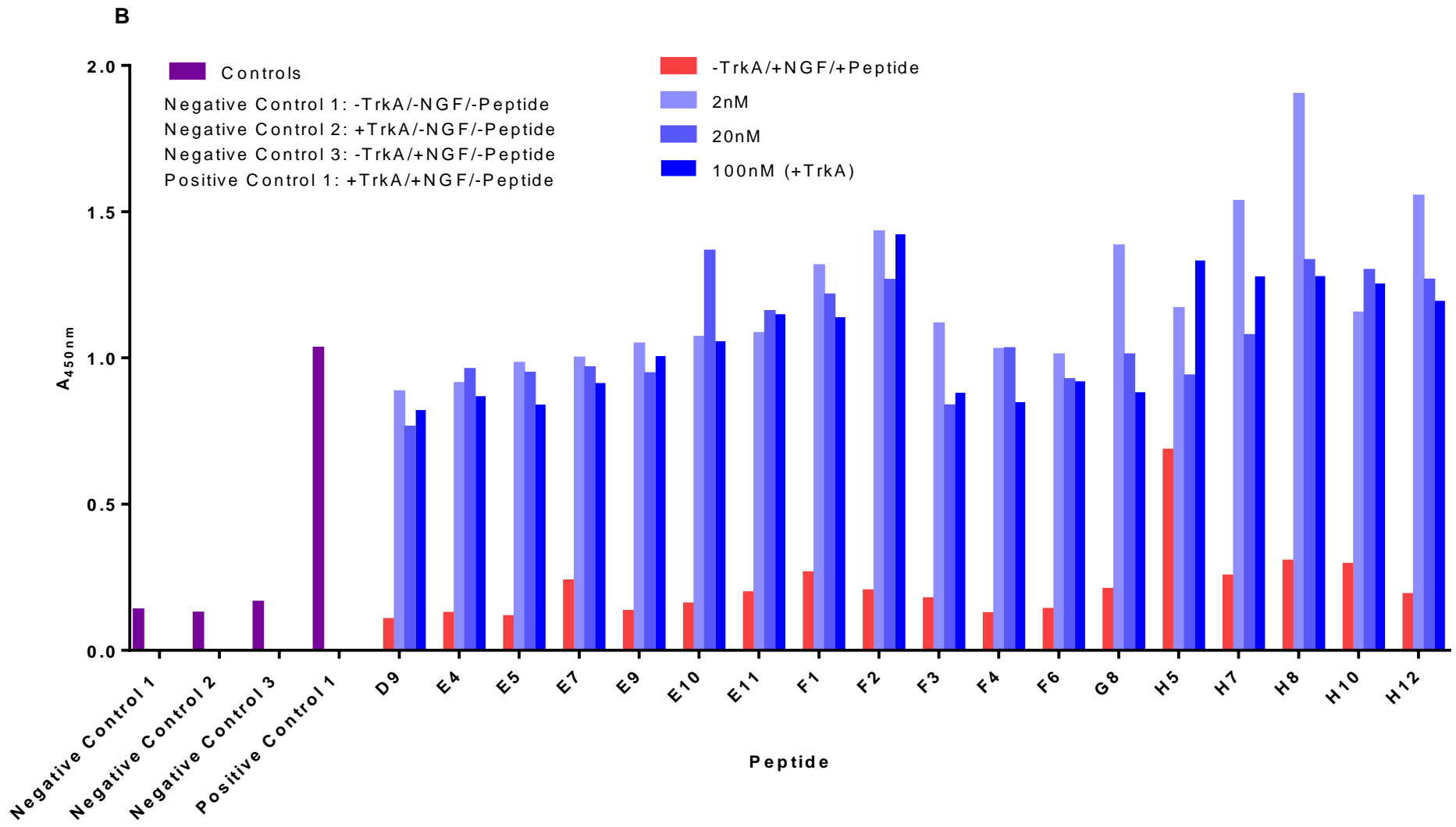
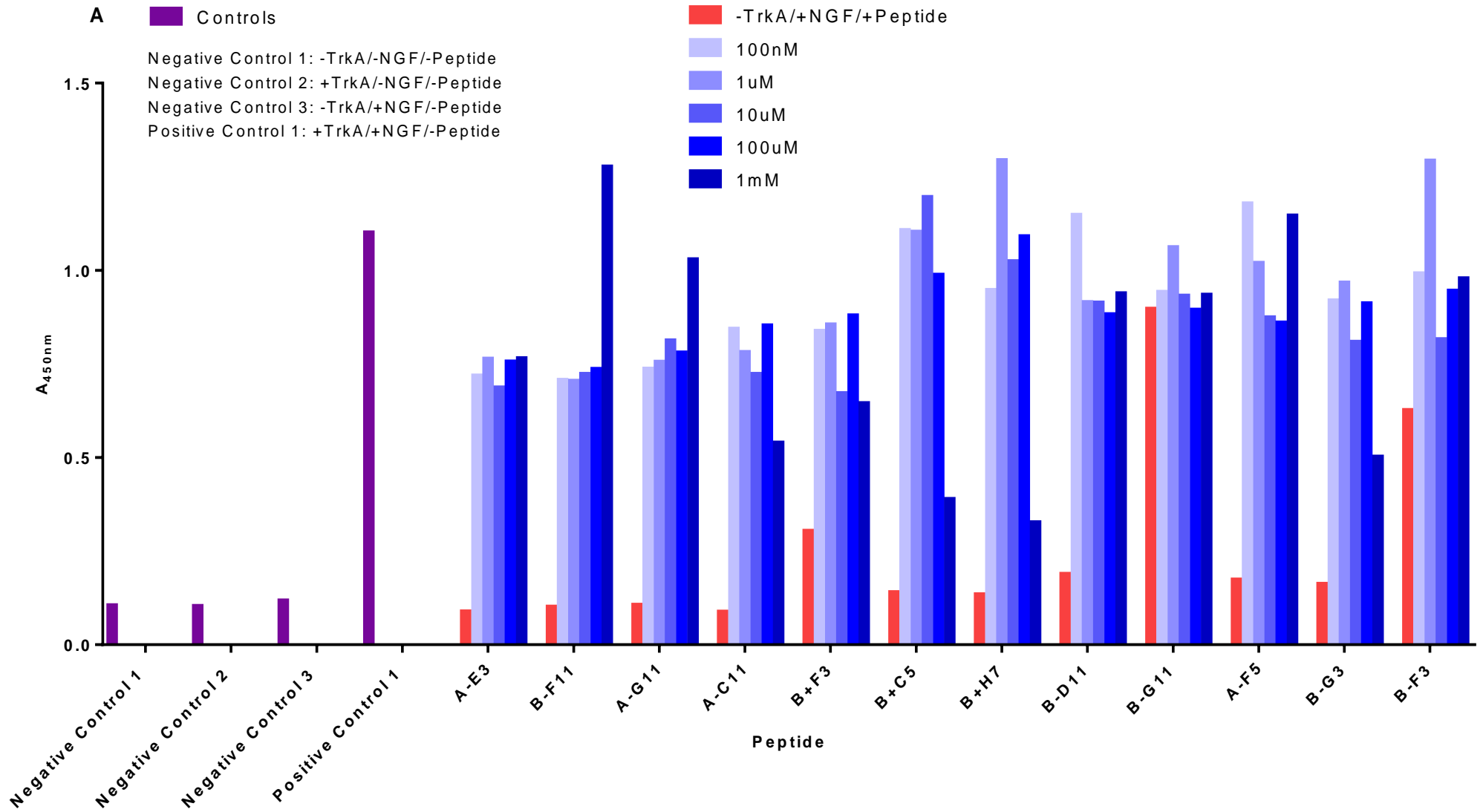
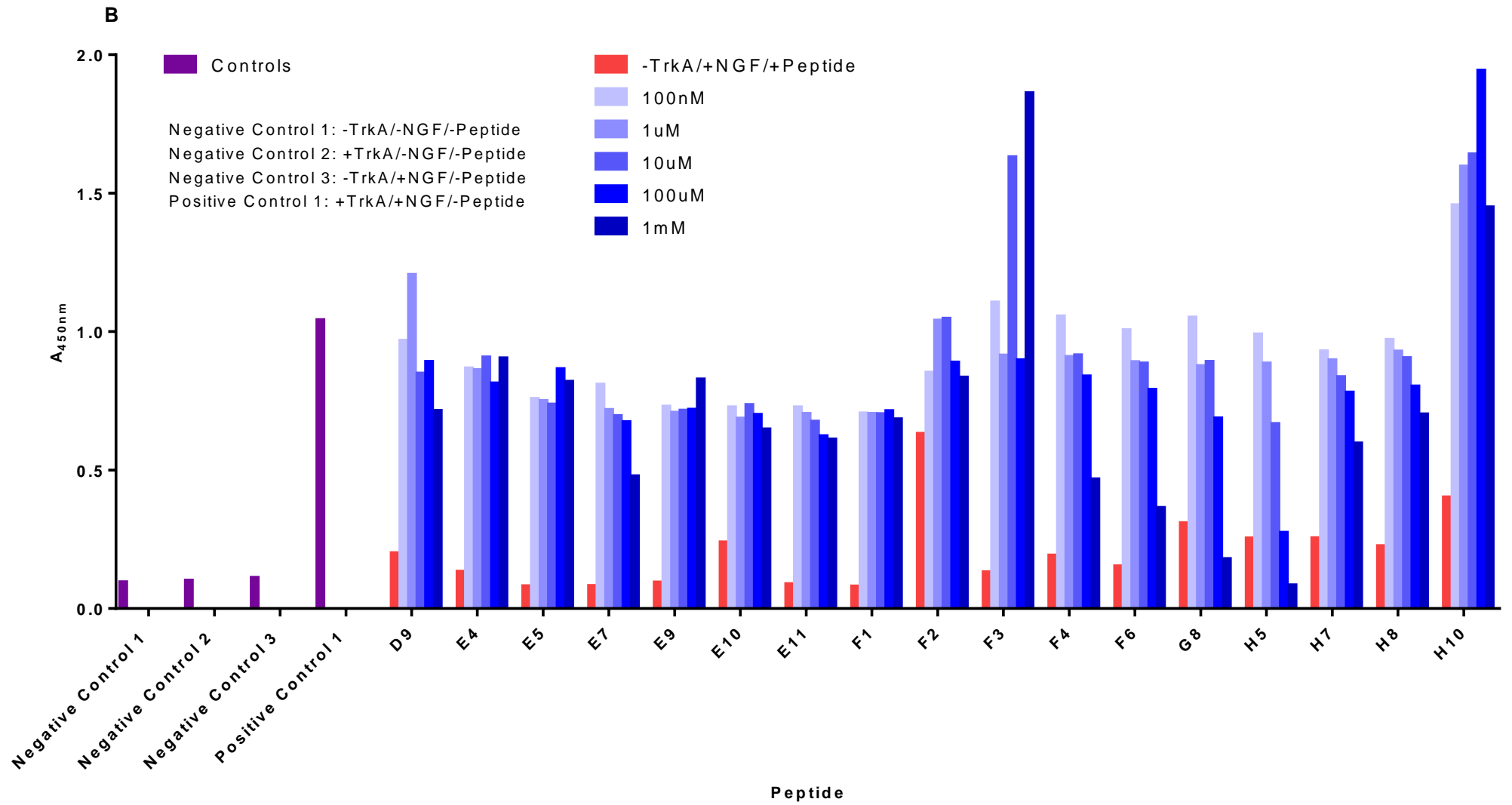


Figure 6.11. Initial Peptide Testing. The peptides identified in screening process underwent ELISA testing, with an immobilised target of TrkA, as described in 2.2.11. Controls as illustrated in Figure 6.10 were used to ensure experimental validity. Every expressed peptide was tested –TrkA (red) and +TrkA (blue). **A:** Library peptides; **B:** Unnatural amino acid peptides.

As the peptides showed little activity at a 2-100nM concentration range it was decided to broaden the testing range to 10µM-1mM. Once again the different peptides were tested using a TrkA inhibition ELISA (2.2.11) as shown in Figure 6.12. This time over the broader concentration range inhibition of rh-βNGF binding to TrkA was observed with the library peptides (Figure 6.12A). Due to the limited reagents values were not repeated so values are variable but for peptides A-C11, B+F3, B+C5, B+H7 and B-G3 a working concentration range of 100µM-1mM was observed. The other peptides show no inherent activity at this range.

The unnatural amino acid peptides likewise showed better activity over this broader range with a selection (F4-H8) showing activity over the 10µM-1mM range (Figure 6.12B). Once a working range had been established for those peptides exhibiting activity it was necessary to further test their activity over a narrower range with repeats to ensure validity. The peptides taken forward for further evaluation are illustrated in Figure 6.12 C.





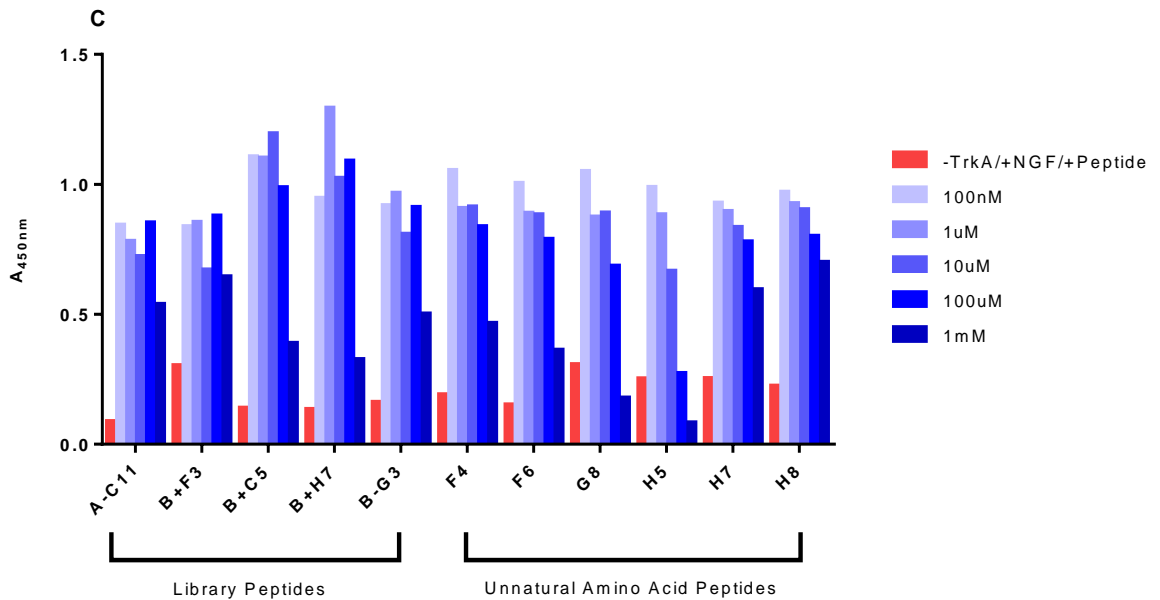


Figure 6.12. Broad Concentration Range Peptide Testing. The peptides identified in screening process underwent ELISA testing, with an immobilised target of TrkA, over a broader concentration range as described in 2.2.11 Controls as illustrated in Figure 6.10 were used to ensure experimental validity. Every expressed peptide was tested –TrkA (red) and +TrkA (blue). **A:** Library peptides; **B:** Unnatural amino acid peptides; **C:** Summary.

Most of the peptides showed activity in inhibiting rh-βNGF-TrkA binding over a concentration range of 10 μM-1 mM, apart from unnatural amino acid peptide H5 which showed activity of a range of 1-100 μM. Due to the high peptide concentrations needed it was not possible to analyse a full inhibition curve, therefore it was decided to test activity of the peptides at incremental steps over their apparent linear ranges. To ensure the validity of these results they were taken in triplicate. Selected library peptides are shown in Figure 6.13 while unnatural amino acid peptides are shown in Figure 6.14. Although not measured at the time the data previously gathered for the A2 and D9 control peptides are shown in Figure 6.13 for reference, although as this is pooled data from different experiments the variability is high.

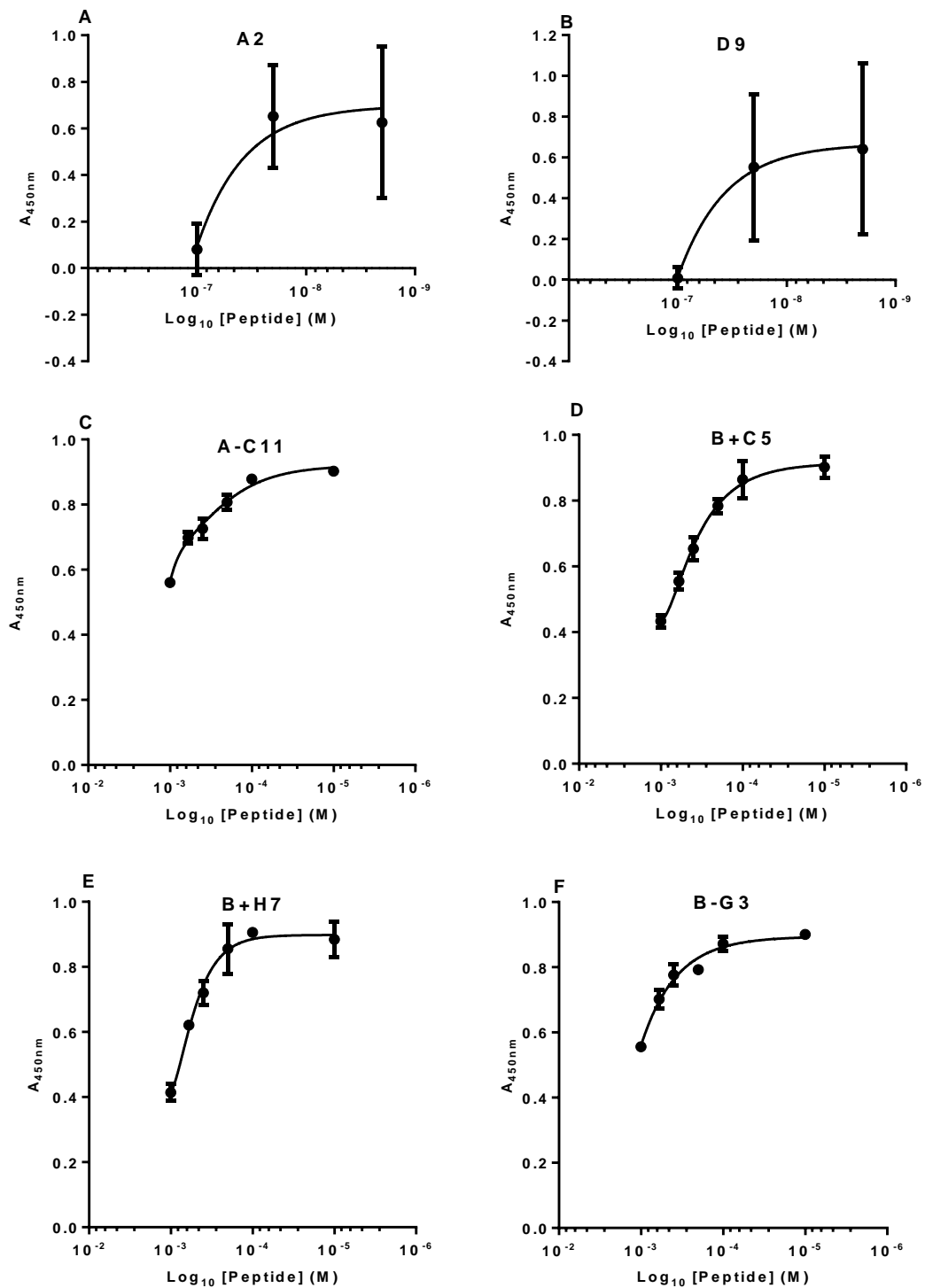


Figure 6.13. Library Peptide Dose Curves. The inhibitory effect of the library peptides was tested using a NGF inhibition assay as described in 2.2.11. Peptides were tested over a range of 10 μM to 1 mM (1mM, 600 μM , 400 μM , 200 μM , 100 μM , and 10 μM), with the higher inhibitory concentration limited by resources. **A:** A2 (control); **B:** D9 (control); **C:** A-C11; **D:** B+C5; **E:** B+H7; **F:** B-G3.

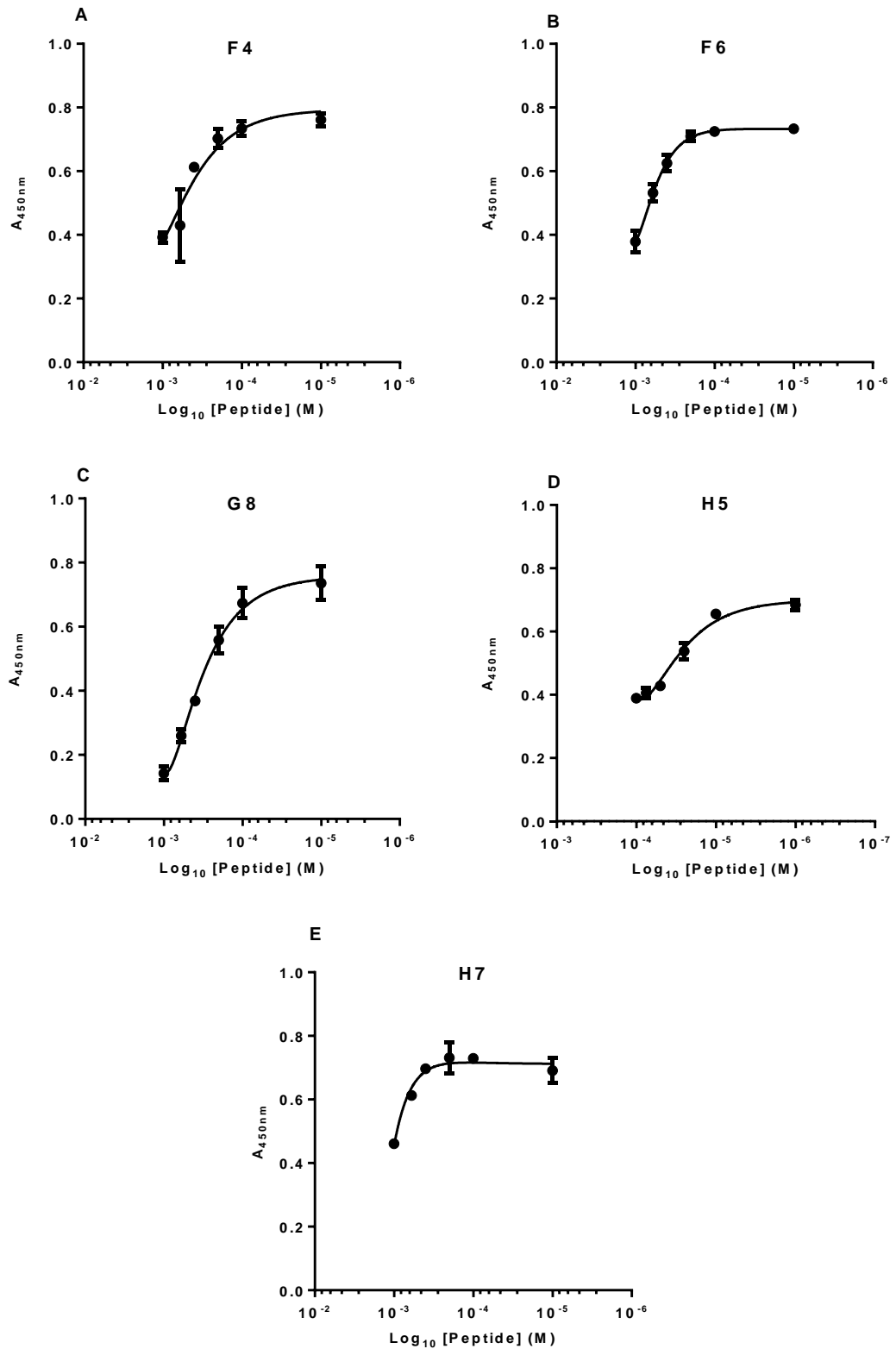


Figure 6.14. Unnatural Amino Acid Peptide Dose Curves. The inhibitory effect of the unnatural amino acid peptides was tested using a NGF inhibition assay as described in 2.2.11. Peptides were tested over a range of 10 μM to 1 mM (1mM, 600 μM , 400 μM , 200 μM , 100 μM , and 10 μM), with H5 tested at 1 μM to 100 μM (100 μM , 75 μM , 50 μM , 25 μM , 10 μM and 1 μM). Higher inhibitory concentrations were limited by resources. **A:** F4; **B:** F6; **C:** G8; **D:** H5; **E:** H7.

As anticipated from the broad peptide concentration range TrkA inhibition ELISA (Figure 6.12) both sets of peptides showed a reasonable downward trend of rh-βNGF binding as the peptide concentration increased, with minimal error seen across most of the data points. The minimal error ensures the validity of the inhibition observed.

All the library peptides showed inhibition of some form Figure 6.13 with some plateauing (B+H7, Figure 6.13 E) at the lowest peptide concentrations. Once again, due to the concentration needed it was not possible to test inhibition at concentrations greater than 1mM although based on the data it would suggest that higher concentrations still are needed for full inhibition of NGF binding to TrkA. B+C5 and B+H7 (Figure 6.13 D and E respectively) had showed the greatest inhibitory response suggesting that these were the most potent of the library peptides.

Once again as expected the unnatural amino acid peptides were seen to be in the active with F4 and F6 showing similar levels of inhibition (Figure 6.14 A and B). Based on Figure 6.12 G8 appeared to be the second most potent NGF inhibitor, behind H5, however based on the higher absorbance observed at 100 μM it was decided to test 100 μM-mM peptide concentration range in Figure 6.14, although in hindsight it may have been more prudent to test over the same range all the other peptides. Whilst H5 (Figure 6.14 D) does not necessarily show the most inhibition it must be noted that this was using a peptide concentration scale 10-fold lower than the other peptides tested due to the better levels of inhibition previously shown. It would also appear that H7 (Figure 6.14 E) was at the limits of activity with its inhibitory effects starting to plateau past 400 μM.

6.8. Discussion

6.8.1. Biotinylation

The biotinylation process was successful with 4-5 biotins attached to the majority of molecules although ideally a biotinylation level of 1-2 biotins per molecule would have been sufficient, as the increased numbers of biotin may interfere with potential peptide binding. Increased biotins on rh- β NGF may have caused some structural changes depending on where they have attached with a possible seven free amines available. However, owing to the limited amount of rh- β NGF available and that any peptides pulled through as a result of binding to structurally different rh- β NGF would be screened out by later testing, the achieved level of biotinylation was deemed acceptable.

6.8.2. Library Screening

Initial inspection of the sequencing results from the screened selection output (Figure 6.8) suggests little, if any amino acid preference at positions 1, 4 and 6 (LH1, 4 and RH6 respectively), whilst valine is preferred at position 2 (LH2) and proline was fixed at position 3 (LH3). Meanwhile, histidine appears to be a preference at position 5 (LH5) and leucine and histidine are preferred at positions 7 (RH5) and 8 (RH4) respectively, whilst aspartic acid, tryptophan and valine are preferred at positions 9, 10 and 11 respectively, within the anti-NGF peptide. However, as discussed in section 1.5.2, all screens assume equal concentrations of library components and thus screening outcomes may be influenced by actual (rather than designed) library composition. In the current data set for example, the over-representation of leucine and histidine at positions 5 & 7 and aspartic acid at position 9 in the original library (Chapter 4) may have influenced subsequent screening results disproportionately.

Therefore, to take into account any bias introduced from variation between designed and observed codon representation, the codon representation before and after selection were compared (Figure 6.15).

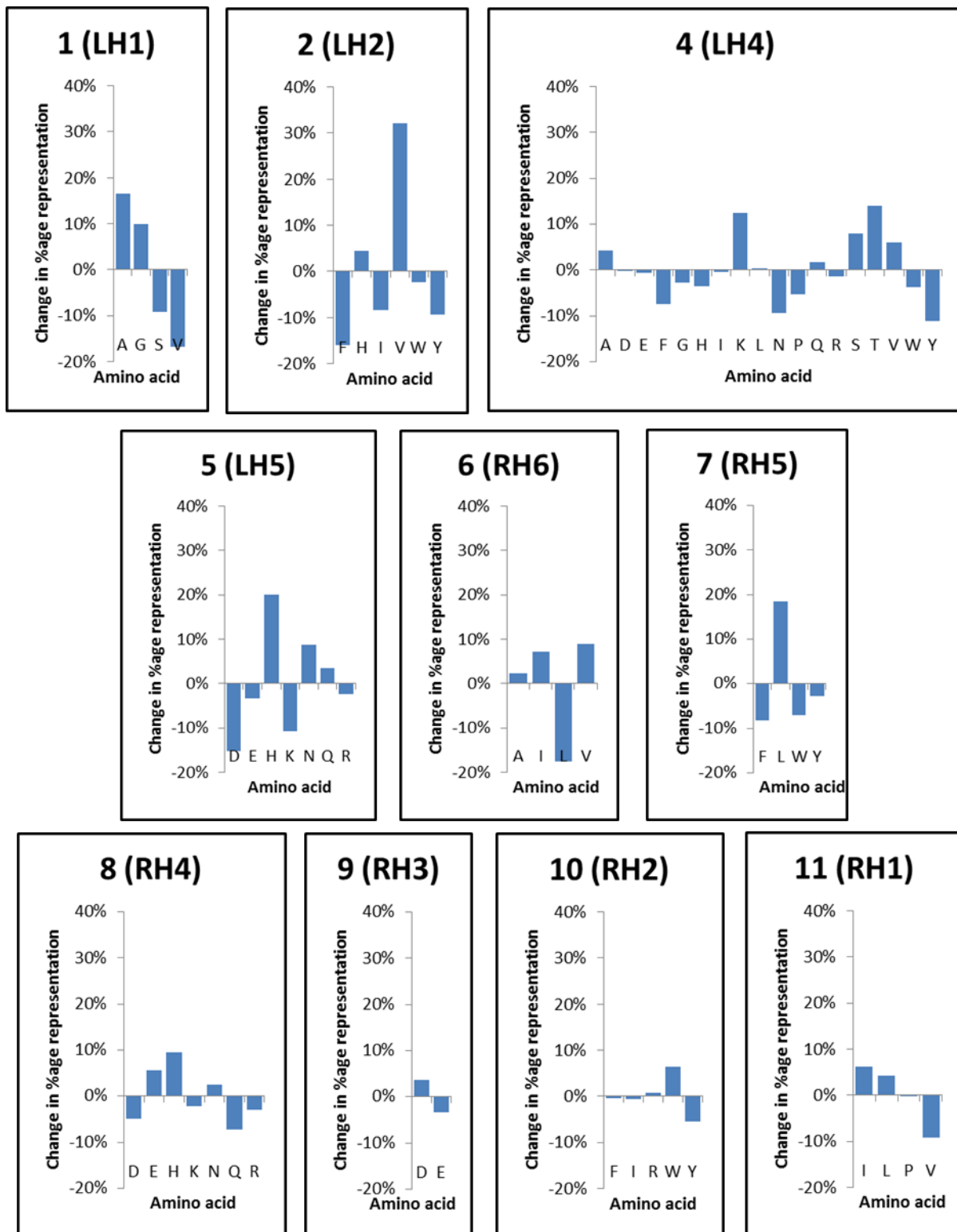


Figure 6.15. Changes in Amino Acid Representation Before and After Selection for NGF Binding. Percentages were calculated by subtracting the percentage codon representation in the original library (Figure 4.13) for each amino acid, at each position in the anti-NGF gene, from amino acid representation in the pool of peptides selected via NGF binding.

The results of the differences before and after suggest that alanine or glycine are preferred at position 1, whilst both valine is preferred at position 2. At position 4, interpretation is less straightforward. Here, 18 amino acids were encoded since Isogenica's proprietary SPOT analysis showed no overall preference and whilst lysine, serine, threonine and valine show increased representation at position 4 after screening, phenylalanine, asparagine, proline and tyrosine appear to be selected against. Thus there is no clear chemical preference at position 4; selected residues include positive charge (lysine), OH-containing (serine, threonine) and hydrophobic (valine). At position 5, histidine and asparagine are preferred (both can form H-bonds), whilst interestingly, both aspartic acid and lysine at position 5 show large decreases in representation at this position after selection. At position 6 leucine is selected against, whereas it is preferred at position 7. Position 8 shows a weak preference for histidine or glutamic acid (opposite charges), whereas positions 9 and 10 show lower relative selectivity once representation in the original library is taken into account. This is particularly relevant for position 9, where initial inspection of the sequencing data (Figure 6.8) would suggest that aspartic acid is strongly-preferred over glutamic acid. However, when library representation is taken into account at that position, the difference is minor. Finally at position 11, based on Isogenica's original, SPOT analysis, position 11 (RH1) was saturated with the hydrophobic amino acids isoleucine, leucine, proline and valine. Of these, valine, which dominated the raw sequencing data, is actually selected against when codon representation is taken into account, whilst there are again minor preferences for structurally-similar leucine and isoleucine. These collective findings are summarised in Table 6.5

Position	1	2	3 (fixed)	4	5	6	7	8	9	10	11
Amino acid	A/G	V	P	K/S/T/V	H/N	I/V (weak)	L	E/H (weak)	D (weak)	W (weak)	I/L (weak)

Table 6.5 Consensus of Amino Acid Preferences in Anti-NGF Peptide Monomers After Taking Library Composition into Account.

Obviously, with $n=1$ for each of the 12 selected full-length peptides, it is difficult to conduct meaningful statistical analysis of the above interpretations which should therefore be treated

with caution. Nonetheless, this small, post-selection population does show some interesting patterns with amino acids particularly favoured (>+15%) at positions 1, 2, 5, and 7. Leucine preference at position 7 is particularly interesting as this backs the sequencing results that leucine is favoured and not just an artefact of biased codon representation with the constructed library.

6.8.3. Peptide Testing - ELISA Results

The activities of the library and unnatural amino acid peptides were not as potent as the dimeric A2 and D9 controls. Although such findings are potentially discouraging, they are not entirely surprising since the control peptides are hypothesised to be dimeric whereas the full-length tested peptides are incapable of forming dimers via disulfide bridges (cysteine is omitted from all positions). As mentioned in chapter 1 NGF and TrkA binding operates through two distinct patches (conserved and specificity patches), as illustrated in Figure 6.16 with the conserved patch (red) and specificity patch (orange) circled, although it is not currently known where the peptides target precisely.



Figure 6.16. NGF-TrkA-d5 binding pocket (original image taken from Wiesmann *et al.* (Wiesmann *et al.*, 1999)). Conserved and specificity patches are circled red and orange respectively.

Thus, the results herein suggest that the dimeric properties (or at least cysteine content) of the control peptides are important in the effective inhibition of NGF-TrkA binding. Such

increased potency of the dimeric control peptides could be due to the presence of two NGF binding motifs (through the dimerization of two peptides containing a single binding motif respectively). On the other hand, only a single binding motif in the dimer may be required but the increased length of the dimerized peptides could physically block the binding patches of NGF.

In this regard, it is particularly interesting that several n-1 genes were selected, with substantial enhancement, when considering the original library composition. The original library encoded 71.0% full-length peptides just 13.2% frameshift mutations caused by n-1 deletions in the genes. Yet after screening, 6 of the 18 returned sequences were of n-1 frameshifted mutants and of these, 5 contained one or more cysteine residues (27.8%). These results suggest that cysteine, although undesirable in terms of manufacturing, may be of importance in NGF binding, either via dimerization or else via direct interaction with either TrkA or NGF, in a manner which inhibits TrkA-NGF binding. Having said this, the presence of the cysteines in the n-1 sequences somehow pulling them through the selection process may also be a misnomer. Due to the one nucleotide deletion the reading frame shifted causing the translation of a poly-arginine tail in the peptides. All of these poly-R n-1 sequences originated from selection reactions containing heparin, whereas none were observed from the selections that did not contain heparin. Whilst this could just be a coincidence it may also have been possible that the n-1 peptides were preferentially selected due to a charge interaction between heparin and their poly-R tail. However, this would have only occurred during the *in vitro* transcription/translation step at the beginning of each round of selections. In order to be recovered at the end of each round there had to have been some affinity of rh- β NGF as the selections underwent a series of wash steps to remove non-specific binders.

Based on the broad peptide concentration range testing (Figure 6.12) it appeared that most of the monomeric peptides showed a minimum inhibition of rh- β NGF at approximately 100 μ M, with H5 from the unnatural amino acid set showing a minimum inhibition at approximately 1-10 μ M. It was not possible to acquire IC_{50} values, since at the highest peptide concentrations that it was possible to analyse. All of the library peptides had a range

of activity over the 100 μ M-1 mM ranges with B+C5 and B+H7 (Figure 6.13 D and E) appearing to have the highest inhibitory effect over this range. Interestingly both B+C5 and B+H7 contained glycine at position 1, proline (fixed) at position 3, glutamine at position 5, alanine at position 6, leucine at position 7 and aspartic acid at position 9 suggesting possible importance (54.5% sequence homology across the randomised region) as well as basic residues at position 8.

In the case of the unnatural amino acid peptides G8 and H5 (Figure 6.14 C and D) were the most potent NGF inhibitors, with H5 showing comparable activity (in relation to the appearance of the plot) to those other peptides tested but at 10-fold lower concentrations. In the case of H5 the proline at position 3, which is critical for peptide activity, is replaced with L-Hydroxyproline, a post-translationally hydroxylated proline, only. With only a single substitution this peptide is the most similar of all the tested peptides to dimeric A2 control, despite which still showed comparative drop in inhibitive activity.

Although disappointingly the monomeric peptides showed a reduced inhibitory effect these results do raise some interesting questions about their overall mechanism of action. In the case of the inhibition of binding events it is easy to assume that the area of action is at the point of binding (in this case the TrkA-NGF interface), although it is possible that conformational changes as a result of inhibitor binding elsewhere on the complex may prevent interaction. As previously mentioned there are two interfaces for NGF to bind a single TrkA, with the NGF homodimer binding two TrkA receptors. Therefore, in this case do the anti-NGF (NGF-binding) peptides block the interaction of NGF and TrkA at their interface or do they bind to the NGF homodimer subsequently interfering with the NGF-TrkA interaction?

The fact that the monomeric peptides show reduced potency than the dimeric versions could suggest some conformational restriction is crucial for inhibition of the complex. Both monomeric and dimeric peptides share the NGF binding motif, albeit with potential optimisation through mutagenesis in the monomeric peptides, so the question is why are two peptides that are linked through a disulfide bond more potent than two single, unlinked

peptides? As illustrated in Figure 1.7, upon binding to TrkA the NGF homodimer undergoes some conformational changes with the N-terminal of each NGF monomer forming a short segment of helix, in the specificity patch, which packs against the receptor. Whilst the two monomeric peptides are able to bind to the NGF monomers their binding may do less to physically alter the conformation as each NGF monomer is still free to move independently, whereas the use of a dimeric peptide could create a physical linkage between the two NGF monomers (via the disulphide linked peptides) thus restricting this conformational change required for binding and thereby inhibiting the interaction between TrkA and NGF.

Conversely, the increased potency of the dimeric peptides could be simply due to a dimeric peptide effectively ensuring that there are two NGF binding peptides (in this case linked) present to bind NGF at the same time, whereas monomeric peptides rely on two individual peptides binding independently of one another, at the same time, to the two constituent NGF monomers of the larger homodimer.

Aside from the obvious difference of disulfide dimerization between the monomeric and dimeric peptides, it is also worth comparing those positions that were randomised in the monomeric peptide NGF binding motif as this may help with understanding the differences in observed inhibition. It should also be noted that while individual residues suitable for substitution had been previously identified by Isogenica Ltd. the use of ProxiMAX enabled analysis of the cumulative effect of these substitutions across the NGF binding motif rather than on an individual basis. It was originally hypothesised based on the composition of the dimeric peptides that they were helical in shape with aromatic residues on one face and charged residues on the other. Analysis of the library sequences does highlight some conserved residues across actual and consensus sequences (Table 6.6), for example Leu7 and Asp9. However, whilst Leu7 is conserved in the library sequences it is in contradiction to the dimeric peptides, which have tyrosine at this position. Having previously said that the pattern of aromatic and charged residues opposing faces is important for the dimeric peptides structure the presence of Leu7, and similar contradictory substitutions, in the library peptides could be a factor for diminished inhibition. In this case it raises the question as to

why these types of substitutions would be enriched if they reduce the inhibitory effect. This may be an effect of the selection process where peptides were selected on their ability to bind NGF resulting in the enrichment sequences that improve NGF binding but do not necessarily effect TrkA inhibition. Interestingly the net charge may also be a factor to be considered with both control peptide showing net negative charge in the binding motif whereas the active library peptides are either neutral or positively charged. Ultimately there is in-sufficient data (when n=12) to truly make firm conclusions regarding consensus sequences, as highlighted by the presence of Gln5 in both actual most active library peptides but not in either consensus sequence.

Position	1	2	3 (fixed)	4	5	6	7	8	9	10	11						
A2	G	W	P	A	E	V	Y	E	D	W	P						
D9	V	W	P	A	E	V	Y	Q	D	W	P						
Non-compensated	None	V	P	None	H	A	L	H	D	W	R	I/V					
Compensated	A	G	V	P	K	V	S	T	H	N	I/V	L	E	H	D	W	I/L
B+C5	G	V	P	A	Q	A	L	H	D	F	P						
B+H7	G	Y	P	K	Q	A	L	R	D	R	V						

Table 6.6. Comparison of Consensus and Actual Peptide Sequences. The two library peptides that showed the best inhibition of NGF-TrkA binding compared to the non-compensated consensus sequence, generated from the sequencing data, and the compensated consensus sequence, accounting for codon bias observed in the anti-NGF peptide library as well as the two dimeric control peptides. Amino acids are highlighted on their structural features: basic, non-polar, polar, uncharged, and acidic.

Chapter 7

Discussion and Conclusions

7. Chapter 7: Discussion and Conclusions

7.1. Summary of Results

The initial aim of this project was to analyse the ProxiMAX process, by producing a generic randomised library, from which changes could be implemented to improve factors such as codon representation and library quality. This improved process could then be used to generate a randomised library with the aim of engineering a high-affinity, monomeric anti-NGF peptide, which was based on the maturation of two dimer peptides that exhibited a conserved NGF binding motif. This library would then be screened using CIS display, a cell free display technique, in order to evaluate the power of new techniques in protein engineering that combine the production of high quality non-degenerate libraries with robust high capacity cell-free display techniques.

To start with the aim was to ligate an equimolar mix of MAX oligonucleotides to an acceptor sequence in a single reaction in order to test the method. A total of six cycles were undertaken using codon subsets in each cycle. Molecular weight comparison of the PCR products from each cycle showed an increase in size throughout the process that suggested the sequential addition of codons cycle-by-cycle had worked correctly. Capillary sequencing of small number of samples confirmed that the additions were successful showing the expected six randomised codons with the correct codons from each set in the right positions.

Library diversity and codon representation was analysed by next-generation sequencing, which showed that there was significant bias to single sequence that made up 64.47% of the entire library. Whilst this representation was obviously an issue with the process it is not only limited to the ProxiMAX methodology but is a common theme in many non-degeneration saturation mutagenesis methods including trinucleotide phosphoramidites. As a result the process was analysed in order to determine area where this bias may have been introduced. This concluded that oligonucleotide quality/quantification and blunt ended ligations using T4 DNA ligase were two critical areas that can greatly affect the outcome.

The use of partially complementary oligonucleotide (5'overhang on forward strand) that required hybridisation lead to the use of the Quant-iT™ PicoGreen® dsDNA assay in order to quantify double stranded DNA in the presence of un-hybridised ssDNA. However, due to light-sensitivity this reagent was liable to degrade quickly that in turn may lead to erroneous quantification. Variations in hybridised MAX oligonucleotide concentration would therefore bias the oligonucleotide mix that would then be carried throughout the process. After initial hybridisation the oligonucleotides may also dissociate from one another whilst in storage causing variations in the true concentrations of the double-stranded oligonucleotide stock. The use of single stranded self-complementary oligonucleotides to form hairpins, which could then be quantified by UV spectrometry, was introduced to improve oligonucleotide stability and improve quantification.

T4 DNA ligase appears to show sequence specificity favouring sequences with codons such as the histidine codon 5'-CAT-3' at the 3' end whilst discriminating against others such lysine and threonine (Ashraf et al., 2013), although the exact point at which sequence preference is inferred is not yet known. In the long term, detailed knowledge of why T4 DNA ligase shows sequences specificity is interesting and could be used to potentially improve the process (and is now the subject of another, ongoing study), in the short term it was necessary to mechanistically circumvent this issue in order to improve the library quality. Ligase preference was addressed by using separate ligations of individual MAX oligonucleotides that would then be amplified, quantified and then mixed at an equimolar level.

Based on Isogenica's proprietary alanine scanning and SPOT analysis of two matured anti-NGF peptides, a 10 amino acid motif was identified. The pattern of substitutions showed the aromatics at W, Y, W (positions 2, 7 and 10) on one side and the charged residues on the other, so as a result it was postulated that the peptides were helical and dimerize through the C-terminal cysteine (common with dimeric peptides (Liu et al., 2009, Wu et al., 2012)) to inhibit NGF binding to TrkA. Based on these peptides, a library for a high affinity monomer peptide was designed, in conjunction with Isogenica, with 11 randomised positions based around the binding motif highlighted from Isogenica's proprietary alanine scanning and SPOT

analysis. Whilst this library was being constructed, the changes in the ProxiMAX procedure with regard to regards to quantification and T4 DNA ligase were incorporated.

Two libraries consisting of 5 and 6 randomised regions (LH and RH respectively) were constructed and ligated together to form the complete library with 11 contiguous randomised positions. NGS analysis showed that over 61% of the read sequences were truncated by 3 codons with only 5% showing the complete library. Despite the truncation, the observed codon representation was much improved, although some positions showed codon bias with the most serious (position LH4) showing significant bias.

Analysis using an internal primer (in order to shorten the LH library framework), followed by polyacrylamide gel electrophoresis suggested that the truncation was introduced by the carry-over of un-digested material from the first cycle product through cycles 2 and 3, which was subsequently re-amplified in cycle 4 when the sequential use of 3 sets of MAX oligonucleotides meant its complementary primer was present. Due to the lower resolving power of agarose gels it was not possible to visualise the difference in size of the different products. Rather than using agarose gel purification, gel purification from PAGE could be used in order to reliably resolve and purify the *MlyI* digests each cycle. The full length 72-mer library represented library diversity of 86.9% although the low number of correct length sequences only equated to 0.1% coverage so should be considered with caution. When taking into account for a reduced library size of 2.51×10^5 the truncated library showed poor diversity (49.8%) with 42.7% coverage.

The combination of the truncation and biased LH4 position meant that the LH portion of the library had to be resynthesized. For the re-synthesis it was decided that the PCR quantification, prior to mixing, should be assessed by nanodrop rather than pixel density after gel electrophoresis. This was due to potential error in quantification being introduced as a result of variation in gel loading and running conditions.

The resynthesized LH library was ligated to the existing RH library and NGS analysis resulted in 71% of the sequences read containing the full length library. Using the adjusted quantification method also resulted in further improvements in the codon representation. In

contrast to the first anti-NGF peptide library, the represented diversity of the final anti-NGF peptide library was good (68.7%) with 1.2% of the potential library covered.

There was remarkable similarity between the RH portion of the final library and the RH portion of both previous anti-NGF libraries and as this was the same all the anti-NGF peptide libraries it validates the consistency of sequencing data. The calculated diversity of the first 72-mer library highlight the need for as large a sample number as possible in order to make the results as statistically accurate as possible. Although the 72-mer library shows a large bias in the LH4 position it had a calculated diversity of 86.9% with only 0.1% coverage of all possible sequences. However, the final anti-NGF peptide library had 68.7% diversity from 1.2% library coverage despite a far improved codon representation at position LH4. A mitigating factor for this drop in diversity, despite the improved representation in the final library can attributed to a failure in the primer introduced mutation at position LH-1, although as is the case in all statistics, the larger the sample size the more faith in the accuracy of the results.

Recombinant human β NGF (rh- β NGF), purchased from R&D systems, was biotinylated, using EZ-Link™ Sulfo-NHS-Biotin (Thermo Scientific), in order to be used as a streptavidin-immobilised target for CIS display. The anti-NGF peptide library then underwent four rounds of CIS display with selection stringency increasing throughout the process.

Library selections and screening are discussed at length in section Chapter 6, Section 6.8. The theoretical library diversity of the ProxiMAX-produced anti-NGF peptide library (2.7×10^7) is well within the screening capacity of CIS display, which can screen libraries with up to 10^{14} members (Odegrip et al., 2004). In order to pre-evaluate the selections, the CIS display output DNA sequences were cloned, expressed as phage fusions and subsequently screened for peptides that exhibited NGF affinity using an ELISA assay with immobilised NGF. Phage display may be considered a bottleneck in the process due to the limited ability to effectively express and screen the clones, but is valuable in that it allows elimination of peptide sequences that do not exhibit the required specificity (in this case for NGF).

Sequences which passed the phage display “test” were subsequently synthesised chemically, for further testing.

The 12 unique peptides from the selection and screening process were synthesised by Alta Biosciences and tested for activity, alongside 18 peptides synthesised by Isogenica, which contain unnatural amino acid substitutions. Screening employed a TrkA inhibition ELISA. Initial testing at a comparable concentration range with that of the working concentration of the original A2 and D9 dimerizing peptides showed very little inhibition of NGF-TrkA binding for any of the tested monomer peptides, suggesting that dimerization may be essential for high affinity for NGF. Expanding the tested peptide concentration range established that five library peptides and five unnatural amino acid peptides showed some form of inhibition over a concentration range of 100 μ M-1 mM with a further unnatural amino acid peptide demonstrating activity down to 10 μ M. Due to limited resources it was not feasible to test peptides over a concentration of 1mM. The inhibitory effect of these peptides was validated by repeated testing over the achievable linear range.

The library peptides were originally screened based on their affinity for NGF. As the literature states NGF has two distinct patches through which TrkA binding is elicited, this suggests those peptides that showed NGF binding during the screening but no inhibitory effect of NGF-TrkA binding were capable of binding NGF but not in the correct area in order to inhibit TrkA binding. Given this result, the dimerization of the original A2 and D9 peptides likely plays an important role in the inhibitory effect of these peptides as the all the active monomers showed a significant reduction in inhibition. Whilst inhibition was observed for the monomers it is questionable that at the concentration required is it practical as for the majority of the peptides full inhibition was still not observed at a concentration of 1mM. The testing of the monomeric peptides has ultimately highlighted that the dimeric nature of the original peptides appears to be fundamental for their inhibitory effect on the NGF-TrkA interaction, despite the proprietary SPOT analysis not highlighting the C-terminal cysteine as critical (most likely due to requirement to immobilise peptide in order to undertake the analysis).

7.2. Discussion and Conclusions

7.2.1. ProxiMAX Randomisation

The generation and refinement of DNA libraries using standard molecular biology techniques and equipment has demonstrated a core principle of ProxiMAX randomisation; its relative simplicity compared to other non-degenerate saturation mutagenesis techniques. In theory this process can be undertaken in any standard lab with access to standard molecular biology techniques, whereas other methods such as trinucleotide phosphoramidites require more specialist knowledge and equipment that are not easily put to use.

Whilst trying to the praise the virtues of ProxiMAX randomisation there is as ever a caveat to this which is, as is the case with many methodologies there is a correct time and place for their use, very few can truly be used universally. Even though MAX oligonucleotides can be reused for multiple libraries, with only the framework oligonucleotides specific to each library, the initial start-up cost is greater than other methods although this would obviously be counteracted the more libraries the MAX oligonucleotides are used to create. The use of iterative cycles of ligation, PCR and digestion, along with purification steps, also make ProxiMAX randomisation quite labour intensive, especially compared to non-degenerate mutagenic primer methods. Aside from the cost, both in money and time, if only a few positions at particularly disparate parts of a protein are targeted then ProxiMAX is not suitable as the library diversity would be a minor issue not to warrant its use and there would be more efficient methods of achieving this goal. Having highlighted some the downsides to ProxiMAX it is also worth saying that there are times when it would also be the best candidate. ProxiMAX has been successfully used in the randomisation of antibody loops where long segments of amino acids have been randomised. As the number of residues targeted increases factors such as library diversity/bias for degenerate mutagenesis, and practicality (i.e. number of primers needed) for non-degenerate methods start to take effect making the use other mutagenesis methods less viable. This is where the ability of ProxiMAX to be selectively choose smaller groups of amino acid to randomise helps maximise the

efficiency of library production by maintaining high diversity across many randomised positions.

This project has further expanded the repertoire for the use of ProxiMAX randomisation by using it to mutagenize peptides, which is potentially easier to undertake than antibody loop mutagenesis, as the whole peptide sequence can be encompassed by the libraries frameworks rather than having to insert back, in-frame, in to an antibody's sequence. Not only this but the mechanisms for subsequent screening processes, such as CIS display, can also be included in the peptides library frameworks rather than sub-cloning into the necessary vectors after the insertions of the randomised portion.

There are still areas of the ProxiMAX process that can be improved in order to increase the quality of the libraries and improve codon representation. For example, current studies into the exact mechanisms that confer sequence preference to T4 DNA ligase will be beneficial, since in the long term, better knowledge this could help to simplify the process back to single reaction with even codon representation, which would reduce costs and process time. Whilst work undertaken in this project has shown improved codon representation in the generated libraries, further work outside of this project has shown that adjustment of donor sequences (rather than the equimolar concentrations of donors used in this study) can be used to compensate for sequence preferences of T4 ligase, to generate a near-equal ratio of codons within the randomised gene (Ashraf et al., 2013). Followed on from this ProxiMAX has also been further optimised to improve codon representation whilst also automating the process and thus removing some the labour intensive steps required to improve codon representation (Frigotto et al., 2015). Obviously the automation process takes the feasibility of use away from the standard laboratory as specialised equipment is required, but the core simplicity of the iterative process remains the same.

7.2.2. CIS Display

As the title to this work suggest, the aim was not only to use ProxiMAX randomisation to generate libraries, but to use it combination with CIS display to screen the resulting libraries. The combination of these modern methods of library generation and screening is meant to highlight the optimisation of modern protein engineering away from more traditional methods such as NNN saturation mutagenesis and phage display. As highlighted in chapter 1, the natural choke point of the whole process is not the ability to generate the libraries but the ability to select and screen them.

CIS display appears to present a viable alternative to these traditional methods by circumventing the drawbacks of both *in vivo* (transformation efficiency) and *in vitro* (complex instability) display technologies. In my experience of using the process it is relatively simple to learn and quick to undertake, both desirable factors for such technologies. The need to transform the selection output for screening may be considered a bottleneck in this process because of the feasibility of picking/growing and tested individual colonies, similar to the drawbacks of phage display. However the important difference is that the library has already undergone selections with desirable sequences enriched and undesirable sequences removed, meaning that the transformations are undertaken with a higher quality pool of DNA and therefore hopefully increasing the chances of finding novel mutants.

Although not used for this work, CIS display is now also routinely used in conjunction with next generation sequencing to allow analysis of sequence enrichment throughout the selection process. However, while this is useful information this does not remove the need for subsequent library screening as the enriched sequences may not necessarily show the desired function, for example in this project peptides were initially selected for their ability to bind to NGF with the ultimate goal to find peptides that caused TrkA inhibition, through binding NGF. Next generation sequencing of the selection output may show enrichment of peptides sequences that bind to NGF but do not necessarily inhibit its interaction with TrkA, hence why the subsequent screening process is still vital.

7.2.3. Peptides: Therapeutics, Interactions and Optimisation

As already highlighted in chapter one (1.7) peptides are becoming increasingly favoured for therapeutic use due to their excellent safety, tolerability and efficacy profiles, like that of larger proteins, with the lower production complexity and costs normally associated with small molecules. Although over 7000 naturally occurring peptides have been identified many of these are necessarily suitable for pharmaceutical use due to weaknesses such as short circulation plasma half-life, aggregation, physical and chemical stability (Fosgerau and Hoffmann, 2015). Therefore these weaknesses make peptides ideal candidates for protein engineering using saturation mutagenesis techniques, especially ProxiMAX randomisation.

Based on either the crystal structure or molecular models of known peptides rationally designed libraries can be designed with the view of identifying essential residues within the peptides in order to counteract their known weaknesses, for example the elimination of hydrophobic patches by substitutions or *N*-methylation of amino acids in order to reduce peptide aggregation. This is of particular importance as, in general, the ultimate goal is to produce liquid drug formulations because of the acidic and enzymatic degradation experienced by oral peptide drugs. Due to their small size this identification, design and substitution process should be comparatively simple and easier to predict compared to that of larger proteins where changes could make much larger conformational changes. However, whilst making all these changes it is obviously important to maintain the pharmacokinetic properties that make the peptides desirable targets to begin with.

As mentioned in 7.2.1, peptides are ideal candidates for ProxiMAX randomisation due to their short length. Once the identification of key residues for activity have been identified through alanine scanning ProxiMAX can be used to quickly substitute residues within the peptides for a group of others that could benefit it pharmaceutically. This would allow the cumulative effect of multiple randomised positions to be analysed and the generation of potentially novel peptides far more efficiently. An example of where ProxiMAX could be used to further improve a peptide's function is the therapeutic use of glucagon. This is normally used in the treatment of hypoglycaemia and is only available in a kit as a lyophilized peptide

powder, which requires reconstitution and agitation. Obviously this is a less than ideal situation where time is critical, so ProxiMAX could potentially be used to improve the stability and solubility in order for glucagon to remain in solution for long periods of time (Fosgerau and Hoffmann, 2015).

In the case of the anti-NGF peptides, either structural studies, such as crystallography, or molecular modelling would help with understanding the mechanics of the inhibitory process of the dimers and would shed light on whether the increased inhibitory effects are due to the presence of two of the binding motifs or whether a single binding motif is required but the increased length of the dimer causes physical obstruction of NGF-TrkA binding. As hypothesised in chapter 6 (6.8.3) I now believe it is more likely that the dimeric peptides bind to the NGF monomers and prevent/limit the structural reordering required for the NGF homodimer to bind to TrkA, rather than physical competition at the NGF-TrkA interface, hence why the dimer peptides show more significant inhibition than the monomeric peptides. C-terminal truncations of the dimeric A2 peptide to remove the cysteine would also help to validate the importance of the C-terminal cysteine for activity, whilst testing dimeric peptides in the presence of a reducing agent would prove or disprove the necessity of the disulphide bond. Conversely, a C-terminal cysteine could be introduced to the active library peptides to enable comparison between the randomised binding motif and the WT, without dimerization becoming a limiting influence. If it was determined that the dimeric peptides restrict the NGF reordering it would also be interesting to design and test a single longer monomeric peptide with two NGF binding motifs, one at each terminal, to see whether this had a similar inhibitory profile. Due to the iterative nature of the ProxiMAX it would be feasible to use on such peptides as there is no physical limit to how many randomised codons can be added, just the theoretical limits based on sequence space and the ability to screen such a library. It may also be iterating to substitute the disulfide link for other means of dimerization such as Cys-maleimide thioether, triazoles or amides, as these may affect the stability, and subsequent activity, of the dimer.

Quantitative binding studies, such as surface plasmon resonance, of those dimer and monomer peptides that show NGF-TrkA could help characterise the peptides affinity for NGF binding, whilst *in vitro* neurite outgrowth inhibition assays would help demonstrate the physiological effect of the peptides activity. Finally, a simple test to attempt to establish the peptide area of inhibition on NGF could be to their inhibitory effects on other neurotrophins and their respective receptors thus establishing or precluding NGF specificity.

Chapter 8

References

8. References

- Abdiche, Y. N., Malashock, D. S. & Pons, J. 2008. Probing the binding mechanism and affinity of tanezumab, a recombinant humanized anti-NGF monoclonal antibody, using a repertoire of biosensors. *Protein Science*, 17, 1326-1335.
- Aloe, L., Braccilaudiero, L., Bonini, S. & Manni, L. 1997. The expanding role of nerve growth factor: from neurotrophic activity to immunologic diseases. *Allergy*, 52, 883-894.
- Aloe, L., Rocco, M. L., Bianchi, P. & Manni, L. 2012. Nerve growth factor: from the early discoveries to the potential clinical use. *J Transl Med*, 10, 239-239.
- Arakawa, T. & Ejima, D. 2014. Refolding Technologies for Antibody Fragments. *Antibodies*, 3, 232-241.
- Ashraf, M., Frigotto, L., Smith, M. E., Patel, S., Hughes, M. D., Poole, A. J., Hebaishi, H. R. M., Ullman, C. G. & Hine, A. V. 2013. ProxiMAX randomization: a new technology for non-degenerate saturation mutagenesis of contiguous codons. *Biochemical Society transactions*, 41, 1189-94.
- Baxter, D., Ullman, C. G. & Mason, J. M. 2014. Library construction, selection and modification strategies to generate therapeutic peptide-based modulators of protein-protein interactions. *Future Medicinal Chemistry*, 6, 2073-2092.
- Beghetto, E. & Gargano, N. 2011. Lambda-Display: A Powerful Tool for Antigen Discovery. *Molecules*, 16, 3089-3105.
- Bertschinger, J. & Neri, D. 2004. Covalent DNA display as a novel tool for directed evolution of proteins in vitro. *Protein Engineering Design & Selection*, 17, 699-707.
- Bessette, P. H., Aslund, F., Beckwith, J. & Georgiou, G. 1999. Efficient folding of proteins with multiple disulfide bonds in the Escherichia coli cytoplasm. *Proceedings of the National Academy of Sciences of the United States of America*, 96, 13703-13708.
- Bessette, P. H., Rice, J. J. & Daugherty, P. S. 2004. Rapid isolation of high-affinity protein binding peptides using bacterial display. *Protein Engineering Design & Selection*, 17, 731-739.

- Bosley, A. D. & Ostermeier, M. 2005. Mathematical expressions useful in the construction, description and evaluation of protein libraries. *Biomolecular Engineering*, 22, 57-61.
- Bradshaw, R. A., Murrayrust, J., Ibanez, C. F., McDonald, N. Q., Lapatto, R. & Blundell, T. L. 1994. Nerve growth-factor- structure-function-relationships. *Protein Science*, 3, 1901-1913.
- Buchwald, H., Dorman, R. B., Rasmus, N. F., Michalek, V. N., Landvik, N. M. & Ikramuddin, S. 2014. Effects on GLP-1, PYY, and leptin by direct stimulation of terminal ileum and cecum in humans: implications for ileal transposition. *Surgery for Obesity and Related Diseases*, 10, 780-786.
- Chao, M. V. 1992. Neurotrophin receptors: a window into neuronal differentiation. *Neuron*, 9, 583-593.
- Chen, J., Song, J. L., Zhang, S., Wang, Y., Cui, D. F. & Wang, C. C. 1999. Chaperone activity of DsbC. *Journal of Biological Chemistry*, 274, 19601-19605.
- Clary, D. O. & Reichardt, L. F. 1994. An alternatively spliced form of the nerve growth factor receptor TrkA confers an enhanced response to neurotrophin 3. *Proceedings of the National Academy of Sciences*, 91, 11133-11137.
- Craik, D. J., Fairlie, D. P., Liras, S. & Price, D. 2013. The Future of Peptide-based Drugs. *Chemical Biology & Drug Design*, 81, 136-147.
- Daugherty, P. S. 2007. Protein engineering with bacterial display. *Current Opinion in Structural Biology*, 17, 474-480.
- Derbyshire, K. M., Salvo, J. J. & Grindley, N. D. 1986. A simple and efficient procedure for saturation mutagenesis using mixed oligodeoxynucleotides. *Gene*, 46, 145-152.
- Diao, L. & Meibohm, B. 2013. Pharmacokinetics and Pharmacokinetic-Pharmacodynamic Correlations of Therapeutic Peptides. *Clinical Pharmacokinetics*, 52, 855-868.
- Doi, N., Takashima, H., Wada, A., Oishi, Y., Nagano, T. & Yanagawa, H. 2007. Photocleavable linkage between genotype and phenotype for rapid and efficient recovery of nucleic acids encoding affinity-selected proteins. *Journal of Biotechnology*, 131, 231-239.

- Edwards, R., Selby, M., Mobley, W., Weinrich, S., Hruby, D. & Rutter, W. 1988. Processing and secretion of nerve growth factor: expression in mammalian cells with a vaccinia virus vector. *Molecular and cellular biology*, 8, 2456-2464.
- Eldridge, B., Cooley, R. N., Odegrip, R., Mcgregor, D. P., Fitzgerald, K. J. & Ullman, C. G. 2009. An in vitro selection strategy for conferring protease resistance to ligand binding peptides. *Protein Engineering Design & Selection*, 22, 691-698.
- Fernandez-Gacio, A., Uguen, M. & Fastrez, J. 2003. Phage display as a tool for the directed evolution of enzymes. *Trends in Biotechnology*, 21, 408-414.
- Fosgerau, K. & Hoffmann, T. 2015. Peptide therapeutics: current status and future directions. *Drug Discovery Today*, 20, 122-128.
- Frade, J. M., Rodríguez-Tébar, A. & Barde, Y.-A. 1996. Induction of cell death by endogenous nerve growth factor through its p75 receptor. *Nature*, 383, 166-168.
- Frigotto, L., Smith, M. E., Brankin, C., Sedani, A., Cooper, S. E., Kanwar, N., Evans, D., Svobodova, S., Baar, C., Ullman, C. G., Glanville, J. & Hine, A. V. 2015. Codon-Precise, Synthetic, Antibody Fragment Libraries Built Using Automated Hexamer Codon Additions and Validated through Next Generation Sequencing. *Antibodies (2073-4468)*, 4, 88-102.
- Fujimori, K., Fukuzono, S., Kotomura, N., Kuno, N. & Shimizu, N. 1992. OVERPRODUCTION OF BIOLOGICALLY-ACTIVE HUMAN NERVE GROWTH-FACTOR IN ESCHERICHIA-COLI. *Bioscience Biotechnology and Biochemistry*, 56, 1985-1990.
- Gai, S. A. & Wittrup, K. D. 2007. Yeast surface display for protein engineering and characterization. *Current Opinion in Structural Biology*, 17, 467-473.
- Gaytan, P., Contreras-Zambrano, C., Ortiz-Alvarado, M., Morales-Pablos, A. & Yanez, J. 2009. TrimerDimer: an oligonucleotide-based saturation mutagenesis approach that removes redundant and stop codons. *Nucleic Acids Research*, 37.
- Gaytan, P., Yanez, J., Sanchez, F., Mackie, H. & Soberon, X. 1998. Combination of DMT-mononucleotide and Fmoc-trinucleotide phosphoramidites in oligonucleotide

- synthesis affords an automatable codon-level mutagenesis method. *Chemistry & Biology*, 5, 519-527.
- Ghilardi, J. R., Freeman, K. T., Jimenez-Andrade, J. M., Coughlin, K. A., Kaczmarek, M. J., Castaneda-Corral, G., Bloom, A. P., Kuskowski, M. A. & Mantyh, P. W. 2012. Neuroplasticity of sensory and sympathetic nerve fibers in a mouse model of a painful arthritic joint. *Arthritis & Rheumatism*, 64, 2223-2232.
- Giordano, C., Marchio, M., Timofeeva, E. & Biagini, G. 2014. Neuroactive peptides as putative mediators of antiepileptic ketogenic diets. *Frontiers in neurology*, 5, 63.
- Hallböök, F., Ibáñez, C. F. & Persson, H. 1991. Evolutionary studies of the nerve growth factor family reveal a novel member abundantly expressed in *Xenopus* ovary. *Neuron*, 6, 845-858.
- Hammond, P. W., Alpin, J., Rise, C. E., Wright, M. & Kreider, B. L. 2001. In vitro selection and characterization of Bcl-X-L-binding proteins from a mix of tissue-specific mRNA display libraries. *Journal of Biological Chemistry*, 276, 20898-20906.
- Hanes, J., Jermutus, L., Schaffitzel, C. & Pluckthun, A. 1999. Comparison of *Escherichia coli* and rabbit reticulocyte ribosome display systems. *Febs Letters*, 450, 105-110.
- Hanes, J. & Pluckthun, A. 1997. In vitro selection and evolution of functional proteins by using ribosome display. *Proceedings of the National Academy of Sciences of the United States of America*, 94, 4937-4942.
- He, L. B., Wang, Y., Wang, G., Chen, C. & Cao, S. G. 2007. Expression and purification of active recombinant human nerve growth factor from *Escherichia coli*. *Chemical Research in Chinese Universities*, 23, 237-240.
- He, M. & Taussig, M. J. 2002. Ribosome display: Cell-free protein display technology. *Briefings in Functional Genomics & Proteomics*, 1, 204-212.
- He, M. Y. & Taussig, M. J. 1997. Antibody-ribosome-mRNA (ARM) complexes as efficient selection particles for in vitro display and evolution of antibody combining sites. *Nucleic Acids Research*, 25, 5132-5134.
- Hoess, R. H. 2001. Protein design and phage display. *Chemical Reviews*, 101, 3205-3218.

- Hu, J. C., O'shea, E. K., Kim, P. S. & Sauer, R. T. 1990. Sequence requirements for coiled-coils: analysis with lambda repressor-GCN4 leucine zipper fusions. *Science*, 250, 1400-1403.
- Hughes, M. D., Nagel, D. A., Santos, A. F., Sutherland, A. J. & Hine, A. V. 2003. Removing the redundancy from randomised gene libraries. *Journal of Molecular Biology*, 331, 973-979.
- Hughes, M. D., Zhang, Z. R., Sutherland, A. J., Santos, A. F. & Hine, A. V. 2005. Discovery of active proteins directly from combinatorial randomized protein libraries without display, purification or sequencing: identification of novel zinc finger proteins. *Nucleic Acids Research*, 33.
- Iacaruso, M. F., Galli, S., Martí, M., Villalta, J. I., Estrin, D. A., Jares-Erijman, E. A. & Pietrasanta, L. I. 2011. Structural model for p75 NTR-TrkA intracellular domain interaction: a combined FRET and bioinformatics study. *Journal of Molecular Biology*, 414, 681-698.
- Ibáñez, C. F., Ebendal, T., Barbany, G., Murray-Rust, J., Blundell, T. L. & Persson, H. 1992. Disruption of the low affinity receptor-binding site in NGF allows neuronal survival and differentiation by binding to the trk gene product. *Cell*, 69, 329-341.
- Ji, R.-R., Samad, T. A., Jin, S.-X., Schmoll, R. & Woolf, C. J. 2002. p38 MAPK activation by NGF in primary sensory neurons after inflammation increases TRPV1 levels and maintains heat hyperalgesia. *Neuron*, 36, 57-68.
- Jimenez-Andrade, J. M., Ghilardi, J. R., Castaneda-Corral, G., Kuskowski, M. A. & Mantyh, P. W. 2011. Preventive or late administration of anti-NGF therapy attenuates tumor-induced nerve sprouting, neuroma formation, and cancer pain. *Pain*, 152, 2564-2574.
- Kahle, P., Burton, L. E., Schmelzer, C. & Hertel, C. 1992. The amino terminus of nerve growth factor is involved in the interaction with the receptor tyrosine kinase p140trkA. *Journal of Biological Chemistry*, 267, 22707-22710.
- Kaplan, D. R. & Miller, F. D. 1997. Signal transduction by the neutrophin receptors. *Current opinion in cell biology*, 9, 213-221.

- Kayushin, A., Korosteleva, M. & Miroshnikov, A. 2000. Large-scale solid-phase preparation of 3'-unprotected trinucleotide phosphotriesters - Precursors for synthesis of trinucleotide phosphoramidites. *Nucleosides Nucleotides & Nucleic Acids*, 19, 1967-1976.
- Kayushin, A., Korosteleva, M., Miroshnikov, A., Kosch, W., Zubov, D., Piel, N., Weichel, W. & Krenz, U. 1999. A new approach to the synthesis of trinucleotide phosphoramidites - Synthons for the generation of oligonucleotide/peptide libraries. *Nucleosides & Nucleotides*, 18, 1531-1533.
- Kayushin, A. L., Korosteleva, M. D., Miroshnikov, A. I., Kosch, W., Zubov, D. & Piel, N. 1996. A convenient approach to the synthesis of trinucleotide phosphoramidites - Synthons for the generation of oligonucleotide/peptide libraries. *Nucleic Acids Research*, 24, 3748-3755.
- Kille, S., Acevedo-Rocha, C. G., Parra, L. P., Zhang, Z. G., Opperman, D. J., Reetz, M. T. & Acevedo, J. P. 2013. Reducing Codon Redundancy and Screening Effort of Combinatorial Protein Libraries Created by Saturation Mutagenesis. *Acs Synthetic Biology*, 2, 83-92.
- Koewler, N. J., Freeman, K. T., Buus, R. J., Herrera, M. B., Jimenez-Andrade, J. M., Ghilardi, J. R., Peters, C. M., Sullivan, L. J., Kuskowski, M. A. & Lewis, J. L. 2007. Effects of a monoclonal antibody raised against nerve growth factor on skeletal pain and bone healing after fracture of the C57BL/6J mouse femur. *Journal of Bone and Mineral Research*, 22, 1732-1742.
- Kraulis, P. J. 1991. MOLSCRIPT: a program to produce both detailed and schematic plots of protein structures. *Journal of Applied Crystallography*, 24, 946-950.
- Krumpe, L. R., Schumacher, K. M., McMahon, J. B., Makowski, L. & Mori, T. 2007. Trinucleotide cassettes increase diversity of T7 phage-displayed peptide library. *Bmc Biotechnology*, 7.
- Kurokawa, Y., Yanagi, H. & Yura, T. 2001. Overproduction of bacterial protein disulfide isomerase (DsbC) and its modulator (DsbD) markedly enhances periplasmic

- production of human nerve growth factor in *Escherichia coli*. *Journal of Biological Chemistry*, 276, 14393-14399.
- Lamballe, F., Klein, R. & Barbacid, M. 1991. trkC, a new member of the trk family of tyrosine protein kinases, is a receptor for neurotrophin-3. *Cell*, 66, 967-979.
- Levi-Montalcini, R. & Hamburger, V. 1951. Selective growth stimulating effects of mouse sarcoma on the sensory and sympathetic nervous system of the chick embryo. *The Journal of experimental zoology*, 116, 321-61.
- Levin, A. M. & Weiss, G. A. 2006. Optimizing the affinity and specificity of proteins with molecular display. *Molecular Biosystems*, 2, 49-57.
- Levy, R., Weiss, R., Chen, G., Iverson, B. L. & Georgiou, G. 2001. Production of correctly folded Fab antibody fragment in the cytoplasm of *Escherichia coli* trxB gor mutants via the coexpression of molecular chaperones. *Protein Expression and Purification*, 23, 338-347.
- Li, S. J. & Hochstrasser, M. 1999. A new protease required for cell-cycle progression in yeast. *Nature*, 398, 246-251.
- Li, S. W., Millward, S. & Roberts, R. 2002. In vitro selection of mRNA display libraries containing an unnatural amino acid. *Journal of the American Chemical Society*, 124, 9972-9973.
- Liu, S., Zhou, L., Chen, L., Dastidar, S. G., Verma, C., Li, J., Tan, D. & Beuerman, R. 2009. Effect of structural parameters of peptides on dimer formation and highly oxidized side products in the oxidation of thiols of linear analogues of human β -defensin 3 by DMSO. *Journal of Peptide Science*, 15, 95-106.
- Lowe, E., Anand, P., Terenghi, G., Williams-Chestnut, R., Sinicropi, D. & Osborne, J. 1997. Increased nerve growth factor levels in the urinary bladder of women with idiopathic sensory urgency and interstitial cystitis. *British journal of urology*, 79, 572-577.
- Ma, S. Y., Saaem, I. & Tian, J. D. 2012. Error correction in gene synthesis technology. *Trends in Biotechnology*, 30, 147-154.

- Makela, A. R. & Oker-Blom, C. 2008. The baculovirus display technology - An evolving instrument for molecular screening and drug delivery. *Combinatorial Chemistry & High Throughput Screening*, 11, 86-98.
- Makowski, L. & Soares, A. 2003. Estimating the diversity of peptide populations from limited sequence data. *Bioinformatics*, 19, 483-489.
- Mantyh, W. G., Jimenez-Andrade, J. M., Stake, J. I., Bloom, A. P., Kaczmarek, M. J., Taylor, R. N., Freeman, K. T., Ghilardi, J. R., Kuskowski, M. A. & Mantyh, P. W. 2010. Blockade of nerve sprouting and neuroma formation markedly attenuates the development of late stage cancer pain. *Neuroscience*, 171, 588-598.
- Mattheakis, L. C., Bhatt, R. R. & Dower, W. J. 1994. An in vitro polysome display system for identifying ligands from very large peptide libraries. *Proceedings of the National Academy of Sciences*, 91, 9022-9026.
- Mcdonald, N. Q., Lapatto, R., Rust, J. M., Gunning, J., Wlodawer, A. & Blundell, T. L. 1991. New protein fold revealed by a 2.3-Å resolution crystal structure of nerve growth factor.
- Meldolesi, J., Sciorati, C. & Clementi, E. 2000. The p75 receptor: first insights into the transduction mechanisms leading to either cell death or survival. *J. Biol. Chem*, 274, 2597-2600.
- Miller, L. J., Fischer, K. A., Goralnick, S. J., Litt, M., Burleson, J. A., Albertsen, P. & Kreutzer, D. L. 2002. Nerve growth factor and chronic prostatitis/chronic pelvic pain syndrome. *Urology*, 59, 603-608.
- Millward, S. W., Fiacco, S., Austin, R. J. & Roberts, R. W. 2007. Design of cyclic peptides that bind protein surfaces with antibody-like affinity. *Acs Chemical Biology*, 2, 625-634.
- Mossessova, E. & Lima, C. D. 2000. Ulp1-SUMO crystal structure and genetic analysis reveal conserved interactions and a regulatory element essential for cell growth in yeast. *Molecular Cell*, 5, 865-876.
- Mossner, E. & Pluckthun, A. 2001. Directed evolution with fast and efficient selection technologies. *Chimia*, 55, 325-329.

- Naismith, J. H. & Sprang, S. R. 1998. Modularity in the TNF-receptor family. *Trends in Biochemical Sciences*, 23, 74-79.
- Nakamura, Y., Gojobori, T. & Ikemura, T. 2000. Codon usage tabulated from international DNA sequence databases: status for the year 2000. *Nucleic Acids Research*, 28, 292-292.
- Negro, A., Martini, I., Bigon, E., Cazzola, F., Minozzi, C., Skaper, S. D. & Callegaro, L. 1992. SYNTHESIS OF THE BIOLOGICALLY-ACTIVE BETA-SUBUNIT OF HUMAN NERVE GROWTH-FACTOR IN ESCHERICHIA-COLI. *Gene*, 110, 251-256.
- Nemoto, N., Miyamotosato, E., Husimi, Y. & Yanagawa, H. 1997. In vitro virus: Bonding of mRNA bearing puromycin at the 3'-terminal end to the C-terminal end of its encoded protein on the ribosome in vitro. *Febs Letters*, 414, 405-408.
- Oddiah, D., Anand, P., McMahon, S. B. & Rattray, M. 1998. Rapid increase of NGF, BDNF and NT-3 mRNAs in inflamed bladder. *Neuroreport*, 9, 1455-1458.
- Odegrip, R., Coomber, D., Eldridge, B., Hederer, R., Kuhlman, P. A., Ullman, C., Fitzgerald, K. & McGregor, D. 2004. CIS display: In vitro selection of peptides from libraries of protein-DNA complexes. *Proceedings of the National Academy of Sciences of the United States of America*, 101, 2806-2810.
- Odegrip, R. & Haggard-Ljungquist, E. 2001. The two active-site tyrosine residues of the A protein play non-equivalent roles during initiation of rolling circle replication of bacteriophage P2. *Journal of Molecular Biology*, 308, 147-163.
- Ono, A., Matsuda, A., Zhao, J. & Santi, D. V. 1995. The synthesis of blocked triplet-phosphoramidites and their use in mutagenesis. *Nucleic Acids Research*, 23, 4677-4682.
- Padhi, A., Sengupta, M., Sengupta, S., Roehm, K. H. & Sonawane, A. 2014. Antimicrobial peptides and proteins in mycobacterial therapy: Current status and future prospects. *Tuberculosis*, 94, 363-373.
- Pattanaik, S., Werkman, J. R., Kong, Q. & Yuan, L. 2010. Site-directed mutagenesis and saturation mutagenesis for the functional study of transcription factors involved in

- plant secondary metabolite biosynthesis. *Plant Secondary Metabolism Engineering*. Springer.
- Patwardhan, R. P., Lee, C., Litvin, O., Young, D. L., Pe'er, D. & Shendure, J. 2009. High-resolution analysis of DNA regulatory elements by synthetic saturation mutagenesis. *Nature Biotechnology*, 27, 1173-1175.
- Praszkier, J., Murthy, S. & Pittard, A. J. 2000. Effect of CIS on activity in trans of the replication initiator protein of an IncB plasmid. *Journal of Bacteriology*, 182, 3972-3980.
- Praszkier, J. & Pittard, A. J. 1999. Role of CIS in replication of an IncB plasmid. *Journal of Bacteriology*, 181, 2765-2772.
- Rattenholl, A., Lilie, H., Grossmann, A., Stern, A., Schwarz, E. & Rudolph, R. 2001a. The pro-sequence facilitates folding of human nerve growth factor from Escherichia coli inclusion bodies. *European Journal of Biochemistry*, 268, 3296-3303.
- Rattenholl, A., Ruoppolo, M., Flagiello, A., Monti, M., Vinci, F., Marino, G., Lilie, H., Schwarz, E. & Rudolph, R. 2001b. Pro-sequence assisted folding and disulfide bond formation of human nerve growth factor. *Journal of Molecular Biology*, 305, 523-533.
- Reetz, M. T. 2013. Biocatalysis in organic chemistry and biotechnology: past, present, and future. *Journal of the American Chemical Society*, 135, 12480-12496.
- Reetz, M. T., Bocola, M., Carballeira, J. D., Zha, D. X. & Vogel, A. 2005. Expanding the range of substrate acceptance of enzymes: Combinatorial active-site saturation test. *Angewandte Chemie-International Edition*, 44, 4192-4196.
- Reetz, M. T. & Carballeira, J. D. 2007. Iterative saturation mutagenesis (ISM) for rapid directed evolution of functional enzymes. *Nature Protocols*, 2, 891-903.
- Reetz, M. T., D Carballeira, J. & Vogel, A. 2006a. Iterative saturation mutagenesis on the basis of B factors as a strategy for increasing protein thermostability. *Angewandte Chemie-International Edition*, 45, 7745-7751.
- Reetz, M. T., Kahakeaw, D. & Lohmer, R. 2008. Addressing the numbers problem in directed evolution. *ChemBiochem*, 9, 1797-1804.

- Reetz, M. T., Wang, L. W. & Bocola, M. 2006b. Directed evolution of enantioselective enzymes: Iterative cycles of CASTing for probing protein-sequence space. *Angewandte Chemie-International Edition*, 45, 1236-1241.
- Reiersen, H., Lobersli, I., Loset, G. A., Hvattum, E., Simonsen, B., Stacy, J. E., McGregor, D., Fitzgerald, K., Welschhof, M., Brekke, O. H. & Marvik, O. J. 2005. Covalent antibody display - an in vitro antibody-DNA library selection system. *Nucleic Acids Research*, 33.
- Roberts, R. W. & Szostak, J. W. 1997. RNA-peptide fusions for the in vitro selection of peptides and proteins. *Proceedings of the National Academy of Sciences of the United States of America*, 94, 12297-12302.
- Robinson, S. D., Safavi-Hemami, H., Mcintosh, L. D., Purcell, A. W., Norton, R. S. & Papenfuss, A. T. 2014. Diversity of Conotoxin Gene Superfamilies in the Venomous Snail, *Conus victoriae*. *Plos One*, 9.
- Rockberg, J., Lofblom, J., Hjelm, B., Uhlen, M. & Stahl, S. 2008. Epitope mapping of antibodies using bacterial surface display. *Nature Methods*, 5, 1039-1045.
- Rydén, M., Hempstead, B. & Ibáñez, C. F. 1997. Differential modulation of neuron survival during development by nerve growth factor binding to the p75 neurotrophin receptor. *Journal of Biological Chemistry*, 272, 16322-16328.
- Rydén, M. & Ibáñez, C. F. 1997. A second determinant of binding to the p75 neurotrophin receptor revealed by alanine-scanning mutagenesis of a conserved loop in nerve growth factor. *Journal of Biological Chemistry*, 272, 33085-33091.
- Samuelson, P., Gunneriusson, E., Nygren, P. A. & Stahl, S. 2002. Display of proteins on bacteria. *Journal of Biotechnology*, 96, 129-154.
- Schneider, R. & Schweiger, M. 1991. A novel modular mosaic of cell adhesion motifs in the extracellular domains of the neurogenic trk and trkB tyrosine kinase receptors. *Oncogene*, 6, 1807-1811.
- Schofield, M. J. & Hsieh, P. 2003. DNA mismatch repair: Molecular mechanisms and biological function. In: ORNSTON, L. N. (ed.) *Annual Review of Microbiology. Volume 57*.

- Sevcik, M. A., Ghilardi, J. R., Peters, C. M., Lindsay, T. H., Halvorson, K. G., Jonas, B. M., Kubota, K., Kuskowski, M. A., Boustany, L., Shelton, D. L. & Mantyh, P. W. 2005. Anti-NGF therapy profoundly reduces bone cancer pain and the accompanying increase in markers of peripheral and central sensitization. *Pain*, 115, 128-141.
- Shih, A., Laramee, G. R., Schmelzer, C. H., Burton, L. E. & Winslow, J. W. 1994. Mutagenesis identifies amino-terminal residues of nerve growth factor necessary for Trk receptor binding and biological activity. *Journal of Biological Chemistry*, 269, 27679-27686.
- Shimizu, Y., Inoue, A., Tomari, Y., Suzuki, T., Yokogawa, T., Nishikawa, K. & Ueda, T. 2001. Cell-free translation reconstituted with purified components. *Nature Biotechnology*, 19, 751-755.
- Shimizu, Y., Kanamori, T. & Ueda, T. 2005. Protein synthesis by pure translation systems. *Methods*, 36, 299-304.
- Sidhu, S. S. & Kossiakoff, A. A. 2007. Exploring and designing protein function with restricted diversity. *Current opinion in chemical biology*, 11, 347-354.
- Sidhu, S. S., Lowman, H. B., Cunningham, B. C. & Wells, J. A. 2000. Phage display for selection of novel binding peptides. *Applications of Chimeric Genes and Hybrid Proteins, Pt C*, 328, 333-363.
- Siloto, R. M. & Weselake, R. J. 2012. Site saturation mutagenesis: methods and applications in protein engineering. *Biocatalysis and Agricultural Biotechnology*, 1, 181-189.
- Smith, G. P. 1985. Filamentous fusion phage- Novel expression vectors that display cloned antigens on the virion surface. *Science*, 228, 1315-1317.
- Smith, J. D., Mcmanus, K. F. & Fraser, H. B. 2013. A novel test for selection on cis-regulatory elements reveals positive and negative selection acting on mammalian transcriptional enhancers. *Molecular biology and evolution*, mst134.
- Snider, W. D. 1994. Functions of the neurotrophins during nervous system development: what the knockouts are teaching us. *Cell*, 77, 627-638.

- Sondek, J. & Shortle, D. 1992. A general strategy for random insertion and substitution mutagenesis: substoichiometric coupling of trinucleotide phosphoramidites. *Proceedings of the National Academy of Sciences*, 89, 3581-3585.
- Stein, A. T., Ufret-Vincenty, C. A., Hua, L., Santana, L. F. & Gordon, S. E. 2006. Phosphoinositide 3-kinase binds to TRPV1 and mediates NGF-stimulated TRPV1 trafficking to the plasma membrane. *The Journal of general physiology*, 128, 509-522.
- Takahashi, T. T., Austin, R. J. & Roberts, R. W. 2003. mRNA display: ligand discovery, interaction analysis and beyond. *Trends in Biochemical Sciences*, 28, 159-165.
- Tang, L. X., Gao, H., Zhu, X. C., Wang, X., Zhou, M. & Jiang, R. X. 2012. Construction of "small-intelligent" focused mutagenesis libraries using well-designed combinatorial degenerate primers. *Biotechniques*, 52, 149-+.
- Tang, L. X., Wang, X., Ru, B. B., Sun, H. F., Huang, J. & Gao, H. 2014. MDC-Analyzer: A novel degenerate primer design tool for the construction of intelligent mutagenesis libraries with contiguous sites. *Biotechniques*, 56, 301-+.
- Tawfik, D. S. & Griffiths, A. D. 1998. Man-made cell-like compartments for molecular evolution. *Nature Biotechnology*, 16, 652-656.
- Tian, J. D., Gong, H., Sheng, N. J., Zhou, X. C., Gulari, E., Gao, X. L. & Church, G. 2004. Accurate multiplex gene synthesis from programmable DNA microchips. *Nature*, 432, 1050-1054.
- Ugolini, G., Marinelli, S., Covaceuszach, S., Cattaneo, A. & Pavone, F. 2007. The function neutralizing anti-TrkA antibody MNAC13 reduces inflammatory and neuropathic pain. *Proceedings of the National Academy of Sciences*, 104, 2985-2990.
- Ullman, C. G., Frigotto, L. & Cooley, R. N. 2011. In vitro methods for peptide display and their applications. *Briefings in Functional Genomics*, 10, 125-134.
- Ultsch, M. H., Wiesmann, C., Simmons, L. C., Henrich, J., Yang, M., Reilly, D., Bass, S. H. & De Vos, A. M. 1999. Crystal structures of the neurotrophin-binding domain of TrkA, TrkB and TrkC. *Journal of Molecular Biology*, 290, 149-159.

- Urfer, R., Tsoulfas, P., Soppet, D., Escandon, E., Parada, L. & Presta, L. 1994. The binding epitopes of neurotrophin-3 to its receptors trkC and gp75 and the design of a multifunctional human neurotrophin. *The EMBO journal*, 13, 5896.
- Valetti, F. & Gilardi, G. 2013. Improvement of biocatalysts for industrial and environmental purposes by saturation mutagenesis. *Biomolecules*, 3, 778-811.
- Van Den Brulle, J., Fischer, M., Langmann, T., Horn, G., Waldmann, T., Arnold, S., Fuhrmann, M., Schatz, O., O'connell, T., O'connell, D., Auckenthaler, A. & Schwer, H. 2008. A novel solid phase technology for high-throughput gene synthesis. *Biotechniques*, 45, 340-343.
- Virnekas, B., Ge, L. M., Pluckthun, A., Schneider, K. C., Wellnhofer, G. & Moroney, S. E. 1994. Trinucleotide phosphoramidites-Ideal reagents for the synthesis of mixed oligonucleotides for random mutagenesis. *Nucleic Acids Research*, 22, 5600-5607.
- Wang, H. H., Isaacs, F. J., Carr, P. A., Sun, Z. Z., Xu, G., Forest, C. R. & Church, G. M. 2009. Programming cells by multiplex genome engineering and accelerated evolution. *Nature*, 460, 894-898.
- Watson, J. J., Fahey, M. S., Van Den Worm, E., Engels, F., Nijkamp, F. P., Stroemer, P., McMahon, S., Allen, S. J. & Dawbarn, D. 2006. TrkAd5: A novel therapeutic agent for treatment of inflammatory pain and asthma. *Journal of Pharmacology and Experimental Therapeutics*, 316, 1122-1129.
- Wiesmann, C. & De Vos, A. 2001. Nerve growth factor: structure and function. *Cellular and Molecular Life Sciences CMLS*, 58, 748-759.
- Wiesmann, C., Ultsch, M. H., Bass, S. H. & De Vos, A. M. 1999. Crystal structure of nerve growth factor in complex with the ligand-binding domain of the TrkA receptor. *Nature*, 401, 184-188.
- Wilson, D. S., Keefe, A. D. & Szostak, J. W. 2001. The use of mRNA display to select high-affinity protein-binding peptides. *Proceedings of the National Academy of Sciences of the United States of America*, 98, 3750-3755.
- Winston, J., Toma, H., Shenoy, M. & Pasricha, P. J. 2001. Nerve growth factor regulates VR-1 mRNA levels in cultures of adult dorsal root ganglion neurons. *Pain*, 89, 181-186.

- Wu, C., Leroux, J.-C. & Gauthier, M. A. 2012. Twin disulfides for orthogonal disulfide pairing and the directed folding of multicyclic peptides. *Nature chemistry*, 4, 1044-1049.
- Yagodkin, A., Azhayev, A., Roivainen, J., Antopolsky, M., Kayushin, A., Korosteleva, M., Miroshnikov, A., Randolph, J. & Mackie, H. 2007. Improved synthesis of trinucleotide phosphoramidites and generation of randomized oligonucleotide libraries. *Nucleosides Nucleotides & Nucleic Acids*, 26, 473-497.
- Yano, H. & Chao, M. V. 2000. Neurotrophin receptor structure and interactions. *Pharmaceutica acta Helvetiae*, 74, 253-60.
- Zahnd, C., Spinelli, S., Luginbuhl, B., Amstutz, P., Cambillau, C. & Pluckthun, A. 2004. Directed in vitro evolution and crystallographic analysis of a peptide-binding single chain antibody fragment (scFv) with low picomolar affinity. *Journal of Biological Chemistry*, 279, 18870-18877.
- Zhu, Y., Colak, T., Shenoy, M., Liu, L., Pai, R., Li, C., Mehta, K. & Pasricha, P. J. 2011. Nerve growth factor modulates TRPV1 expression and function and mediates pain in chronic pancreatitis. *Gastroenterology*, 141, 370-377.

Chapter 9

Appendices

9. Appendices

9.1. Appendix 1. Single Reaction Ligation Library Codon Representation Table

MAX Codons		R1		R2		R3		R4		R5		R6	
		Exp	Obs										
A	GCG	20.00%	0.00%	0.00%	0.00%	0.00%	0.00%	0.00%	0.00%	0.00%	0.00%	0.00%	0.00%
C	TGC	0.00%	0.00%	0.00%	0.00%	0.00%	0.00%	0.00%	0.00%	0.00%	0.00%	33.33%	90.41%
D	GAC	0.00%	0.00%	0.00%	0.00%	50.00%	0.00%	0.00%	0.02%	0.00%	0.00%	0.00%	0.00%
E	GAA	0.00%	0.00%	0.00%	0.00%	50.00%	99.93%	0.00%	0.00%	0.00%	0.00%	0.00%	0.00%
F	TTT	0.00%	0.01%	33.33%	0.04%	0.00%	0.00%	0.00%	0.00%	0.00%	0.00%	0.00%	0.00%
G	GGC	20.00%	0.00%	0.00%	0.00%	0.00%	0.00%	0.00%	0.00%	0.00%	0.00%	0.00%	0.00%
H	CAT	0.00%	0.00%	0.00%	0.00%	0.00%	0.00%	0.00%	0.03%	33.33%	99.04%	0.00%	0.00%
I	ATT	20.00%	99.90%	0.00%	0.00%	0.00%	0.00%	0.00%	0.00%	0.00%	0.00%	0.00%	0.00%
K	AAA	0.00%	0.00%	0.00%	0.00%	0.00%	0.00%	0.00%	0.02%	33.33%	0.03%	0.00%	0.00%
L	TTA	20.00%	0.02%	0.00%	0.00%	0.00%	0.00%	0.00%	0.00%	0.00%	0.00%	0.00%	0.00%
M	ATG	0.00%	0.00%	0.00%	0.00%	0.00%	0.00%	0.00%	0.00%	0.00%	0.00%	33.33%	7.28%
N	AAC	0.00%	0.00%	0.00%	0.00%	0.00%	0.00%	25.00%	72.50%	0.00%	0.00%	0.00%	0.00%
P	CCG	25.00%	0.00%	0.00%	0.00%	0.00%	0.00%	0.00%	0.00%	0.00%	0.00%	33.33%	2.19%
Q	CAG	0.00%	0.00%	0.00%	0.00%	0.00%	0.00%	25.00%	18.12%	0.00%	0.00%	0.00%	0.00%
R	CGT	0.00%	0.00%	0.00%	0.00%	0.00%	0.00%	0.00%	0.00%	33.33%	0.83%	0.00%	0.00%
S	TCT	0.00%	0.00%	0.00%	0.00%	0.00%	0.00%	25.00%	6.01%	0.00%	0.00%	0.00%	0.00%
T	ACC	0.00%	0.00%	0.00%	0.00%	0.00%	0.00%	25.00%	3.21%	0.00%	0.00%	0.00%	0.00%
V	GTG	20.00%	0.00%	0.00%	0.00%	0.00%	0.00%	0.00%	0.00%	0.00%	0.00%	0.00%	0.00%
W	TGG	0.00%	0.00%	33.33%	0.00%	0.00%	0.00%	0.00%	0.00%	0.00%	0.00%	0.00%	0.01%
Y	TAT	0.00%	0.00%	33.33%	99.93%	0.00%	0.00%	0.00%	0.00%	0.00%	0.00%	0.00%	0.00%
Design		AGILV		FWY		DE		NQST		HKR		CMP	
Codons >1%		I		Y		E		NQST		H		CMP	

9.2. Appendix 2. Anti-NGF PeptideLibrary Framework Sequences

LH Acceptor (Q)	5'-CGGCGGTTAGAACGCGGCTACAATTAATACATAACCCCATCCCC CTGTGACAATTAATCATCGGCTCGTATAATGTGTGGAATTGTGAG-3'
LH Acceptor RC	5'-PHO-TTCCTGTTTAAACGCCGCATGGCCATGGTAGATCCTGTTT CCTGTGTGAAATTGTTATCCGCTCACAAATCCACACATT-3'
LH Acceptor PCR Primer (Q)	5'-PHO-TTCCTGTTTAAACGCCGC-3'
LH Acceptor PCR Primer(P)	5'-PHO-TTCCGGTTTAAACGCCGC-3'
LH Universal RC Primer	5'-CGG-CGGTTAGAACGCGGC-3'
RH acceptor	5'-PHO-TCTGCGGCGGCGGGCAGCGTTCTAGTCTAGCGGCCCA ACTGATCTTCACCAAACGGAGACCTGTACCGGC-3'
RH acceptor RC	5'-GCCGGTACAGGTCTCCGTTTGGTGAAGATCAGTTGGGGCCGCTA GACTAGAACCGCTGCCCCGCCGCCGAGA-3'
RH Universal RC Primer	5'-GCCGGTACAGGTCTCCGT-3'

9.3. Appendix 3. 72-mer Anti-NGF Peptide Library Codon Representation Tables

MAX Codons		LH R1		LH R2		LH R3		LH R4		LH R5	
		Exp	Obs	Exp	Obs	Exp	Obs	Exp	Obs	Exp	Obs
A	GCT	25.0%	25.6%	0.0%	0.0%	0.0%	0.0%	5.6%	0.2%	0.0%	0.0%
C	TGC	0.0%	0.0%	0.0%	0.0%	0.0%	0.0%	0.0%	0.0%	0.0%	0.0%
D	GAT	0.0%	0.1%	0.0%	0.0%	0.0%	0.0%	5.6%	0.3%	14.3%	10.1%
E	GAA	0.0%	0.0%	0.0%	0.0%	0.0%	0.0%	5.6%	0.0%	14.3%	3.7%
F	TTC	0.0%	0.0%	16.7%	6.0%	0.0%	0.0%	5.6%	0.8%	0.0%	0.0%
G	GGC	25.0%	13.9%	0.0%	0.0%	0.0%	0.0%	5.6%	0.4%	0.0%	0.0%
H	CAT	0.0%	0.0%	16.7%	17.8%	0.0%	0.0%	5.6%	0.3%	14.3%	28.6%
I	ATC	0.0%	0.0%	16.7%	43.4%	0.0%	0.0%	5.6%	6.4%	0.0%	0.0%
K	AAG	0.0%	0.0%	0.0%	0.0%	0.0%	0.0%	5.6%	1.1%	14.3%	18.0%
L	CTG	0.0%	0.0%	0.0%	0.0%	0.0%	0.1%	5.6%	6.3%	0.0%	0.0%
M	ATG	0.0%	0.0%	0.0%	0.0%	0.0%	0.0%	0.0%	0.1%	0.0%	0.0%
N	AAC	0.0%	0.0%	0.0%	0.0%	0.0%	0.0%	5.6%	10.9%	14.3%	10.8%
P	CCG	0.0%	0.0%	0.0%	0.0%	100.0%	98.1%	5.6%	1.5%	0.0%	0.0%
Q	CAG	0.0%	0.0%	0.0%	0.0%	0.0%	0.3%	5.6%	0.3%	14.3%	18.5%
R	CGT	0.0%	0.0%	0.0%	0.0%	0.0%	0.0%	5.6%	0.0%	14.3%	9.8%
S	TCT	25.0%	39.5%	0.0%	0.0%	0.0%	0.0%	5.6%	1.1%	0.0%	0.0%
T	ACC	0.0%	0.0%	0.0%	0.0%	0.0%	0.0%	5.6%	0.8%	0.0%	0.0%
V	GTG	25.0%	20.3%	16.7%	12.8%	0.0%	0.0%	5.6%	2.6%	0.0%	0.0%
W	TGG	0.0%	0.0%	16.7%	12.3%	0.0%	0.0%	5.6%	1.0%	0.0%	0.0%
Y	TAC	0.0%	0.0%	16.7%	6.9%	0.0%	0.0%	5.6%	65.4%	0.0%	0.0%
Design		GAVS		WFYIVH		P		18 codons		NEQDKRH	
Codons >1%		AGSV		FHIVWY		P		ILNPSVY		DEHKNQR	
Other Codons		0.6%		0.7%		1.5%		0.5%		0.4%	

MAX Codons		RH R6		RH R5		RH R4		RH R3		RH R2		RH R1	
		Exp	Obs	Exp	Obs	Exp	Obs	Exp	Obs	Exp	Obs	Exp	Obs
A	GCT	25.0%	51.6%	0.0%	0.0%	0.0%	0.0%	0.0%	0.0%	0.0%	0.0%	0.0%	0.2%
C	TGC	0.0%	0.0%	0.0%	0.0%	0.0%	0.0%	0.0%	0.0%	0.0%	0.0%	0.0%	0.0%
D	GAT	0.0%	0.2%	0.0%	0.0%	14.3%	12.7%	50.0%	88.1%	0.0%	0.0%	0.0%	0.1%
E	GAA	0.0%	0.0%	0.0%	0.0%	14.3%	2.3%	50.0%	11.6%	0.0%	0.0%	0.0%	0.1%
F	TTC	0.0%	0.0%	25.0%	6.2%	0.0%	0.0%	0.0%	0.0%	20.0%	8.0%	0.0%	0.1%
G	GGC	0.0%	0.0%	0.0%	0.0%	0.0%	0.0%	0.0%	0.0%	0.0%	0.0%	0.0%	0.0%
H	CAT	0.0%	0.0%	0.0%	0.0%	14.3%	60.2%	0.0%	0.0%	0.0%	0.0%	0.0%	0.0%
I	ATC	25.0%	13.7%	0.0%	0.0%	0.0%	0.0%	0.0%	0.0%	20.0%	8.5%	25.0%	9.8%
K	AAG	0.0%	0.0%	0.0%	0.0%	14.3%	1.7%	0.0%	0.0%	0.0%	0.0%	0.0%	0.0%
L	CTG	25.0%	18.9%	25.0%	78.1%	0.0%	0.0%	0.0%	0.0%	0.0%	0.0%	25.0%	4.3%
M	ATG	0.0%	0.2%	0.0%	0.2%	0.0%	0.0%	0.0%	0.0%	0.0%	0.0%	0.0%	0.0%
N	AAC	0.0%	0.0%	0.0%	0.0%	14.3%	5.2%	0.0%	0.0%	0.0%	0.0%	0.0%	0.0%
P	CCG	0.0%	0.0%	0.0%	0.0%	0.0%	0.0%	0.0%	0.0%	0.0%	0.0%	25.0%	17.1%
Q	CAG	0.0%	0.0%	0.0%	0.0%	14.3%	6.9%	0.0%	0.0%	0.0%	0.0%	0.0%	0.1%
R	CGT	0.0%	0.0%	0.0%	0.0%	14.3%	10.7%	0.0%	0.0%	20.0%	24.5%	0.0%	0.0%
S	TCT	0.0%	0.3%	0.0%	0.0%	0.0%	0.0%	0.0%	0.0%	0.0%	0.0%	0.0%	0.0%
T	ACC	0.0%	0.0%	0.0%	0.0%	0.0%	0.0%	0.0%	0.0%	0.0%	0.0%	0.0%	0.0%
V	GTG	25.0%	14.6%	0.0%	0.1%	0.0%	0.0%	0.0%	0.0%	0.0%	0.0%	25.0%	67.4%
W	TGG	0.0%	0.0%	25.0%	6.0%	0.0%	0.0%	0.0%	0.0%	20.0%	36.0%	0.0%	0.1%
Y	TAC	0.0%	0.0%	25.0%	9.0%	0.0%	0.0%	0.0%	0.0%	20.0%	22.4%	0.0%	0.0%
Design		VILA		YWFL		NEQDKRH		DE		WIRFY		PIVL	
Codons >1%		AILV		FLWY		DEHKNQR		DE		FIRWY		ILPV	
Other Codons		0.5%		0.5%		0.4%		0.3%		0.5%		0.6%	

9.4. Appendix 4. 63-mer Anti-NGF Peptide Library Codon Representation Tables

MAX Codons		LH1		LH2		LH3		LH4		LH5	
		Exp	Obs	Exp	Obs	Exp	Obs	Exp	Obs	Exp	Obs
A	GCT	25.0%	11.6%							0.0%	0.0%
C	TGC	0.0%	0.2%							0.0%	0.0%
D	GAT	0.0%	0.0%							14.3%	11.2%
E	GAA	0.0%	0.0%							14.3%	5.1%
F	TTC	0.0%	0.0%							0.0%	0.2%
G	GGC	25.0%	45.9%							0.0%	0.0%
H	CAT	0.0%	0.0%							14.3%	24.5%
I	ATC	0.0%	0.0%							0.0%	1.3%
K	AAG	0.0%	0.0%							14.3%	17.7%
L	CTG	0.0%	0.0%							0.0%	0.0%
M	ATG	0.0%	0.0%							0.0%	0.0%
N	AAC	0.0%	0.0%							14.3%	11.6%
P	CCG	0.0%	0.0%							0.0%	0.3%
Q	CAG	0.0%	0.0%							14.3%	12.5%
R	CGT	0.0%	0.0%							14.3%	14.0%
S	TCT	25.0%	11.9%							0.0%	0.0%
T	ACC	0.0%	0.0%							0.0%	0.0%
V	GTG	25.0%	29.3%							0.0%	0.5%
W	TGG	0.0%	0.0%							0.0%	0.3%
Y	TAC	0.0%	0.0%							0.0%	0.2%
Design		GAVS		WFYIVH		P		18 codons		NEQDKRH	
Codons >1%		AGSV								DEHIKNQR	
Other Codons		1.0%								0.5%	

MAX Codons		RH6		RH5		RH4		RH3		RH2		RH1	
		Exp	Obs	Exp	Obs	Exp	Obs	Exp	Obs	Exp	Obs	Exp	Obs
A	GCT	25.0%	46.9%	0.0%	0.0%	0.0%	0.0%	0.0%	0.1%	0.0%	0.0%	0.0%	0.2%
C	TGC	0.0%	0.0%	0.0%	0.0%	0.0%	0.0%	0.0%	0.0%	0.0%	0.0%	0.0%	0.0%
D	GAT	0.0%	0.1%	0.0%	0.0%	14.3%	12.6%	50.0%	87.6%	0.0%	0.0%	0.0%	0.1%
E	GAA	0.0%	0.0%	0.0%	0.0%	14.3%	2.6%	50.0%	11.6%	0.0%	0.0%	0.0%	0.1%
F	TTC	0.0%	0.0%	25.0%	6.2%	0.0%	0.0%	0.0%	0.0%	20.0%	8.1%	0.0%	0.1%
G	GGC	0.0%	0.0%	0.0%	0.0%	0.0%	0.0%	0.0%	0.0%	0.0%	0.0%	0.0%	0.0%
H	CAT	0.0%	0.0%	0.0%	0.0%	14.3%	58.8%	0.0%	0.1%	0.0%	0.0%	0.0%	0.0%
I	ATC	25.0%	13.2%	0.0%	0.1%	0.0%	0.0%	0.0%	0.1%	20.0%	8.9%	25.0%	10.4%
K	AAG	0.0%	0.0%	0.0%	0.0%	14.3%	1.9%	0.0%	0.0%	0.0%	0.0%	0.0%	0.0%
L	CTG	25.0%	21.9%	25.0%	75.2%	0.0%	0.1%	0.0%	0.1%	0.0%	0.1%	25.0%	4.1%
M	ATG	0.0%	0.1%	0.0%	0.2%	0.0%	0.0%	0.0%	0.0%	0.0%	0.0%	0.0%	0.0%
N	AAC	0.0%	0.0%	0.0%	0.1%	14.3%	5.9%	0.0%	0.0%	0.0%	0.0%	0.0%	0.0%
P	CCG	0.0%	2.0%	0.0%	0.0%	0.0%	0.0%	0.0%	0.0%	0.0%	0.0%	25.0%	16.5%
Q	CAG	0.0%	0.0%	0.0%	0.0%	14.3%	7.1%	0.0%	0.0%	0.0%	0.0%	0.0%	0.1%
R	CGT	0.0%	0.0%	0.0%	0.0%	14.3%	10.5%	0.0%	0.0%	20.0%	25.0%	0.0%	0.0%
S	TCT	0.0%	0.3%	0.0%	0.0%	0.0%	0.0%	0.0%	0.0%	0.0%	0.0%	0.0%	0.0%
T	ACC	0.0%	0.0%	0.0%	0.0%	0.0%	0.0%	0.0%	0.0%	0.0%	0.0%	0.0%	0.0%
V	GTG	25.0%	14.9%	0.0%	0.1%	0.0%	0.0%	0.0%	0.1%	0.0%	0.0%	25.0%	67.5%
W	TGG	0.0%	0.0%	25.0%	6.0%	0.0%	0.0%	0.0%	0.0%	20.0%	35.7%	0.0%	0.1%
Y	TAC	0.0%	0.0%	25.0%	11.4%	0.0%	0.0%	0.0%	0.0%	20.0%	21.4%	0.0%	0.0%
Design		VILA		YWFL		NEQDKRH		DE		WIRFY		PIVL	
Codons >1%		AILPV		FLWY		DEHKNQR		DE		FIRWY		ILPV	
Other Codons		0.6%		0.5%		0.4%		0.4%		0.7%		0.7%	

9.5. Appendix 5. Re-Synthesised Final Anti-NGF Peptide Library Codon Representation Tables

MAX Codons		LH1		LH2		LH3		LH4		LH5	
		Exp	Obsv	Exp	Obsv	Exp	Obsv	Exp	Obsv	Exp	Obsv
A	GCT	25.0%	25.1%	0.0%	0.0%	0.0%	0.0%	5.6%	4.1%	0.0%	0.0%
C	TGC	0.0%	0.0%	0.0%	0.0%	0.0%	0.0%	0.0%	0.0%	0.0%	0.0%
D	GAT	0.0%	0.0%	0.0%	0.0%	0.0%	0.0%	5.6%	0.0%	14.3%	15.2%
E	GAA	0.0%	0.0%	0.0%	0.0%	0.0%	0.0%	5.6%	0.7%	14.3%	3.3%
F	TTC	0.0%	0.0%	16.7%	16.0%	0.0%	0.0%	5.6%	7.5%	0.0%	0.0%
G	GGC	25.0%	15.0%	0.0%	0.0%	0.0%	0.0%	5.6%	2.7%	0.0%	0.0%
H	CAT	0.0%	0.0%	16.7%	12.3%	0.0%	0.0%	5.6%	3.5%	14.3%	21.6%
I	ATC	0.0%	0.0%	16.7%	33.3%	0.0%	0.0%	5.6%	0.5%	0.0%	0.0%
K	AAG	0.0%	0.0%	0.0%	0.0%	0.0%	0.0%	5.6%	4.3%	14.3%	19.2%
L	CTG	0.0%	0.0%	0.0%	0.0%	0.0%	0.0%	5.6%	8.0%	0.0%	0.0%
M	ATG	0.0%	0.0%	0.0%	0.0%	0.0%	0.0%	0.0%	0.1%	0.0%	0.0%
N	AAC	0.0%	0.0%	0.0%	0.0%	0.0%	0.0%	5.6%	9.4%	14.3%	7.9%
P	CCG	0.0%	0.0%	0.0%	0.0%	100.0%	99.3%	5.6%	5.3%	0.0%	0.0%
Q	CAG	0.0%	0.0%	0.0%	0.0%	0.0%	0.1%	5.6%	6.6%	14.3%	13.3%
R	CGT	0.0%	0.0%	0.0%	0.0%	0.0%	0.0%	5.6%	1.5%	14.3%	19.0%
S	TCT	25.0%	25.9%	0.0%	0.0%	0.0%	0.0%	5.6%	8.8%	0.0%	0.0%
T	ACC	0.0%	0.0%	0.0%	0.0%	0.0%	0.0%	5.6%	10.9%	0.0%	0.0%
V	GTG	25.0%	33.4%	16.7%	17.8%	0.0%	0.0%	5.6%	10.7%	0.0%	0.0%
W	TGG	0.0%	0.0%	16.7%	2.3%	0.0%	0.0%	5.6%	3.7%	0.0%	0.0%
Y	TAC	0.0%	0.0%	16.7%	17.7%	0.0%	0.0%	5.6%	11.2%	0.0%	0.0%
Design		GAVS		WFYIVH		P		18 codons exc C&M		NEQDKRH	
Codons >1%		AGSV		FHIVWY		P		AFGHKLNPNRSTVWY		DEHKNQR	
Other Codons		0.5%		0.4%		0.5%		0.8%		0.5%	

MAX Codons		RH6		RH5		RH4		RH3		RH2		RH1	
		Exp	Obsv	Exp	Obsv	Exp	Obsv	Exp	Obsv	Exp	Obsv	Exp	Obsv
A	GCT	25.0%	39.4%	0.0%	0.0%	0.0%	0.0%	0.0%	0.0%	0.0%	0.0%	0.0%	0.2%
C	TGC	0.0%	0.0%	0.0%	0.0%	0.0%	0.0%	0.0%	0.0%	0.0%	0.0%	0.0%	0.0%
D	GAT	0.0%	0.1%	0.0%	0.0%	14.3%	13.2%	50.0%	88.0%	0.0%	0.0%	0.0%	0.1%
E	GAA	0.0%	0.0%	0.0%	0.0%	14.3%	2.6%	50.0%	11.7%	0.0%	0.0%	0.0%	0.1%
F	TTC	0.0%	0.0%	25.0%	8.2%	0.0%	0.0%	0.0%	0.0%	20.0%	8.8%	0.0%	0.1%
G	GGC	0.0%	0.0%	0.0%	0.0%	0.0%	0.0%	0.0%	0.0%	0.0%	0.0%	0.0%	0.0%
H	CAT	0.0%	0.0%	0.0%	0.0%	14.3%	57.2%	0.0%	0.0%	0.0%	0.0%	0.0%	0.0%
I	ATC	25.0%	17.8%	0.0%	0.0%	0.0%	0.0%	0.0%	0.0%	20.0%	9.0%	25.0%	10.4%
K	AAG	0.0%	0.0%	0.0%	0.0%	14.3%	2.1%	0.0%	0.0%	0.0%	0.0%	0.0%	0.0%
L	CTG	25.0%	26.0%	25.0%	73.2%	0.0%	0.0%	0.0%	0.0%	0.0%	0.0%	25.0%	4.1%
M	ATG	0.0%	0.1%	0.0%	0.1%	0.0%	0.0%	0.0%	0.0%	0.0%	0.0%	0.0%	0.0%
N	AAC	0.0%	0.0%	0.0%	0.0%	14.3%	5.8%	0.0%	0.0%	0.0%	0.0%	0.0%	0.0%
P	CCG	0.0%	0.0%	0.0%	0.0%	0.0%	0.0%	0.0%	0.0%	0.0%	0.0%	25.0%	16.7%
Q	CAG	0.0%	0.0%	0.0%	0.0%	14.3%	7.3%	0.0%	0.0%	0.0%	0.0%	0.0%	0.1%
R	CGT	0.0%	0.0%	0.0%	0.0%	14.3%	11.4%	0.0%	0.0%	20.0%	24.2%	0.0%	0.0%
S	TCT	0.0%	0.1%	0.0%	0.0%	0.0%	0.0%	0.0%	0.0%	0.0%	0.0%	0.0%	0.0%
T	ACC	0.0%	0.0%	0.0%	0.0%	0.0%	0.0%	0.0%	0.0%	0.0%	0.0%	0.0%	0.0%
V	GTG	25.0%	16.2%	0.0%	0.0%	0.0%	0.0%	0.0%	0.0%	0.0%	0.0%	25.0%	67.5%
W	TGG	0.0%	0.0%	25.0%	7.0%	0.0%	0.0%	0.0%	0.0%	20.0%	35.4%	0.0%	0.2%
Y	TAC	0.0%	0.0%	25.0%	11.0%	0.0%	0.0%	0.0%	0.0%	20.0%	22.1%	0.0%	0.0%
Design		VILA		YWFL		NEQDKRH		DE		WIRFY		PIVL	
Codons >1%		AILV		FLWY		DEHKNQR		DE		FIRWY		ILPV	
Other Codons		0.5%		0.4%		0.3%		0.2%		0.5%		0.6%	

9.6. Appendix 6. pET SUMO/CAT Positive Expression Control Plasmid Map (taken from Champion™ pET SUMO Protein Expression System manual, Invitrogen)



9.7. Appendix 7. pET SUMO Sequencing Primers

SUMO Fwd	5' AGATTCTTGTACGACGGTATTAG 3'
T7 Rev	5' CCACCGCTGAGCAATAACTA 3'